# SYNTHESIS OF OXY AND AMINO CYCLOPENTADIENYL RHENIUM COMPLEXES

DISSERTATION

zur

Erlangung der naturwissenschaftlichen Doktorwürde

(Dr. sc. nat.)

vorgelegt der

Mathematisch-naturwissenschaftlichen Fakultät

der

Universität Zürich

von

Gabriel Lastennet

aus

Frankreich

Promotionskomitee

Prof. Dr. Heinz Berke (Vorsitz und Leitung)

Prof. Dr. Roger Alberto

Zürich 2008

# Contents

# List of Abbreviations

| | |
|---|---|
| Cp | cyclopentadienyl |
| Cbz | Benzyloxycarbonyl |
| Me | methyl |
| Et | ethyl |
| Ar | aryl |
| $^{i}$Pr | isopropyl |
| Ph | Phenyl |
| IR | infrared |
| MS | mass spectroscopy |
| NMR | Nuclear Magnetic Resonance |
| FAB | Fast Atom Bombardment |
| EI | Electron Impact Ionization |
| ESI | Electrospray Ionization |
| Hz | hertz |
| THF | tetrahydrofuran |
| δ | chemical shift |
| ν | frequency |
| br | broad |
| d | doublet |
| m | multiplet (NMR), medium (IR) |
| quart | quartet |
| quint | quintet |
| s | singlet (NMR, strong (IR) |
| t | triplet |
| rt | room temperature |
| equiv. | equivalent |

# List of Prepared Compounds

**1** ($\eta^5$-$C_5H_5$)$Re(CO)_3$

**2** ($\eta^5$-$C_5H_4Li$)$Re(CO)_3$

**3** ($\eta^5$-$C_5H_4SiMe_3$)$Re(CO)_3$

**5** ($\eta^5$-$C_5H_4OLi$)$Re(CO)_3$

**6** ($\eta^5$-$C_5H_4OH$)$Re(CO)_3$

**7** ($\eta^5$-$C_5H_4OMe$)$Re(CO)_3$

**8** ($\eta^5$-$C_5H_4OEt$)$Re(CO)_3$

**9** ($\eta^5$-$C_5H_4O^iPr$)$Re(CO)_3$

**10** ($\eta^5$-$C_5H_4OCH_2CH{=}CH_2$)$Re(CO)_3$

**11** ($\eta^5$-$C_5H_4OCH_2Ph$)$Re(CO)_3$

**12** ($\eta^5$-$C_5H_4OCOMe$)$Re(CO)_3$

**13** ($\eta^5$-$C_5H_4OCOPh$)$Re(CO)_3$

**14** ($\eta^5$-$C_5H_4N_3$)$Re(CO)_3$

**15** ($\eta^5$-$C_5H_4NH_2$)$Re(CO)_3$

**16** ($\eta^5$-$C_5H_4N{=}CHPh$)$Re(CO)_3$

**17** ($\eta^5$-$C_5H_4NHCH_2Ph$)$Re(CO)_3$

**18** ($\eta^5$-$C_5H_4NHCbz$)$Re(CO)_3$

**19** ($\eta^5$-$C_5H_4NHCOMe$)$Re(CO)_3$

**20** ($\eta^5$-$C_5H_4NHC_4H_8$)$Re(CO)_3$

**21** ($\eta^5$-$C_5H_4NHCONHC_8H_3F_6$)$Re(CO)_3$

**22** ($\eta^5$-$C_5H_4NHCONHC_6F_5$)$Re(CO)_3$

**23** [($\eta^5$-$C_5H_4OMe$)$Re(CO)_2(NO)$]$^+BF_4^-$

**24** $[(\eta^5\text{-}C_5H_4NHCbz)Re(CO)_2(NO)]^+BF_4^-$

**25** $[(\eta^5\text{-}C_5H_4OCH_2Ph)Re(CO)_2(NO)]^+BF_4^-$

**26** $(\eta^5\text{-}C_5H_4OCH_2Ph)Re(CO)(NO)H$

**27** $[(\eta^5\text{-}C_5H_4OH)Re(CO)_2(NO)]^+BF_4^-$

# 1 Introduction

## 1.1 Rhenium in general

### 1.1.1 Discovery

Rhenium was the last naturally occurring element to be discovered. Predicted by Henry Moseley in 1914, it was isolated the first time by two young german physicists in 1925, Walter Noddack and Ida Tacke. They separated 10 parts per million of material from a sample of gadolinite and named the new element Rhenium in homage to their native river Rhine. Later in 1928, they produced a gram of rhenium from 660 kg of molybdenite from Scandinavia.[1]

### 1.1.2 Occurence and recovery

Rhenium is present in the Earth's crust at approximately 1 ppb and indeed occurs principally in molybdenite in porphyry copper deposits. It is recovered from molybdenite, itself extracted from copper ores by froth flotation. The roasting of the molybdenum concentrates produces molybdenum trioxide and rhenium oxides, captured with the sulphur emission when the flue dusts are wet scrubbed. Ammonium perrhenate $NH_4ReO_4$ (APR) is the most common form of rhenium prior to conversion and pure rhenium powder can be prepared from APR with $H_2$ at high temprature.[2-5]

The first pure rhenium mineral was discovered in 1994 in Russia at Kudriavy vulcano, Iturup Island in the Kurile arc[6]. It was found to be rhenium sulphide $ReS_2$, named rheniite.

### 1.1.3 Production

Chile, USA, Peru, Kazahkstan, Canada, Russia and Armenia are the main producers of rhenium. The world production is about 50 tons/year and recycling of Pt-Re catalysts provides another10 tons/year.

### 1.1.4 Applications and consumption

Rhenium is used as a catalyst in petroleum reforming for the production of high-octane hydrocarbons, used in the production of lead free gasoline. Platinum-rhenium catalysts are exceptionally resistant to poisoning from nitrogen sulfur and phosphorus and allow to operate at lower pressures and higher temperatures, which leads to improved yields.
Rhenium alloys, particularly molybdenum and tungsten alloys, have shown significant properties such as improved ductility and superconductivity. Molybdenum-rhenium alloys become superconducting at 10 K and ductile at temperatures above 196°C. Alloys of tungsten containing 24 % of rhenium have lower ductile to brittle transition temperatures than pure tungsten and rhenium improves the strenght of nickel alloys at high temperatures (1000° C). These alloys are principally used in aerospace for the design of turbine blades.

Rhenium is also used in thermocouples, temperature control, heating elements, ionization gauges, mass spectrographs, electron tubes and targets, electrical contacts, metallic coatings, vacuum tubes, crucibles, electromagnets and semiconductors. However on a very small scale, rhenium can also be used in medical applications. After neutron bombardment, radioactive rhenium is used in prevention and treatment of restenosis and can be highly effective in the treatment of liver tumors.

In 2001, catalytic uses of rhenium represented 25 % of rhenium consumption, metallurgical uses 75 % and the other uses collectively 5 % of total consumption.[7-11]

## 1.2 Rhenium catalysis in laboratory

### 1.2.1 Epoxidation

Epoxidation has been investigated intensively, because epoxides are versatile electrophilic intermediates in organic synthesis, which can be easily converted into polyethers, diols and amino alcohols. Catalytic asymmetric epoxidation has contributed to the great advances in generation of compounds with chiral centers the past 30 years and has widespread application in bulk, fine chemistry and in the pharmaceutical industry. The most efficient epoxidation catalysts apply transition metals, such as titanium, manganese, osmium and tungsten.
Methyltrioxorhenium (MTO) was also found to be an efficient catalyst, capable of oxidizing various functional groups using $H_2O_2$ (Scheme 1.1)[12-17]. The first catalyst was developed by Herrmann and coworkers. This catalyst showed moderate selectivity due the high Lewis acidity of MTO, catalyzing the ring opening of the epoxide to the diol. Addition of tertiary amines proved beneficial to the selectivity of the process, but appeared to work at the expense of the catalytic activity. The loss in activity was established to be the consequence of the competing formation of N-oxide. The process was improved with the use of more oxidation resistant N-donor ligands such as pyridine, quinuclidine, pyrazole, under biphasic conditions. Thus N-oxide formation can be compensated by the extraction of N-oxide to the aqueous phase.

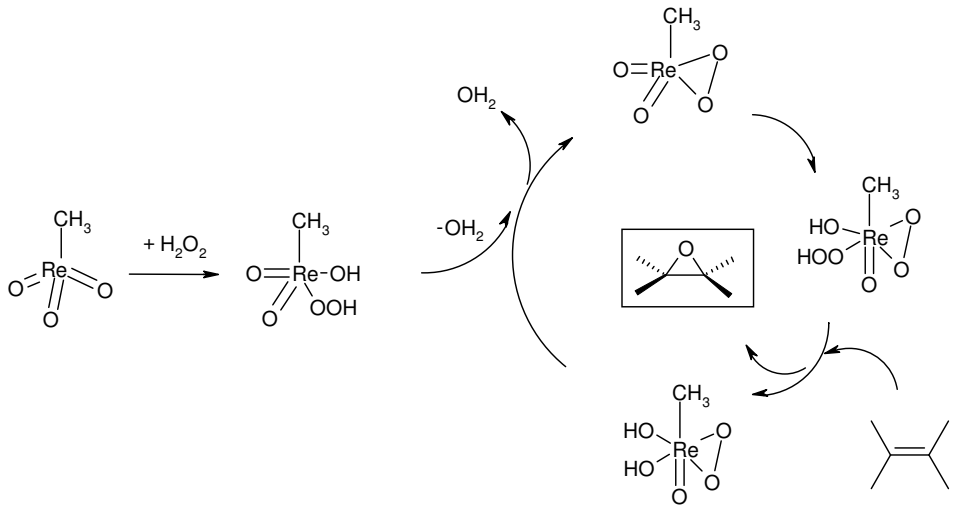


**Scheme 1.1** Mechanism of MTO-based catalytic epoxidation

Recently the asymmetric version of the MTO-based catalytic epoxidation has been studied with various chiral ligands such as ferrocenyl pyridine, chiral pyrazole and glycol derivatives. Promising enantiomeric excesses up to 40 % have been observed.

### 1.2.2 Olefin metathesis

Olefin metathesis has become one of the most important chemical reactions and a very useful process in various disciplines of chemistry and in industry. Some of the first olefin metathesis catalysts used in industry in the 1960s for the transformation of propene to ethylene and butenes were prepared by impregnating alumina with aqueous solution of ammonium perrhenate or perrhenic acid followed by drying and calcination steps. These catalysts have been intensively studied, because of their high activity and selectivity at low temperatures (273-373 K). Methyltrioxorhenium (MTO) on silica alumina has also exhibited good activity in olefin metathesis at room temperatures[18-25]. Various studies with dirhenium heptoxide on alumina have demonstrated that the initiation step is probably a pseudo Wittig reaction with formation of oxametallacyclobutane followed by the formation of carbene species (Scheme 1.2).

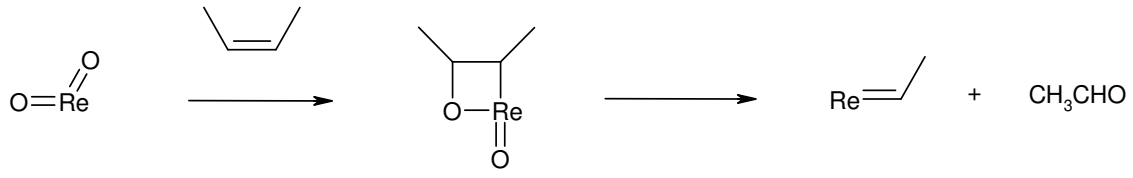


**Scheme 1.2** Oxametallacyclobutane (pseudo Wittig mechanism)

After these observations in the 1990's, J.M. Basset and coworkers developed a new heterogeneous rhenium catalyst supported by a silica surface (Figure 1.1).[26-29]

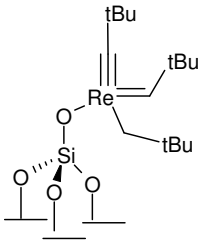


**Figure 1.1.** Rhenium-carbene surface

This new system catalyses the metathesis of propene at 25 °C with an initial rate (TOF) of 0.25 mol per mol Re per second, which corresponds to the best for rhenium catalysts. The formation of 3,3-dimethyl butene and 4,4-dimethyl pentene in a 3:1 ratio results from cross metathesis between propene and the neopentylidene ligand. Moreover this surface is also able to catalyse alkyne metathesis.

### 1.2.3 Isomerization of olefins

Isomerization of allylic alcohols can be catalyzed by various complexes at high temperatures such as $VO(OR)_3$ (130-200° C) or $WO(OR)_3$ and at room temperature by $VO(acac)_2$ or $MoO_2$ when activated by hexamethylsilylperoxide. Rhenium oxides are also able to catalyse this reaction and particularly MTO[30,31]. Additionally MTO, the analogous triphenylsiloxy derivative and rhenium heptoxide can catalyse the isomerization of allylic silyl ethers. The mechanism of 1, 3-transposition of allylic alcohols catalysed by MTO involves a transfer of the metal bonded O atom to the alcohol as shown below (Scheme 1.3).

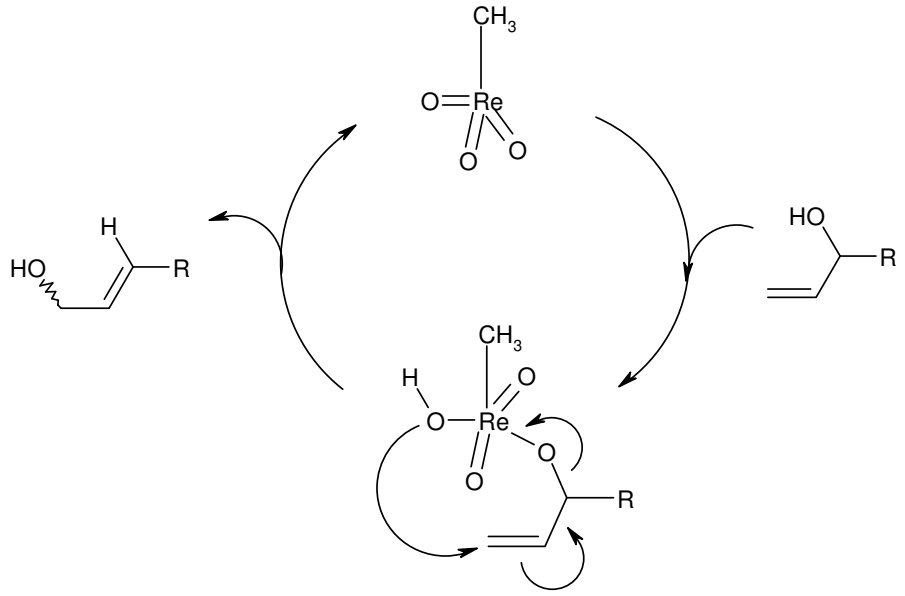


**Scheme 1.3** Mechanism of 1,3-rearrangement of allylic alcohols catalyzed by MTO

Rhenium has shown great catalytic activity in epoxidation, olefin metathesis and isomerization of olefins and particularly the rhenium trioxide MTO. These catalytic reactions are important branches of chemistry. However, rhenium has not been utilized yet in a catalytic hydrogenation as an important achievement in catalysis and to profitable industrial processes.

## 1.3 Catalytic hydrogenation

Hydrogenation consists of 1,2-addition of dihydrogen to unsaturated organic compounds such as alkenes, alkynes, ketones, imines or nitriles. The classical reaction is the reduction of alkenes to alkanes as shown below (Scheme 1.4).

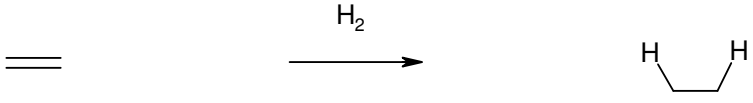


**Scheme 1.4**

The addition of dihydrogen proceeds here formally with the homolytic splitting of the H-H bond. However in certain cases the H-H bond splits in a heterolytic way giving a proton and hydride both appearing in the end in a base and a metal bound form (Scheme 1.5):

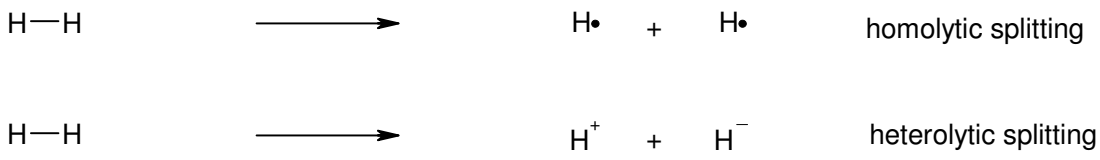


**Scheme 1.5**

Hydrogenation reactions apply hydrogen gas or as a chemically bound source of dihydrogen hydrazine, dihydroanthracene, formic acid or quinines, which are usually then called transfer hydrogenations. Most of the hydrogenation reactions occur in the presence of a catalyst that lowers the activation energy of the process and thus accelerates the reaction. Two classes of catalysts have been developed. Heterogeneous catalysts, which are not soluble in the solvent in which the reaction is carried out. Whereas homogeneous catalysts are completely soluble and in the same phase as the reactants.

## 1.4 Historical perspectives of catalytic hydrogenation

### 1.4.1 Heterogeneous catalysis

Döbereiner's lamp[32,33], commercialized in 1823, is the first catalytic application of dihydrogen adsorption. This ingenious device produces dihydrogen gas generated from zinc and sulphuric acid. The gas streams through a narrow outlet toward a holder in which platinum is suspended on a thin platinum wire whereupon it ignites by reaction with ambient oxygen.

Fifty years later J.P. Sabatier[34-38] and Senderens developed the catalytic hydrogenation of organic compounds in the gaseous state including the transformation of oleic to stearic acid

and nitrobenzene to aniline. Today Sabatier's process is known as the reaction of carbon dioxide with dihydrogen leading to methane and water (Scheme 1.6).

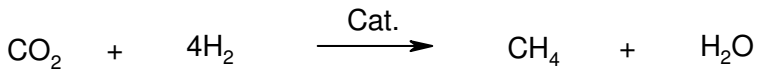


**Scheme 1.6** Sabatier Process

In 1908 F. Haber developed a catalytic process to produce ammonia (scheme 1.7). He reacted nitrogen gas generated by the Linde process and hydrogen gas under high pressure and high temperature over an iron catalyst. Later, this process was scaled up by C. Bosch working for the chemical company BASF. Nitric acid produced from ammonia was then used to manufacture agricultural fertilizers as well as explosives. Today, the Haber-Bosch process[39-45] is used to produce more than 500 million tons of artificial fertilizer per year; about 1 % of the world's annual energy supply[41] is consumed in the process, and it sustains about 40 % of the Earth's population[42].

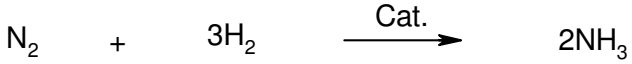


**Scheme 1.7** Haber-Bosch Process

In the 1920s F. Fischer and H. Tropsch discovered a new catalytic process applying cobalt and iron catalysts (Scheme 1.8). Today this process is still very useful in petrochemistry to produce synthetic fuels and food grade wax. In this reaction carbon monoxide and hydrogen gas are converted into liquid hydrocarbons of various forms.[46-57]

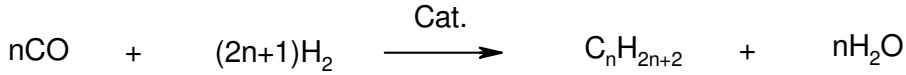


**Scheme 1.8** Fischer-Tropsch Process

In the 1930s hydroformylation[58-62] of olefins using cobalt catalysts was discovered by O. Roelen. and has become the main industrial process for the production of oxo compounds (7

millions tons per year). The reaction involves carbon monoxide and dihydrogen gas under high pressure (10-200 atm) and high temperature (Scheme 1.9). This reaction has continuously been improved and today the process applies various cobalt, rhodium, palladium and nickel catalysts. The process produces aldehydes, versatile compounds which can be converted into many secondary products. The main application is devoted to the transformation of propene into butanal, precursor of butyl acrylate, a feedstock for the production of polymers.

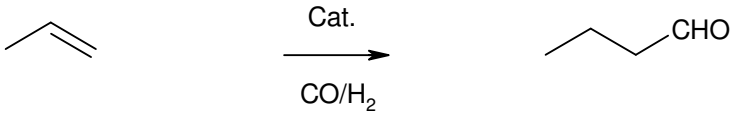


**Scheme 1.9** Oxo Synthesis

### 1.4.2 Homogeneous and asymmetric catalysis

In 1966 J. A. Osborn and G. Wilkinson (Nobel laureate[63]) published the synthesis of a new transition metal complex able to hydrogenate various olefins[64-66]. For the first time hydrogenation of various olefins was carried out in a solution, in which both the catalyst and the reagents were soluble. Based on Wilkinson's discovery, R. H. Crabtree in 1968 synthesized an iridium complex with a higher activity and capable of reducing a wider range of olefin types, particularly tri- and tetra-substituted alkenes (Figure 1.2)[67].


**Figure 1.2**

Asymmetric catalysis arose with the utilization of chiral phosphine as ligands. In 1968 W. S. Knowles (Nobel laureate[68]) could obtain an enantiomeric excess of 68% of (*R*) 2-phenyl-

propionic acid from 2-phenyl-acrylic acid with chiral isopropyl-methyl-phenyl-phosphine as ligand. First large enantiomeric excess obtained with a chiral phosphine (scheme 1.10)[69-71]:

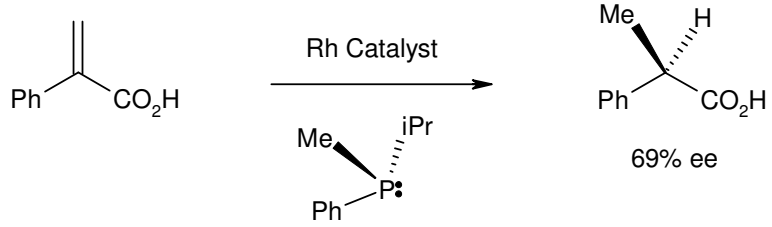


**Scheme 1.10**

In 1971 H. B. Kagan introduced chirality into a rhodium(I)-based catalytic system with a biphosphine (DIOP)[72]. Since the advent of this concept a large range of biphosphines have been synthesized and the eniantomeric excesses have been considerably enhanced[73-79]. The first industrial catalytic asymmetric synthesis employed such a biphosphine (DiPAMP) and was elaborated in 1974 by W. S. Knowles at Mosanto for the synthesis of L-DOPA[80,81].

Complexes of rhodium(I) have exhibited very high activity in catalytic hydrogenation, but their application has been limited to dehydroamino acids. A second generation of catalyst was discovered by T. Ikariya-M. Saburi and R. Noyori (Nobel Laureate[82]) in the 1980s. This ruthenium(II) catalysts are highly efficient and can be used for the enantioselective reduction of allylic alcohols, α,β-unsaturated acids and keto groups (Scheme 1.11)[83-89].

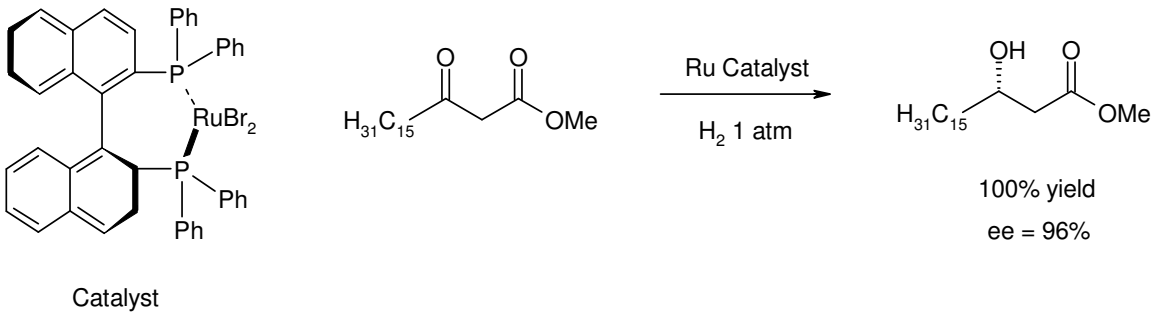


**Scheme 1.11** Noyori's catalyst

Heterogeneous catalysis has led to great industrial processes still used today. Homogeneous catalysts were the next generation of catalysts, highly reactive and able to transfer chirality to the substrate in the presence of an appropriate chiral ligand.

## 1.5 Mechanisms of hydrogenation

The mechanisms of hydrogenation of the best catalytic systems applying rhodium, iridium and ruthenium have been intensively studied and many mechanisms have been suggested and recently most of the mechanisms presented in the next chapter have been accepted. Rhodium and iridium mechanisms will be presented and then an overview about mechanistic aspects of ruthenium catalysis including the Shvo complex.

### 1.5.1 Rhodium and iridium catalysts

Crabtree reported the first homogeneous iridium catalysis in 1977[90]. Crabtree's catalyst has exhibited high catalytic activity in hydrogenation of olefins, particularly in reduction of tri and tetra substituted olefins[91]. The active species was isolated and described as a dihydrido olefin complex of the type $[IrH_2(olefin)_2L_2]^+$. The asymmetric version of the catalysis was developed by Pfaltz and coworkers in the 1990s with various chiral ligands such as phosphine-oxazoline ligands[92]. The catalytic cycle (Scheme 1.12)[93] has been studied by several groups and recently new detailed mechanisms based on experimental observations and DFT calculations have been suggested. All cycles suggested involves dihydride intermediates after oxidative addition and solvation steps during the hydrogenation process. The cycle ends with the reductive elimination of the saturated hydrocarbons.

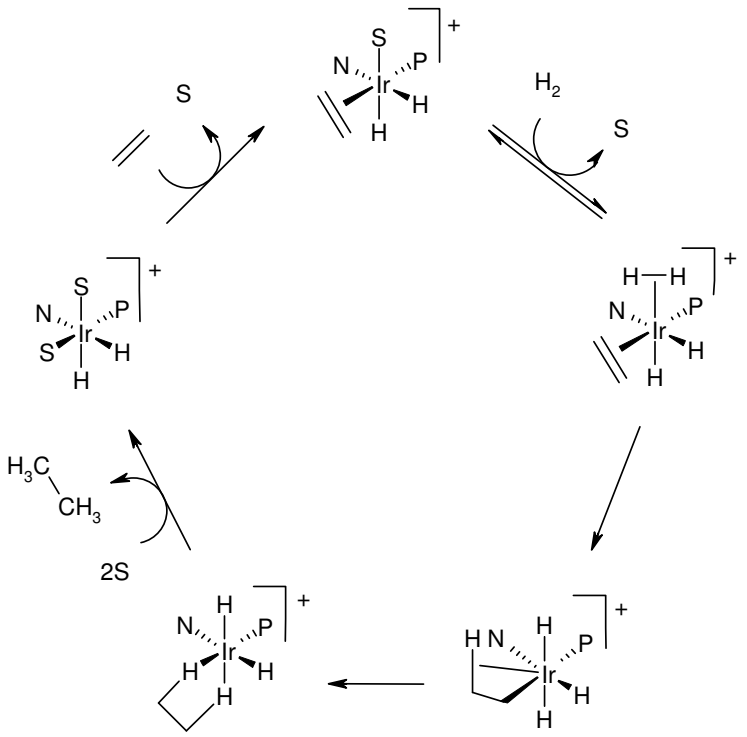


**Scheme 1.12**

The mechanism of rhodium catalyzed hydrogenation was studied by J. Halpern and coworkers. They proposed a mechanism in 1982 based on kinetic and spectroscopic studies and DFT calculations (Scheme 1.13)[94].

J. Halpern and coworkers found that the reaction of $[Rh(diphos)]^+$ with mac was a rapid process and complete at room temperature. Complex $[Rh(diphos)(mac)]^+$was even isolated and characterized by NMR spectroscopy ($^{31}P$, $^{13}C$, $^{1}H$) and the structure of the $BF_4$ salt was determined by X-ray analysis. The crystallographic data revealed a chelation of the substrate to the rhodium via the oxygen of the carbonyl. Step 2 was found to be the rate determining step of the catalytic reaction. The activation energy of Step 3 was lower than Step 2 but high enough to be rate determining at low temperature (-40°C) and thus the complex $[Rh(H)(diphos)(mac)]^+$could be characterized. The spectroscopic data showed clearly for the first time that during the reductive process the hydride migrates to the β carbon while the α-carbon binds to the rhodium center.

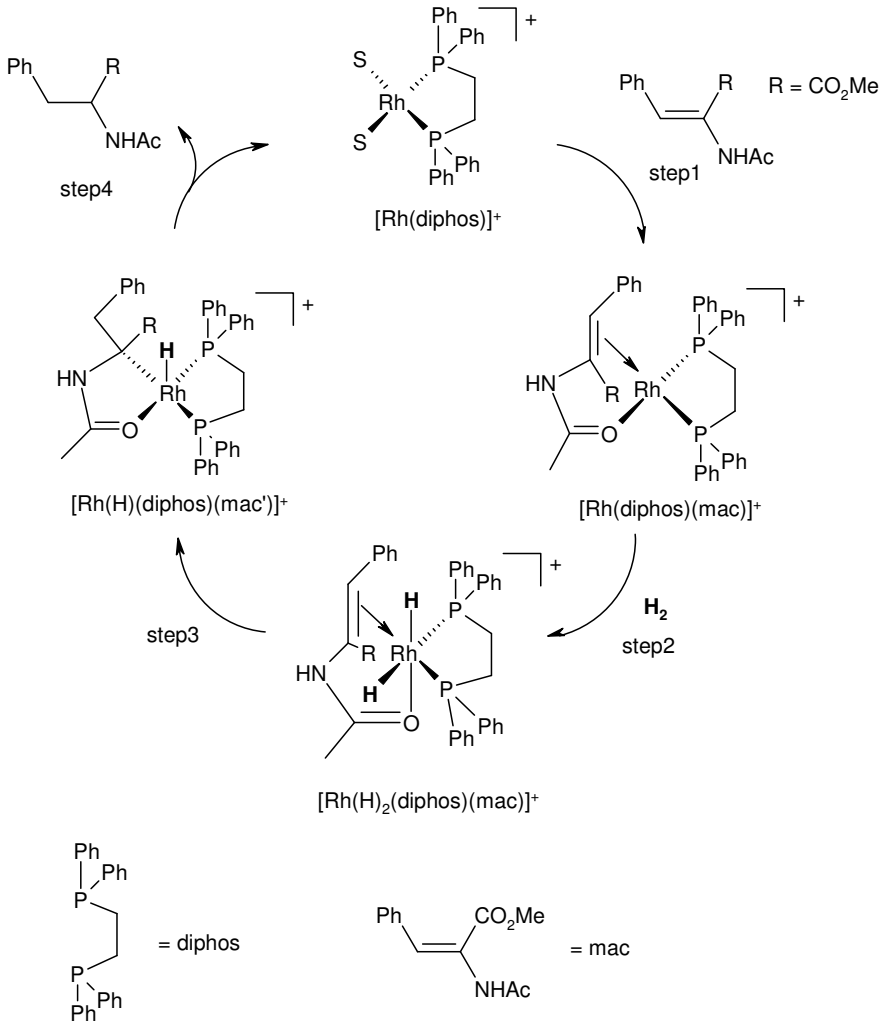


**Scheme 1.13**

The complex $[Rh(H)_2(diphos)(mac)]^+$ has never been observed, yet, but oxidative addition to analogous rhodium complexes has been well recognized and recent DFT calculations performed by R. Landis and coworkers have confirmed the structures of the intermediates that form during the catalytic processes[95].

### 1.5.2 Ruthenium catalysts

Usually hydrogen gas first coordinates to the ruthenium at a vacant site as a $\eta^2$-dihydrogen ligand and then in most common cases this ligand undergoes heterolytic splitting to give the ruthenium hydride and a protonated base (Scheme 1.14-pathway a). In certain cases the hetero

splitting results in the formation of ruthenium (IV) hydride compound with a proton anchored onto a ligand (pathway b) and the oxidative addition of dihydrogen to a ruthenium (II) gives a ruthenium (IV) dihydriden (pathway c).[96,97]

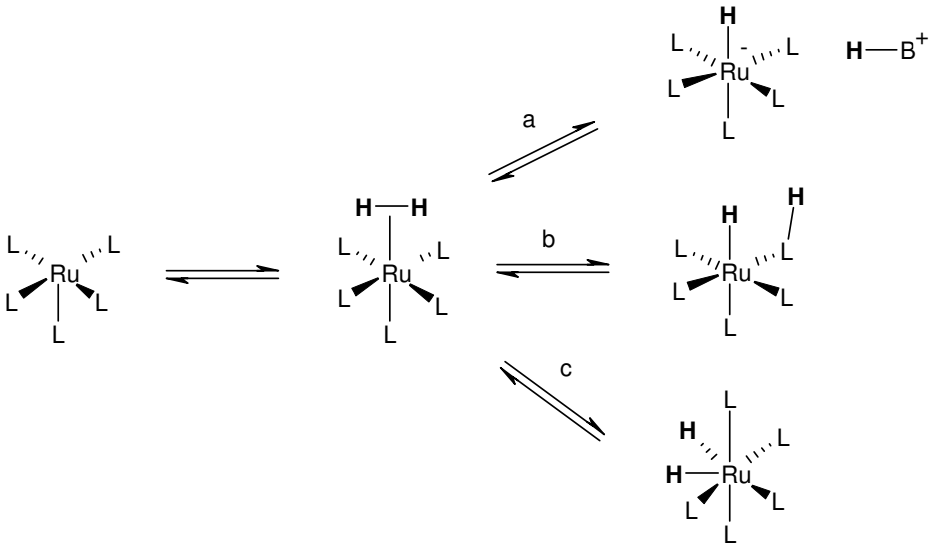


**Scheme 1.14**

The classical mechanism of hydrogenation involves a coordination of the substrate at a vacant site on the ruthenium after release of a molecule of solvent. This coordination in the inner coordination sphere activates the carbonyl or imine group and thus facilitates the migration of the hydride to the carbon β (Scheme 1.15).

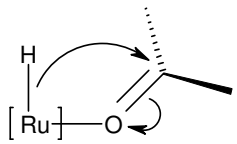


**Scheme 1.15**

However Noyori and coworkers discovered that ruthenium complexes can also reduce a substrate by a non-classical mechanism involving an interaction with the outer coordination sphere of the ruthenium complex. In this mechanism the ketone or imine is activated by an external electrophile or an internal electrophile attached to an ancillary ligand (Scheme1.16).

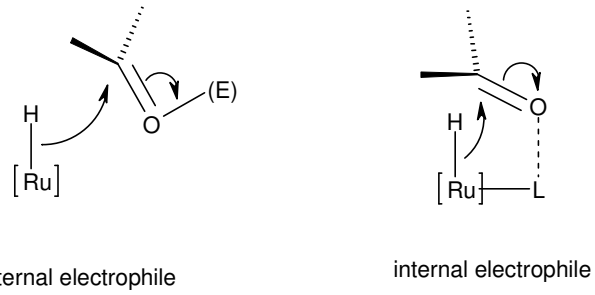


external electrophile internal electrophile

**Scheme1.16**

The first example of ligand-assisted catalysis was reported by Noyori and involves a NH group. They found that the addition of primary diamines and a base in isopropanol increased considerably the activity of the ruthenium catalyst $RuCl_2(PPh_3)_3$. Similar compounds of the form $RuCl_2$(diphosphine)(diamine)[98] with chiral diphosphines combined with the appropriate primary chiral amines were found to be extremely active and are enantioselective catalysts for the hydrogenation of a wide range of ketones[99-121] and imines[122,123].

Since the first observations of this phenomenon called the "NH-effect", it has been established that $RuCl_2$(diphosphine)(diamine) compounds are not the catalysts directly, but catalysts precursors to the active dihydride catalytic species $Ru(H)_2$(diphosphine)(diamine).

### 1.5.3 The NH effect and its mechanism

In 2001 R. H. Morris and coworkers prepared and isolated the dihydride $Ru(H)_2$((*R*)-(binap)($NH_2CMe_2CMe_2NH_2$). The crystal structure determination revealed an octahedral *trans*-dihydride Ru(II) complex[124]. This dihydride loses $H_2$ under $N_2$ or Ar atmosphere to produce the hydridoamido complex Ru(H)((*R*)-(binap)($NHCMe_2CMe_2NH_2$). This complex reacted with 1 atm $H_2$ to produce $Ru(H)_2$((*R*)-(binap)($NH_2CMe_2CMe_2NH_2$). They also obtained a first structural evidence for a hydridoamido complex from the crystal structure of the analogous triphenylphosphine complex, Ru(H)$(PPh_3)_2$($NHCMe_2CMe_2NH_2$). They found that its structural features allows dihydrogen addition *trans* to the hydride with a minimal structural reorganisation.

According to these observations, R. H. Morris and coworkers proposed the following catalytic cycle (Scheme 1.17)[125,126]. The initiation of the catalysis starts with the formation of a hydrogen bond between the oxygen of the ketone and the axial proton of the NH group (Step 1). Then the ketone receives both the hydride from the metal and the proton from the diamine in a concerted fashion (Step 2). This step leads to the hydridoamido complex Ru(H)(diphosphine)($NHCMe_2CMe_2NH_2$), which reacts with hydrogen gas (Step 3). The dihydrogen molecule coordinates to the ruthenium center and then becomes more acidic. The nitrogen of the amide becomes pyramidal and basic and thus initiates the hetero-splitting of the H-H bond (Step 4).

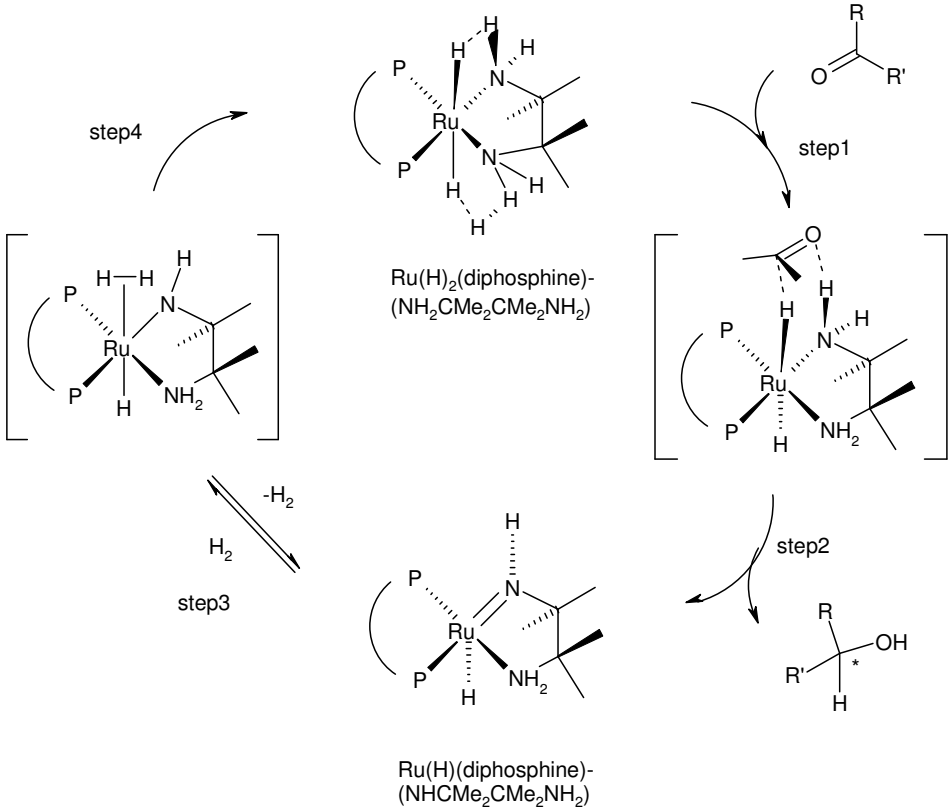


**Scheme 1.17**

Step 4 was found to be the rate determining step of this catalytic system because of the sensitivity of the catalyst to the hydrogen pressure. Indeed DFT calculations showed that the reaction of the dihydride with the ketone is a very easy process with a low activation energy

barrier whereas the noticeable loss of the Ru-N π bonding is responsible for the higher activation energy of the hetero splitting of the H-H bond.

### 1.5.4 Catalysis assisted by an acidic OH group

An early example of ligand-assisted catalytic hydrogenation involving hetero-splitting of the H-H bond was provided by Shvo and coworkers[127-131]. The Shvo catalyst is a dimeric hydrido carbonyl cyclopentadienyl ruthenium complex with a bridging hydride and an O-H-O hydrogen bond (Scheme 1.18). Structural evidence for the dimeric form was obtained from the X-ray structure determination of a single crystal of the complex $Ru_2(\mu\text{-}H)(\mu\text{-}C_5Ph_2(C_6H_4Cl)_2O\text{-}H\text{-}OC_5Ph_2(C_6H_4Cl)_2)(CO_4)$. Shvo and coworkers found that the catalyst is in equilibrium with the monomers and. The monomer is capable of hydrogenating ketones, imines or aldehydes by hydride/proton transfers, whereas the monomer can receive dihydrogen directly from $H_2$ gas or by dehydrogenation of a hydrogen donor such as quinone.

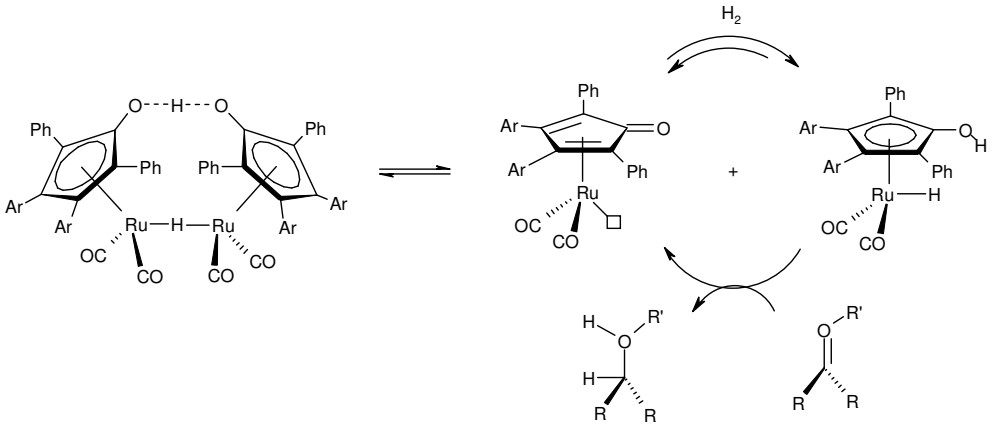


**Scheme 1.18** Shvo's catalyst

Shvo and coworkers originally proposed a mechanism where the substrate coordinates to ruthenium prior to hydrogen transfer (Scheme 1.19).

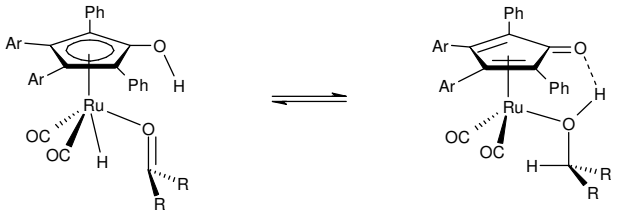

**Scheme 1.19**

In 2001, Casey and coworkers studied the deuterium isotope effects on benzaldehyde reduction by selective deuteration of the hydroxyl and the hydride positions and provided the strongest evidence for a concerted hydrogen transfer mechanism. As expected for a concerted reaction, a large kinetic isotope effect (KIE) $k_{OHRuH}/k_{ODRuD} = 3.6$ was found as approximately the product of the two individual KIE's $k_{OHRuH}/k_{OHRuD} = 1.5$ and $k_{ODRuH}/k_{ODRuH} = 2.2$, ($1.5 \times 2.2 = 3.3$)[132].

The acidity of the hydroxyl group was also determined to evaluate the role of the hydroxyl proton in the reduction of the substrate. The pKa of the hydroxyl group was calculated to be 17.5 in acetonitrile. For comparison, the pKa of phenol is 26.6 and the pKa of benzoic acid 20.7 in acetonitrile. Thus, the relatively low pKa of the hydroxyl proton would favour a hydrogen bonding interaction between the oxygen or the nitrogen atom of the substrate and would match also with the hypothesis of a concerted reaction. The following scheme shows the mechanism proposed by Casey's group (Scheme 1.20).

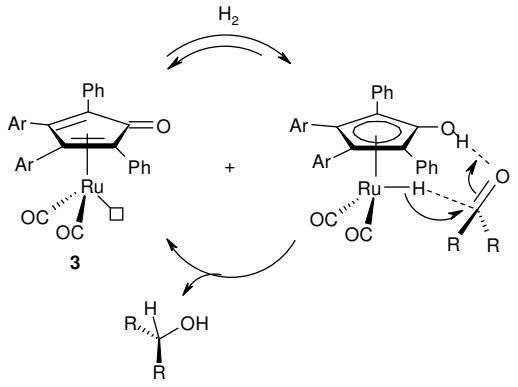

**Scheme 1.20**

During the hydrogenation step the ketone or the imine is outside the coordination sphere of the metal and interacts with the hydride in the secondary coordination sphere and the proton

of the hydroxyl group. The simultaneous transfer of the hydride and the proton to the carbonyl or the imine group leads to the formation of the coordinatively unsaturated complex [$\eta^4$-$Ph_4C_4(CO)$]$Ru(CO)_2$. The vacant site on the ruthenium allows $\eta^2$ recoordination of the dihydrogen ligand to the ruthenium. The subsequent heterolytic splitting of the H-H bond results in the formation of complex [$\eta^5$-$Ph_4C_5OH$)]$Ru(CO)_2H$.

Park and coworkers synthesized a complex similar to the monomer of the Shvo catalyst with a NH group on the cyclopentadienyl ring (Figure 1.3)[133]. This complex does not dimerize because of the the substituent on the nitrogen group. It was found to catalyze the racemization of secondary alcohols at room temperature, but attempts of the reduction of benzaldehyde were unsuccessful.

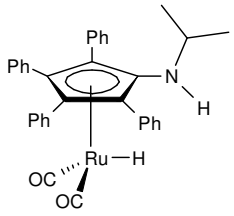


**Figure 1.3.**

Casey's group prepared the analogous complex. Reduction of benzaldehyde failed, too[134]. It was clear that the amine protons of the complexes were not acidic enough to facilitate the proton transfer. When therefore a proton source was added, reduction occurred even at low temperatures, as low as -80 °C.

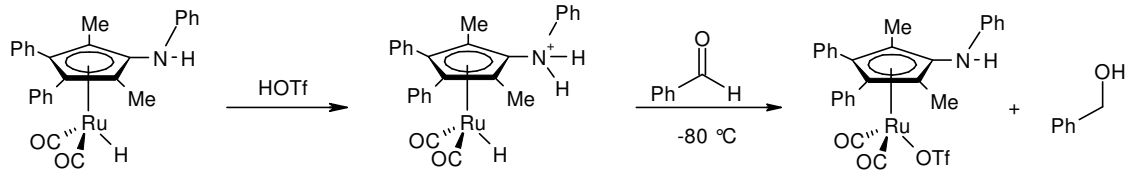


**Scheme 1.21**

## 1.6 Objective of this work

### 1.6.1 Goal

As shown in the previous chapter, the Shvo diruthenium complex dissociates into the hydroxycyclopentadienyl ruthenium hydride $[\eta^5\text{-}Ph_4C_5OH)]Ru(CO)_2H$ and the coordinatively unsaturated cyclopentadienone $[\eta^4\text{-}Ph_4C_4(CO)]Ru(CO)_2$. This system is assumed to transfer $H_2$ in form of an acidic and a hydridic hydrogen to the ketone in a concerted fashion ("Ionic Hydrogenation") (Scheme 1.22).

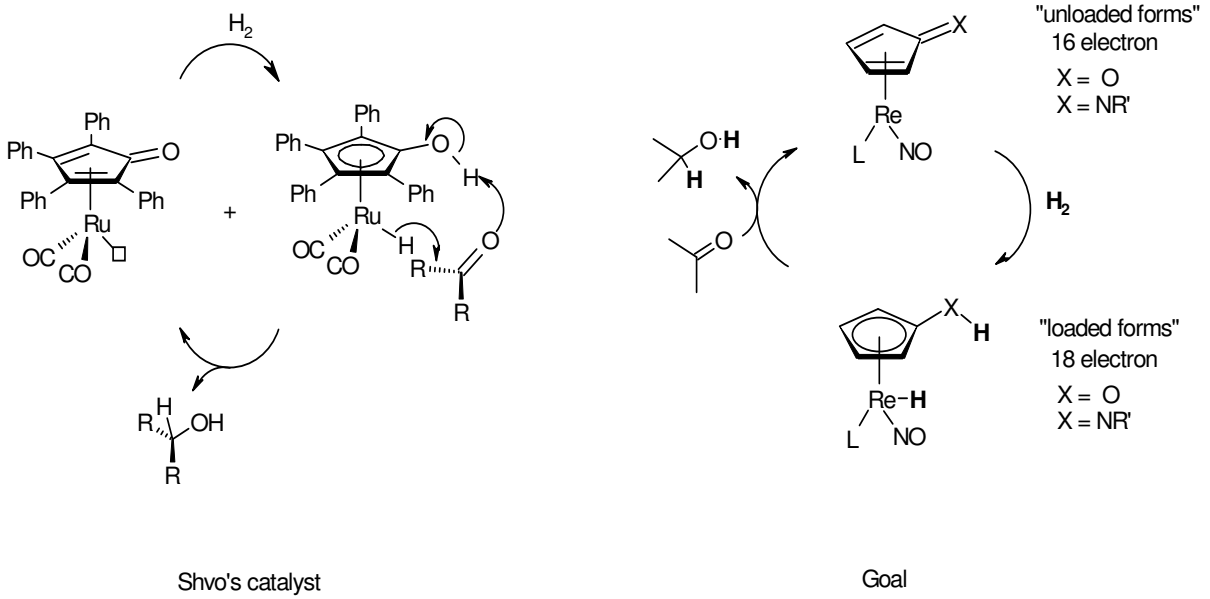


**Scheme 1.22**

We were interested in the design of a new "Ionic Hydrogenation" catalyst utilizing polar rhenium hydrides. The catalytic system involves a hydroxy or an amino cyclopentadienyl hydrido nitrosyl rhenium complex $[\eta^5\text{-}C_5H_4(XH)]Re(L)(NO)H$ (X = O, NR'), isoelectronic to the ruthenium system. This type complex bears both an acidic function and a hydride ("loaded forms"). After $H^-$ and $H^+$ transfers a corresponding cyclopentadienone or an imino nitrosyl rhenium complex $[\eta^5\text{-}C_4H_4(CX)]Re(L)(NO)H$ (X = O, NR') results ("unloaded forms"). The loaded forms are regenerated by heterolytic $H_2$ uptake.

### 1.6.2 Strategy

The target molecule is a cyclopentadienyl hydrido nitrosyl rhenium complex bearing an OH group or a NH group [$\eta^5$-$C_5H_4$(XH)]Re(CO)(NO)H (X = O, NR') (Figure 1.4).

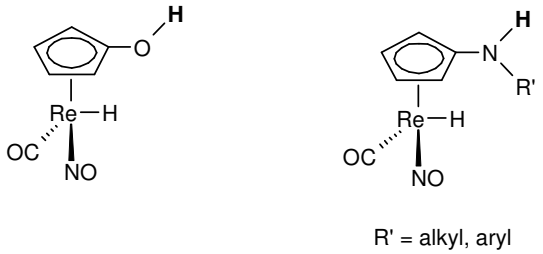


**Figure 1.4.**

We were interested in synthesizing the target molecule in a straightforward and facile way so that the synthesis does not involve complicated steps. The retrosynthetic strategy (Scheme 1.24) was based on the synthesis of the similar cyclopentadienyl hydrido nitrosyl rhenium complex ($\eta^5$-$C_5H_5$)Re(CO)$_2$(NO)H that can be prepared in two steps from ($\eta^5$-$C_5H_5$)Re(CO)$_3$ (Scheme 1.23), which reacts with nitrosonium ($NO^+$) to give the nitrosyl rhenium complex [($\eta^5$-$C_5H_5$)Re(CO)$_2$(NO)]$^+$. This nitrosyl complex under particular basic conditions can be converted into the hydrido compound ($\eta^5$-$C_5H_4$OH)Re(CO)(NO)H.

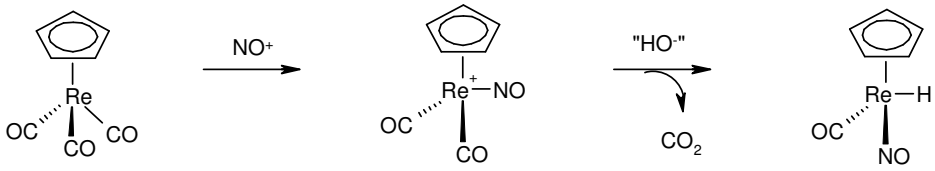


**Scheme 1.23**

Along the retrosynthesis the OH and the NH groups were protected to prevent any side reaction. For instance secondary amines react with nitrosonium required for the nitrosylation step to give nitrosamines. The preparation of hydrido rhenium complexes involves basic medium that could interact with the acidic protons of either the amine or the hydroxyl group. Thus the retrosynthesis of the complexes [$\eta^5$-$C_5H_4$(XH)]Re(CO)(NO)H (X = O, NR') starts

with the deprotection of [$\eta^5$-$C_5H_4$(XR)]Re(CO)(NO)H (X = O, NR', R = protecting group) that are obtained under basic conditions from the nitrosyl precursors [$\eta^5$-$C_5H_4$(XR)]Re(CO)$_2$(NO)]$^+$, both the products themselves of the nitrosylation of the substituted tricarbonyl rhenium complexes [$\eta^5$-$C_5H_4$(XR)]Re(CO)$_3$, which are the protected forms of the hydroxy and the amino cyclopentadienyl tricarbonyl rhenium compounds [$\eta^5$-$C_5H_4$(XH)]Re(CO)$_3$. Their preparation requires the functionalization of ($\eta^5$-$C_5H_5$)Re(CO)$_3$ with an OH or a NH group.

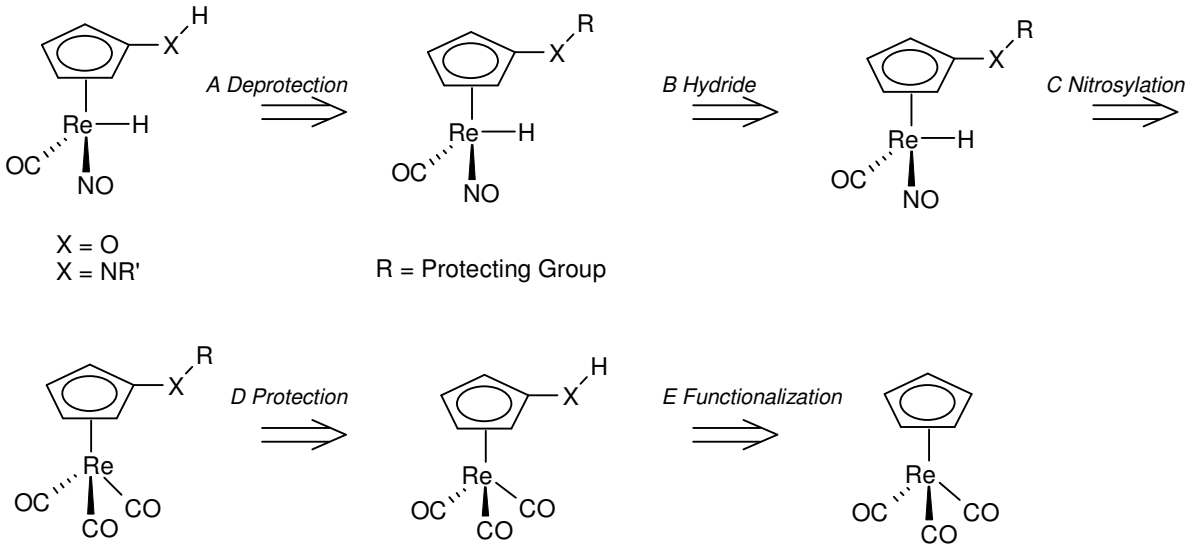


**Scheme 1.24** Retrosynthesis of the complexes [$\eta^5$-$C_5H_4$(XH)]Re(CO)(NO)H (X = O, NR')

## 1.7 References

[1] T. A. Millensifer, Rhenium and Rhenium Compounds, *Kirk-Othmer Encyclopedia of Chemical Technology*, 16 April **2001**.

[2] U.S. Patent 2,414,965 (**1947**) A. D. Melaven, J. A. Bacon.

[3] A. Sutulov, *Molybdenum and Rhenium Recovery from Porphyry Coppers*, University of Concepcion, Chile, **1970**.

[4] A. Sutulov, *Molybdenum and Rhenium* 1778–1977, University of Concepcion, Chile, **1976**.

[5] A. M. Chekmarev, I. D. Troshkina, "Rhenium Recovery from Non-Traditional Resource", in B. D. Bryskin, ed., *Rhenium and Rhenium Alloys*, TMS, **1996**.

[6] M. A. Krzhinsky, S. I Tkachenko, K. I Shmulovich, Y. A. Taran, G. S. Steinberg, *Nature* **1994**, *369*, 51.

[7] F. Habashi, "Rhenium Seventy Years Old", in B. D. Bryskin, ed., *Rhenium and Rhenium Alloys*, TMS, **1996**.

[8] V. Dolejsek and J. Heyrovsky, *Nature* **1925**, *116*, 782.

[9] F. H. Loring, J. G. F. Druce, *Chem. News* **1925**, *131*, 337.

[10] L. C. Hurd, *J. Chem. Ed.* Oct. **1933**, 605–608.

[11] K. B. Lebedev, *The Chemistry of Rhenium*, translated from the Russian by L. Ronson and A.A. Woolf, Butterworth's, London, **196**2.

[12] J. Rudolph, K. L. Reddy, P. Chiang, K. B. Sharpless, *J. Am. Chem. Soc.* **1997**, *119*, 6189.

[13] M. Nakajima, Y. Sasaki, H. Iwamoto, S. Hashimoto, *Tetrahedron lett.* **1998**, *39*, 87.

[14] D. Mandelli, C. A. Vliet, U. Arnold, R. A. Sheldon, U. Schuchardt, *J. Mol. Catal. A: Chem.* **2001**, *168*, 165.

[15] F. E. Kühn, J. Zhao, W. A. Herrmann, *Tetrahedron: Assymetry* **2005**, *16*, 3469.

[16] W. A. Herrmann, R. M. Kratzer, H. Ding, W. R. Thiel, H. Glas, *J. Organomet. Chem.* **1998**, *555*, 293.

[17] W. A. Herrmann, W. Wagner, U. N. Flessner, U. Volkhardt, H. Komber, *Angew.Chem.* 1991, *103*, 1704.

[18] A. Salameh, C. Copéret, J. M. Basset, V. P. Böhm, M. Röper, *Adv. Synth. Catal.* **2007**, *349*, 238.

[19] M. Chabanas, C. Copéret, J. M. Basset, *Chem. Eur. J.* **2003**, *9*, 971.

[20] M. Chabanas, A. Baudouin, C. Copéret, J. M. Basset, *J. Am. Chem. Soc.* **2001**, *123*, 2062.

[21] P. G. Menond, Z. Paál, *Ind. Eng. Chem. Res.* **1997**, *36*, 3282.

[22] R. Burch, *Platinum Met. Rev.***1978**, *22*, 57.

[23] M. Yang, G. Somorjai, *J. Am. Chem. Soc.* **2004**, *126*, 7698.

[24] M. F. Schneider, H. Junga, S. Blechert, *Tetrahedron* **1995**, *51*, 13003.

[25] D. A. Perry, J. C. Hemminger, *J. Am. Chem. Soc.* **2000**, *122*, 8079.

[26] M. Chabanas, A. Baudouin, C. Copéret, J. M. Basset, *J. Am. Chem. Soc.* **2001**, *123*, 2062.

[27] A. Lesage, L. Emsley, M. Chabanas, C. Copéret, J. M. Basset, *Angew. chem. Int. Ed* **2002**, *41*, 4535.

[28] A. Salameh, C. Copéret, J. M. Basset, V. P. Böhm, M. Röper, *Adv. Synth. Catal.* **2007**, *349*, 238.

[29] M. Chabanas, C. Copéret, J. M. Basset, *Chem. Eur. J.* **2003**, *9*, 971.

[30] G. Wang, A. Jimtaisong, R. L. Luck, *Organometallics* **2004**, *23*, 4522.

[31] S. Bellemin-Laponnaz, J . P Le Ny, J. A. Osborn, *Tetrahedron lett.* **2000**, *41*, 1549.

[32] G. B. Kauffman, *Platinum Met. Rev.* **1999**, *43*, 122.

[33] P. M. D. Collins, *Platinum Met. Rev.* **1986**, *30*, 141.

[34] P. Sabatier, J. B. Senderens, *Annales de Chimie et de Physique* **1905**, *4*, 335.

[35] P. Sabatier, J. B. Senderens, *Comptes Rendus de l'Académie des Sciences* **1902**, *134*, 689.

[36] P. Sabatier, Nobel Lecture 1912, *Nobel Lectures 1922-1941,* Elsevier Publishing Company, Amsterdam, **1966**.

[37] P. J. Lunde, *Industrial and Engineering Chemistry Process Design and Development* **1974**, *13*, 226.

[38] P. J. Lunde, F. L. Kester, *Industrial and Engineering Chemistry Process Design and Development* **1974**, *13*, 27.

[39] F. Haber, Nobel Lecture 1920, *Nobel Lectures 1901-1921, Elsevier Publishing Company, Amsterdam,* **1966**.

[40] C. Bosh, Nobel Lecture 1932, *Nobel Lectures 1922-1941, Elsevier Publishing Company, Amsterdam,* **1966**.

[41] B. E. Smith, *Science* **2002**, *297*, 1654.

[42] M. D. Fryzuk, *Nature* **2004**, *427*, 498-

[43] V. Smil, *Nature* **1999**, *400*, 415.

[44] Z. Kowalczyk, S. Jodiz, J. Sentek, *Appl. Catal., A* **1996**, *138*, 83.

[45] *German Patent 293,787*, assigned to BASF, granted March 8, **1913**.

[46] F. Fischer and H. Tropsh, *German Patent 484,337*, granted to the inventors July 22, **1925**, made public on October 3, 1929.

[47] H. Pichler, *Adv. Catal.* **1952**, *4*, 271.

[48] M. A. Vannice, *J. Catal.* **1975**, *37*, 449.

[49] R. C. Reuel, C. H. Bartholoew, *J. Catal.* **1984**, *85*, 63.

[50] R. C. Reuel, C. H. Bartholoew, *J. Catal.* **1984**, *85*, 78.

[51] C. H. Bartholomew, *Catal. Lett.s* **1990**, *7*, 27.

[52] B. G. Johnson, C. H. Bartholomew, D. W. Goodman, *J. Catal.* **1991**, *128*, 231.

[53] G. W. Hubert, S. J. M. Butala, M. L. Lee, C. H. Bartholomew, *Catal.s Lett.* **2001**, *74*, 45.

[54] G. W. Hubert, C. H Bartholomew, *Studies on Surface Science and catalysis* **2001**,*136*, 283.

[55] G. W. Hubert, C. G. Guymon, T. L. Conrad, B. C. Stephenson, C. H. Bartholomew, *Studies on Surface Science and catalysis* **2001**,*139*, 423.

[56] H. D. Burtron, M. Occelli, *Studies on Surface Science and catalysis* **2007**, *163*.

[57] E. Iglesia, *Appl. Catal.*1997, *161*, 59.

[58] D. Evans, J. A. Osborn, g. Wilkinson, *J. Chem. Soc. A: Inorganic, Physical, Theoretical* **1968**, 3133.

[59] B. Cornils, E. G. Kuntz, *J. Organomet. Chem.* **1995**, *502*, 177.

[60] B. Cornils, W. A. Herrmann (eds), *Applied Homogeneous Catalysis with Organometallic Compounds Part 1+2*, VCH, Weinheim **1996**.

[61] B. Cornils, W. A. Herrmann (eds), *Aqueous-Phase Organometallic Catalysis*, VCH, Weinheim **1996**.

[62] B. Cornils, W. A. Herrmann, M. Rasch, *Angew. chem.* **1994**, *33*, 2144.

[63] G. Wilkinson Nobel Lecture 1973, *Nobel Lectures, Chemistry 1971-1980*, Tore Frängsmyr, Sture Forsén, World Scientific Publishing Co., Singapore, **1993**.

[64] J. A. Osborn, F. H. Jardine, J. F. Young, G. Wilkinson, *J. Chem. Soc. A* **1966**, *1711*.

[65] C. O'Connor, G. Yagupsky, D. Evans, G. Wilkinson, *Chemical Communications (London)* **1968**, 420.

[66] D. Evans, J. A. Osborn, G. Wilkinson, *J. Chem. Soc. A* **1968**, 3133.

[67] R. Crabtree, *Acc. Chem. Res.* **1979**, *12*, 331.

[68] W. S. Knowles Nobel Lecture 2001, *Nobel Lectures, Chemistry 1971-1980*, Tore Frängsmyr, Stockholm, **2002**.

[69] W. S Knowles, J. Sabacky, *Chem. Commun.s* 1**968**, 1445.

[70] *Chem. Eng. News* **1970**, 40.

[71] L. Horner, H. Siegel, H. Büthe, *Angew. chem. Int. Ed.* **1968**, *7*, 942.

[72] T. P. Dang, H. B. Kagan, *Chemi. Commun.* **1971**, 481.

[73] B. D. Vineyard, W. S. Knowles, M. J. Sabacky, G. L. Bachman, D. J. Weinkauff, *J. Am. Chem. Soc.* **1977**, *99*, 5946.

[74] A. Miyashita, A. Yasuda, H. Takaya, K. Toriumi, T. Ito, T. Souchi, R. Noyori, *J. Am. Chem. Soc.* **1980**, *102*, 7932.

[75] H. Brunner, *Top. Stereochem.*, E. L. Eliel, N. Y. **1988**, *18*, 129.

[76] M. J. Burk, J. E. Feaster, W. A. Nugent, R. L. Harlow, *J. Am. Chem. Soc.* **1993**, *115*, 10125.

[77] A. Togni, C. Breutel, A. Schnyder, F. Spindler, H. Landert, A. Tijani, *J. Am. Chem. Soc.* **1994**, *116*, 4062.

[78] F. Robin, F. Mercier, L. Ricard, F. Mathey and M. Spagnol, *Chem. Eur. J.* **1997**, *8*, 1365.

[79] F. Mathey, M. Spagnol, F. Mercier, F. Robin, V. Mouries, *United States Patent 6521795*.

[80] H. B. Kagan, *Bull. Soc. Chim. Fr.,* **1988**, 846.

[81] W. S. Knowles, *Acc. Chem. Res.* **1983**, *16*, 106.

[82] R. Noyori, Nobel Lecture 2001, *The Nobel Prizes 2001*, Tore Frängsmyr, Stockholm, **2002**.

[83] R. Noyori, T. Ohkuma, M. Kitamura, H. Takaya, N. Sayo, H. Kumobayashi, S. Akutagawa, *J. Am. Chem. Soc.* **1987**, *109*, 5856.

[84] M. Kitamura, M. Tokunaga, T. Ohkuma, R. Noyori, *Tetrahedron lett.* **1991**, *32*, 4163.

[85] B. Heiser, E. A. Broger, Y. Crameri, *Tetrahedron: Asymmetry* **1991**, *2*, 51.

[86] Steven A. King, Andrew S. Thompson, Anthony O. King, Thomas R. Verhoeven, *J. Org. Chem.* **1992**, *57*, 6689.

[87] J. P. Genêt, V. Ratovelomanana-Vidal, M. C. Caño de Andrade, X. Pfister, P. Guerreiro, J. Y. Lenoir, *Tetrahedron lett.* **1995**, *36*,4801.

[88] I. Gautier, V. Ratovelomanana-Vidal, P. Savignac, J. P. Genêt, *Tetrahedron lett.* **1996**, *37*, 7721.

[89] P. Bertus, P. Phansavath, V. Ratovelomanana-Vidal, J. -P. Genêt, A. R. Touati, T. Homri, B. Ben Hassine, J. Y. Lenoir, *Tetrahedron: Asymmetry* **1999**, *10*,1369.

[90] R. H. Crabtree, H. Felkin, G. E. Morris, *J. Organomet. Chem.* **1977**, *141*, 205.

[91] R. Crabtree, *Acc. Chem.l Res.* **1979**, *12*, 331.

[92] S. P. Smidt, A. Pfaltz, E. Martínez-Viviente, P. S. Pregosin, A. Albinati, *Organometallics* **2003**, *22*, 1000.

[93] a) K. Källström, I. Munslow, P. G. Anderson, *Chem. Eur. J.* **2006**, *12*, 3194.

[94] J. Halpern, *Science* **1982**, *217*, 401.

[95] S. Feldgus, C. R. Landis., *J. Am. Chem. Soc.* **2000**, *122*, 12714.

[96] J. S. M. Samec, J. E. Bäckvall, P. G. Andersson, P. Brandt, *Chem. Soc. Rev.* **2006**, 35, 237.

[97] S. E. Clapham, A. Hadzovic, R. H. Morris, *Coord. Chem. Rev.* **2004**, *248*, 2201.

[98] T. Ohkuma, H. Ooka, S. Hashiguchi, T. Ikariya, R. Noyori, *J. Am. Chem. Soc.* **1995**, *117*, 2675.

[99] R. Noyori, T. Ohkuma, *Angew. chem. Int.l Ed.* 2001, *40*, 40.

[100] R. Noyori, *Angew. chem. Int. Ed.* **2002**, *41*, 2008.

T. Ohkuma, H. Doucet, T. Pahm, K Mikami, T. Korenaga, M. Terada, R. Noyori, *J. Am. Chem. Soc.* **1998**, *120*, 1086.

[101] H. Doucet, T. Ohkuma, K. Murata, T. Yokozawa, M. Kozawa, E. Katayama, A.F. England, T. Ikariya, R. Noyori, *Angew. chem. Int. Ed.* **1998**, *37*, 1703.

[102] T. Ohkuma, M. Koizumi, H. Doucet, T. Pham, M. Kozawa, K. Murata, E. Katayama, T. Yokozawa, T. Ikariya, R. Noyori, *J. Am. Chem. Soc.* **1998**, *120*, 13529.

[103] T.Ohkuma, R. Noyori, in: E.N. Jacobs, A. Pfaltz, H. Yamamoto (Eds.), *Comprehensive Asymmetric Catalysis*, vol. 1, Springer, Berlin, **1999** (Chapter 6.1).

[104] T. Ohkuma, M. Kitamura, R. Noyori, in: I. Ojima (Ed.), *Catal. Asym. Synth.*, *second ed*., Wiley VCH, New York, **2000** (Chapter 1).

[105] T. Ohkuma, D. Ishii, H. Takeno, R. Noyori, *J. Am. Chem. Soc.* **2000**, *122*, 6510.

[106] T. Ohkuma, M. Koizumi, H. Ikehira, T. Yokozawa, R. Noyori. *Org. Lett.* **2000**, *2*, 659.

[107] K. Mikami, T. Korenaga, T. Ohkuma, R. Noyori, *Angew. chem. Int. Ed.* **2000**, *39*, 3707.

[108] R. Noyori, M. Yamakawa, S. Hashiguchi, *J. Org. Chem.* **2001**, *66*, 7931.

[109] T. Ohkuma, M. Koizumi, K. Muñiz, G. Hilt, C. Kabuto and R. Noyori, *J. Am. Chem. Soc.* **2002**, *124*, 6508.

[110] C.A. Sandoval, T. Ohkuma, K. Muñiz, R. Noyori, *J. Am. Chem. Soc.* **2003**, 125, 13490.

[111] K. Abdur-Rashid, A.J. Lough and R.H. Morris, *Organometallics* **2001**, *20*, 1047.

[112] O.M. Akotsi, K. Metera, R.D. Reid, R. McDonald, S.H. Bergens, *Chirality* **2000**, *12*, 514.

[113] M.J. Burk, W. Hems, D. Herzberg, C. Malan, A. Zanotti-Gerosa, *Org. Lett.* **2000**, *2*, 4173.

[114] G.-J. Deng, Q.-H. Fan, X.-M. Chen, G.-H. Liu, *J. Mol. Catal. A: Chem.* **2003**, *193*, 21.

[115] E. Lindner, S. Al-Gharabli, H.A. Mayer, *Inorg. Chim. Acta* **2002**, *334*, 113.

[116] E. Lindner, S. Al-Gharabli, I. Warad, H.A. Mayer, S. Steinbrecher, E. Plies, M. Seiler, H. Bertagnolli, *Z. Anorg. Allg. Chem.* **2003**, *629*, 161.

[117] E. Lindner, H.A. Mayer, I. Warad, K. Eichele, *J. Organomet. Chem.* **2003**, 665, 176.

[118] E. Lindner, I. Warad, K. Eichele, H.A. Mayer, *Inorg. Chim. Acta*, **2003**, *350*,. 49.

[119] K. Mikami, T. Korenaga, Y. Yusa, M. Yamanaka, *Advanced Synthesis and Catalysis,* **2003**, *345*, 246.

[120] J.-H. Xie, L.-X. Wang, Y. Fu, S.-F. Zhu, B.-M. Fan, H.-F. Duan and Q.-L. Zhou, *J. Am. Chem. Soc.* **2003**, *125*, 4404.

[121] C. Bianchini and P. Barbaro, *Top. Catal.* **2002**, *19*, 17.

[122] K. Abdur-Rashid, A. L. Lough, R. H. Morris, *Organometallics* **2001**, *20*, 1047.

[123] C. J. Cobley, J. P. Henschke, *Adv. Synth. Catal.* **2003**, *345*, 195.

[124] K. Abdur-Rashid, M. Faatz, A. J. Lough, R. H. Morris, *J. Am. Chem. Soc.* **2001**, *123*, 7473.

[125] K. Abdur-Rashid, S. E. Claphan, A. Hadzovic, J. N. Harvey, A. J. Lough, R. H. Morris, *J. Am. Chem. Soc.* **2002**, *124*, 15104.

[126] K. Abdur-Rashid, A. J. Lough, R. H. Morris, *Organometallics* **2000**, *19*, 2655.

[127] Y. Blum, D. Czarkie, Y. Rahamim, Y. Shvo, *Organometallics* **1985**, *4*, 1459.

[128] Y. Shvo, D. Czarkie, Y. Rahamim, *J. Am. Chem. Soc.* **1986**, *108*, 7400.

[129] C. P. Casey, T. E. Vos, G. A. Bikzhanova, J. E. Bäckvall, L. Johansson, J. Park, Y. H. Kim, *Organometallics* **2002**, *21*, 1955.

[130] C. P. Casey, T. E. Vos, G. A. Bikzhanova, *Organometallics* **2003**, *22*, 901.

[131] A. H. Éll, J. B. Johnson, J. E. Bäckvall, *Chem. Commun.* **2003**, 1652.

[132] C. P. Casey, S. W. Singer, D. R. Powell, R. K. Hayashi, M. Kavana, *J. Am. Chem. Soc.* **2001**, *123*, 1090.

[133] J. H. Choi, Y. K. Choi, Y. H. Kim, E. S. Park, E. J. Kim, M. J. Kim, J. Park, *J. Org. Chem.* **2004**, *69*, 1972.

[134] C. P. Casey, T. E. Vos, S. W. Singer, I. A. Guzei, *Organometallics* **200**2, *21*, 5038.

# 2 Preparation of ($\eta^5$-Hydroxycyclopentadienyl)(tricarbonyl)rhenium

## 2.1 Introduction

Previously we elaborated a synthetic route for the preparation of the target molecule ($\eta^5$-$C_5H_4OH)Re(CO)_2(NO)H$ (Scheme 2.1). The first step of the synthetic pathway to ($\eta^5$-$C_5H_4OH)Re(CO)(NO)H$ consists of the OH functionalization of the rhenium coordinated cyclopentadienly moiety of ($\eta^5$-$C_5H_5)Re(CO)_3$ to give of ($\eta^5$-$C_5H_4OH)Re(CO)_3$.

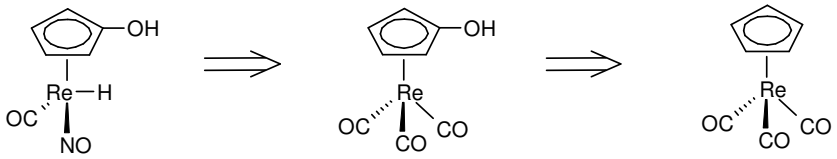


**Scheme 2.1** First step of the retrosynthesis to the hydrido complex 5

In this chapter the preparation of ($\eta^5$-hydroxycyclopentadienyl)(tricarbonyl)rhenium ($\eta^5$-$C_5H_4OH)Re(CO)_3$ will be reported. After a short overview over the literature to this complex, a new and efficient route is presented. The new route applies dioxybis(trimethylsilane) $(Me_3SiO)_2$ as an excellent hydroxylating agent for metal coordinated cyclopentadienyl rings.

## 2.2 Literature

### 2.2.1 Rhenabenzene as intermediate for the preparation of ($\eta^5$-1,3-diphenyl-2-hydroxy-cyclopentadienyl)(tricarbonyl)rhenium

In 1985, R. Ferede and coworkers reported the preparation of ($\eta^5$-1,3-diphenyl-2-hydroxy-cyclopentadienyl)(tricarbonyl)rhenium [$\eta^5$-$Ph_2C_5H_2(OH)]Re(CO)_3$[1]. Reaction of (E,E)-1,4-dilithium-1,4-diphenyl-1,3-butadiene with bromo(tetracarbonyl)(triphenylphosphine)rhenium $(CO)_4PPh_3ReBr$[2] followed by protonation gave ($\eta^1$-4-lithium-1,4-diphenyl-1,3-butadienyl)rhenium, leading after cyclisation to formation of rhenabenzene. Subsequent

reductive elimination and loss of triphenyl phosphine generates [$\eta^5$-$Ph_2C_5H_2(OH)$]$Re(CO)_3$ (Scheme 2.2).

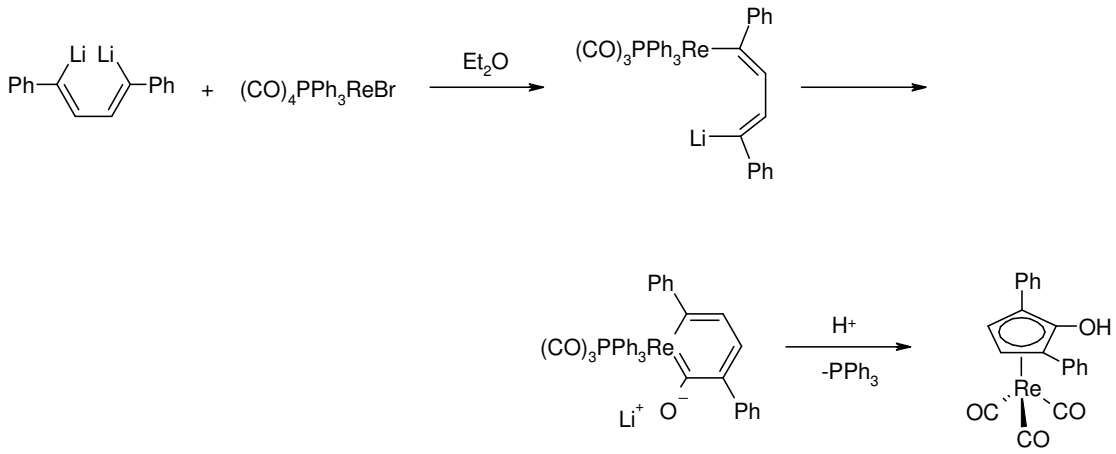


**Scheme 2.2**

This method was tested in our laboratory and the expected product was obtained with a yield of 20% vs 84 % reported in the literature[1].

### 2.2.2 A three-component-preparation of ($\eta^5$-hydroxycyclopentadienyl)(tricarbonyl)-rhenium

Another remarkable procedure was developed by A. Katzenellenbogen and coworkers in 1998[4,5,6]. Their preparation of ($\eta^5$-hydroxycyclopentadienyl)(tricarbonyl)rhenium ($\eta^5$-$C_5H_4OH)Re(CO)_3$ involves three components, the rhenium complex $(Et_4N)_2[ReBr_3(CO)_3]$, diazocyclopentadiene $(C_5H_4)N_2$ and a nucleophile (halide or carboxylates anions). The insertion reactions of $(C_5H_4)N_2$ with pentacarbonylrhenium halides $XRe(CO)_5$ for the preparation of halogen substituted complexes ($\eta^5$-$C_5H_4X)Re(CO)_3$ was already reported, but the use of pentacarbonyl precursors required long reaction times with refluxing benzene to obtain ($\eta^5$-bromocyclopentadienyl)(tricarbonyl)rhenium ($\eta^5$-$C_5H_4Br)Re(CO)_3$ or ($\eta^5$-iodoyclo-pentadienyl)tricarbonyl)rhenium ($\eta^5$-$C_5H_4I)Re(CO)_3$. A. Katzenellenbogen was able to enhance the reactivity of the starting material using another precursor prepared by R. Alberto and coworkers. Alberto's complex $(Et_4N)_2[ReBr_3(CO)_3]$[7-9] reacted in an even more facile

fashion with the diazocyclopentadiene $(C_5H_4)N_2$ and afforded $(\eta^5\text{-}C_5H_4Br)Re(CO)_3$ (26) [10] in a good yield of 62 % after 45 min at 80 °C (Scheme 2.3).

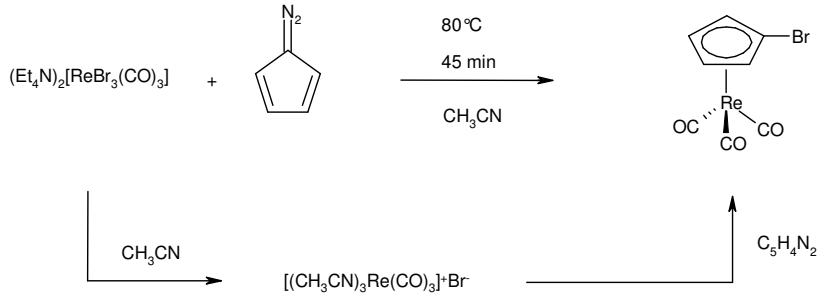


**Scheme 2.3**

The authors also prepared the triflate complex $[(CH_3CN)Re(CO)_3]^+TfO^-$ by the reaction of $(Et_4N)_2[ReBr_3(CO)_3]$ with silver triflate AgOTf (Scheme 2.4). The triflate anion very often is a non-coordinating counteranion and a poor nucleophile and it therefore allows the introduction of an external nucleophile replacing the triflate substituent in the Cp ring. Reaction of potassium acetate with $(C_5H_4)N_2$ and the triflate complex $[(CH_3CN)Re(CO)_3]^+TfO^-$ gave $(\eta^5\text{-}C_5H_4OCOCH_3)Re(CO)_3$, which led after hydrolysis to the desired complex $(\eta^5\text{-}C_5H_4OH)Re(CO)_3$.

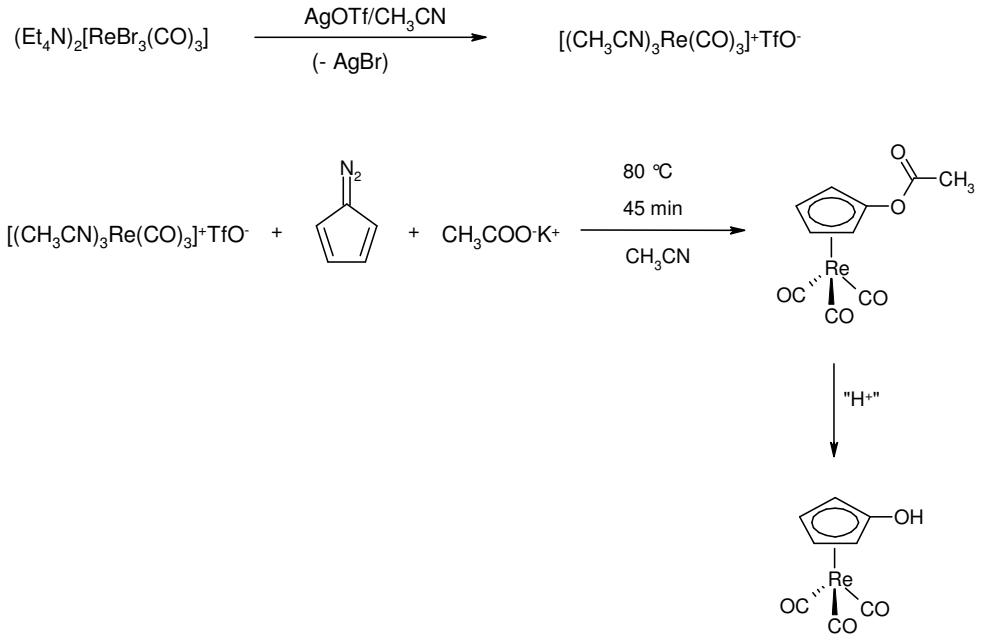


**Scheme 2.4**

This method has been tested but only a few tens of milligrams of ($\eta^5$-$C_5H_4OH$)$Re(CO)_3$ was obtained with 30 % yield compared with the given yield of 62 % in the literature. There is still another disadvantage of this route, the preparation of $(C_5H_4)N_2$ is a long and delicate procedure[11]. $(C_5H_4)N_2$ is an unstable compound at room temperature, higly explosive[12] in pure form and must be kept in solution at low temperature (-78°C). Another complication is that the concentration of the solution has to be determined for each preparative batch by adding a known amount of the dissolved compound to an ethereal solution containing excess of triphenyl phosphine. The concentration is calculated from the weighed adduct $(C_5H_4)N_2.PPh_3$[13] which crystallizes from solution.

Although A. Katzenellenbogen's procedure seems ingenious in its chemical pathway, it is impractical especially in large scale preparations which principally imply reagents easy to access and to handle.

### 2.2.3 Electrophilic hydroxylation of the rhenium coordinated cyclopentadienyl ligands

Electrophilic hydroxylation of arenes was first reported by M. Taddei and coworkers. In 1985[14] they described a simple method to obtain phenols from arene compounds. In such procedures dioxybis(trimethylsilane)[15-21] $(Me_3SiO)_2$ was used as a hydroxylating agent. The reaction of $(Me_3SiO)_2$ with aryl lithium gave trimethylsilyloxy derivatives $ROSiMe_3$ (Table 2.1). Then the trimethylsilyloxy derivatives $ROSiMe_3$ were desilylated with a solution of methanol and hydrochloric acid to afford the corresponding phenols ROH. Indeed the trimethyl silyl group is very suitable as a hydroxyl protecting group and is labile in slightly acidic solutions. But when heterocyclic compounds were used as starting materials the reaction led to trimethylsilyl derivatives $RSiMe_3$.

As shown in Table 2.1, the aryl lithium compounds ArX (Entry 1, 2, 3) gave the alcohols ROH with the excepted regioselectivity by electrophilic hydroxylation. But furan and tiophene (Entry 4, 5) furnished the corresponding trimethylsilyl derivatives $RSiMe_3$. This observation was also reported by S. Florio and coworkers in 1989[15].

**Table 2.1** Electrophilic hydroxylation of various arene compounds with $(Me_3SiO)_2$.

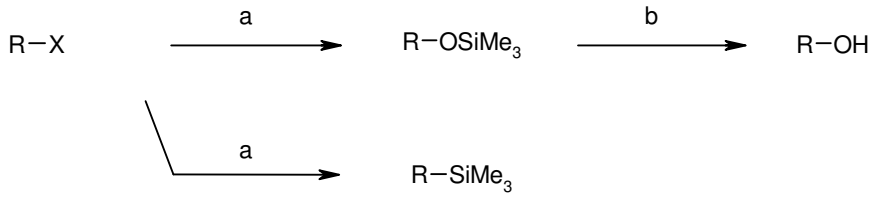


| Entry | R | X | Product | Yield (%) |
|---|---|---|---|---|
| 1 |  | Br | ROH | 86 |
| 2 |  | Br | ROH | 83 |
| 3 | 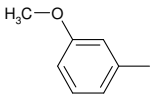 | Br | ROH | 88 |
| 4 | 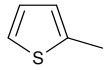 | H | $RSiMe_3$ | 40-70 |
| 5 | 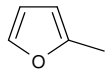 | H | $RSiMe_3$ | 40-70 |

1) nBuLi, THF, -78°C, 30min; 2) $(Me_3SiO)_2$, THF; (b) HCl, MeOH, rt

Dioxybis(trimethylsilane) $(Me_3SiO)_2$ can be used as an appropriate synthetic equivalent of the $[Me_3SiO]^+$ cation and in a more extended view as a good synthetic equivalent of the cation $HO^+$. It was applied successfully in the preparation of phenols from arenes, even though in the case of heterocyclic compounds, a different pathway may be seen leading to trimethyl silyl derivatives.

## 2.3 Strategy

In the search for a new route to hydroxylation of **1**, electrophilic hydroxylation with dioxybis(trimethylsilane) $(Me_3SiO)_2$ appeared to be a suitable method. The synthon type cation $[Me_3SiO]^+$ looked very intriguing for me. The rhenium coordinated cyclopentadienyl ring of **1** behaves as an aromatic moiety possessing similar features in comparison with the

arene group. In particular, ($\eta^5$-$C_5H_5$)$Re(CO)_3$ reacts with butyl lithium to give the nucleophilic lithium salt ($\eta^5$-$C_5H_4Li$)$Re(CO)_3$ which can react with halogens to give the corresponding substituted derivatives[22-24]. As shown in Scheme 2.5 ($\eta^5$-$C_5H_4Li$)$Re(CO)_3$ reacts with $I_2$ to produce the iodo derivative ($\eta^5$-$C_5H_4I$)$Re(CO)_3$ or $Br_2$ to give the bromo derivative ($\eta^5$-$C_5H_4Br$)$Re(CO)_3$.

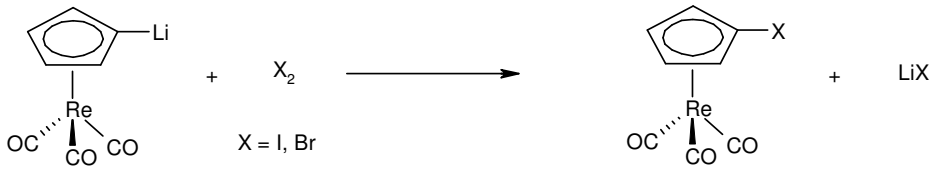


**Scheme 2.5**

Since related to Taddei's work deprotonation of ($\eta^5$-$C_5H_5$)$Re(CO)_3$ with a lithium base leads to formation of the lithium derivative ($\eta^5$-$C_5H_4Li$)$Re(CO)_3$, addition of $(Me_3SiO)_2$ to ($\eta^5$-$C_5H_4Li$)$Re(CO)_3$ was expected to afford ($\eta^5$-$C_5H_4OSiMe_3$)$Re(CO)_3$ and ($\eta^5$-$C_5H_4OH$)$Re(CO)_3$ after treatment with a solution of an acid (Scheme 2.6).

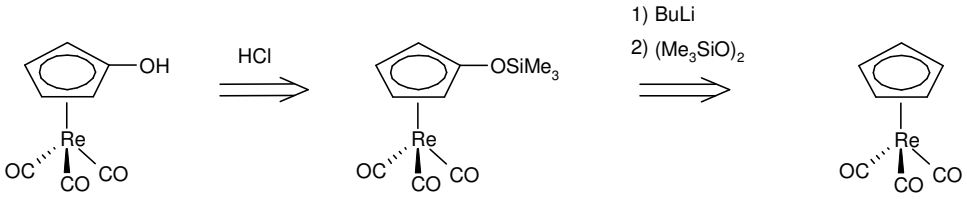


**Scheme 2.6** Retrosynthesis of **16**

## 2.4 Preparation of ($\eta^5$-$C_5H_4OH$)$Re(CO)_3$ (6).

### 2.4.1 Electrophilic hydroxylation of lithium ($\eta^5$-cyclopentadienyl)(tricarbonyl)rhenium with dioxybis(trimethylsilane).

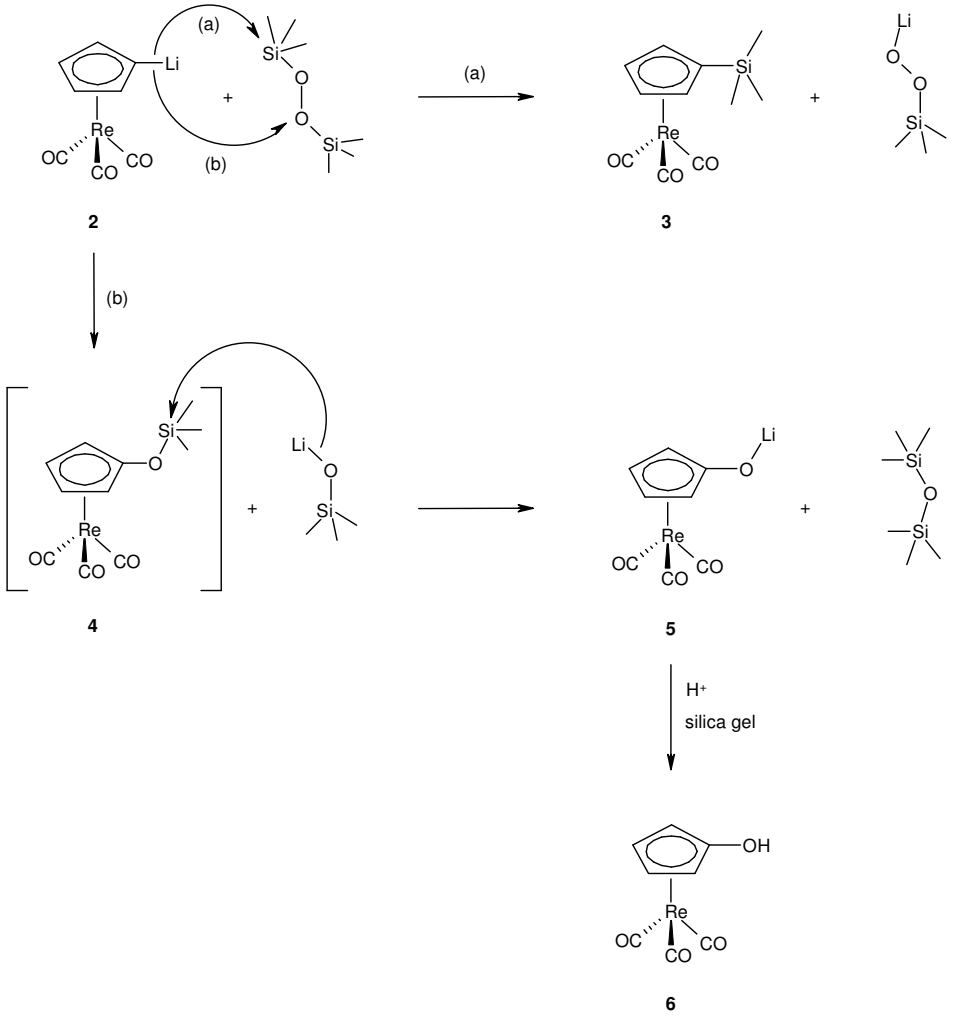


**Scheme 2.7**

($\eta^5$-Cyclopentadienyl)(tricarbonyl)rhenium (**1**) was deprotonated with 1.2 equivalents of *n*-butyllithium in THF (Scheme 2.7). *n*-Butyllithium was added drop wise to the solution of **1** in THF at low temperature (-78°C). After addition, the solution became slightly yellow. The reaction was followed by $^1$H NMR to assure that the deprotonation of **1** was complete. The singlet corresponding to **1** at 5.48 ppm disappeared. Two new triplets signals were observed at 5.38 and 4.78 ppm. These two triplets were assigned to the protons of the $C_5H_4$ ring of lithium

($\eta^5$-cyclopentadienyl)(tricarbonyl)rhenium (**2**). In $^{13}C$ NMR spectrum, **2** displayed two signals at 88.5 and 93.0 ppm. The $^{1}H$, $^{13}C$ correlation (HSQC) indicates that these two resonances correspond to the carbon atoms of the $C_5H_4$ ring in proximal and distal positions of the lithium substituent (Figure 2.1). In the $^{7}Li$ NMR spectrum, only one signal was observed at 0.93 ppm.

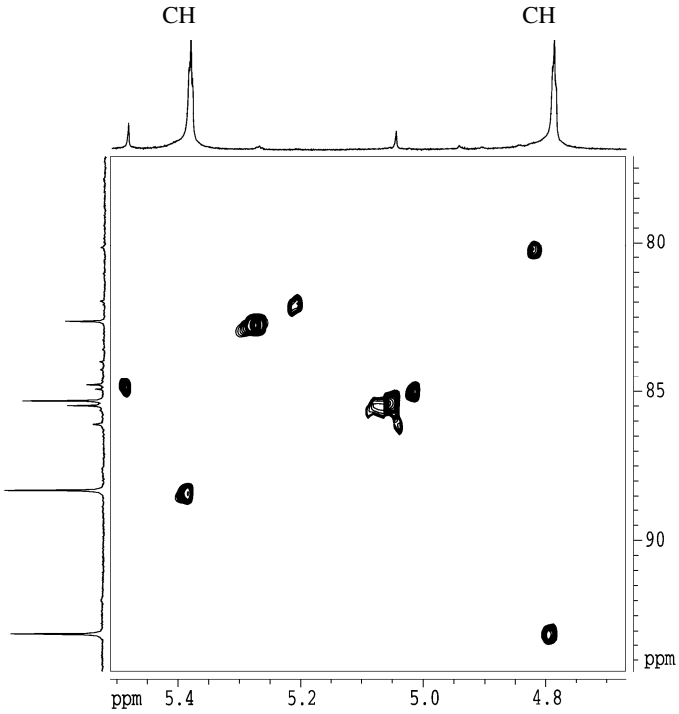


**Figure 2.1**. $^{1}H$,$^{13}C$ correlation (HSQC) spectrum of **2** in THF-$d_8$ at 20 °C

Once the full deprotonation to generate **2** had been assured by $^{1}H$ and $^{7}Li$ NMR spectroscopy, 1 equivalent of dioxybis(trimethylsilane) $(Me_3SiO)_2$ was added to the mixture at low temperature and then the mixture was slowly warmed up to room temperature (Scheme 2.7). The yellow solution turned to orange and then to brown. After stirring overnight the solvent was removed *in vacuo*.

Addition of ether to the crude reaction mixture revealed a white precipitate, which was filtered off and dried *in vacuo* to give the lithium salt **5**. The ethereal layer was collected and removal of the solvent afforded **3**. The structure of **5** was revealed by a single crystal X-ray

diffraction study and it was confirmed by $^{1}H$, $^{13}C$ NMR, IR and mass spectroscopy. The elemental analysis of crystals of **5** revealed that **5** contained two molecules of water.

When the crude reaction mixture was chromatographed on silica gel, we obtained the products **3** and **6** in 45 and 40 % respectively. Formation of **3** was explained by protonation of **5** on the slightly acidic silica gel. **3** and **6** were identified by $^{1}H$, $^{13}C$ NMR, IR and mass spectroscopy and their composition was confirmed by elemental analysis. Recrystallization of **6** could be effected from a mixture dichloromethane/pentane (2:1) and yielded colorless crystals. A single crystal X-ray diffraction study confirmed the structure of **6**.

Given that ($\eta^5$-$C_5H_4OLi$)$Re(CO)_3$ (**5**) is a salt and ($\eta^5$-$C_5H_4SiMe_3$)$Re(CO)_3$ (**3**) can be sublimed easily, these two products could also be separated in a sublimation apparatus at 150°c *in vacuo*. Sublimed **3** grew as thin needles. The lithium salt **5** remained at the bottom of the flask and could thus be easily collected and used without any further purification for the preparation of **6**. The lithium salt **5** was then protonated in an aqueous solution of hydrochloric acid in dichloromethane. The organic layer was extracted with ether and filtered. Evaporation of the ethereal filtrate gave **6** in a yield over 96 %.

The formation of **5** and **3** can be explained by nucleophilic attack of **2** at the O-O bond of $(Me_3SiO)_2$ to give **4**. Splitting of the O-O occurs with formation of a new carbon-oxygen bond. **4** is then attacked at silicon by the silyloxy lithium salt $Me_3SiO^-Li^+$ to give the lithium oxido derivative **5** and hexamethyldisiloxane $(Me_3Si)_2O$ which is thermodynamically very stable. The formation of **3** is explained by silicon attack of **2** to the peroxide $(Me_3SiO)_2$.

According to Tadei's work, heteroatoms in the aromatic ring influence the direction of the nucleophilic attack. In the case of aryl lithium, the nucleophilic attack is oriented to the O-O bond whereas in the case of heterocycle or in the case of **2** the attack is oriented to the Si atom. The hetero atoms or the metal is directly involved in the nucleophilicity. These examples tend to show that the presence of electron withdrawing moieties are favorable to the nucleophilic attack at the silicon.

### 2.4.2 Characterization of compounds 3, 5 and 6

The $^{1}H$ NMR of **3** in $CDCl_3$ displays two triplets at 5.40 and 5.43 ppm assigned to the protons of the rhenium coordinated $C_5H_4$ group. In fact two doublets of doublets could be theoretically expected. The distance H1-H3 is larger than H1-H2 but the angle between H1 and H3 is about 180°, which induces a coupling similar to H1-H2. The trimethyl silyl group was identified by a singlet at 0.24 ppm (Figure 2.3).

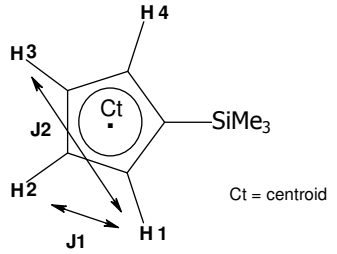


**Figure 2.2**. $^{1}H$ NMR couplings of **3**

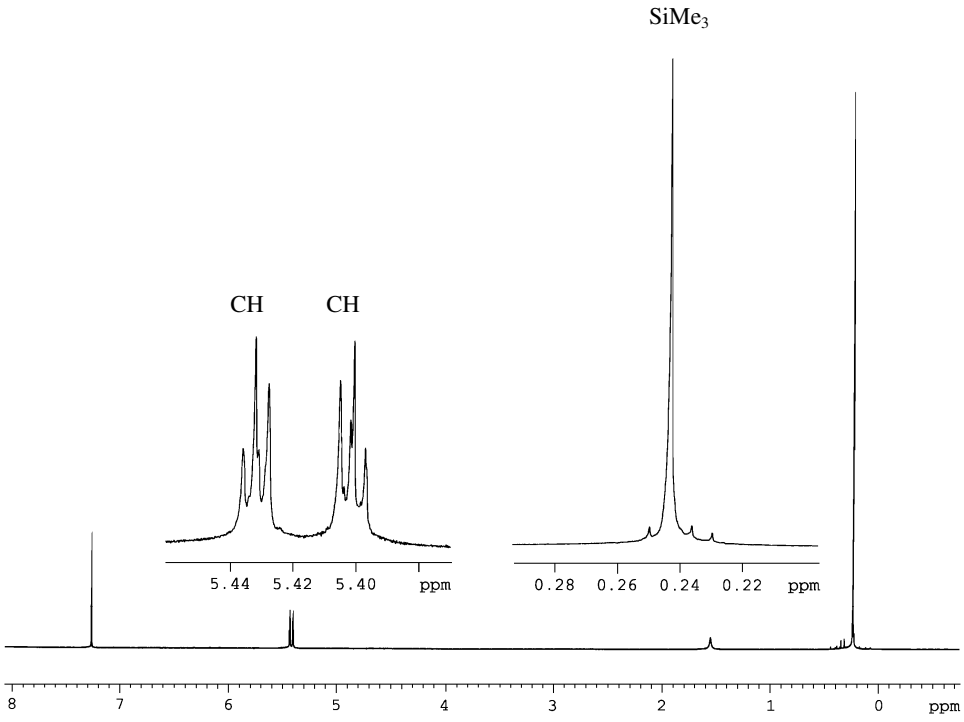


**Figure 2.3.** $^{1}H$ NMR spectrum of **3** in chloroform-d at 20 °C

The $^{1}H$ NMR spectrum of **6** showed in two triplets at 5.02 and 5.10 ppm (Figure 2.4). The $^{13}C$ NMR of **6** displayed a resonance at 194.4 ppm assigned the carbonyl groups, a resonance at

140.1 ppm attributed to the $C_{ipso}$ of the $C_5H_4$ group and two resonances at 78.4 and 67.8 ppm attributed to the carbons in proximal and distal positions of the OH group. The IR spectrum of **6** displayed two ν(CO) bands at 1980 and 2020 $cm^{-1}$ (Figure 2.5). The mass spectrum of **6** displayed the expected molecular-ion peak at *m/z* 352 and fagment ion peaks corresponding to elimination of CO at *m/z* 324, 296 and 268 (Figure 2.6)

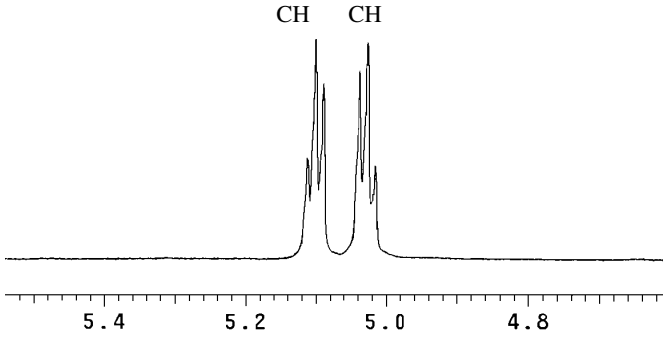


**Figure 2.4**. $^1H$ NMR in chloroform-d of **6** at 20 °C

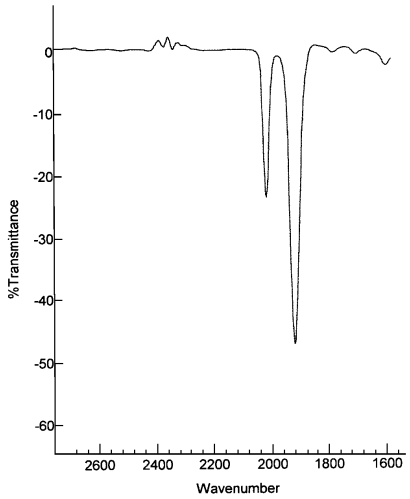


**Figure 2.5.** IR spectrum of **6** in dichloromethane

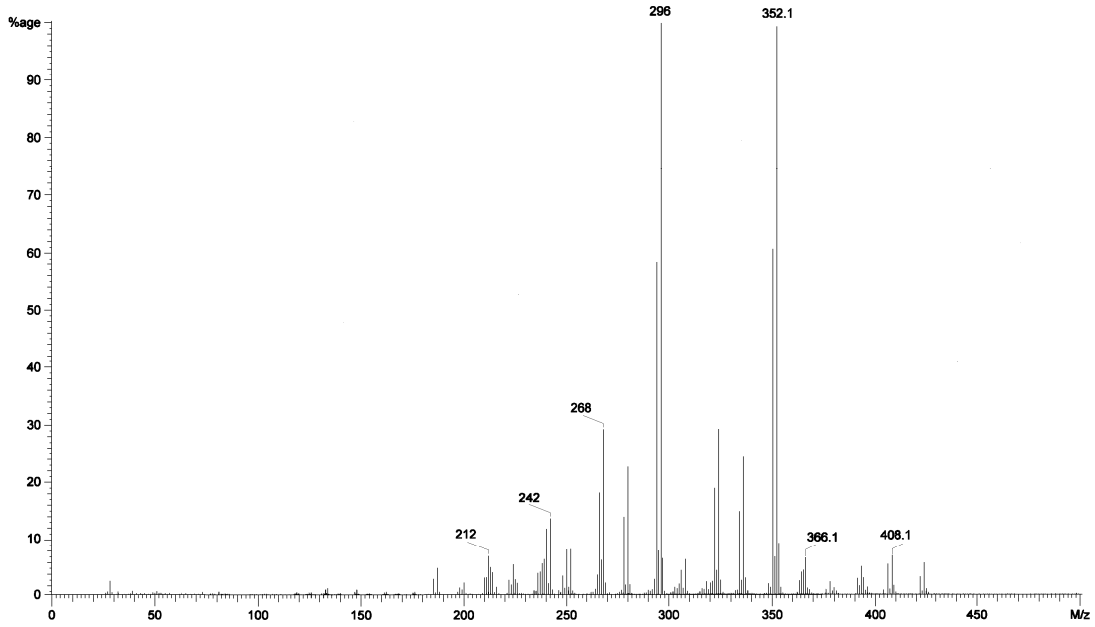


**Figure 2.6** Mass spectrum (EI) of **6**

X-ray diffraction studies showed that the compound **6** crystallized in a monocyclic system $P2_1/C$ (Figure 2.7). Selected bond distances and bond angles are listed in Table 2.2[25-30]. The X-ray data collection and processing parameters are listed in Table 7.3.2.

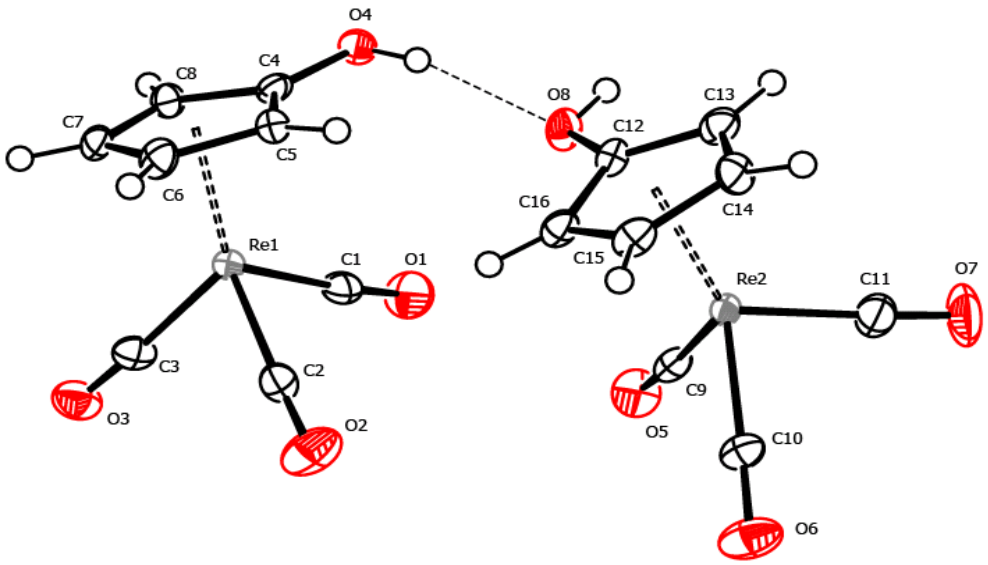


**Figure 2.7.** X-ray structure of **6** (ORTEP representation with selected atomic labels). Thermal ellipsoids are shown with a 30 % probability level.

**Table 2.2** Selected bond distances (Å) and bond angles (°) of **6**

| Selected bond distances (Å) | | Selected angles (°) | |
|---|---|---|---|
| Re1-C1 | 1.910(8) | C8-C4-C5 | 109.0(6) |
| Re1-C2 | 1.922(8) | C6-C5-C4 | 108.3(6) |
| Re1-C3 | 1.924(7) | C7-C6-C5 | 107.1(7) |
| C4-O4 | 1.356(6) | C6-C7-C8 | 109.1(6) |
| C1-O1 | 1.153(8) | C4-C8-C7 | 106.3(6) |
| C2-O2 | 1.144(8) | C1-Re1-C3 | 90.8(3) |
| C3-O3 | 1.142(8) | C1-Re1-C2 | 90.1(3) |
| C4-C5 | 1.402(11) | C3-Re1-C2 | 89.8(3) |
| C5-C6 | 1.438(9) | C4-O4-H1 | 109.5(8) |
| C6-C7 | 1.415(11) | O1-C1-Re1 | 175.7(6) |
| C7-C8 | 1.430(11) | O2-C2-Re1 | 176.5(7) |
| C8-C4 | 1.422(9) | O3-C3-Re1 | 176.8(6) |

The $^{1}H$ NMR of **5** displayed two triplets at 4.32 and 4.84 ppm in THF-$d_8$ (Figure 2.8). These two chemical shifts were attributed to the $C_5H_4$ ring were situated in higher field than those of compounds **6** and **3**. The $^{13}C$ NMR of **5** displayed a resonance at 199.0 ppm which confirmed the presence of CO groups. The two resonances at 76.4 and 66.0 ppm were attributed to the $C_5H_4$ group and the resonance at 164.0 ppm to the $C_{ipso}$. The mass spectrum of **5** showed the expected molecular-ion peak at *m/z* 351 corresponding to $[M - Li]^+$. The elemental analysis of a sample of **5** revealed that **5** was solvated by two water molecules.

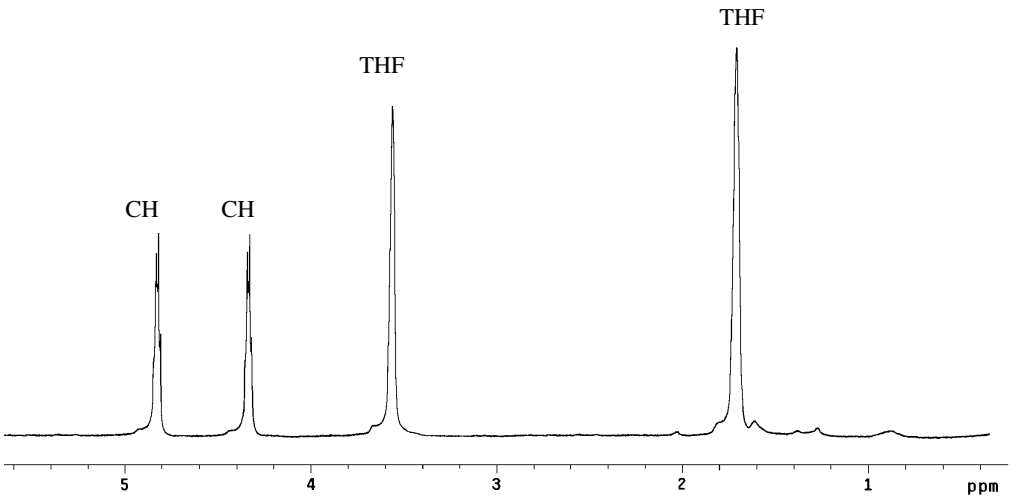


**Figure 2.8.** $^{1}$H NMR spectrum in THF-$d_8$ of compound **5** at 20 °C

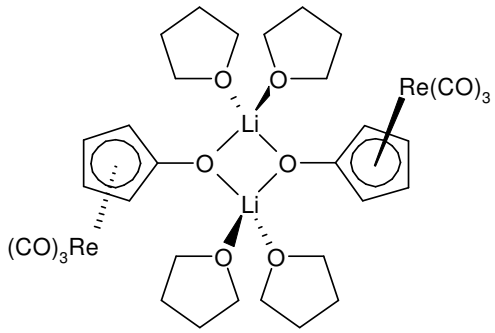


**Figure 2.9.** Compound **5** coordinated by two molecules of THF

Crystals of **5** were obtained in a solution of THF-hexane at -30°C. X-ray diffraction studies of **5** showed that the compound crystallized in the monocyclic system $P2_1/n$ (Figure 2.10). **5** was found to be coordinated by two molecules of THF via the lithium cation (Figure 2.9). Selected bond distances and bond angles are listed in Table 2.3. The X-ray data collection and processing parameters are listed in Table 7.3.1.

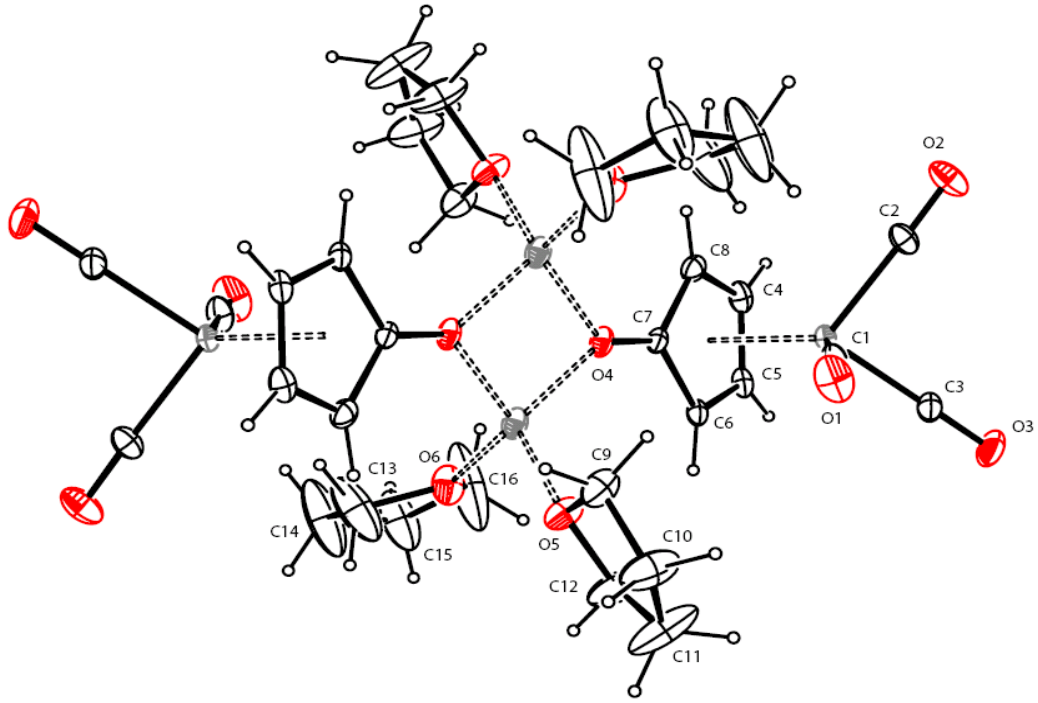


**Figure 2.10.** X-ray structure of **5** (ORTEP representation with selected atomic labels). Thermal ellipsoids are shown with a 20% probability level.

**Table 2.3** Selected bond distances (Å) and bond angles (°) of **5**

| Selected bond distances (Å) | | Selected angles (°) | |
|---|---|---|---|
| Re1-C1 | 1.917(5) | C8-C4-C5 | 108.0(4) |
| Re1-C2 | 1.923(5) | C6-C5-C4 | 108.7(4) |
| Re1-C3 | 1.912(5) | C7-C6-C5 | 108.2(4) |
| C7-O4 | 1.285(5) | C6-C7-C8 | 105.3(4) |
| C1-O1 | 1.143(6) | C4-C8-C7 | 109.0(4) |
| C2-O2 | 1.140(6) | C1-Re1-C3 | 91.5(2) |
| C3-O3 | 1.148(6) | C1-Re1-C2 | 93.0(2) |
| C4-C5 | 1.386(7) | C3-Re1-C2 | 89.8(2) |
| C5-C6 | 1.424(6) | C7-O4-Li1 | 136.3(4) |
| C6-C7 | 1.443(6) | O1-C1-Re1 | 175.8(4) |
| C7-C8 | 1.429(9) | O2-C2-Re1 | 178.1(5) |
| C8-C4 | 1.427(7) | O3-C3-Re1 | 177.5(5) |

### 2.4.3 Summary

($\eta^5$-$C_5H_5$)$Re(CO)_3$ (**1**) was deprotonated in the cyclopentadienyl ring with butyl lithium in THF. The resulting lithium salt ($\eta^5$-$C_5H_4Li$)$Re(CO)_3$ (**2**) reacted with dioxybis(trimethylsilane) $(Me_3SiO)_2$ to give ($\eta^5$-$C_5H_4OH$)$Re(CO)_3$ (**6**) and ($\eta^5$-$C_5H_4SiMe_3$)$Re(CO)_3$ (**3**) after chromatographic separation. Surprisingly the expected primary product the trimethylsilyloxy compound ($\eta^5$-$C_5H_4OSiMe_3$)$Re(CO)_3$ (**4**) could neither be isolated nor spectroscopically detected.

## 2.5 Recycling of ($\eta^5$-$C_5H_4SiMe_3$)$Re(CO)_3$ (3)

### 2.5.1 Removal of the trimethylsilyl group with tetrabutylammonium fluoride

In order to improve the global yield of the reaction, it was attempted to reconvert **3** into **1**. The deprotection of silyl groups with fluoride is well known and tetra butyl ammonium fluoride (TBAF) is usually used to cleave the C-Si bond of silylated alcohols[31-38]. Pure **3** was dissolved in THF and vigorously stirred at room temperature (Scheme 2.8). An excess of TBAF (1.5 equiv.) was added and the colourless solution turned brown. After evaporation, the product was isolated by flash chromatography with a short plug of silica gel and then the mixture was subjected to sublimation. The product was identified as ($\eta^5$-$C_5H_5$)$Re(CO)_3$ (**1**) by $^1$H NMR spectrocopy. The yield of **1** was found to be in the range of 70-100 %.

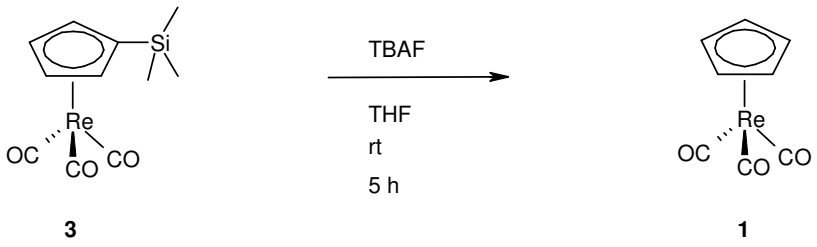


**3** **1**

**Scheme 2.8**

### 2.5.2 Yield optimization for 16

The yield of the compound **6** was found to be low, approximately 35%. Fortunately, the side product **3** could be reconverted into starting material **1** by removal of the trimethylsilyl group in a THF solution of TBAF and the global yield of the reaction could be optimized. In Table 2.4 are reported the experimental data for the preparation of **6** starting with 3700 mg of **1**. 3700 mg (11.08 mmol) of **7** gave 1396 mg (3.99 mmol) of **6** and 2164 mg (5.32 mmol) of **3**. The isolated yields were found to be 36 % (**6**) and 48 % (**3**) (entry 1). These 2164 mg of **3** were reconverted into **1** in an excellent 100% yield (1776 mg, 5.32 mmol), which gave 614 mg (1.75 mmol) of **6** and 952 mg (2.34 mmol) of **3**, 34 and 44 % respectively (entry 2). After

2 other cycles (entries 3 and 4), we obtained at all 2291 mg (6.55 mmol) of **6** (entry 5). Thus the yield of **6** could be finally optimized after 3 cycles up to 59 %.

**Table 2.4.** Recycling of **3**-Experimental data

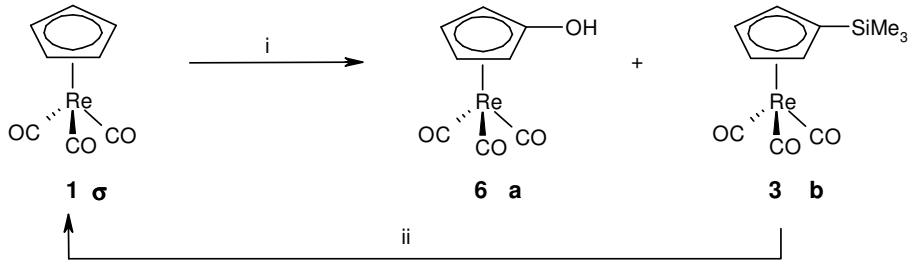


| Entry | **1** | | **6** | | **3** | |
|---|---|---|---|---|---|---|
| | mg (mmol) | Yield $\sigma$ (%) | mg (mmol) | Yield *a* (%) | mg (mmol) | Yield *b* (%) |
| 1 | 3700 (11.08) | _ | 1396 (3.99) | 36 | 2164 (5.32) | 48 |
| 2 | 1776 (5.32) | 100 | 614 (1.75) | 33 | 952 (2.34) | 44 |
| 3 | 547 (1.64) | 70 | 195 (0.56) | 34 | 346 (0.85) | 52 |
| 4 | 273 (0.82) | 96 | 86 (0.24) | 30 | 160 (0.39) | 48 |
| 5 | Sum | | 2291 (6.55) | 59 | | |

(i) n-BuLi, THF, then $(Me_3SiO)_2$, -78°C to rt (ii) TBAF, THF, rt

The recycling of the compound **3** increased the global yield of the reaction. The gain of the recycling can be also theoretically calculated. The three compounds **1**, **6** and **3** were renamed S, A and B respectively for more clarity.

Let us consider now the reaction S → A + B (Figure 2.11).

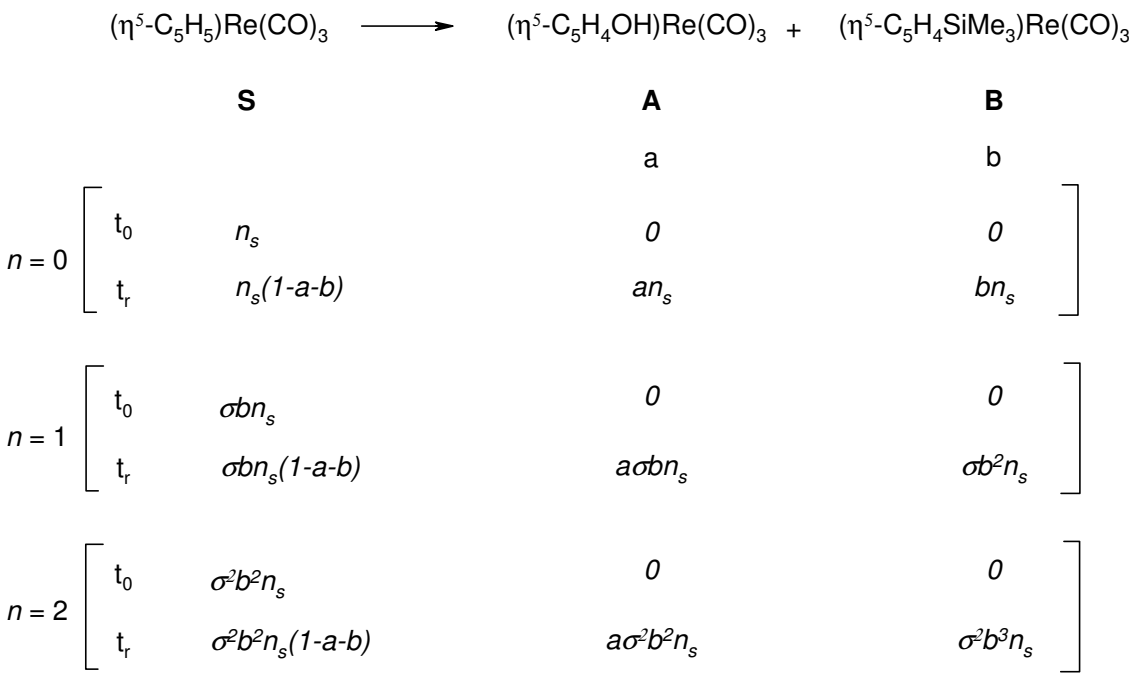


**Figure 2.11.**

$a$ is the isolated yield of A, $0 \le a \le 1$,

$b$ is the isolated yield of B, $0 \le b \le 1$

$\sigma$ is the isolated yield of S after the recycling reaction B $\rightarrow$ S, $0 \le \sigma \le 1$

$n$ is the number of times B is recycled

$n_S$ is the amount in moles of S at t = $t_0$, $n = 0$

$n = 0$ : The reaction starts at time t = $t_0$, the amount of S in moles is $n_s$ then, the amount in moles of both A and B is 0. At time t = $t_r$, the reaction is finished, the two products are isolated, $an_s$ moles of A and $bn_s$ moles of B are obtained. These $bn_s$ moles of B are reconverted into S, the yield of the reaction is $\sigma$, it means $\sigma bn_s$ ($\sigma \times bn_s$) moles of S are regenerated.

$n = 1$ : These $\sigma bn_s$ moles of S afford $a\sigma bn_s$ ($a \times \sigma bn_s$) moles of A and $\sigma b^2 n_s$ ($b \times \sigma bn_s$) moles of B. These $\sigma b^2 n_s$ moles of B are reconverted into S, the yield of the reaction is $\sigma$, it means that $\sigma^2 b^2 n_s$ ($\sigma \times \sigma b^2 n_s$) moles of S are reobtained

$n = 2$ : These $\sigma^2 b^2 n_s$ moles of S afford $a\sigma^2 b^2 n_s$ ($a \times \sigma^2 b^2 n_s$) moles of A and $\sigma^2 b^3 n_s$ ($b \times \sigma^2 b^2 n_s$) moles of B etc…

After *n* recyclings, we obtain the following progressions (Table 2.5):

**Table 2.5** Theoretical progressions of the reaction S → A + B with recycling of B

| Number of recycling | S | A | B |
|---|---|---|---|
| *n = 0* | $n_s$ | $an_s$ | $bn_s$ |
| *n = 1* | $\sigma b n_s$ | $a\sigma b n_s$ | $\sigma b^2 n_s$ |
| *n = 2* | $\sigma^2 b^2 n_s$ | $a\sigma^2 b^2 n_s$ | $\sigma^2 b^3 n_s$ |
| *n = 3* | $\sigma^3 b^3 n_s$ | $a\sigma^3 b^3 n_s$ | $\sigma^3 b^4 n_s$ |
| *n = 4* | $\sigma^4 b^4 n_s$ | $a\sigma^4 b^4 n_s$ | $\sigma^4 b^5 n_s$ |
| *n* | $\sigma^n b^n n_s$ | $a\sigma^n b^n n_s$ | $\sigma^n b^{n+1} n_s$ |

*σ:* isolated yield of S produced from B, *a*: isolated yield of A, *b*: isolated yield of B, $n_s$: initial amount in moles of S,
*n*: number of cycles

If $n_A$ is the amount in moles of compound A obtained after *n* recycling reactions, then

$$n_A = an_s + a\sigma b n_s + a\sigma^2 b^2 n_s + a\sigma^3 b^3 n_s + a\sigma^4 b^4 n_s + a\sigma^5 b^5 n_s + ... + a\sigma^n b^n n_s$$

$$n_A = an_s(1 + \sigma b + \sigma^2 b^2 + \sigma^3 b^3 + \sigma^4 b^4 + \sigma^5 b^5 + ... + \sigma^n b^n)$$

$$G = 1 + \sigma b + \sigma^2 b^2 + \sigma^3 b^3 + \sigma^4 b^4 + \sigma^5 b^5 + ... + \sigma^n b^n$$

The sum *G* is a geometric series; multiplying both sides by *σb* gives

$$\sigma bG = \sigma b + \sigma^2 b^2 + \sigma^3 b^3 + \sigma^4 b^4 + \sigma^5 b^5 + ... + \sigma^{n+1} b^{n+1}$$

and substracting *σbG* from *G* then gives

$$G - \sigma bG = 1 - \sigma^{n+1} b^{n+1}$$

$$G(1 - \sigma b) = 1 - \sigma^{n+1} b^{n+1}$$

$$G = \frac{1 - \sigma^{n+1} b^{n+1}}{1 - \sigma b}$$

so

$$n_A = an_s \left( \frac{1 - \sigma^{n+1} b^{n+1}}{1 - \sigma b} \right)$$

The formula above is true only for

$a + b \leq 1$

The yield $y_A$ of A in percentage of moles is then

$$y_A = 100a\left(\frac{1-\sigma^{n+1}b^{n+1}}{1-\sigma b}\right)$$

Experimentally, the yields obtained for A and B were always close in the range 30-45%. To visualize the influence of the yields *a* and *b* onto the global yield of A $y_A$, let *a* be equal to *b*, after *n* recycling reactions, then

$$n_A = a\left(\frac{1-\sigma^{n+1}a^{n+1}}{1-\sigma a}\right)$$

$$y_A = 100a\left(\frac{1-\sigma^{n+1}a^{n+1}}{1-\sigma a}\right)$$

The formula above is valid only for $a \leq 0,5$ ($a + b \leq 1,$ if $a = b$ then $2a \leq 1$ and $a \leq 0,5$).

If the recycling is repeated 4 times ($n = 4$) which seems reasonable practically, then

$$y_A = f(a) = 100a\left(\frac{1-\sigma^5 a^5}{1-\sigma a}\right)$$

$a \leq 0,5$

The values $y_A$ were calculated for $\sigma$ = 50%, $\sigma$ = 95% and $\sigma$ = 100%. Selected values are reported in Table 2.15. The graph $y_A = f(a)$ is showed below (Graph 2.1). Three curves were plotted for $\sigma$ = 50%, $\sigma$ = 95% and $\sigma$ = 100%. The graph 2.1 gives a visual representation of the yield $y_A$ of A obtained after 4 recyclings vs. *a*. It indicates for instance that if $a = b$ = 40 %, the yield of A is 64% for $\sigma$ = 95% and 66% for $\sigma$ = 100% after 4 recyclings.

As mentioned previously, the observed *a* was in the range of 30-45% which gives a global yield $y_A$ in the range 42-77% for $\sigma$ = 95% (Table 2.6).

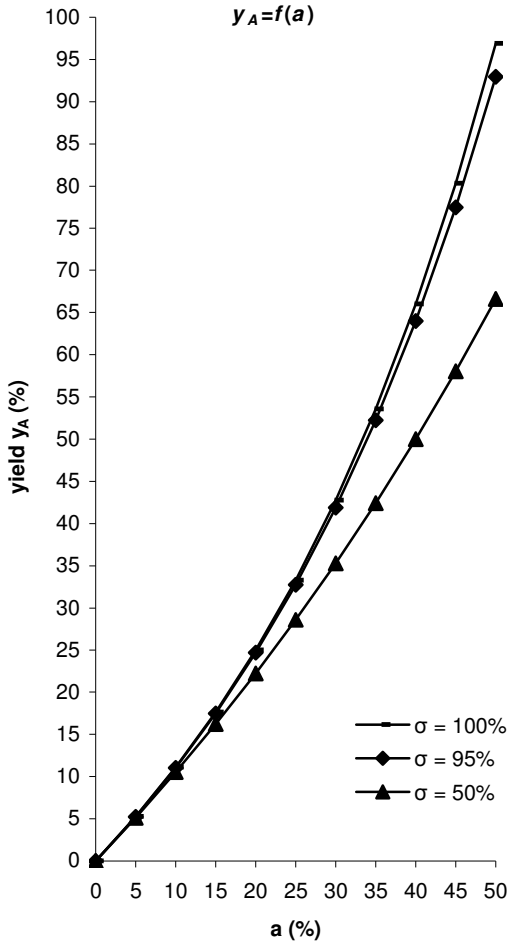


**Graph 2.1**

**Table 2.6.** Approximate values $y_A$ vs. $a$

| $a$ (%) | $y_A$ (%), $\sigma$ = 50% | $y_A$ (%), $\sigma$ = 95% | $y_A$ (%),$\sigma$ = 100% |
|---|---|---|---|
| 0 | 0 | 0 | 0 |
| 5 | 5 | 5 | 5 |
| 10 | 11 | 11 | 11 |
| 15 | 16 | 17 | 18 |
| 20 | 22 | 25 | 25 |
| 25 | 29 | 33 | 33 |
| 30 | 35 | 42 | 43 |
| 35 | 42 | 52 | 54 |
| 40 | 50 | 64 | 66 |
| 45 | 58 | 77 | 80 |
| 50 | 67 | 93 | 97 |

$Y_A$: global isolated yield of A after $n$ cycles, $a$: isolated yield of A and B, $\sigma$: isolated yield of S obtained from the recycling of B

Now let $a$ be expressed as a function of $b$,

$$y_A = a\left(\frac{1-\sigma^5 b^5}{1-\sigma b}\right)$$

if $a$ is expressed as a percentage, then

$$a = f(b) = \frac{y_A(1-\sigma b)}{1-\sigma^5 b^5}$$

This formula above is true only for $a + b \leq 100\,\%$

$\sigma$ is known, experimentally $\sigma = 95\%$ and $0 \leq y_A \leq 100$

$a$ can be expressed as a function of $b$ for $y_A$ = 10%, $y_A$ = 20%, $y_A$ = 30%, …, $y_A$ = 100%.

The graphs $a = f(b)$ (Graph 2.2) are showed below and selected approximate values are reported in Table 2.7.

From these graphs, if we know $a$ and $b$, we can determine the yield $y_A$. For example, if $b$ = 45 % and $a$ = 37%, what's the yield $y_A$? If we trace the two lines b = 45% and a = 37%, then the two lines cross is situated on the curve $a = f(b)$ ; $y_A$ = 60%. The yield $y_A$ is 60% for $b$ = 45 % and $a$ = 37%.

The other way around, if $b$ = 65% and $y_A$ = 70%, what's the value of $a$? The line $b$ = 65% crosses the curve $a = f(b)$ ; $y_A$ = 70% for a = 29%.

As mentioned before, both yields $a$ and $b$ were found to be in the range 30-45% The values corresponding to $30 \le a \le 45\%$ ; $30 \le b \le 45\%$ and $50 \le y_A \le 100\%$ were greyed out in Table 2.6. This data set shows that good yields close to 80% can be reached for values of $a$ and $b$ around 45%. For instance if $a$ = 46.5% and $b$ = 45%, $y_A$ = 80%.

It is also remarkable that good yields are obtained for low values of $a$. If $25 \le a \le 35\%$ and $55 \le b \le 65\%$ then $50 \le y_A \le 80\%$.

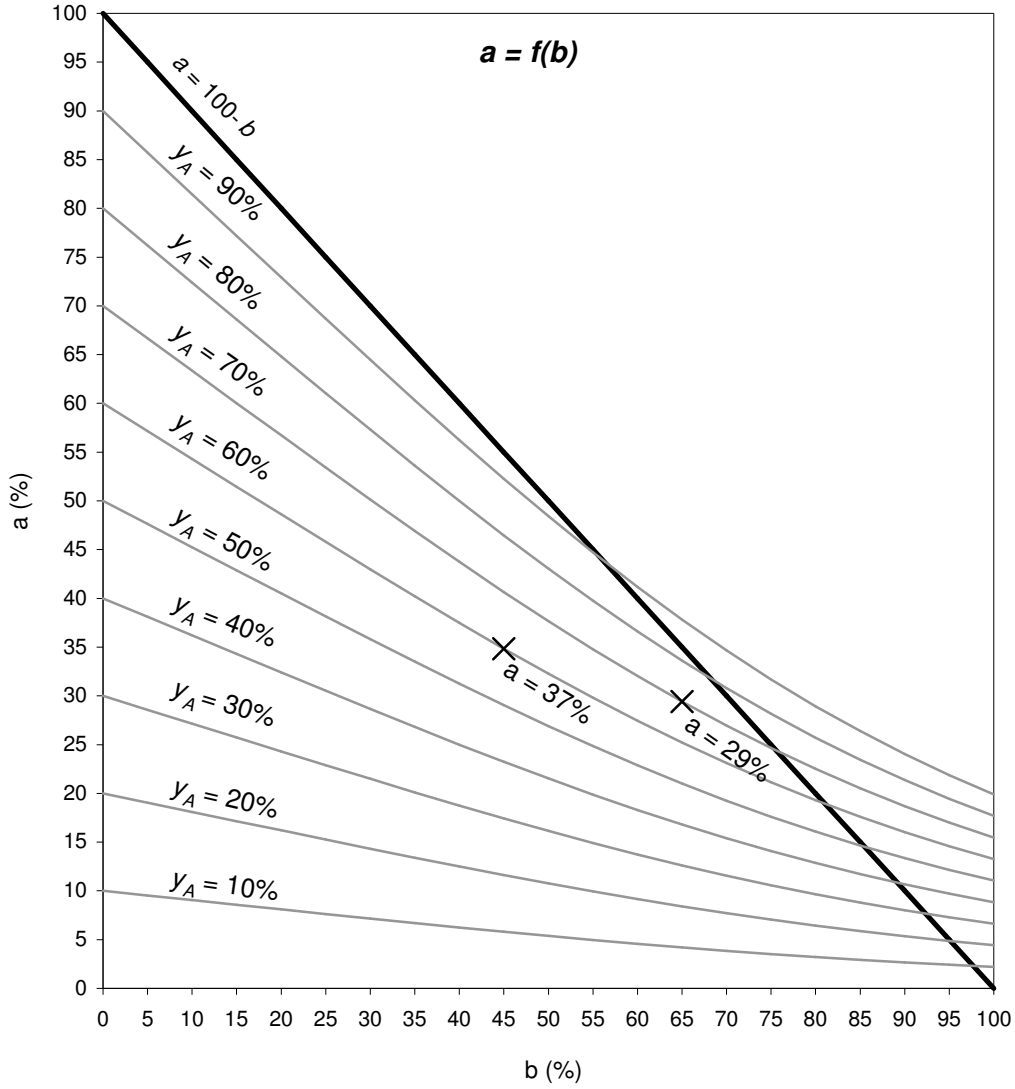


**Graph 2.2**

**Table 2.7** Selected approximate values of *a* vs. *b*

| *b*(%) | *a*(%) $y_A$ = 10% | *a*(%) $y_A$ = 20% | *a*(%) $y_A$ = 30% | *a*(%) $y_A$ = 40% | *a*(%) $y_A$ = 50% | *a*(%) $y_A$ = 60% | *a*(%) $y_A$ = 70% | *a*(%) $y_A$ = 80% | *a*(%) $y_A$ = 90% |
|---|---|---|---|---|---|---|---|---|---|
| 30 | 7.2 | 14.3 | 21.5 | 28.7 | 35.8 | 43 | 50.1 | 57.3 | 64.5 |
| 35 | 6.7 | 13.4 | 20.1 | 26.8 | 33.5 | 40.2 | 46.9 | 53.6 | 60.3 |
| 40 | 6.2 | 12.5 | 18.7 | 25 | 31.2 | 37.5 | 43.7 | 50 | 56.2 |
| 45 | 5.8 | 11.6 | 17.4 | 23.2 | 29 | 34.8 | 40.7 | 46.5 | 52.3 |
| 50 | 5.4 | 10.8 | 16.1 | 21.5 | 26.9 | 32.3 | 37.7 | 43 | 48.4 |
| 60 | 4.6 | 9.2 | 13.7 | 18.3 | 22.9 | 27.5 | 32 | 36.6 | - |
| 70 | 3.9 | 7.7 | 11.6 | 15.4 | 19.3 | 23.1 | 27 | - | - |

$Y_A$: global isolated yield of A, *a*: isolated yield of A, *b*: isolated yield of B, *σ*: isolated yield of S

### 2.5.3 Conclusion

The undesired compound ($\eta^5$-$C_5H_4SiMe_3$)$Re(CO)_3$ (**3**) could be reconverted into ($\eta^5$-$C_5H_5$)$Re(CO)_3$ (**1**). The recycling of **3** allowed us to improve significantly the yield of ($\eta^5$-$C_5H_4OH$)$Re(CO)_3$ (**6**). Indeed experimentally, we were able to obtain **6** in a yield of 60% after several recycling steps versus 35% initially. This result was also confirmed by theoretical calculations that demonstrate that very good yields can reach even higher values than 60%, up to 80% after 4 recycling cycles.

## 2.6 Conclusion

The key molecule of our retrosynthesis was prepared successfully. The novel route to ($\eta^5$-hydroxycyclopentadienyl)(tricarbonyl)rhenium (**6**) consists in the electrophilic hydroxylation of ($\eta^5$-cyclopentadienyl)(tricarbonyl)rhenium (**1**) with dioxybis(trimethylsilane). This method allowed for a large scale synthesis with compounds easy to handle and to prepare. The modest yield of **6** could be largely compensated by the recycling of the side product [$\eta^5$-(trimethylsilyl)cyclopentadienyl](tricarbonyl)rhenium (**3**) (Scheme 2.9).

## 2.7 Summary

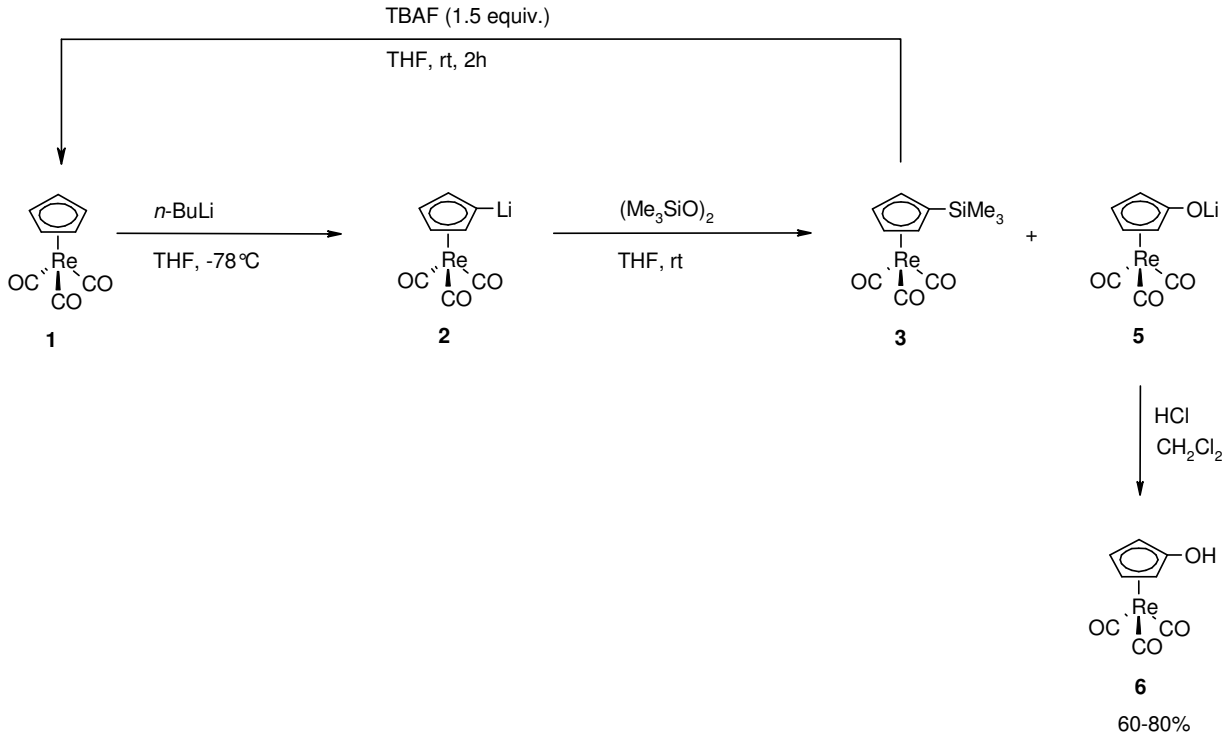


**Scheme 2.9**

## 2.8 References

[1] R. Ferede, J. F.Hinton, W. A. Korfmacher, J. P. Freeman, T. Allison, *Organomet.* **1985**, *4*, 614.

[2] D. W. Parker, M. Marsi, J. A. Gladysz, *J. Organomet. Chem.* **1980**, *194*, C1.

[3] H. J. Reich, I. L. Reich, *J. Org. Chem.* **1975**, *40*, 2248.

[4] F. Minutolo, J. A.Katzenellenbogen, *J. Am. Chem. Soc.* **1998**, *120*, 4514.

[5] F. Minutolo, J. A. Katzenellenbogen, *J. Am. Chem. Soc.* **1998**, *120*, 13264.

[6] F. Minutolo, J. A. Katzenellenbogen, *Organometallics* **1999**, *18*, 2519.

[7] R. Alberto, A. Egli, U. Abram, K. Hegetschweiler, V. Gramlich, P. A. Schubiger, *J. Chem. Soc., Dalton Transactions* **1994**, 2815.

[8] R. Alberto, R. Schibli, P. A. Schubiger, *Polyhedron* **1996**, 15, 1079.

[9] R. Alberto, R. Schibli, A. Egli, P. A. Schubiger, W. A. Herrmann, G. Artus, U. Abram, T. A. Kaden, *J. Organomet. Chem.* **1995**, *492*, 217.

[10] J. L. Thomas, R. Dominguez, M. C. Helvenston, *Organometallics* **1988**, *7*, 2566.

[11] F. Ramirez, S. Levy, *J. Am. Chem. Soc.* **1958**, *23*, 2036.

[12] T. Weil, M. Cais, *J. Am. Chem. Soc.* **1963**, *28*, 2472.

[13] K. J. Reimer, A. Shaver, *J. Organomet. Chem.* **1975**, *93*, 239.

[14] M. Tadei, A. Ricci, *Synthesis-Communications* **1985**, 633.

[15] S. Florio, L. Troisi, *Tetrahedron lett.* **1989**, *30*, 3721.

[16] W. P. Jackson, *Synlett* **1990**, 536.

[17] M. Suzuki, H. Takada, R. Noyori, *J. Org. Chem.* **1982**, *47*, 902

[18] D. H. R. Barton, B. M. Chabot, *Tetrahedron* **1997**, *53*, 487.

[19] P. Kocienski, M. Todd, *J. Chem. Soc. Chem. Commun.* **1982**, 1078.

[20] D. Brandes, A. Blaschette, *J. Chem. Soc. Chem.Commun.* **1974**, 217.

[21] S. Kanemoto, K. Oshima, Wong Victor, S. Matsubara, K. Takai, Wong Victor, H. Nozaki, *Tetrahedron lett.* **1983**, *24*, 2185.

[22] C. Lo Sterzo, M. Miller, J. K. Stille, *Organometallics* **1989**, *9*, 687.

[23] W. A. Herrmann, *Chem. Ber.* **1978**, *111*, 2458.

[24] L. V. Dinh,; J. A. Gladysz, *Chemistry -A European Journal* **2005**, *11*, 7211.

[25] I. A. Lobanova, V. I. Zdanovich, P. V. Petrovskii, N. E. Kolobova, *J. Organomet. Chem.* **1985**, *292*, 395.

[26] W. Harrison, J. Trotter, *J. Chem. Soc., Dalton Transactions: Inorg. chem.* **1972**, *5*, 678.

[27] P. J. Fitzpatrick, Y. Le Page, Y. S. Butler, *Acta Crystallogr., Sect. B: Structural Crystallography and Crystal Chemistry* **1981**, *B37(5)*, 1052.

[28] Y. Huang, I. S. Butler, D. F. R. Gilson, *Inorg. chem.* **1992**, *31*, 4762.

[29] L. V. Dinh, F. Hampkel, J. A. Gladysz, *J. Organomet. Chem.* **2005**, 690, 493.

[30] D. Kurz, R. Fröhlich, G. Erher, *Organometallics* **2001**, *20*, 572.

[31] *Inorg. Synth.* **1992**, *29*, 211.

[32] J. H. Clark, *Chemical Reviews* **1980**, *80*, 429.

[33] I. Kuwajima, E. Nakamura, *Accounts of Chemical Research* **1985**, *18*, 181.

[34] K. Jarowicki, P. J. Kocienski, *J. Chem. Soc., Perkin Transactions 1* **1999**, 1589.

[35] T. D. Nelson, R. D. Crouch, *Synthesis* **1996**, 1031.

[36] J. S. Davies, L. C. L Higginbotham, E.J. Tremeer, C. Brown, R. C. Treadgold, *J. Chem. Soc., Perkin Transactions 1* **1992**, 3043.

[37] J. W. Gillard, R. Fortin, H. E. Morton, C. Yoakim, C. A. Quesnell, S. Daignault, Y. Guindon, *J. Org. Chem.* **1988**, *53*, 2602.

[38] P. J. Kocienski, *Protecting Groups*, Thieme Stuttgart, **1994**.

# 3 Preparation of Alkoxy and Acyloxy Cyclopentadienyl Tricarbonyl Rhenium Complexes

## 3.1 Introduction

In this chapter we investigate the possibility to alkylate/ acylate the OH group of ($\eta^5$-$C_5H_4OH$)$Re(CO)_3$ **6**. In our retrosynthesis the protection of **6** was envisaged in order to avoid side reactions with the OH function in the following steps: nitrosylation and formation of hydride (Scheme 3.1). Indeed according to the literature, formation of hydride from rhenium complexes similar to ($\eta^5$-$C_5H_4OH$)Re(CO)(NO)H involves basic media that could interact with the acidic proton of the OH group.

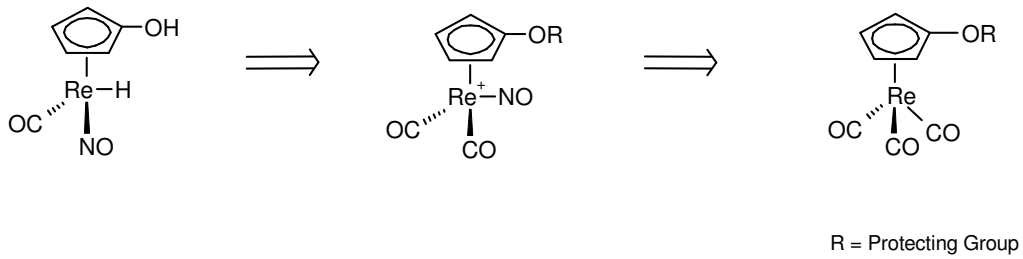


**Scheme 3.1**

The preparation of various alkoxy and acyloxy cyclpentadienyl rhenium complexes is described in this chapter.

## 3.2 Preparation of alkoxy cyclopentadienyl tricarbonyl rhenium complexes

### 3.2.1 Literature

The first ether synthesis was reported by Williamson in 1850[1-3]. This reaction is still widely used today. It is the simplest method for preparing symmetrical and asymmetrical ethers. This reaction involves an alkoxide ($RO^-$) generated in situ from an alcohol in the presence of a base such as sodium carbonate or potassium hydroxide and an alkylating agent, generally an alkyl

halide (R'X). The alkoxide reacts with the alkyl halide via a nucleophilic substitution to give the desired ether (Scheme 3.2). The reaction is carried out in polar solvents to favor the nucleophilic substitution, particularly acetonitrile or dimethylformamide. The reaction occurs under reflux within a few hours. The reaction was extended to aryl halides and many examples can be found in the literature[4-17].

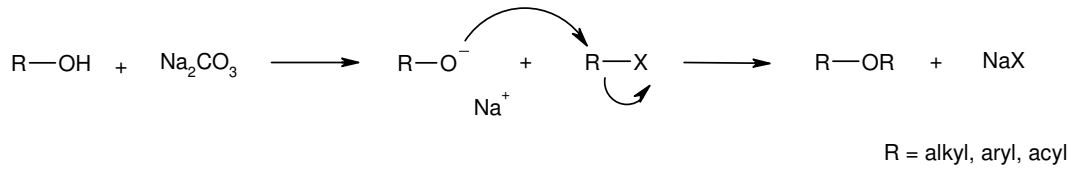


**Scheme 3.2**

### 3.2.2 Preparation of the alkoxy rhenium complexes 7-11

A series of alkoxy rhenium complexes was prepared under Williamson condtions. ($\eta^5$-$C_5H_4OH)Re(CO)_3$ (**6**) was dissolved in acetonitrile with an excess of alkyl halide R-X. 2 equivalents of sodium carbonate were added to the mixture and the solution was heated under reflux for 10 hours (Table 3.1).

The first attempt with methyl iodide in acetonitrile and sodium carbonate under reflux for 10 hours afforded the expected product **7** in a yield of 60 %[1-4]. The reaction of **6** with ethyl bromide gave the expected product **8** in a yield of 65 %. The reaction of **6** with isopropyl bromide afforded the product **9** in a 68 % yield. The nucleophilic substitution failed with the bulky *tert*-butyl bromide.

The success of the substitution encouraged us to test other groups that could play the role of protecting groups. Benzyl bromide is well known as a protecting group for alcohols[21-29]. The benzyl group is labile in the presence of dihydrogen gas under a pressure of 1.5 bar $H_2$ and in the presence of a catalyst. Usually palladium on activated carbon is used. The allyl group is also commonly used as protecting group for alcohols[30-37]. Isomerization of the more labile enol ether employing $KO^tBu$ with subsequent mild acidic hydrolysis is one of the most common deprotection methods. Isomerization of allyl ether can be also carried out with a palladium catalyst such as $Pd(PPh_3)_4$ under basic conditions.

**Table 3.1** Preparation of ethers **7**-**11** from **6**

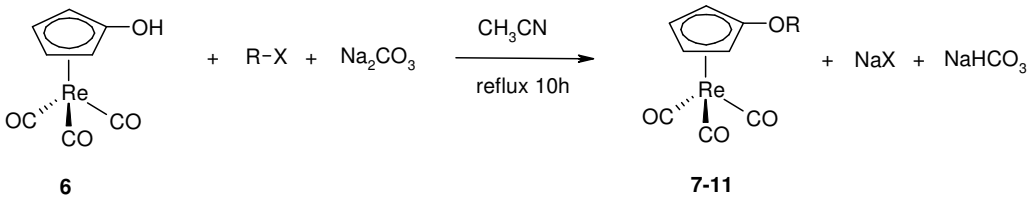


**6** **7-11**

| Entry | R-X | Product | Yield (%)[a] |
|---|---|---|---|
| 1 |  | **7** | 60 |
| 2 |  | **8** | 60 |
| 3 |  | **9** | 61 |
| 5[b] | 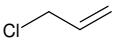 | **10** | 90 |
| 6 | 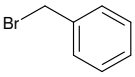 | **11** | 90 |

[a]isolated yields

[b]a crystal of KI was added to the reaction mixture

As showed in Table 3.1, the benzyl ether and the allyl ether derivatives reacted with 16 and the corresponding products **10** and **11** were isolated in the good yields of 70 and 85 % respectively[19]. Both benzylic and allylic halides undergo nucleophilic substitution reactions very readily even with weak nucleophiles, because the electronic deficiency of either the benzylic or the allylic position is resonance stabilized. In the case of allylic groups the mechanism can be simply a $S_N1$ or a $S_N2$, but it can also proceed through a rearrangement where the nucleophile can attack both the electron deficient sites (Scheme 3.3). Allyl chloride was employed instead of allyl bromide. A catalytic amount of potassium iodide was added to the reaction mixture to facilitate the substitution[38]. Iodide replaces chloride and thus catalyses its elimination.

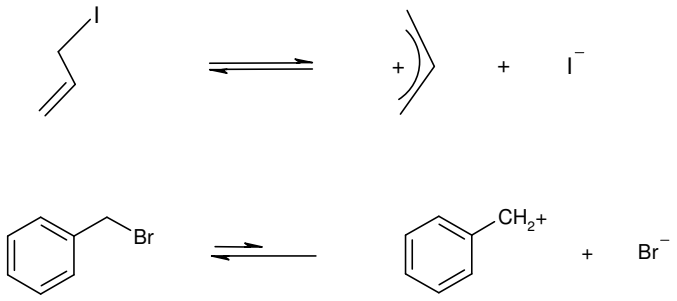


**Scheme 3.3**

### 3.2.3 Characterization of the rhenium complexes 7-11

Compounds **7**, **8**, **9** and **11** were isolated as white powders at room temperature. Compound **10** is a colourless oil at ambient temperature. All the compounds were fully characterized by $^{1}H$, $^{13}C$ NMR, IR and mass spectroscopy. Their composition was determined by elemental analysis. Compounds **7** and **11** were recrystallized from a solution of hexane-dichloromethane and crystals of compounds **7** and **11** were suitable for X-ray diffraction.

The $^{1}H$ NMR spectrum of ($\eta^5$-$C_5H_4OMe$)$Re(CO)_3$ (**7**) showed two signals, a multiplet at 5.08 ppm attributed to the $C_5H_4$ group and a singlet at 3.59 ppm attributed to the methoxy group (Figure 3.1). The integrals of these signals are in accord with the expected number of protons. In the $^{13}C$ NMR spectrum, the presence of carbonyl groups was confirmed by a resonance at 194.1 ppm. The methoxy group was identified by a signal at 58.3 ppm and the carbon atoms of the $C_5H_4$ group ring were observed at 145.1, 78.3 and 66.1 ppm. The IR spectrum revealed two ν(CO) 2021 and 1922 $cm^{-1}$ confirming the $Re(CO)_3$ unit.

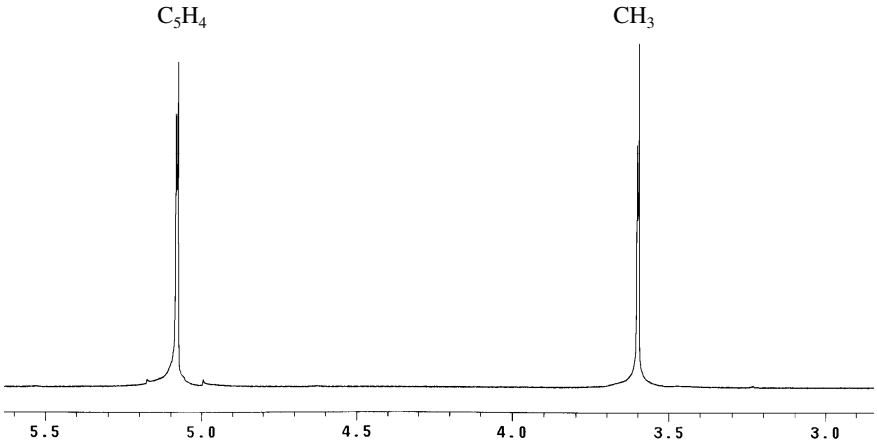


**Figure 3.1.** $^{1}$H NMR spectrum of **7** in chloroform-d at 20 °C

X-ray diffraction studies of **7** showed that the compound crystallized in a triclinic space group P-1 (Figure 3.2). Selected bond distances and bond angles are listed in Table 3.2. The X-ray data collection and processing parameters are listed in Table 7.3.3.

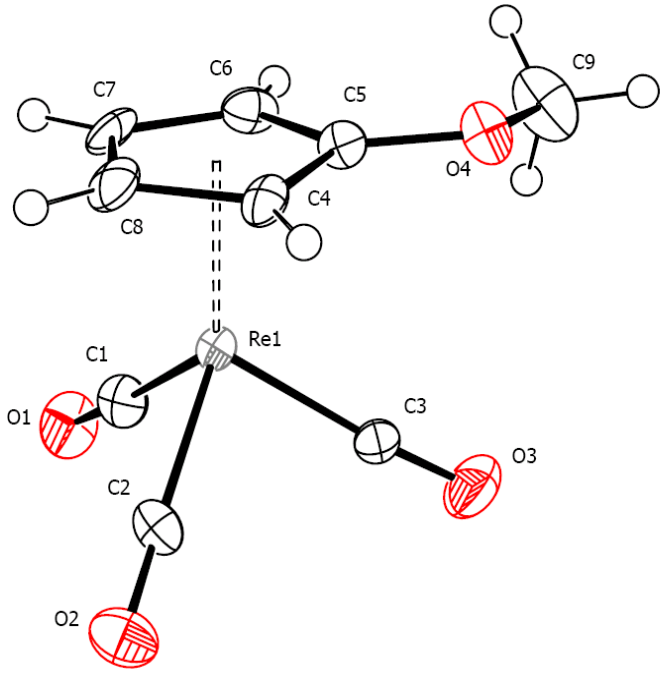


**Figure 3.2.** X-ray structure of **7** (ORTEP representation with selected atomic labels). Thermal ellipsoids are shown with a 50% probability level.

**Table 3.2** Selected bond distances (Å) and bond angles (°) of **7**

| Selected bond distances (Å) | | Selected angles (°) | |
|---|---|---|---|
| Re1-C1 | 1.925(13) | C8-C4-C5 | 105.9(11) |
| Re1-C2 | 1.925(12) | C6-C5-C4 | 110.0(16) |
| Re1-C3 | 1.923(12) | C7-C6-C5 | 107.5(11) |
| C5-O4 | 1.365(14) | C6-C7-C8 | 107.7(11) |
| C1-O1 | 1.141(16) | C4-C8-C7 | 108.7(11) |
| C2-O2 | 1.139(15) | C1-Re1-C3 | 91.3(5) |
| C3-O3 | 1.129(16) | C1-Re1-C2 | 89.8(5) |
| C4-C5 | 1.410(16) | C3-Re1-C2 | 88.9(5) |
| C5-C6 | 1.410(17) | C5-O4-C9 | 117.3(10) |
| C6-C7 | 1.427(18) | O1-C1-Re1 | 177.1(12) |
| C7-C8 | 1.413(19) | O2-C2-Re1 | 178.5(11) |
| C8-C4 | 1.446(17) | O3-C3-Re1 | 175.7(10) |

The $^{1}$H NMR spectrum of ($\eta^5$-$C_5H_4OEt$)$Re(CO)_3$ (**8**) in $CDCl_3$ showed also a singlet at 5.06 ppm attributed to the $C_5H_4$ ring protons (Figure 3.3). The ethyl group could be identified by a triplet and a quartet at 1.33 and 3.77 ppm respectively. For comparison ethyl bromide shows in $CDCl_3$ a triplet and a quartet at 1.68 and 3.43 ppm. The integration 5:2:3 is consistent with the given assignement. Additionally, the presence of the carbonyl groups was confirmed by a resonance at 194.3 ppm in the $^{13}$C NMR spectrum. The $C_5H_4$ ring carbons were found at 144.4, 78.4 and 67.4 ppm and the two carbon atoms of the ethyl group were assigned to the two resonances at 66.2 and 14.4 ppm. In the IR spectrum of **8**, two ν(CO) bands of the $Re(CO)_3$ local unit appeared at 2021 and 1922 cm$^{-1}$. The mass spectrum of **8** showed the correct molecular-ion peak peak at *m/z* 380 fragment ion peaks at *m/z* 352, 324, 296 corresponding to elimination of CO.

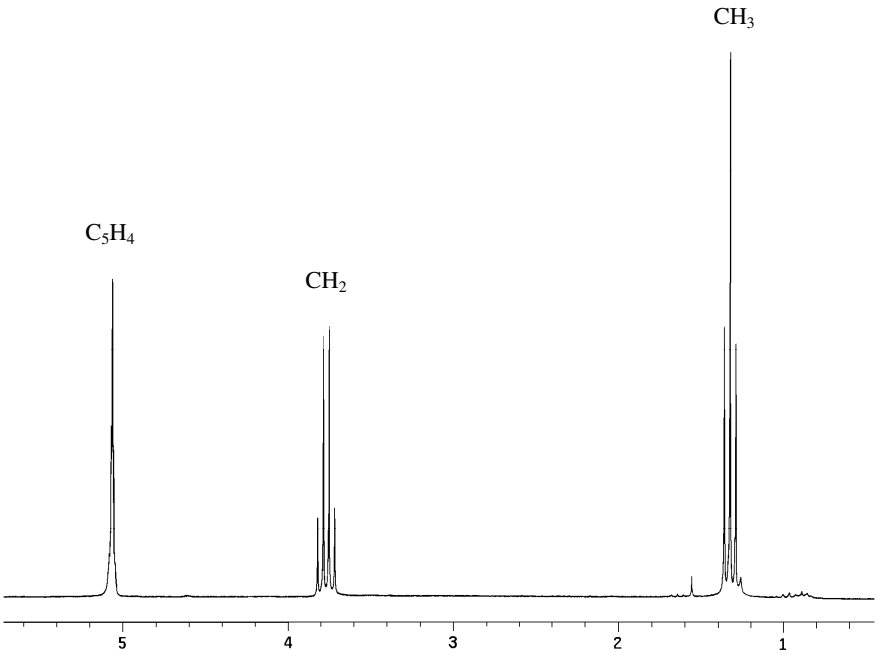


**Figure 3.3.** $^{1}$H NMR spectrum of **8** in chloroform-d at 20 °C

The $^{1}$H NMR spectrum of ($\eta^5$-$C_5H_4O^iPr$)$Re(CO)_3$ (**9**) in $CDCl_3$ showed two triplets at 5.06 and 5.02 ppm proving the presence of a substituted ($\eta^5$-$C_5H_4$) ring (Figure 3.4). The isopropyl group was identified by two resonances: a multiplet at 4.03 ppm (characteristic of the CH proton of the isopropyl group) and a doublet at 1.30 ppm for the protons of the three methyl groups $CH_3$ both coupled to each other. In the $^{13}$C NMR spectrum, the carbonyl groups appeared at 194.5 ppm. The carbon atoms of the ($\eta^5$-$C_5H_4$) group resonated at 144.2, 78.4 and 67.8 ppm, which is in accord with what we observed in the $^{13}$C spectra of the previous compounds **7** and **8**. In the IR spectrum **9** showed two bands at 2020 and 1921 $cm^{-1}$ attributed to the stretching of the CO groups of the $Re(CO)_3$ unit. The mass spectrum confirmed **9**. The molecular-ion peak appeared at *m/z* 394 as expected.

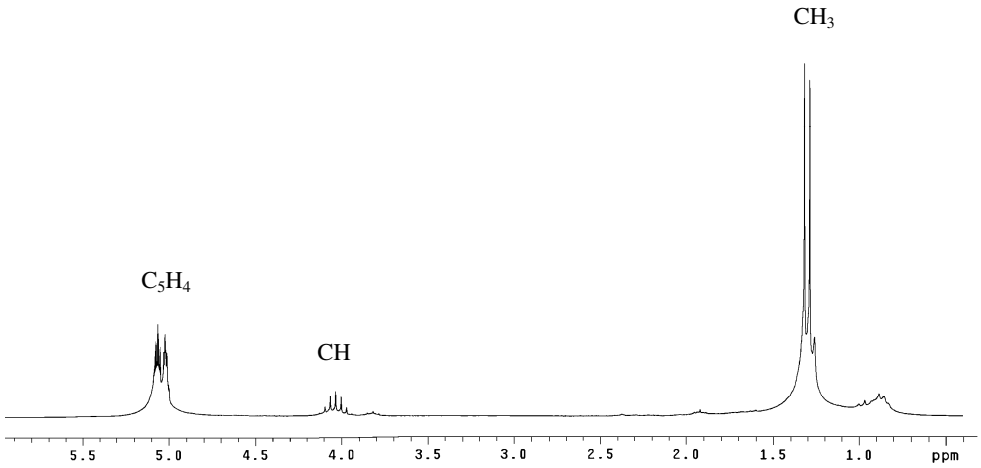


**Figure 3.4.** $^{1}$H NMR spectrum of **9** in chloroform-d at 20 °C

The $^{1}$H NMR spectrum of ($\eta^5$-$C_5H_4OC_3H_5$)$Re(CO)_3$ (**10**) displayed a multiplet at 5.09 ppm attributed to the ($\eta^5$-$C_5H_4$) ring protons (Figure 3.5). The assignement of the allyl protons is given below (Figure 3.5). In $^{13}$C NMR spectrum of **10** the $C_{CO}$ resonated at 194.1, the $C_{ipso}$ of the $C_5H_4$ gave rise to a signal at 143.8 ppm. The two resonances at 78.4 and 72.4 were attributed to the carbon atoms of the $C_5H_4$ group in proximal and distal position of the allyl group, which was confirmed by three resonances at 66.7, 119.2 and 131.4 ppm.

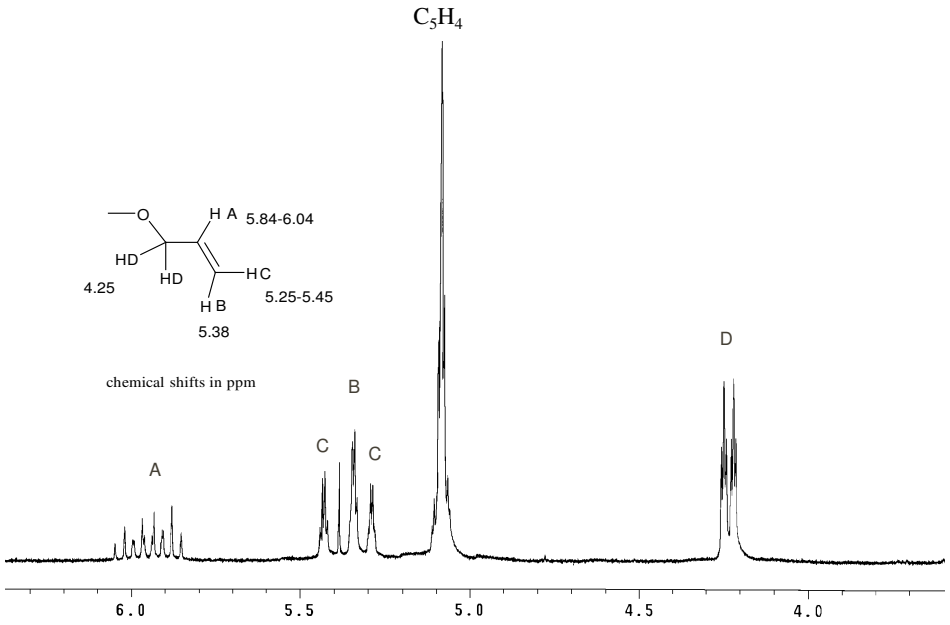


**Figure 3.5.** $^{1}$H NMR spectrum of **9** in chloroform-d at 20 °C

The IR spectrum of **10** confirmed the existence of a $Re(CO)_3$ unit. Two bands apparead at 2020 and 1914 $cm^{-1}$. The mass spectrum showed the expected molecular-ion peak at *m/z* 392 and fragment ion peak corresponding to elimination of CO and to the release of the allyl group.

The $^1H$ NMR spectrum of ($\eta^5$-$C_5H_4OCH_2Ph$)$Re(CO)_3$ (**11**) in $CDCl_3$ showed two triplets at 5.13 and 5.11 ppm attributed to the ($\eta^5$-$C_5H_4$) ring protons (Figure 3.6). The two H benzylic protons appeared at 4.73 ppm and the aromatic protons were attributed to the singlet at 7.41 ppm. In the $^{13}C$ NMR spectrum, the carbonyl groups gave rise to a signal at 194.2 ppm and the carbon atoms of the ($\eta^5$-$C_5H_4$) ring were identified by resonances at 143.8, 134.7 and 128.8 ppm. In the IR spectrum two bands corresponding to the CO groups of the $Re(CO)_3$ unit appeared at 2020 and 1930 $cm^{-1}$. The mass spectrum of **11** displayed a molecular-ion peak at m/z 442 corresponding to the cation [($\eta^5$-$C_5H_4COCH_2Ph$)$Re(CO)_3$]$^+$ and fragment-ion peaks corresponding to CO elimination and benzyl elimination at m/z 386 [($\eta^5$-$C_5H_4CO$ $CH_2Ph$)$Re(CO)$]$^+$, 358 [($\eta^5$-$C_5H_4CH_2Ph$)$Re$]$^+$ , 351 [($\eta^5$-$C_5H_4$)$Re(CO)_3$]$^+$ and 267 [($\eta^5$-$C_5H_4$)$Re$]$^+$

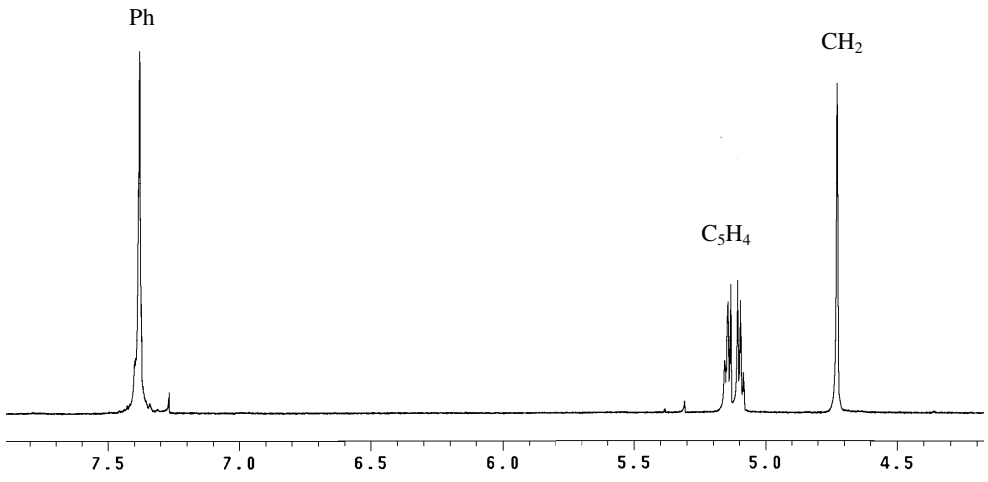


**Figure 3.6.** $^1H$ NMR spectrum of **11** in chloroform-d at 20 °C

X-ray diffraction studies of **11** showed that the compound crystallizes in a monoclinic system $P2_1/C$ (Figure 3.7). Selected bond distances and bond angles are listed in Table 3.3. The X-ray data collection and processing parameters are listed in table 7.3.4.

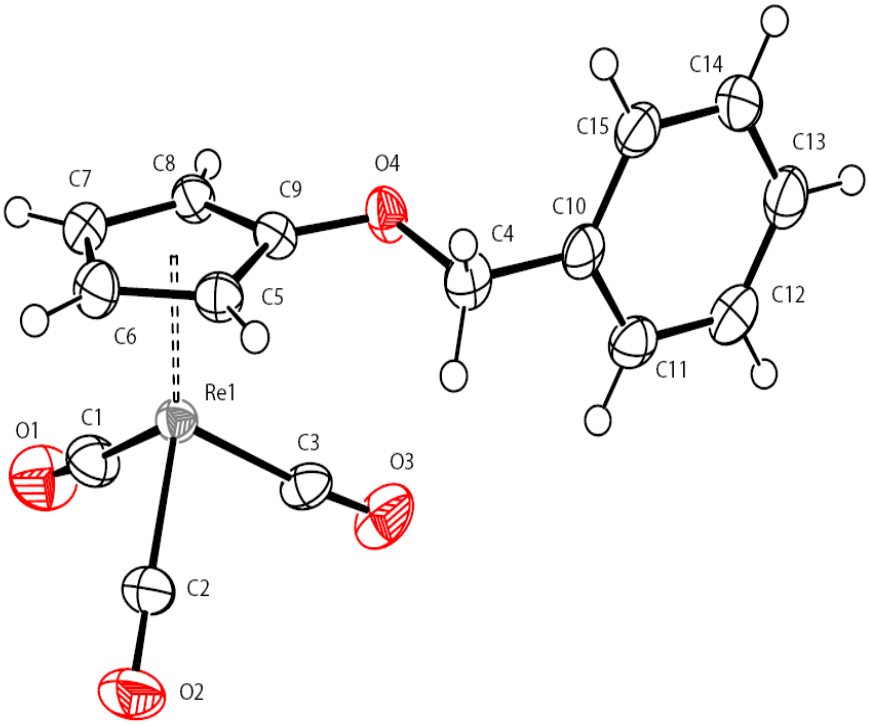


**Figure 3.7.** X-ray structure of **11** (ORTEP representation with selected atomic labels). Thermal ellipsoids are shown with a 50% probability level.

**Table 3.3** Selected bond distances (Å) and bond angles (°) of **11**

| Selected bond distances (Å) | | Selected angles (°) | |
|---|---|---|---|
| Re1-C1 | 1.909(5) | C8-C4-C5 | 108.8(3) |
| Re1-C2 | 1.921(4) | C6-C5-C4 | 117.3(3) |
| Re1-C3 | 1.923(4) | C7-C6-C5 | 108.2(4) |
| C9-O4 | 1.448(5) | C6-C7-C8 | 108.3(4) |
| C1-O1 | 1.156(6) | C4-C8-C7 | 107.4(3) |
| C2-O2 | 1.148(5) | C1-Re1-C3 | 91.2(2) |
| C3-O3 | 1.144(5) | C1-Re1-C2 | 92.3(19) |
| C4-C5 | 1.419(5) | C3-Re1-C2 | 89.95(18) |
| C5-C6 | 1.432(6) | O1-C1-Re1 | 176.4(4) |
| C6-C7 | 1.418(6) | O2-C2-Re1 | 177.3(4) |
| C7-C8 | 1.425(6) | O3-C3-Re1 | 175.3(4) |
| C8-C4 | 1.425(6) | | |

## 3.3 Preparation of acyloxy tricarbonyl rhenium complexes

### 3.3.1 Preparation of acyloxy rhenium complexes from ($\eta^5$-$C_5H_4OH$)$Re(CO)_3$ (6)

($\eta^5$-$C_5H_4OH$)$Re(CO)_3$ (**6**) was expected to react with acyl halides under the conditions described previously for the preparation of alko rhenium complexes because they are more reactive than alkyl halides. Both the oxygen and the halogen atoms of acyl halides[39] enhance the electrophilicity of the carbon of the carbonyl group, which promotes the nucleophilic attack.

An excess of acyl chloride was added to a solution of acetonitrile containing 2 equivalents of sodium carbonate. After 10 hours under reflux, the solvent of the reaction mixture was removed under vacuum and the reaction products were isolated on silica gel. The compounds **12** and **13** were identified by $^1H$ and $^{13}C$ NMR and compared with pure samples (Table 3.4).

**Table 3.4** Preparation of acyloxy rhenium complexes.

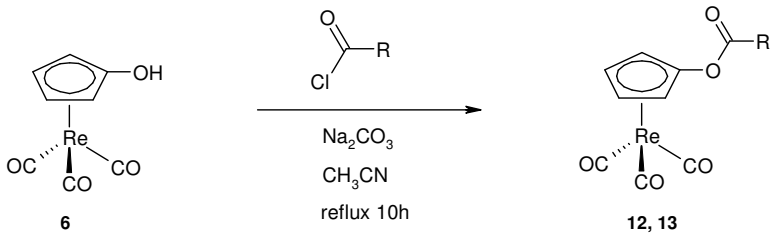


| Entry | RCOX | Product | Yield |
|---|---|---|---|
| 1 | 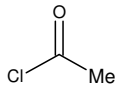 | **12** | 67 % |
| 2 | 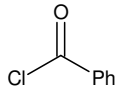 | **13** | 68 % |

The compounds **12** and **13** were characterized by $^1H$ and $^{13}C$ NMR, IR and their composition was determined by elemental analysis. X-ray diffraction studies on **13** confirmed its structure.

The $^{1}H$ NMR spectrum of **12** showed two triplets at 5.56 and 5.16 ppm corresponding to the $C_5H_4$ ring protons (Figure 3.8). A singlet at 2.19 ppm confirmed the presence of the methyl of the acyl group. In the $^{13}C$ NMR spectrum the presence of the $Re(CO)_3$ unit was also confirmed by a signal at 193.4 ppm and the $C_{CO}$ of the acyl moiety was confirmed by a resonance at 167.4 ppm. The $C_5H_4$ ring carbons were identified by three signals at 128.8, 79.4 and 74.5 ppm. A resonance at 20.8 ppm confirmed the existence of the $C_{Me}$ atom. Finally the IR spectrum revealed two bands at 2026 and 1929 $cm^{-1}$ attributed to the stretching of the carbonyl groups coordinated to rhenium.

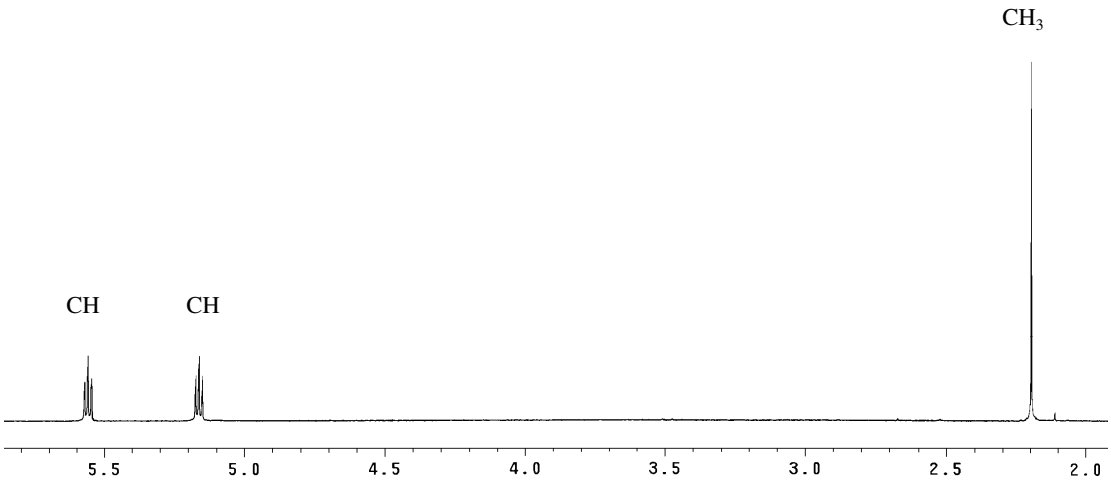


**Figure 3.8.** $^{1}H$ NMR spectrum of **12** in chloroform-d at 20 °C

The $^{1}H$ NMR of compound **13** revealed two triplets at 5.69 and 5.24 ppm attributed to the Cp ring protons. A multiplet at 8.07-8.05 ppm and two triplets at 7.48 and 7.66 ppm confirmed the presence of aromatic protons (Figure 3.9). The $^{13}C$ NMR spectra with two resonances at 193.4 and 163.4 ppm confirmed the presence of carbonyl groups. The signals at 128.8, 79.7 and 74.8 ppm were attributed to the carbon atoms of the Cp ring. The aromatic carbon atoms were identified by the resonances at 134.3, 130.2, 129.3 and 127.9 ppm. Finally the IR spectrum of **13** revealed two bands at 2026 and 1929 $cm^{-1}$ attributed to the $C_{CO}$ carbonyl groups coordinated to rhenium. The mass spectrum of **12** displayed a molecular-ion peak at m/z 456 corresponding to the cation $[(\eta^5\text{-}C_5H_4COPh)Re(CO)_3]^+$ and fragment-ion peaks corresponding to CO elimination and benzylcarbonyl elimination at m/z 428 $[(\eta^5\text{-}$

$C_5H_4COPh)Re(CO)_2]^+$, 400 $[(\eta^5\text{-}C_5H_4COPh)Re(CO)]^+$, 372 $[(\eta^5\text{-}C_5H_4COPh)Re]^+$ and 323 $[(\eta^5\text{-}C_5H_4)Re(CO)_2]^+$.

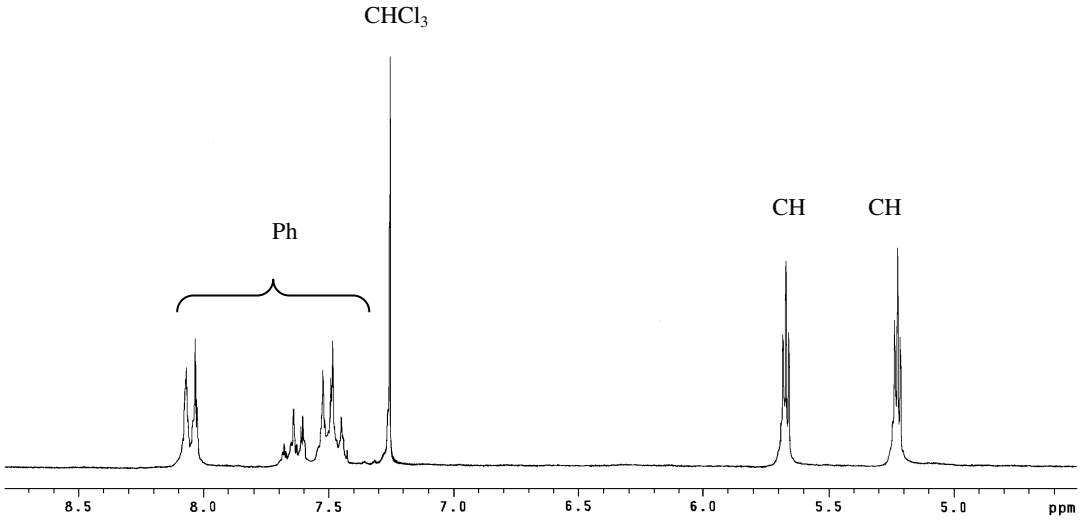


**Figure 3.9.** $^1$H NMR spectrum of **13** in chloroform-d at 20 °C

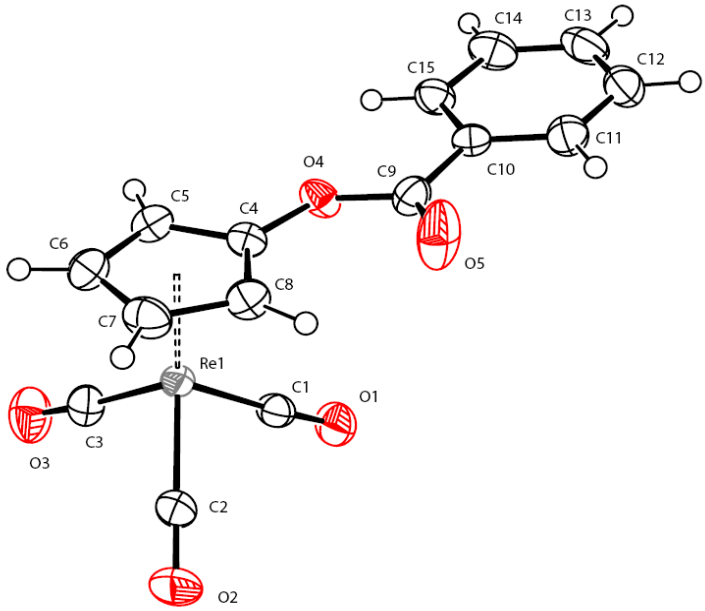


**Figure 3.10.** X-ray structure of **13** (ORTEP representation with selected atomic labels). Thermal ellipsoids are shown with a 50% probability level.

A few hundred milligrams of **13** were dissolved in ether and the solvent was allowed to evaporate slowly in a vial. The colorless crystals were suitable for X-ray diffraction. X-ray

diffraction studies showed that compound **13** crystallized in a triclinic system P-1 (Figure 3.10). Selected bond distances and bond angles are listed in Table 3.5.

**Table 3.5** Selected bond distances (Å) and bond angles (°) of **13**

| Selected bond distances (Å) | | Selected angles (°) | |
|---|---|---|---|
| Re1-C1 | 1.910(5) | C8-C4-C5 | 110.0(4) |
| Re1-C2 | 1.912(5) | C6-C5-C4 | 106.3(5) |
| Re1-C3 | 1.906(5) | C7-C6-C5 | 108.8(5) |
| C4-O4 | 1.381(5) | C6-C7-C8 | 107.7(5) |
| C1-O1 | 1.150(6) | C4-C8-C7 | 107.2(5) |
| C2-O2 | 1.146(7) | C1-Re1-C3 | 88.4(2) |
| C3-O3 | 1.144(7) | C1-Re1-C2 | 91.9(2) |
| C4-C5 | 1.424(7) | C3-Re1-C2 | 90.8(2) |
| C5-C6 | 1.413(7) | O1-C1-Re1 | 176.1(4) |
| C6-C7 | 1.427(9) | O2-C2-Re1 | 175.8(5) |
| C7-C8 | 1.422(8) | O3-C3-Re1 | 177.9(6) |
| C8-C4 | 1.402(7) | | |
| C9-O5 | 1.183(7) | | |

### 3.3.2 Preparation of acyloxy rhenium complexes in “one-pot”.

In the conditions of Williamson that we described previously, the base generates the cyclopentadienyl oxide ($\eta^5$-$C_5H_4ONa$)$Re(CO)_3$ in situ. Then the nucleophilic attack can take place on the acyl chloride (RCOCl) to give the corresponding acyloxy cyclopentadienyl complex ($\eta^5$-$C_5H_4OCOR$)$Re(CO)_3$ (Scheme 3.4).

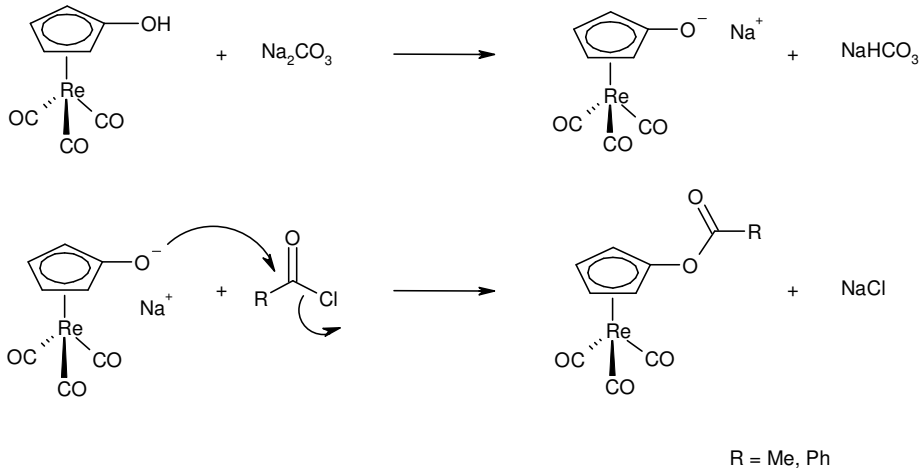


**Scheme 3.4**

We previously showed that the reaction of **2** with $(Me_3SiO)_2$ produced the cyclopentadienyl oxide **5**. We decided to utilize this oxide in situ to produce acyloxy rhenium complexes at room temperature in "one pot". The reaction of **2** with $(Me_3SiO)_2$ produced also the side product **3**, but it was expected not to react with acyl chloride.

Practically ($\eta^5$-cyclopentadienyl)(tricarbonyl)rhenium (**1**) was dissolved in THF and treated with butyl lithium at -78°C. After 30 min, the solution was allowed to warm to room temperature and dioxybis(trimethylsilane) $(Me_3SiO)_2$ was added to the mixture. After another 30 min, the mixture was treated with an excess of acyl chloride (ClCOR, R = Me, Ph) (1.2 equivalents). After 4 h, the solvent was removed *in vacuo* and the products were isolated by chromatography on silica gel and identified by $^1$H NMR spectroscopy. The reaction afforded the expected compound **12** in the presence of acetyl chloride and **13** in the presence of benzoyl chloride. **12** and **13** were obtained in the moderate yields of 22 and 25 % respectively (Table 3.6). These low yields are due to the formation of **3**. This undesired compound could be however reconverted into **6** as described in the previous chapter in the presence of TBAF in THF.

**Table 3.6** Preparation of the acyloxy derivatives **12** and **13** in "one pot"

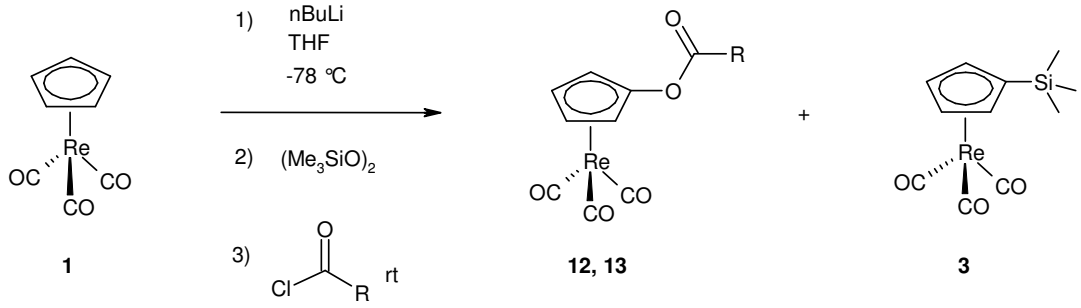


| Entry | XCOR | Products | Yields (%)[a] |
|---|---|---|---|
| 1 | 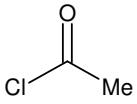 | **12 / 3** | 22 / 55 |
| 2 | 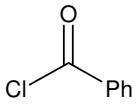 | **13 / 3** | 25 / 57 |

[a]isolated yields

### 3.3.3 Conclusion

Treatment of **1** with successively butyl lithium, dioxybis(trimethylsilane) and acyl chloride, ethanoyl chloride or benzoyl chloride, produced the corresponding acyloxy cyclopentadienyl tricarbonyl rhenium complexes **12** and **13**. It is a novel, quick and simple procedure to generate various acyloxy cyclopentadienyl tricarbonyl rhenium complexes.

## 3.4 Spectroscopic data

**Table 3.7** Spectroscopic data

| Entry | Product | $^{1}$H (δ ppm, 200 MHz, $CDCl_3$) | $^{13}$C (δ ppm, 200 MHz, $CDCl_3$) | IR ([a]:DCM, [b]:KBr, $cm^{-1}$) |
|---|---|---|---|---|
| 1 | **1** | 5.38 (s, 5H) | 193.8, 84.5 | 2024 (s), 1926 (vs) [a] |
| 2 | **6** | 5.10 (*pseudo* t, 2H, J = 2.2Hz), 5.03 (*pseudo* t, 2H, J = 2.2Hz) | 194.4, 140.1, 78.4, 67.8 | 3100 (w), 2021 (s), 1923 (vs) [a] |
| 3 | **12** | 5.56 (*pseudo* t, 2H, J = 2.2Hz), 5.16 (*pseudo* t, 2H, J = 2.2Hz), 2.19 (s, 3H) | 193.4, 167.4, 128.8, 79.4, 74.5, 20.8 | 2026 (vs), 1929 (vs) [a] |
| 4 | **3** | 5.42 (*pseudo* t, 2H, J = 2.2Hz), 5.40 (*pseudo* t, 2H, J = 2.2Hz), 0.25 (s, 9H) | 194.2, 91.8, 91.8, 86.3, 0.0 | 2021 (vs), 1922 (vs), 1263 (s), 840 (w) [a] |
| 5 | **13** | 8.07-8.05 (m, 1H), 7.66 (m, 2H), 7.48(m, 2H), 5.69 (pseudo t, 2H, J = 2.2Hz), 5.24 (pseudo t, 2H, J = 2.2Hz) | 193.4, 163.4, 134.3, 130.2, 129.3,128.8, 127.9, 79.7, 74.8 | 2026 (vs), 1929 (vs) [a] |
| 6 | **7** | 5.08 (m, 4H), 3.59 (s, 3H) | 194.1, 145.1, 78.3, 66.1, 58.3 | 2021 (s), 1924 (vs) [a] |
| 7 | **8** | 5.06 (m, 4H), 3.77 (q, 2H, *J* = 6Hz), 1.33 (t, 3H, *J* = 6Hz) | 194.3, 144.4, 78.4, 67.4, 66.2, 14.4 | 2021 (s), 1922 (vs) [a] |
| 8 | **9** | 5.06 (m, 2H), 5.02 (m, 2H), 4.03 (m, 1H, *J* = 6Hz), 1.30 (d, 6H, *J* = 6Hz) | 194.5, 144.2, 78.4, 67.8, 66.3, 21.9 | 2020 (vs), 1921 (vs), 1488 (w) [a] |
| 9 | **10** | 6.04-5.84 (m, 1H), 5.36 (dquart, 1H) 5.34 (t, 1H), 5.09 (m, 4H), 4.23 (t, 1H), 4.25(t, 1H) | 194.0, 143.8, 131.4, 119.2, 78.4, 72.4, 66.7 | 2019 (vs), 1914 (vs) [a] |
| 10 | **11** | 5.13 (*pseudo* t, 2H, *J* = 2.4Hz), 5.11 (*pseudo* t, 2H, *J* = 2.4Hz), 4.73 (s, 2H) | 194.2, 143.8, 134.7, 128.8, 128.2, 78.5, 73.7, 66.8 | 2020 (s), 1930 (vs) [a] |

## 3.5 Crystallographic data

**Table 3.8** Relevant structural parameters for the complexes ($\eta^5$-$C_5H_4R$)$Re(CO)_3$.

| -R | Mean *d* [Re – C(O)] | Mean ∠ (O)C – Re – C(O) | Mean ∠ Re – C – O | *d* [Re – C(R)] | *d* [Re – Ct] | *d* [C – R] |
|---|---|---|---|---|---|---|
| -H (**1**) | 1.894 Å | 90.0° | 177.7° | 2.284 Å | 1.957 Å | 0.806 Å |
| -$SiMe_3$ (**3**) | 1.855 | 91.1 | 175.5 | 2.280 | 1.949 | - |
| -OH (**6**) | 1.915 | 89.9 | 177.5 | 2.359 | 1.967 | 1.356 |
| -OLi (**5**) | 1.917 | 91.4 | 177.1 | 2.465 | 1.977 | 1.285 |
| -OCOPh (**13**) | 1.909 | 90.4 | 176.6 | 2.328 | 1.963 | 1.381 |
| -OMe (**7**) | 1.924 | 90.0 | 177.1 | 2.356 | 1.966 | 1.365 |
| -$OCH_2Ph$ (**11**) | 1.918 | 91.1 | 176.3 | 2.361 | 1.968 | 1.352 |

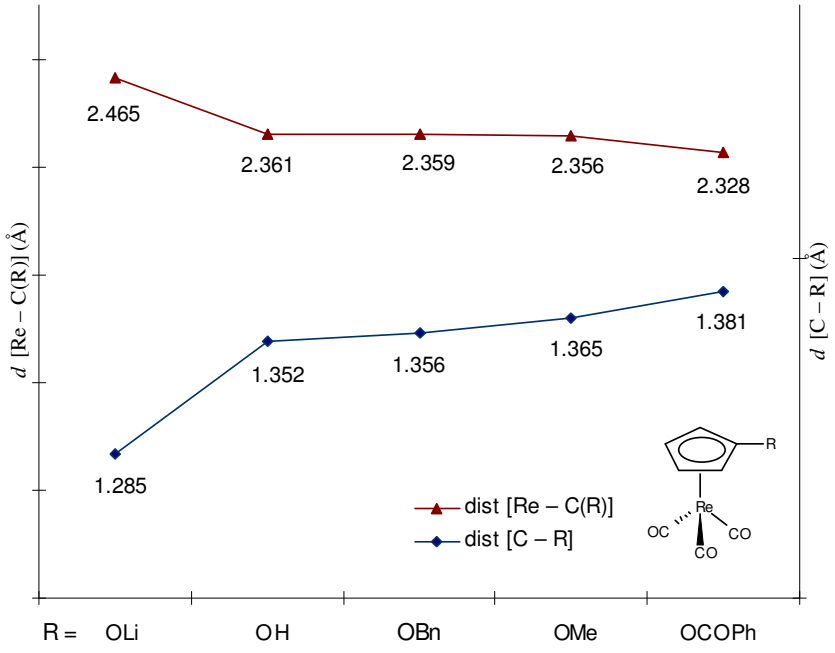


**Figure 3.11.** Distances [Re – C(R)] and [C – R] in the ($\eta^5$-cyclopentadienyl)-(tricarbonyl)rhenium complexes ($\eta^5$-$C_5H_4R$)$Re(CO)_3$.

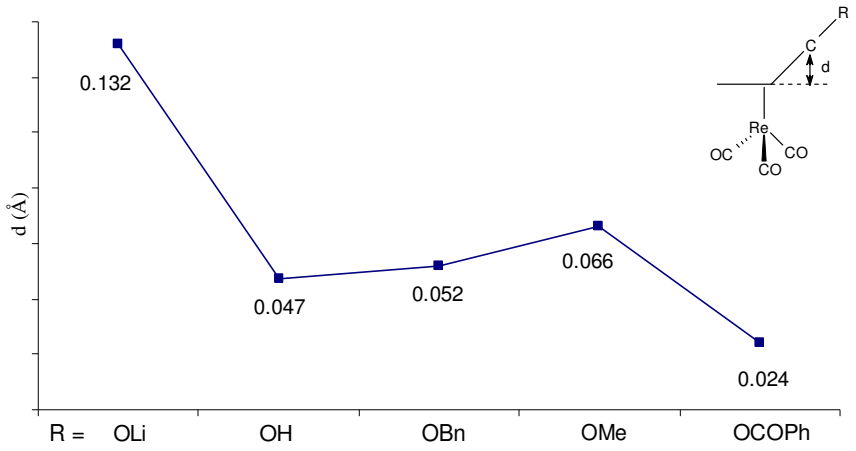


**Figure 3.12.** Deviation d in the ($\eta^5$-cyclopentadienyl)(tricarbonyl)rhenium complexes ($\eta^5$-$C_5H_4R$)$Re(CO)_3$.

### 3.6 Deprotection of ($\eta^5$-$C_5H_4OCH_2Ph$)$Re(CO)_3$ (11)

The benzyl group is commonly used as a protecting group. This group is stable under basic and acidic conditions, withstand oxidizing agents and common nucleophiles and electrophiles. Hydrogenation with nickel or palladium is the common method used to remove the benzyl group[40-45]. Under a pressure of 1.5 atmosphere with palladium on activated carbon, the deprotection is quantitative.

[$\eta^5$-(Benzyloxy)cyclopentadienyl](tricarbonyl)rhenium **11** was dissolved in deuterated methanol. A catalytic amount of palladium was added to the mixture. The tube was filled with hydrogen gas (1.5 atm) and the mixture was heated to 40°C. The deprotection of **11** was controlled by $^1$H NMR spectroscopy, the sample was measured at different times (t = 0 h, t = 4 h, t = 20, t = 24 h) (Scheme 3.5).

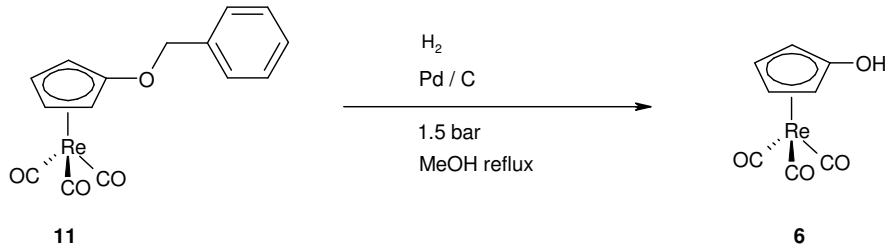


**Scheme 3.5**

At t = 0 h, the $^1$H NMR spectrum of the deprotection shows two triplets at 5.13 and 5.11 ppm corresponding to the protons of the ($\eta^5$-$C_5H_4$) ring and a singlet at 4.73 ppm corresponding to the protons at the benzylic position. A pure sample of **6** was measured in methanol. The $^1$H NMR spectrum showed two signals at 5.03 and 5.11 ppm. At t = 0 h, we observed the two signals of **11** at 5.13 and 5.11 ppm and an intense signal at 4.88 ppm corresponding to methanol. At t = 4 h, the $^1$H NMR spectrum showed two new signals at 5.03 and 5.11 ppm corresponding to **6**. After twenty hours, $^1$H NMR spectroscopy indicated that conversion of **11** into **6** was already quantitative (Figure 3.13). After 24 hours, the conversion was almost total. And after 30 hours, the proton signals of **11** disappeared.

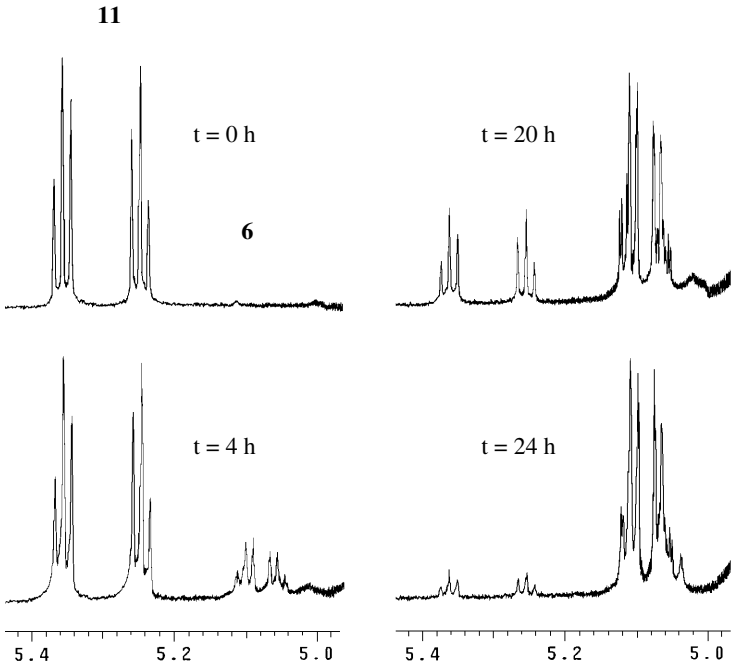


**Figure 3.13.** Hydrogenolysis of **11** - $^1$H NMR spectrum in methanol-$d_4$

The removal of the benzyl group by hydrogenation was successful with a total conversion of **11** into **6**.

## 3.7 Summary

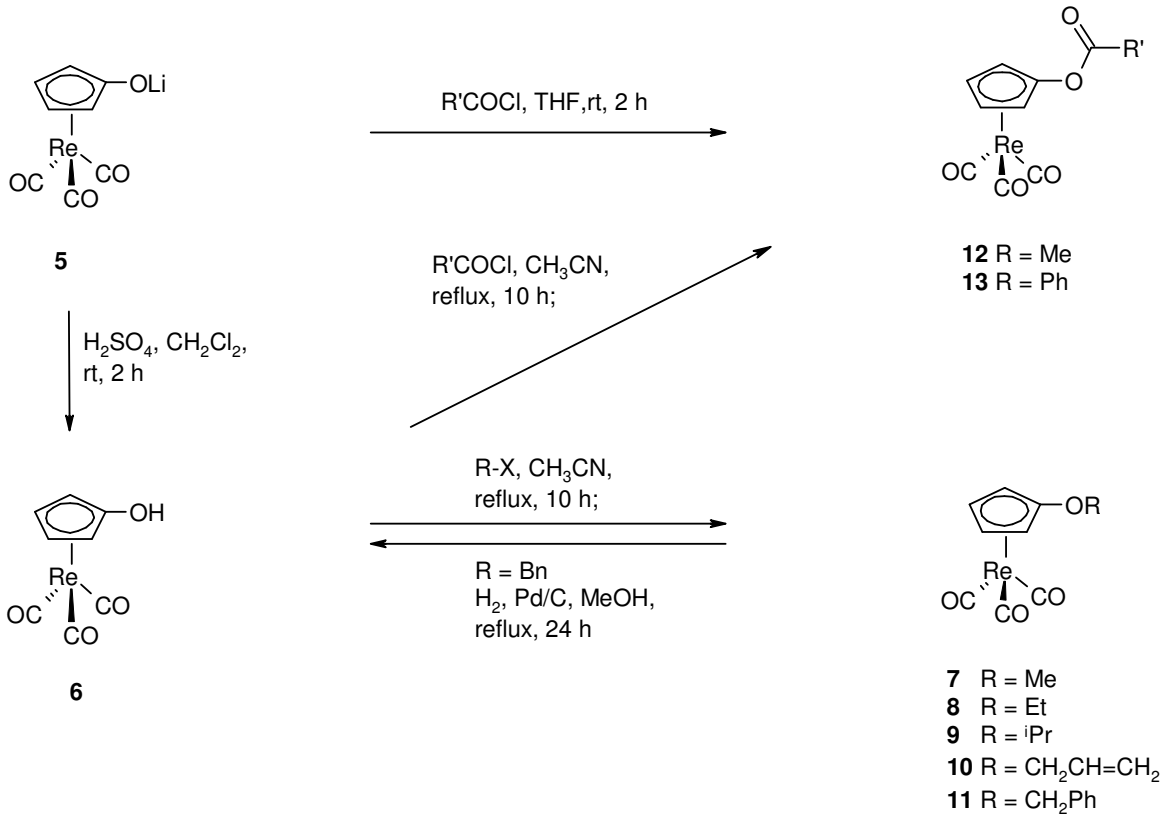


**Scheme 3.6**

The compound **5** was protonated in a biphasic solution of dichloromethane and aqueous sulfuric acid to give the hydroxyl compound **6**. The hydroxyl derivative **6** was reacted with various alkyl and acyl halides in acetonitrile under reflux on sodium carbonate. The corresponding products **12**, **13**, **7**, **8**, **9**, **10** and **11** were obtained in good yields. The products **12** and 1**3** could be also obtained from **5** at room temperature. Finally the benzyl derivative **11** was subjected to hydrogenolysis which regenerated the compound **6** (Scheme 3.6).

## 3.8 Conclusion

The preparation of ester and ether derivatives was facile. The compounds are stable under ambient atmosphere and they can be purified by flash chromatography on silica gel. The ether series is a new class of compounds. These series show that the hydroxyl group can be easily protected. The removal of the benzyl group from **11** regenerating **6** shows also that the deprotection of the OH group is feasible under mild conditions.

## 3.9 References

[1] W. Williamson, *J. Chem. Soc.* **1852**, *4*, 106.

[2] W. Williamson, *J. Chem. Soc.* **1852**, *4*, 229.

[3] O. C. Dermer, *Chem. Rev.* **1934**, *14*, 385.

[4] A. Hassner, C. Stumer, *Org. Synth. Based on Name reactions and Unnamed Reactions*, Pergamon: Kidlington, **1994**, 419.

[5] S. R. Sandler, W. Karo, *Organic Functional Group Preparations 1*, Academic: New York **1983**, 132.

[6] F. Montanari, P. Tundo, *J. Org. Chem.* **1981**, *46*, 2125.

[7] J. G. Hefferman, D. C. Sherrington, *Tetrahedron lett.* **1983**, *24*, 1661.

[8] R. Neumann, Y. Sasson, *J. Mol. Catal.* **1985**, *31*, 81.

[9] C. J. Thoman, T. D. Habeeb, M. Huhn, M. Korpusik, D. F. Slish, *J. Org. Chem.* **1989**, *54*, 4476.

[10] J. Alvarez-Builla, J. J. Vaquero, J. L. Garcia-Navio, J. F. Cabello, C. Sunkel, M. Fau de Casa-Juana, F. Dorrego, L. Santos, *Tetrahedron* **1990**, *46*, 967.

[11] S. N. Tan, R. A. Dryfe, H. H. Girault, *Helvetica Chimica Acta* **1994**, *77*, 231.

[12] A. Banerjee, K. Lee, D. E. Falvey, *Tetrahedron* **1999**, *55*, 12699.

[13] G. D. Yadav, N. M. Desai, *Catal. Commun.* **2006**, *7*, 325.

[14] K. K. Park, J. S. Jeong, *Tetrahedron* **200**5, *61*, 545.

[15] M. Lloung, A. Loupy, S. Marque, A. Petit, *Heterocycles* **2004**, *63*, 297.

[16] K. D. Raner, C. R. Strauss, R. W. Trainor, J. S. Thorn, *J. Org. Chem.* **1995**, *60*, 2456.

[17] N. Bagett, *Comprehensive Organic Chemistry* **1979**, Pergamon Press, New York, 799-850.

[18] U. E. Diner, F. Sweet, R. K. Brown, *Can. J. Chem.* **1966**, *4*, 1591.

[19] H. Plenio, A. Warnecke, *Organometallics* **1996**, *15*, 5066.

[20] K. Jarowicki, P. Kocienski, *J. Chem. Soc., Perkin Transactions 1* **1998**, 4005.

[21] M. Bruce, Y. Roshan-Ali, *J. Chem. Res. S*. **1981**, 193.

[22] T. Ogawa, S. Nakabayasi, *Carbohydr. Res.* **1981**, *93*, C1-C5.

[23] T. Nukada, T. Kitajima, Y. Nakahara, T. Ogawa, *Carbohydr. Res.* **1992**, *228*, 157.

[24] T. Ogawa, S. Nakabayasi, T. Kitajima, *Carbohydr. Res.* **1983**, *114*, 225.

[25] T. Ogawa, T. Horisaki, *Carbohydr. Res.* **1983**, *123*, C1-C4.

[26] H. Iijima, T. Ogawa, *Carbohydr. Res.* **1988**, *172*, 183.

[27] H. Iijima, T. Ogawa, *Carbohydr. Res.* **1989**, *186*, 95.

[28] H. Iijima, T. Ogawa, *Carbohydr. Res.* **1989**, *186*, 107.

[29] H. Kunz, K. von dem Bruch, *Angew. Chem. Int. Ed. Engl.* **1994***, 33,* 101.

[30] K. Inomata, T. Yamamoyo, H. Kotake, *Chem. Lett.* **1981**, 1357.

[31] J. Tsuji, T. Yamakawa, *Tetrahedron lett.* **1979**, 63.

[32] M. Honda, H. Morita, I. Nagakura, *J. Org. Chem.* **1997**, *62*, 8932.

[33] M. Ishizaki, M. Yamada, S.-I. Watanabe, O. Hoshino, K. Nishitani, M. Hayashida, A. Tanaka, H. Hara, *Tetrahedron* **2004**, *60*, 7973.

[34] D. R. Vutukuri, P. Bharathi, Z. Yu, K. Rajasekaran, M.-H. Tran, S. Thayumanavan, *J. Org. Chem.* **2003**, *68*, 1146.

[35] A. Dahlen, A. Sundgren, M. Lahmann, S. Oscarson, G. Hilmersson, *Org. Lett.*, **2003**, *5*, 4085.

[36] S. Chandrasekhar, R. Reddy, R. J. Rao, *Tetrahedron* **2001**, *57*, 3435.

[37] T. W. Greene, P.G. M. Wuts, *Protective groups in Org. Synth., 3rd ed*. John Wiley & Sons: New York, **1991**.

[38] J. L. Romera, J. M. Cid, A. A Trabanco, *Tetrahedron lett.* **2004**, *45*, 8797.

[39] S. Patai, *The Chemistry of Acyl Halides* **1972**, Wiley-Interscience, New York.

[40] E. Llàcer, P. Romea, F. Urpí, *Tetrahedron lett.* **2006**, *47*, 5815.

[41] V. S. Rao, A. S. Perlin, *Carbohydr. Res.* **1980**, *83*, 175.

[42] J. S. Bajwa, *Tetrahedron lett.* **1992**, *33*, 2299.

[43] A. R. Vaino, W. T. Depew, W. A. Szarek, *Carbohydr. Res.* **1997**, *305*, 27.

[44] S. Hanessain, T. J. Liak, B. Vanasse, *Synthesis* **1981**, 396.

[45] D. C. Johnson, T. S. Widlanski, *Org. Lett.* **2004**, *6*, 4643.

# 4 Preparation of Amino Cyclopentadienyl Tricarbonyl Rhenium Complexes

## 4.1 Introduction

The initial retrosynthesis scheme presents the target molecule ($\eta^5$-$C_5H_4NHR$)Re(CO)(NO)H as a potential catalyst for "ionic hydrogenation" reactions. Its design was based on similar Shvo's bifunctional complexes possessing a NH acidic group on the cyclopentadienyl moiety and a hydride coordinated to the rhenium center. We suggested that ($\eta^5$-$C_5H_4NHR$)Re(CO)(NO)H could reduce unsaturated substrates via a concerted transfer of both the hydride from the rhenium and the proton from the NH group.

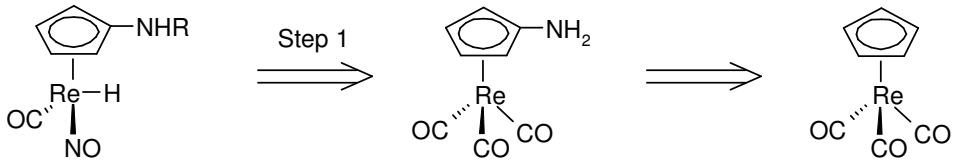


**Scheme 4.1**

The synthetic pathway to ($\eta^5$-$C_5H_4NHR$)Re(CO)(NO)H includes logically the tricarbonyl rhenium complex ($\eta^5$-$C_5H_4NH_2$)$Re(CO)_3$ as a precursor. This compound was not known and a synthetic route had to be developed. The preparation of ($\eta^5$-$C_5H_4NH_2$)$Re(CO)_3$ and various amino cyclopentadienyl rhenium complexes were reported in the following chapter.

## 4.2 ($C_5H_4NH_2$)$Re(CO)_3$ (15)

The similar manganese compound ($\eta^5$-$C_5H_4NH_2$)$Mn(CO)_3$ was reported in the literature[1], but not the related rhenium derivative. It is a two steps reaction. Cymantrene was treated with butyl lithium and then with tosyl azide. Cymantrenyl azide was then reduced with $NaBH_4$ in situ to yield ($\eta^5$-$C_5H_4NH_2$)$Mn(CO)_3$, which was isolated in a good yield of 70 %. Analogous to the preparation of ($\eta^5$-$C_5H_4NH_2$)$Mn(CO)_3$, hexane solution of *n*-butyl lithium (1.6 M, 1.2 equiv.) was added to a THF solution of **1** at -78°C. After 1 hour of stirring, para-toluenetosyl

azide was added to the mixture generating ($\eta^5$-cyclopentadienylazide)tricarbonylrhenium (**14**) that was reduced in situ with $NaBH_4$ to give **15** (Scheme 4.2).

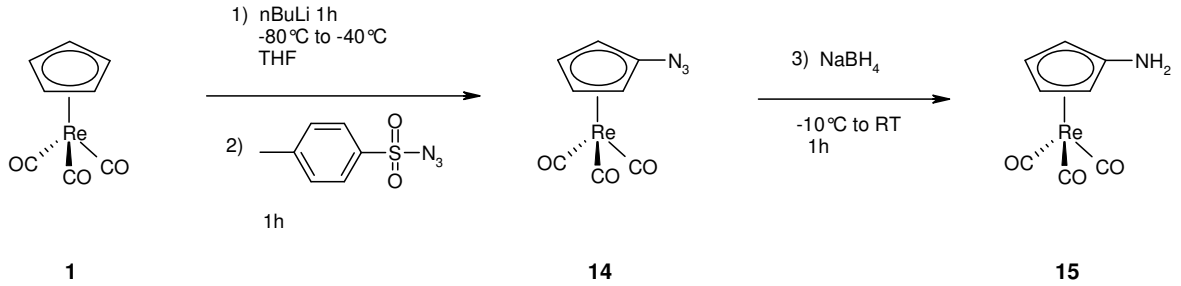


**Scheme 4.2**

The solvent of the reaction mixture was removed *in vacuo* and then the brown crude product **15** was transferred into a sublimation apparatus. Sublimation was carried out *in vacuo* at 130 °C to obtain **15**. Recrystallization could be effected in dichloromethane at –30°C by slow diffusion of hexane. Crystals of **15** were obtained, unfortunately the crystals were not suitable for X-ray diffraction analysis. After purification and recrystallization, the yield was 50 %. **15** was fully characterized by $^1H$, $^{13}C$ NMR and IR spectroscopy.

The reactive azide intermediate ($\eta^5$-$C_5H_4N_3$)$Re(CO)_3$ (**14**) could not be isolated, but characterized by $^1H$ NMR spectroscopy. $^1H$ NMR spectrum of **14** in $CD_3CN$ revealed two signals at 5.36 and 5.53 ppm which were assigned to the protons of the rhenium coordinated $\eta^5$-$C_5H_4$ group. (Figure 4.1).

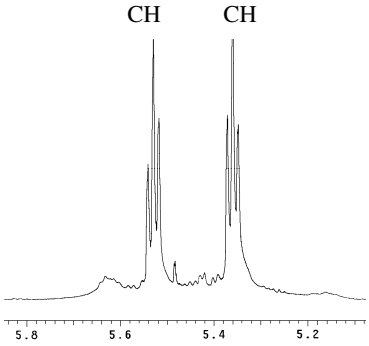


**Figure 4.1.** $^1H$ NMR spectrum of **14** in acetonitrile-$d_3$ at 20 °C

**15** was characterized by $^{1}H$, $^{13}C$ NMR, IR and mass spectroscopy. The $^{1}H$ NMR of **15** in acetonitrile-$d_3$ showed two triplets at 4.72 and 5.13 ppm, which confirmed the presence of a substituted ($\eta^5$-$C_5H_4$) group and a broad singlet at 4.05 ppm that confirmed the existence of a $NH_2$ group (Figure 4.2).

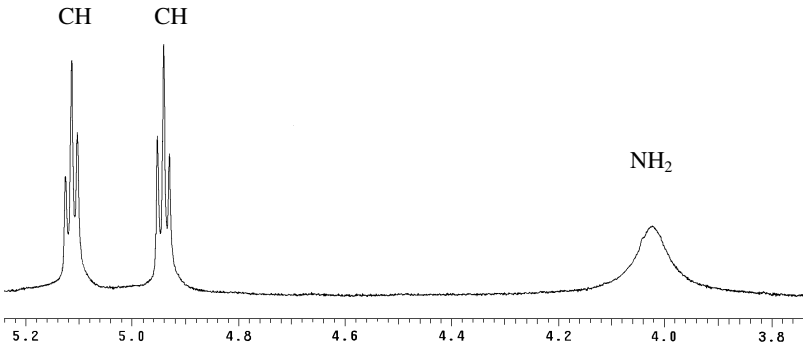


**Figure 4.2.** $^{1}H$ NMR spectrum of **15** in acetonitrile-$d_3$ at 20 °C

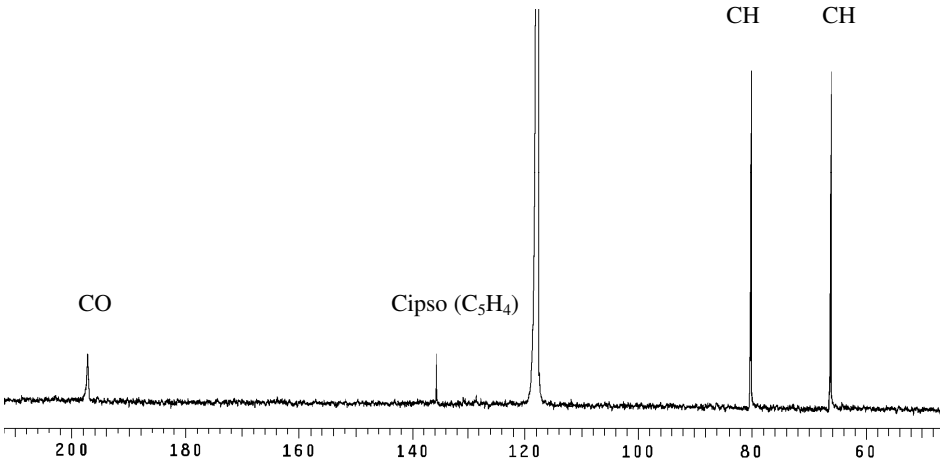


**Figure 4.3.** $^{13}C$ NMR spectrum of **15** in acetonitrile-$d_3$ at 20 °C

The $^{13}C$ NMR spectrum of **15** displayed two resonances at 66.4 ppm and 80.3 ppm attributed to the $C_5H_4$ ring carbon atoms. The resonance at 138.7 ppm was assigned to the ipso carbon atom bearing the $NH_2$ group. The presence of carbonyl groups was confirmed by a resonance at 197.3 ppm (Figure 4.3). The IR spectrum showed two ν(CO) bands at 2012 and 1917 $cm^{-1}$ confirming the $Re(CO)_3$ pattern. The mass spectrum of **15** revealed a molecular-ion peak at m/z 353 corresponding to the cation $[(\eta^5\text{-}C_5H_4NH_2)Re(CO)_3 + 2H]^+$.

## 4.3 $(C_5H_4N=CHPh)Re(CO)_3$ (16)

### 4.3.1 Preparation of 16

The reaction of primary amines with either alydehydes or ketones gives Shiff bases[2-16]. The mechanism involves a nucleophilic addition of the amine to the carbonyl group resulting in the formation of carbinolamine. Dehydratation of carbinolamine produces the corresponding imine. This condensation reaction is usually acid catalyzed. However condensation between aryl amines and aromatic aldehydes is favored and then does this reaction not require any catalyst. Shiff bases from aldehydes and aryl amines are very stable compounds (Scheme 4.4).

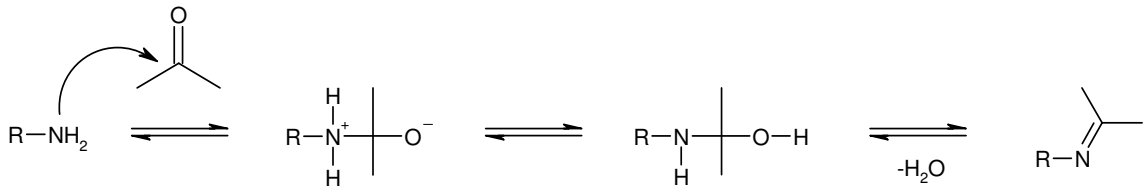


**Scheme 4.3** Schiff base formation

As expected ($\eta^5$-$C_5H_4NH_2$)$Re(CO)_3$ (**15**) reacted with benzaldehyde to afford [$\eta^5$-(phenylmethyleneamino)cyclopentadienyl](tricarbonyl)rhenium (**16**) (Scheme 4.5). The reaction was carried out in ethanol at room temperature. After 10 hours of stirring, the solvent was removed *in vacuo* and the product was crystallized by slow diffusion of hexane into a solution of dichloromethane at –30°C.

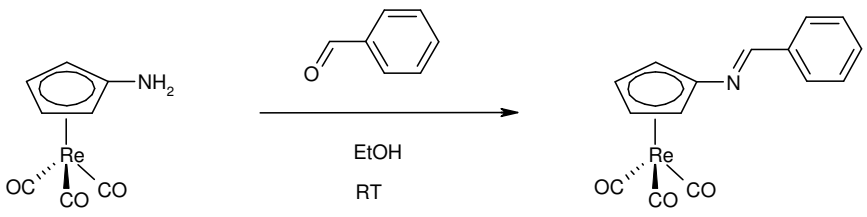


**15** **16**

**Scheme 4.4**

### 4.3.2 Characterization of 16.

**16** was fully characterized by $^{1}H$,$^{13}C$ NMR, IR, MS and elemental analysis. The $^{1}H$ NMR spectrum of the new compound **16** displayed a singlet at 8.40 ppm assigned to the imine proton, its chemical shift is consistent with that of other aromatic imines (Figure 4.4)[17-21]. The two triplets at 5.50 and 5.28 ppm were assigned to the $C_5H_4$ ring protons. The doublet of doublet at 7.82 ppm and the multiplet at 7.49 ppm confirmed the presence of the phenyl group. The $^{13}C$ NMR spectrum displayed a resonance at 164.9 ppm which also confirmed the existence of the imine carbon (Figure 4.5). The resonance at 194.1 ppm indicated the presence of carbonyl groups and the resonances at 134.9, 84.4 and 81.6 ppm were assigned to the carbons of the Cp ring. The four resonances at 132.2, 129.1, 128.9 and 127.8 ppm were assigned to the carbons of the phenyl group. The IR spectrum of **16** displayed two ν(CO) bands at 2021 and 1928 $cm^{-1}$ in accord with the local $C_{3v}$ symmetry of the $Re(CO)_3$ group. The mass spectrum of **16** revealed a molecular-ion peak at m/z 441, which corresponds to the cation $[(\eta^5\text{-}C_5H_4N{=}CHPh)Re(CO)_3 + 2H]^+$. The crystals obtained were suitable for X-ray diffraction. X-ray studies revealed that the compound crystallized in the monocyclic system $P2_1/_C$ (Figure 4.6). Selected bond distances and bond angles are listed in Table 4.1. The X-ray data collection and processing parameters are listed in Table 7.3.6.[22-24]

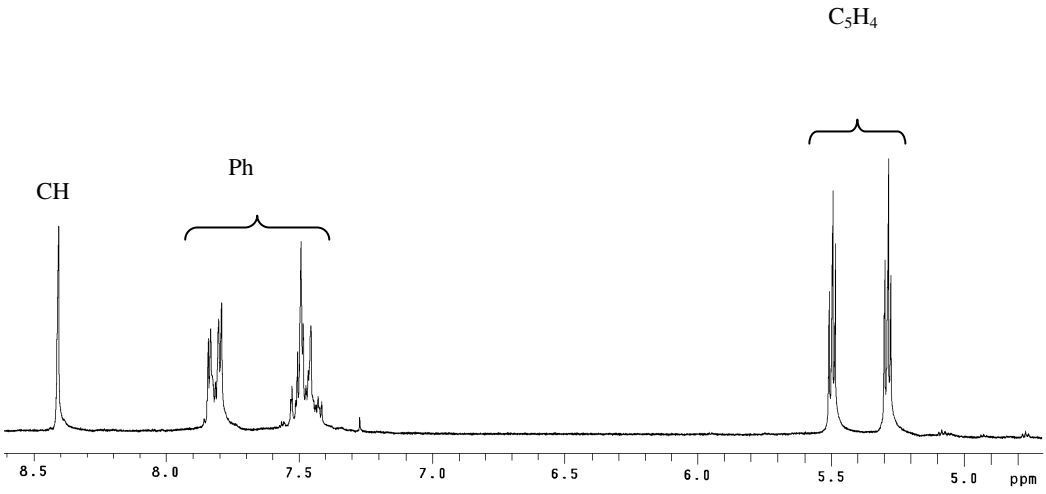


**Figure 4.4.** $^{1}H$ NMR spectrum in acetonitrile-$d_3$ of compound **16** at 20 °C

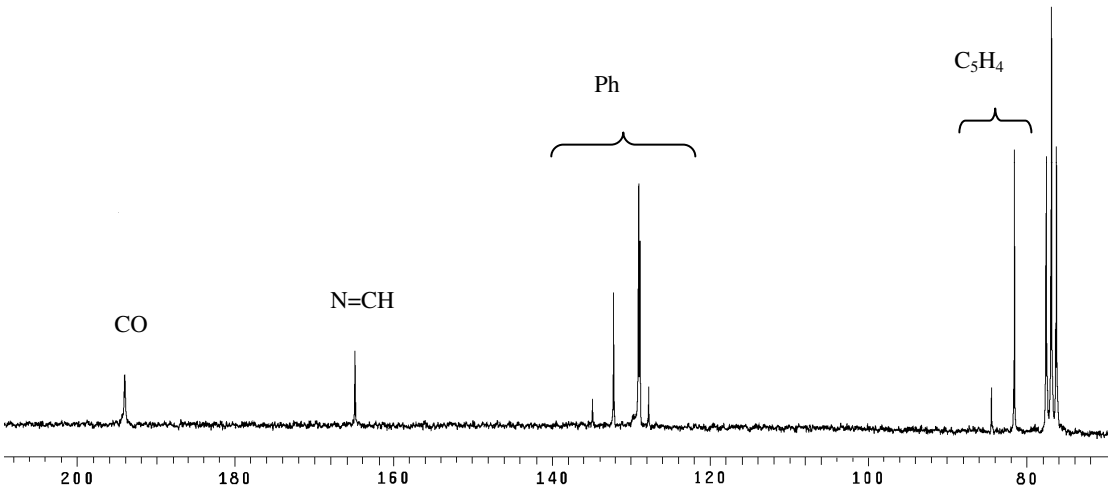


**Figure 4.5.** $^{13}C$ NMR spectrum of **16** in acetonitrile-$d_3$ at 20 °C

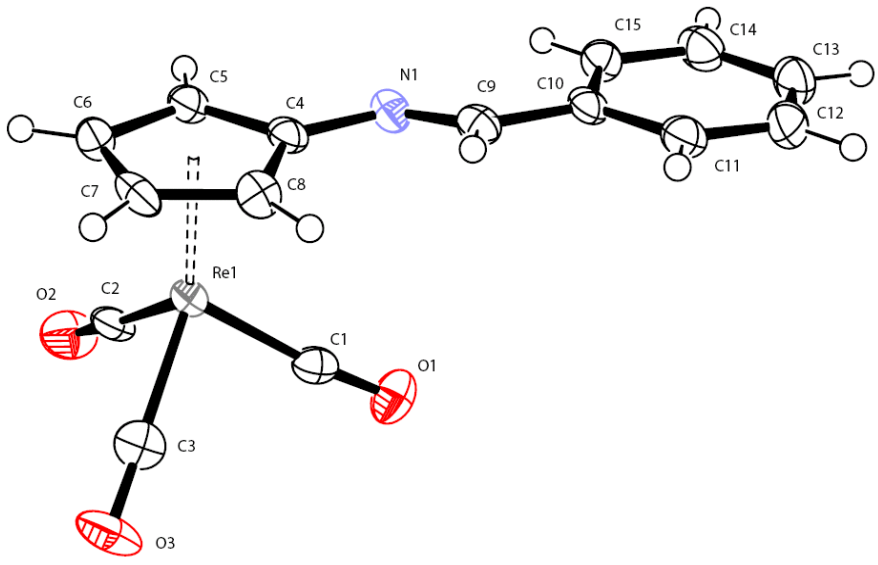


**Figure 4.6.** X-ray structure of **16** (ORTEP representation with selected atomic labels). Thermal ellipsoids are shown with a 50% probability level.

**Table 4.1** Selected bond distances (Å) and bond angles (°) of **16**

| Selected bond distances (Å) | | Selected angles (°) | |
|---|---|---|---|
| Re1-C1 | 1.911(8) | C8-C4-C5 | 107.7(6) |
| Re1-C2 | 1.922(6) | C6-C5-C4 | 108.5(5) |
| Re1-C3 | 1.926(7) | C7-C6-C5 | 106.9 (5) |
| C4-N1 | 1.414(8) | C6-C7-C8 | 110.2(6) |
| N1-C9 | 1.281(8) | C4-C8-C7 | 108.2(6) |
| C2-O2 | 1.142(7) | C1-Re1-C3 | 90.2(3) |
| C3-O3 | 1.138(8) | C1-Re1-C2 | 90.3(3) |
| C4-C5 | 1.418(8) | C3-Re1-C2 | 89.2(3) |
| C5-C6 | 1.426(9) | C4-N1-C9 | 117.3(5) |
| C6-C7 | 1.408(9) | N1-C9-C10 | 123.4(6) |
| C7-C8 | 1.406(9) | N1-C4-C8 | 131.0(5) |
| C8-C4 | 1.440(8) | | |

### 4.4 ($\eta^5$-$C_5H_4NHCH_2Ph$)$Re(CO)_3$ (17)

[$\eta^5$-(benzylamino)cyclopentadienyl](tricarbonyl)rhenium (**17**) was prepared from **15** and benzyl bromide. The reaction was carried out in acetonitrile under reflux. After 10 hours, the reaction mixture was removed *in vacuo*. **17** was purified by flash chromatography on silica gel in a 63 % yield (Scheme 4.5). The benzyl derivative **17** was also obtained by reduction of the imine **16** with 2 equivalents of $NaBH_4$ in ethanol[26-28].

**17** was isolated as a white solid. The $^1$H NMR spectrum of **17** in $CDCl_3$ revealed two triplets at 5.08 and 4.81 ppm. The benzylic carbon atom was confirmed by a signal at 4.00 ppm. The $^1$H NMR integration ratio confirmed the *mono* substitution. The NH group gave a signal at 3.30 ppm. The $^{13}$C NMR spectrum displayed the $C_{CO}$ at 195.2 ppm and the benzylic carbon atom gave rise to a signal at 51.6 ppm.

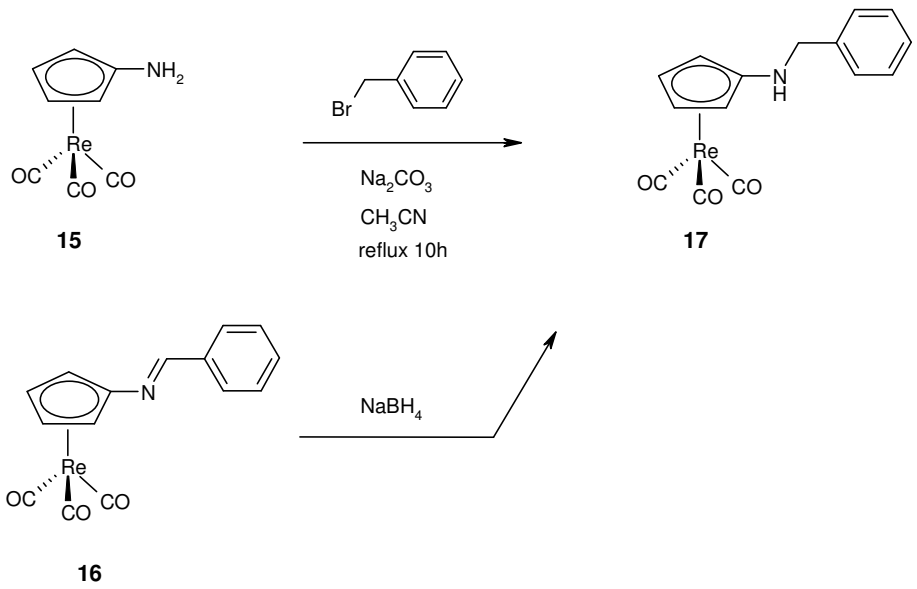


**Scheme 4.5**

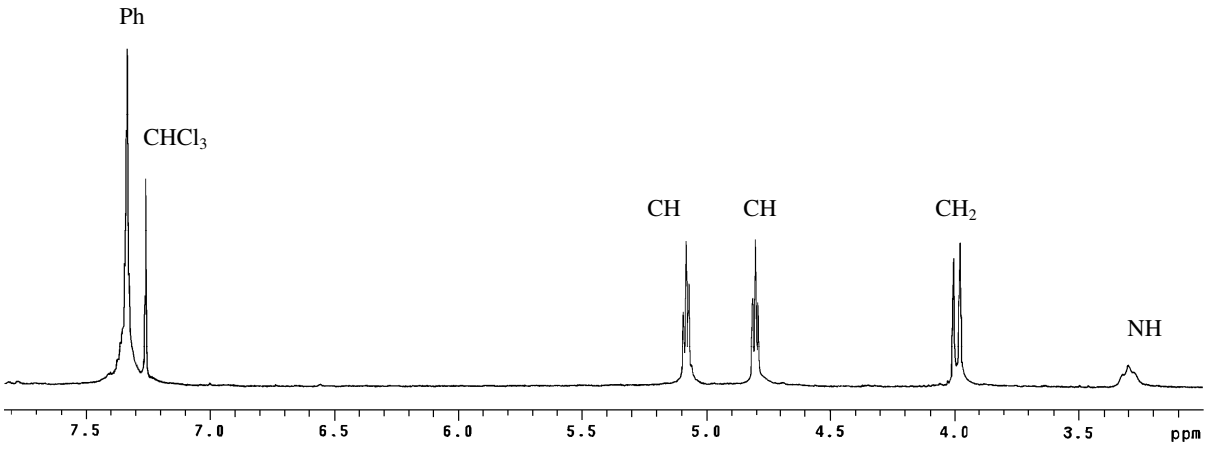


**Figure 4.7** $^{1}$H NMR spectrum in $CDCl_3$ of compound **17** at 20 °C

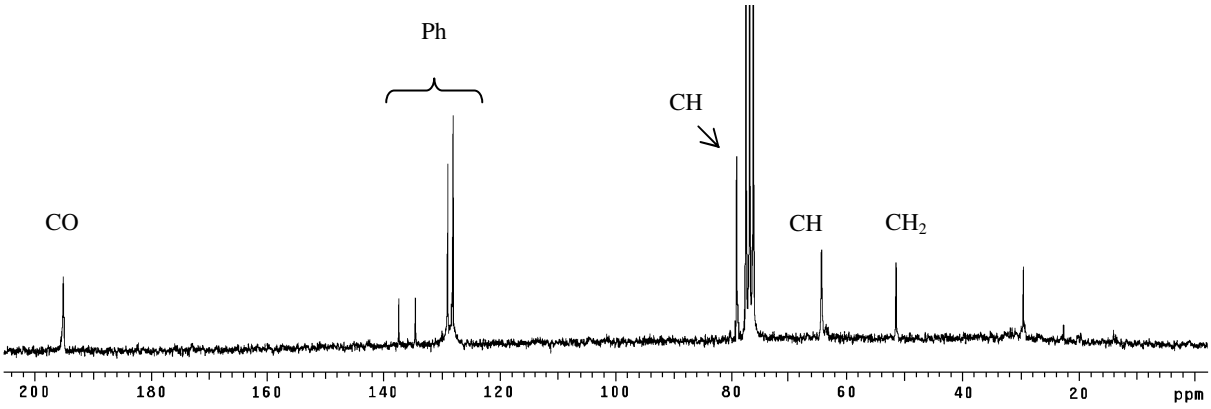


**Figure 4.8** $^{13}C$ NMR spectrum of **17** in $CDCl_3$ at 20 °C

## 4.5 $(C_5H_4NHCOCH_2Ph)Re(CO)_3$ (18)

### 4.5.1 Preparation of 18

The benzyloxycarbonyl group (Z) has proved to be a very useful functionality for the protection of amines and amine derivatives. This group is very convenient, since it is easily removable by catalytic hydrogenation. The Z group is stable to basic and most aqueous acidic conditions. Usually the protection of amino groups with Z is carried out in aqueous media in the presence of a base.

The Z group is particularly used in amino acid chemistry which requires protection of the carboxylic and amino groups[29-31]. The scheme below shows the synthesis of N-benzyloxycarbonyl-L-aspartate (Z-aspartate) (Scheme 4.6). The reaction is carried out in a biphasic medium. Benzylchloroformate, insoluble in water, is dissolved in toluene before addition to an aqueous basic solution of aspartic acid. The reaction affords at room temperature the protected Z-aspartate after 2 h of vigorous stirring.

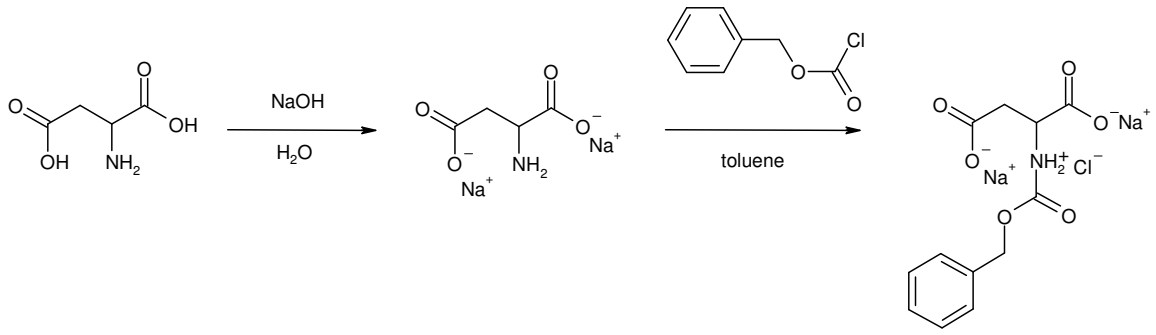


**Scheme 4.6** Protection of aspartate in a biphasic medium

We used this protection procedure to prepare ($\eta^5$-{[(benzyloxy)carbonyl]amino}-cyclopentadienyl)(tricarbonyl)rhenium (**18**). Given that both reagents **15** and benzychloroformate are not soluble in water, we selected an organic solvent in which water is miscible. Thus, an ethanol solution of ($\eta^5$-$C_5H_4NH_2$)$Re(CO)_3$ (**15**) and benzylchloroformate were added to an aqueous solution of $K_2CO_3$ (Scheme 4.7). After 10 h with vigorous stirring, the organic layer was collected and the solvent was removed *in vacuo*. The reaction afforded a new compound which was isolated and crystallized by slow diffusion of hexane into dichloromethane at – 30°C.

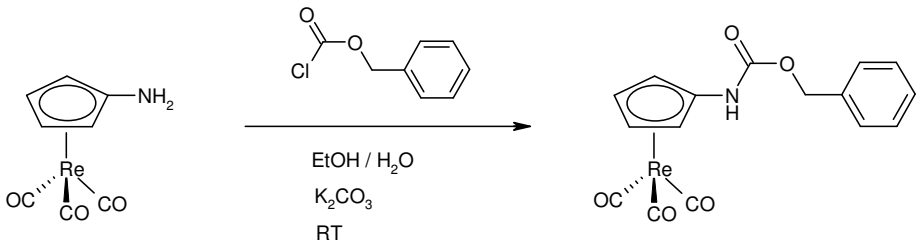


**15** **18**

**Scheme 4.7**

### 4.5.2 Characterization of 18

The new compound **18** was analytically pure and was fully characterized by $^1H$, $^{13}C$ NMR, IR, MS and elemental analysis. The $^1H$ NMR of **18** in acetonitrile displayed two triplets at

5.66 and 5.29 ppm, which were assigned to the $C_5H_4$ ring protons (Figure 4.7). The singlet at 5.12 ppm was assigned to the benzylic protons and the multiplet at 7.35 ppm to the phenyl protons. The broad signal at 7.75 ppm was attributed to the carbamate NH proton. Indeed, in $CDCl_3$ the $^1H$ NMR showed a resonance at 6.39 ppm which is consistent with the shift of a phenyl carbamate proton in this solvent. The proton chemical shifts of various phenyl carbamates are reported in Table 3.2. The chemical shifts values are located in the range of 6.59 to 7.13 ppm. The chemical shift value of 7.13 ppm corresponds to the *ortho* chloro substituted phenyl carbamate. The chlorine atom at the *ortho* position on the phenyl group enhances the acidity of the carbamate proton which then appears at lower field. The δ value for the new compound **18** is shifted upfield, which indicates that the cyclopentadienyl tricarbonyl rhenium moiety is slightly less electron withdrawing than the phenyl group. In $CDCl_3$ the $C_5H_4$ ring protons appear at noticeably different chemical shift as a multiplet at 5.17 ppm.

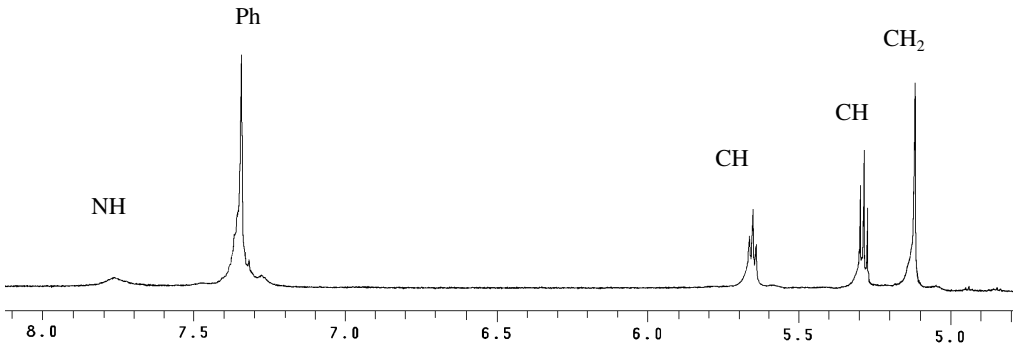


**Figure 4.9** $^1H$ NMR spectrum of **18** in acetonitrile-$d_3$ at 20 °C

The $^{13}C$ NMR spectrum of **18** showed a resonance at 193.9 ppm which confirmed the existence of metal bound carbonyl groups. The resonance at 152.5 ppm was assigned to the $C_{CO}$ atom of the carbamate group, which is consistent with the normal range for carbamate chemical shifts (Table 4.2). The resonance at 71.6 ppm was attributed to the $C_{benzyl}$.

**Table 4.2** Chemical shifts of various carbamates

| Phenylcarbamate | $^{1}$H NMR δ (ppm) in $CDCl_3$ | $^{13}$C NMR δ (ppm) in $CDCl_3$ |
|---|---|---|
| methyl phenylcarbamate[10] | 6.79 | 154.3 |
| ethyl phenylcarbamate[11] | 6.74 | 154.0 |
| dodecyl phenylcarbamate[12] | 6.68 | 153.8 |
| 8-dodecylthio-5,7-octadiynyl(o-chlorophenyl)carbamate[34] | 7.13 | 153.2 |
| 8-dodecylthio-5,7-octadiynyl(p-chlorophenyl)carbamate[35] | 6.59 | 153.3 |
| 8-dodecylthio-5,7-octadiynyl(m-chlorophenyl)carbamate[36] | 6.64 | 153.2 |
| **18** | 6.39 | 152.5 |

In the IR spectrum of **18** the two ν(CO) bands at 2020 (m) and 1907 $cm^{-1}$ confirmed the existence of the $Re(CO)_3$ unit. The mass spectrum showed the molecular-ion peak at m/z 508, which corresponds to the cation $[(\eta^5\text{-}C_5H_4NHCOOCH_2Ph)Re(CO)_3 + Na]^+$.

The colorless crystals of **18** obtained were suitable for X-ray diffraction. The X-ray diffraction study confirmed the structure of **18**. The X-ray diffraction showed that the compound crystallized in a monocyclic system $P2_1/_C$ (Figure 4.10). Selected bond distances and bond angles are listed in Table 4.3. The X-ray data collection and processing parameters are listed in Table 7.3.7.

**Table 4.3** Selected bond distances (Å) and bond angles (°) of **18**.

| Selected bond distances (Å) | | Selected angles (°) | |
|---|---|---|---|
| Re1-C1 | 1.918(6) | C8-C4-C5 | 108.3(5) |
| Re1-C2 | 1.914(6) | C6-C5-C4 | 107.9(5) |
| Re1-C3 | 1.912(6) | C7-C6-C5 | 107.5(5) |
| C4-N1 | 1.408(7) | C6-C7-C8 | 109.0(5) |
| N1-C9 | 1.352(7) | C4-C8-C7 | 107.1(5) |
| C9-O4 | 1.208(7) | C4-N1-C9 | 124.4(5) |
| C9-O5 | 1.347(6) | N1-C9-O4 | 126.0(5) |
| O5-C10 | 1.462(7) | C9-O5-C10 | 117.2(4) |
| C1-O1 | 1.145(7) | O5-C10-C11 | 110.2(5) |
| C2-O2 | 1.150(7) | C1-Re1-C3 | 89.8(3) |
| C3-O3 | 1.148(7) | C1-Re1-C2 | 92.9(3) |
| C4-C5 | 1.411(8) | C3-Re1-C2 | 88.4(3) |
| C5-C6 | 1.424(8) | | |
| C6-C7 | 1.399(9) | | |
| C7-C8 | 1.419(8) | | |
| C8-C4 | 1.416(8) | | |

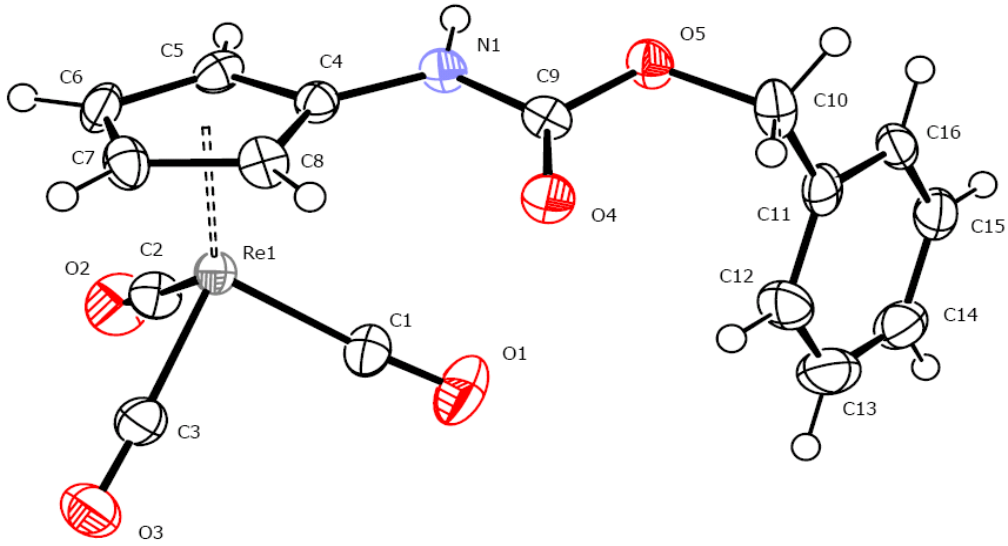


**Figure 4.8.** X-ray structure of **18** (ORTEP representation with selected atomic labels). Thermal ellipsoids are shown with a 30% probability level.

## 4.6 $(C_5H_4NHCOCH_2Ph)Re(CO)_3$ (19)

### 4.6.1 Preparation of 19

($\eta^5$-acetamidocyclopentadienyl)(tricarbonyl)rhenium (**19**) was prepared according to the method described previously. The amine **15** was dissolved in a biphasic solution EtOH / $H_2O$ in the presence of a base ($K_2CO_3$). The mixture was stirred vigorously overnight at room temperature. The new compound **19** was isolated by flash chromatography in a good yield of 67 %.

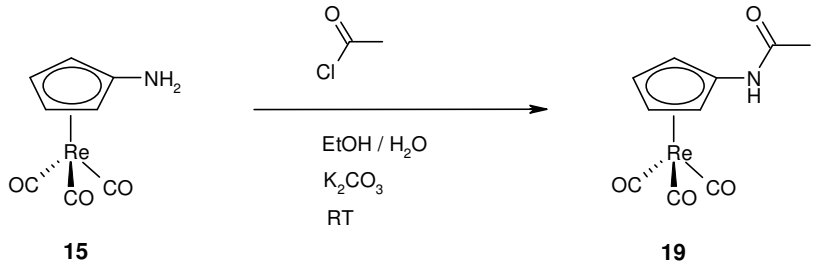


**Scheme 4.9**

### 4.6.2 Characterization of 19

**19** was fully characterized by $^1H$, $^{13}C$ NMR, IR spectroscopy, MS and elemental analysis. The $^1H$ NMR spectrum of **19** in benzene displayed two triplets at 5.08 and 4.24 ppm assigned to the aromatic protons (Figure 4.11). The singlet at 1.24 ppm was attributed to the methyl group and the broad signal at 5.20 ppm to the NH proton. The $^{13}C$ NMR spectrum in benzene-$d_6$ showed a resonance at 194.7 ppm assigned to the carbonyl groups coordinated to rhenium. The $C_{CO}$ atom of the amide group appeared at 165.2 ppm and the $C_{Me}$ at 23.0 ppm. Two resonances for the cyclopentadienyl ring carbons were observed at 80.1 and 72.3 ppm. The resonance of the carbon bound to the NH group could not be observed probably due to a too long relaxation time of this atom and the resulting low intensity for this resonance. C atom with benzylic carbon-nitrogen bonds are often difficult to observe. The IR spectrum of **19** in KBr displayed two ν(CO) bands at 2020 (m) and 1908 $cm^{-1}$ (s). The intensity pattern of these bands speaks for a $C_{3v}$ $Re(CO)_3$ subunit. The mass spectrum showed the molecular-ion peak at m/z 416, which corresponds to the cation $[(\eta^5\text{-}C_5H_4NHCOCH_3)Re(CO)_3 + Na]^+$.

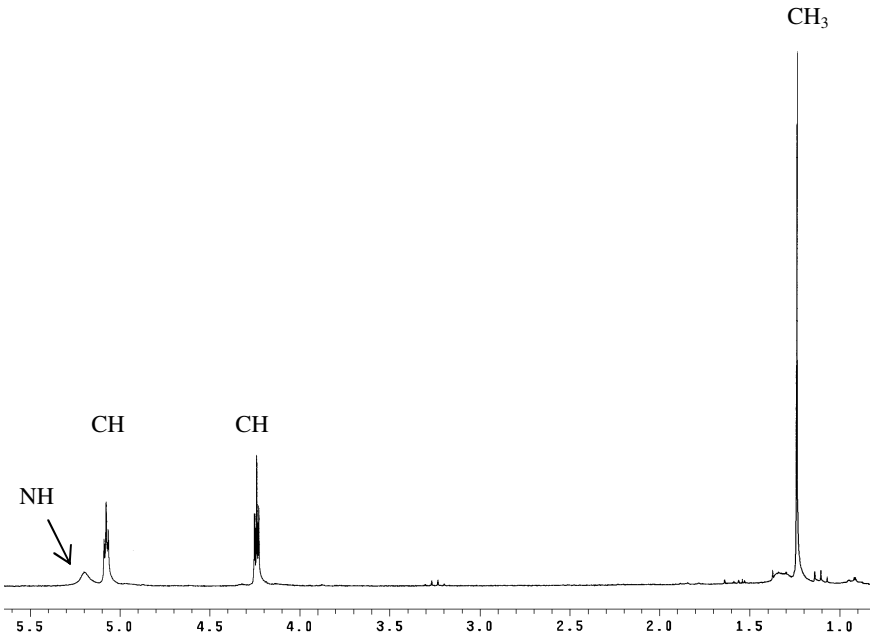


**Figure 4.11** $^{1}$H NMR spectrum of **19** in benzene-$d_6$ at 20 °C.

## 4.7 ($\eta^5$-$C_5H_4NC_4H_8$)$Re(CO)_3$ (20)

### 4.7.1 Preparation of 20

Heterocyclization of primary amines and particularly of aniline derivatives were reported by Ju and Varma in 2005. They prepared a series of N-aryl azacycloalkanes in one pot in an aqueous medium from alkyldihalides and aniline derivatives. Usually azacyloalkanes are prepared via alkylation of primary amines with glycol sulfonate in refluxing anhydrous dioxane using complicated multistep reactions under harsh conditions or through coupling reactions using expensive metal catalysts. The reaction described by Ju and Varma was carried out in an aqueous potassium carbonate medium and accelerated with micro wave irradiation in order to establish a green chemistry[37]. The reaction time was shortened under micro wave irradiation, but it was found that the reaction occurred also with conventional heating (oil bath) (Scheme 4.9 and Table 4.4). This interesting example of pyrrolidine synthesis in one pot was the base for the preparation of the new compound **20**[38-40].

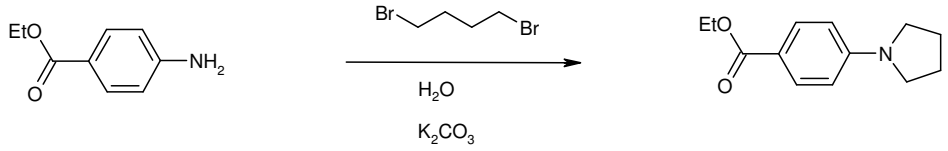


**Scheme 4.9** Reaction of ethyl 4-aminobenzoate with 1,4-dibromobutane

**Table 4.4** Reaction conversion under conventional heating (oil bath)[a]

| entry | Reaction time (h) | Conversion based on ethyl 4-aminobenzoate (%) |
|---|---|---|
| 1 | 1.0 | 26 |
| 2 | 3.0 | 41 |
| 3 | 8.0 | 64(58)[c] |
| 4 | 24.0 | 63(57)[c] |
| 5 | 33.0 | 95(91)[c] |

[a]The temperature of the oil bath was 120°C. [b]Conversions based on quantitative GC-MS analyses. [c]Isolated yields in parentheses

**15** was dissolved in ethanol with one equivalent of 1,4-diodobutane at room temperature. An aqueous solution of $K_2CO_3$ was added to the mixture and it was heated under reflux overnight. The reaction afforded ($\eta^5$-pyrrolidinylcyclopentadienyl)-(tricarbonyl)rhenium (**20**) in a good yield of 60 % (Scheme 4.11). **20** was purified by flash chromatography. Further purification was effected by recrystallization from a dichloromethane-hexane solution.

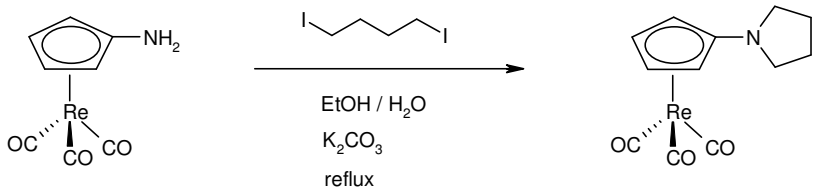


**15** **20**

**Scheme 4.10**

The mechanism of this reaction presumably involves a double base-supported nucleophilic substitution pathway at the iodo ends of the diodobutane as sketched in the Scheme 4.11 below.

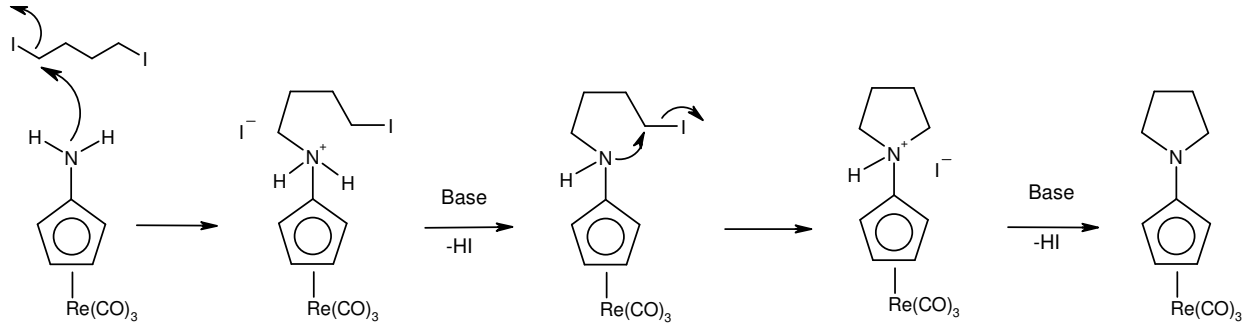


**Scheme 4.11**

### 4.7.2 Characterization of 20

The new compound **20** was characterized by $^{1}H$, $^{13}C$ NMR, IR spectroscopy, MS and the composition of **20** was confirmed by elemental analysis. The $^{1}H$ NMR spectrum of **20** in $CD_3CN$ showed two triplets at 5.23 and 4.71 ppm assigned to the $C_5H_4$ protons (Figure 4.12). The two triplets at 2.87 and 1.91 ppm were assigned to the protons of the pyrrolidine ring. The signal at 2.87 ppm downfield corresponds to the four equivalent protons on the two carbon atoms bound to the nitrogen atom of the pyrrolidine group and the signal upfield at 1.91 ppm corresponds to the four equivalent protons on the two other ring carbons atoms. The $^{13}C$ NMR spectrum displayed a resonance at 196.9 ppm, which confirmed the existence of rhenium bound carbonyl groups (figure 4.13). The $C_5H_4$ group was identified by three $^{13}C$ NMR resonances at 137.8, 80.6 and 65.0 ppm. The carbon atoms of the pyrrolidine group appeared at 51.2 and 25.6 ppm, which were in their chemical shift range consistent with that of organic pyrrolidine compounds (Table 4.5). The IR spectrum of **20** in KBr displayed two ν(CO) bands at 2007 (s) and 1895 (s) $cm^{-1}$ in accord with the local $C_{3v}$ symmetry of the $Re(CO)_3$ group. The mass spectrum of **20** displayed the molecular-ion peak at m/z 406, which corresponds to the cation $[(\eta^5\text{-}C_5H_4NHC_4H_8)Re(CO)_3 + H]^+$.

**Table 4.5** Proton and carbon chemical shifts of the pyrrolidine ring

| Pyrrolidine compounds | $^{1}$H NMR chemical shifts (ppm) | $^{13}$C NMR chemical shifts (ppm) | Deuterated solvent |
|---|---|---|---|
| **20** | 2.87<br>1.91 | 51.2<br>25.6 | $CD_3CN$ |
| 4-(1-pyrrolidinyl)pyridine[41] | 3.27<br>2.01 | 47.0<br>25.3 | $CDCl_3$ |
| N-methylpyrrolidine [42] | 2.47<br>1.78 | 56.3<br>24.1 | $CDCl_3$ |
| 1-Phenylpyrrolidine[43] | 3.23<br>1.94 | 47.4<br>25.3 | $CDCl_3$ |

The crystals of **20** obtained after recrystallization from a dichloromethane-hexane solution were suitable for X-ray diffraction. The X-ray studies confirmed the expected structure of **20** and indicated that the compound crystallized in an orthorhombic system $P2_1\ 2_1\ 2_1$ (Figure 4.14). Selected bond distances and bond angles are listed in Table 4.6. The X-ray data collection and processing parameters are listed in Table 7.3.8.

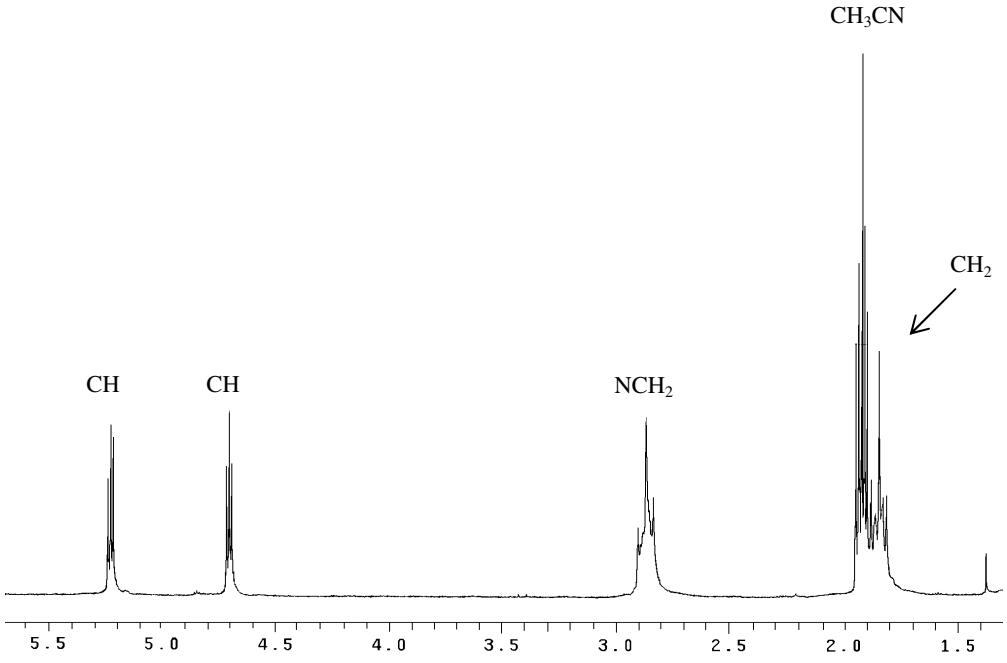


**Figure 4.12** $^{1}$H NMR spectrum in acetonitrile-$d_3$ of compound **20** at 20 °C

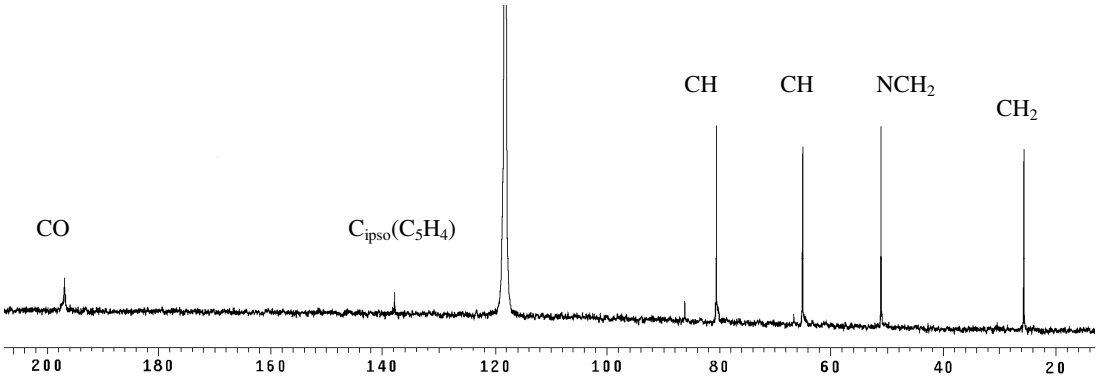


**Figure 4.13** $^{13}$C NMR spectrum in acetonitrile-$d_3$ of compound **20** at 20 °C.

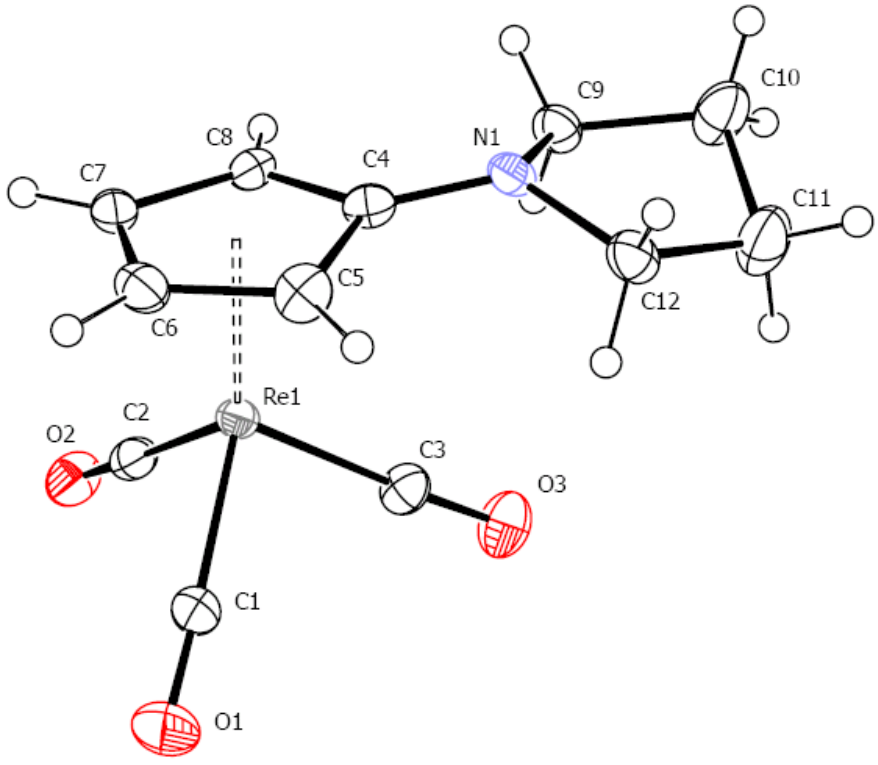


**Figure 4.12.** X-ray structure of **20** (ORTEP representation with selected atomic labels). Thermal ellipsoids are shown with a 30% probability level.

**Table 4.6** Selected bond distances (Å) and bond angles (°) of **20**.

| Selected bond distances (Å) | | Selected angles (°) | |
|---|---|---|---|
| Re1-C1 | 1.910(5) | C8-C4-C5 | 106.3(4) |
| Re1-C2 | 1.914(5) | C6-C5-C4 | 108.3(4) |
| Re1-C3 | 1.920(4) | C7-C6-C5 | 108.7(4) |
| C4-N1 | 1.339(6) | C6-C7-C8 | 108.3(4) |
| C1-O1 | 1.153(6) | C4-C8-C7 | 107.7(4) |
| C2-O2 | 1.157(6) | C1-Re1-C3 | 90.19(19) |
| C3-O3 | 1.152(5) | C1-Re1-C2 | 90.5(2) |
| C4-C5 | 1.452(6) | C3-Re1-C2 | 90.37(19) |
| C5-C6 | 1.425(7) | C4-N1-C9 | 120.1(3) |
| C6-C7 | 1.397(6) | N1-C9-C10 | 102.3(3) |
| C7-C8 | 1.453(7) | C10-C11-C12 | 104.3(4) |
| C8-C4 | 1.435(6) | | |
| N2-C9 | 1.464(4) | | |
| N1-C12 | 1.473(5) | | |

## 4.8 ($\eta^5$-$C_5H_4NHCONHC_8H_3F_6$)$Re(CO)_3$ (21)

Urea and thiourea were intensively investigated in the area of molecular recognition due to their strong hydrogen-bonding activity. Recent reports suggest that urea and thiourea not only recognized organic compounds (carboxylic acids, sulfonic acids, nitrates etc…) but also activated them as an acid catalyst[44, 45]. They were found as good organocatalysts in many reactions such as Michael addition to α,β-unsaturated carbonyl compounds, Diels Alder reaction, asymmetric Strecker and Mannich reactions etc…[46-51]

Urea functions could be also used for ionic hydrogenations to polarize in particular organic carbonyl compounds and facilitate the hydride transfer to the electrophilic center of the substrate. The acidic urea protons would stabilize the substrate in the close vicinity to the

hydride. The strong double hydrogen bonding between the substrate and the urea cyclopentadienyl rhenium complex could then initiate the transfer of the hydride, as sketched in Fig.4.15.

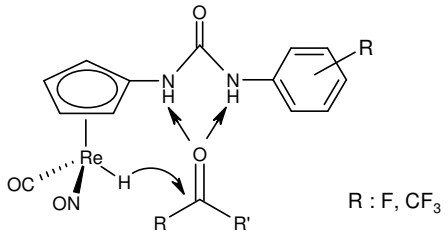


**Figure 4.15**

### 4.8.1 Preparation of 21

($\eta^5$-$C_5H_4NH_2$)$Re(CO)_3$ (**15**) was reacted with 1.5 equivalents of triphosgene in chloroform at room temperature in the presence of triethylamine[52]. After 10 min the reaction mixture was treated with 1.5 equivalents of 3,5-bis(trifluoromethyl)aniline and the mixture was stirred further 1 h at room temperature (Scheme 4.12). Removal of the solvent afforded [$\eta^5$-({[3,5-bis(trifluoromethyl)phenyl]carbamoyl}amino)cyclopentadienyl](tricarbonyl)rhenium (**21**) in 70 % yield. **21** could be purified by recrystallization from a solution hexane-dichloromethane-THF at -30°C.

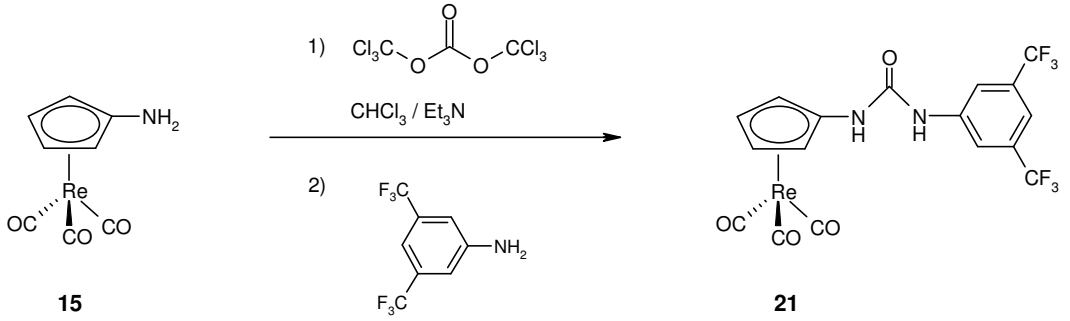


**Scheme 4.12**

### 4.8.2 Triphosgene : safety and mechanistic aspect

Phosgene is commonly used for the preparation of urea derivatives. Primary amines react with phosgene to give the corresponding isocyanate. Addition of another equivalent of amine gives the corresponding urea derivative as demonstrated in Scheme 4.13. But phosgene is a highly toxic gas classified as a pulmonary irritant[53-56]. During World War I, it was used in combination with chlorine gas for combat purposes[57]. Inhalation of phosgene induces serious lung injuries. Exposure to concentrations of 3 ppm may not cause noticeable symptoms for 12-24 hours but exposures to 50 ppm may be rapidly fatal[58-63]. Nowadays phosgene is generally replaced by triphosgene in laboratory syntheses of urea derivatives. Triphosgene is a white powder which is easier and safer in handling than $COCl_2$. However triphosgene generates phosgene on heating and upon reaction with any nucleophile. Traces of moisture also lead to formation of phosgene. That is why triphosgene should be handled with exactly the same precautions taken with phosgene.

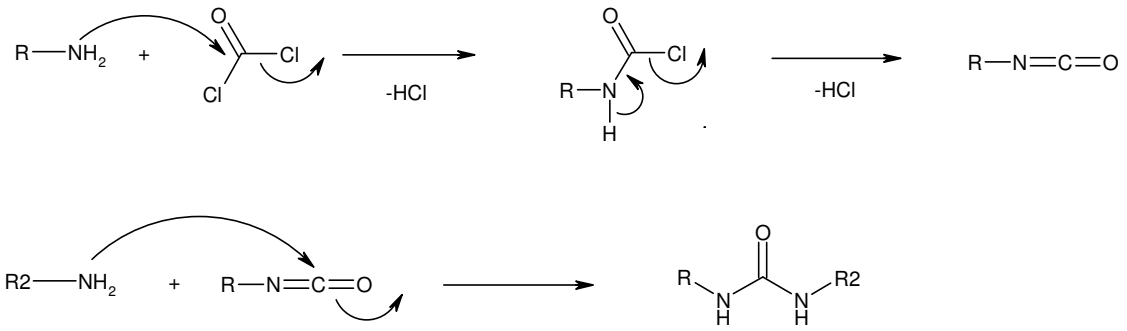


**Scheme 4.13** Preparation of ureas applying phosgene

As shown below (Scheme 4.14), one mole of triphosgene generates three moles of phosgene. The primary amine attacks at the carbonyl group of the triphosgene and induces the elimination of the highly unstable trichloromethanol HO-$CCl_3$ that is spontaneously converted into phosgene under basic conditions. The process results in the formation of isocyanates (Scheme 4.14) and phosgene that can react with amine to further generate another equivalent of isocyanate.

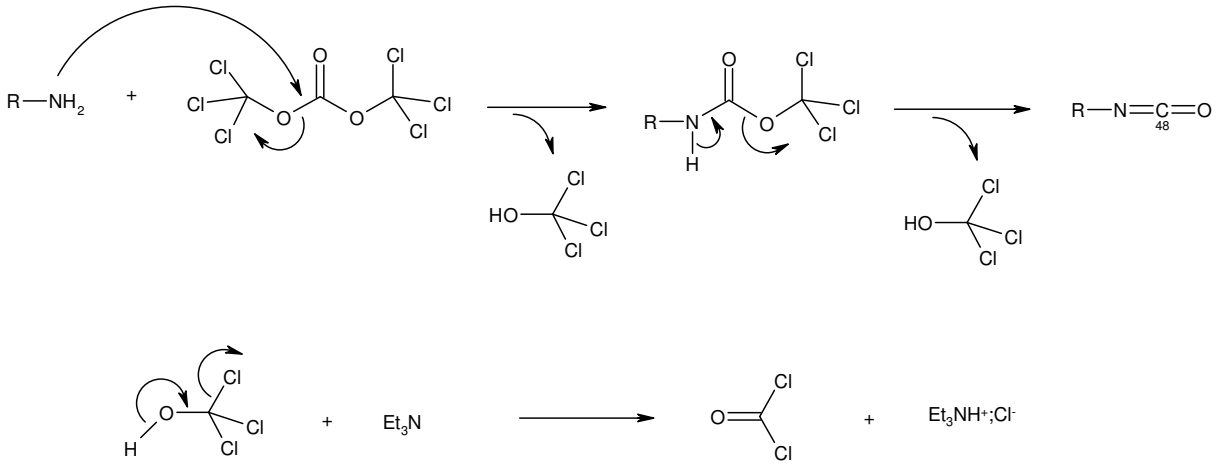


**Scheme 4.14** Trisphosgene as substitute of phosgene

### 4.8.3 Characterization of 21

**21** was fully characterized by $^{1}H$, $^{13}C$, $^{19}F$ NMR, IR spectroscopy, MS and its composition was determined by elemental analysis. The $^{1}H$ NMR spectrum of **21** in acetonitrile-$d_3$ displayed two triplets at 5.75 and 5.32 ppm for the cyclopentadienyl ring (Figure 4.16). The two singlets at 8.01 and 7.62 ppm were first attributed to the aromatic protons and the NH groups, respectively. The integration ration of 3:2 was also in agreement and moreover according to the one-dimensional NOE spectrum of **21** (Figure 4.17), the singlet at 7.62 could be attributed to the proton of the NH moiety. However the $^{13}C$, $^{1}H$ correlation spectrum of **21** (Figure 4.18) demonstrated that the two $^{1}H$ NMR signals correlate with two $^{13}C$ NMR resonances located in the region of $C_{Ar}$ atoms, which means that the two signals at 8.01 and 7.62 ppm correspond both to aromatic protons and the NH protons. As a matter of fact, the NH protons and the aromatic protons accidentally overlap. The $^{19}F$ NMR spectrum of **21** displayed one signal at –65.2 ppm proving the presence of chemically equivalent $CF_3$ groups (Figure 4.19). The IR spectroscopy the two ν(CO) bands at 2020 and 1917 $cm^{-1}$. The mass spectrum of **21** showed the molecular-ion peak at m/z 629, which corresponds to the cation $[(\eta^5\text{-}C_5H_4NHCONHC_8H_3F_6)Re(CO)_3 + Na]^+$.

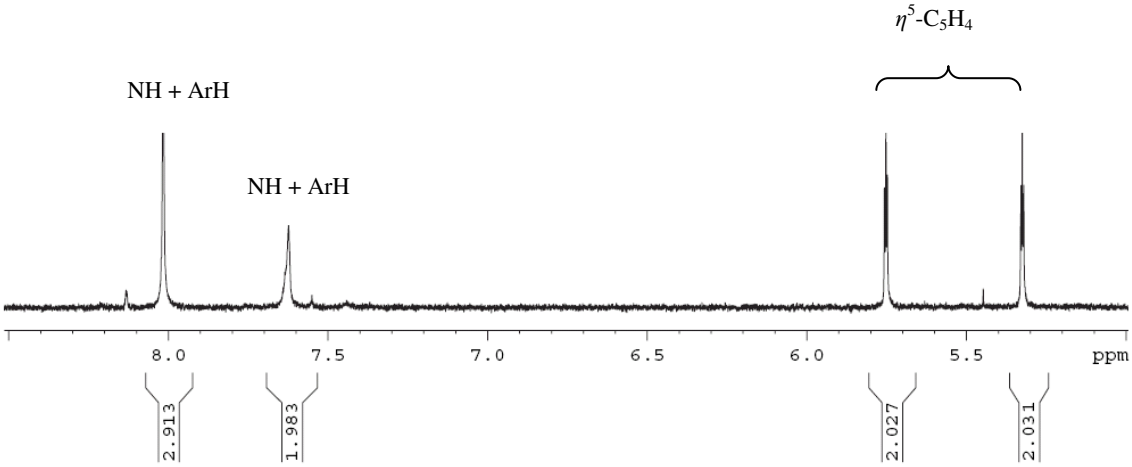


**Figure 4.16.** $^1$H NMR spectrum in acetonitrile-$d_3$ of **21** at 20 °C

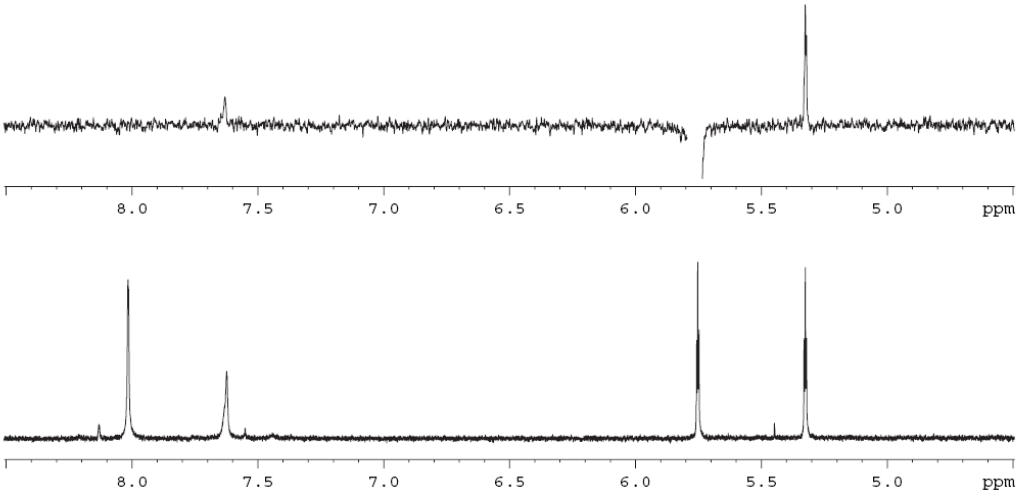


**Figure 4.17.** 1D NOE spectrum of **21** in acetonitrile-$d_3$ at 20 °C

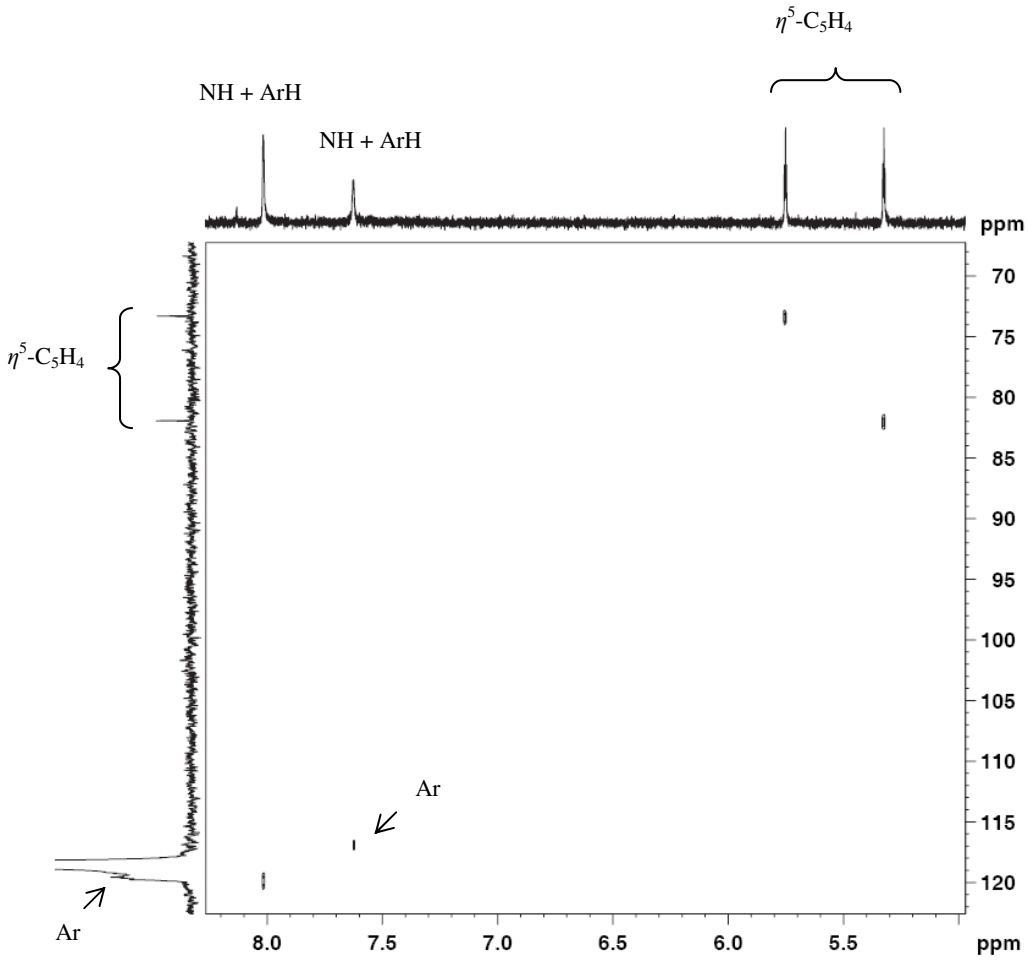


**Figure 4.18** $^{13}C$, $^{1}H$ correlation spectrum of 21 in acetonitrile-$d_3$ at 20 °C

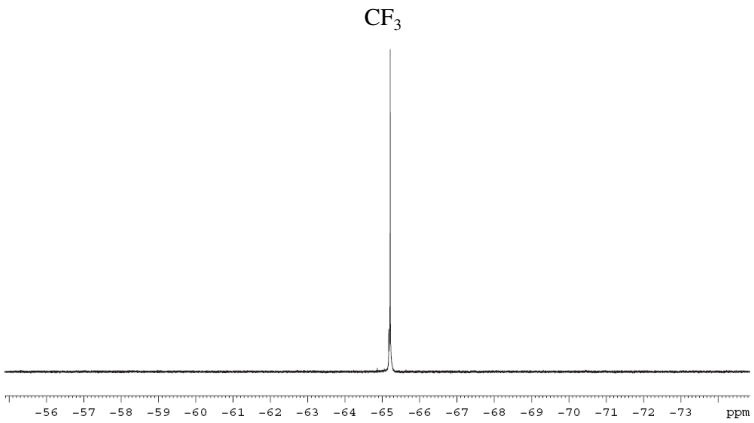


**Figure 4.19** $^{19}F$ NMR spectrum of **21** in acetonitrile-$d_3$ at 20 °C

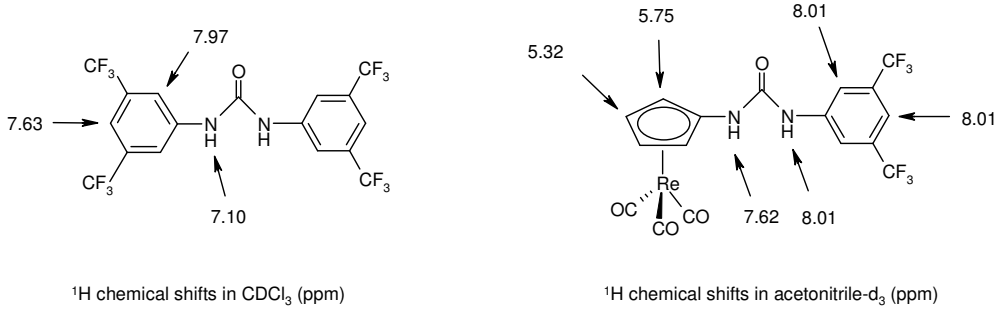


**Figure 4.20** Comparison of $^1$H NMR chemical shifts of 1,3-bis-(3,5-bis-trifluoromethyl-phenyl)urea (left)and in $CDCl_3$ and of **21** in acetonitrile-$d_3$ at 20 °C (right).

A single crystal of **21** was studied by X-ray diffraction, which confirmed the structural assignment by NMR and IR spectroscopy. **21** cocrystallized with a THF solvate molecule, which showed three-centred hydrogen bonding from the THF acceptor oxygen and to the chelating urea NH-donors (Figure 4.21). **21**.THF crystallized in the monocyclic system C2/c (Figure 4.22). Selected bond distances and bond angles are listed in Table 4.7. The X-ray data collection and processing parameters are given in Table 7.3.9.

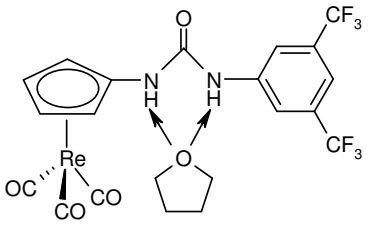

**Figure 4.21** Hydrogen bonding for **21**.THF

**Table 4.7** Selected bond distances (Å) and bond angles (°) of **21**.THF

| Selected bond distances (Å) | | Selected angles (°) | |
|---|---|---|---|
| Re1-C1 | 1.912(8) | C8-C4-C5 | 107.2(5) |
| Re1-C2 | 1.912(6) | C6-C5-C4 | 107.5(5) |
| Re1-C3 | 1.908(8) | C7-C6-C5 | 108.3(6) |
| N1-C4 | 1.384(6) | C6-C7-C8 | 108.2(5) |
| C1-O1 | 1.598(8) | C4-C8-C7 | 106.7(5) |
| C2-O2 | 1.144(7) | C1-Re1-C3 | 91.1(4) |
| C3-O3 | 1.140(9) | C1-Re1-C2 | 90.2(3) |
| C4-C5 | 1.414(7) | C3-Re1-C2 | 91.0(3) |
| C5-C6 | 1.428(8) | O4-C9-N2 | 125.9(4) |
| C6-C7 | 1.401(9) | N1-C9-O4 | 122.3(4) |
| C7-C8 | 1.399(9) | C4-N1-C9 | 124.9(4) |
| C8-C4 | 1.427(7) | N2-C9-N1 | 111.8(4) |
| N1-H1 | 0.8600 | C9-N2-C10 | 126.4(4) |
| N2-H2 | 0.8600 | | |
| C9-O4 | 1.212(5) | | |

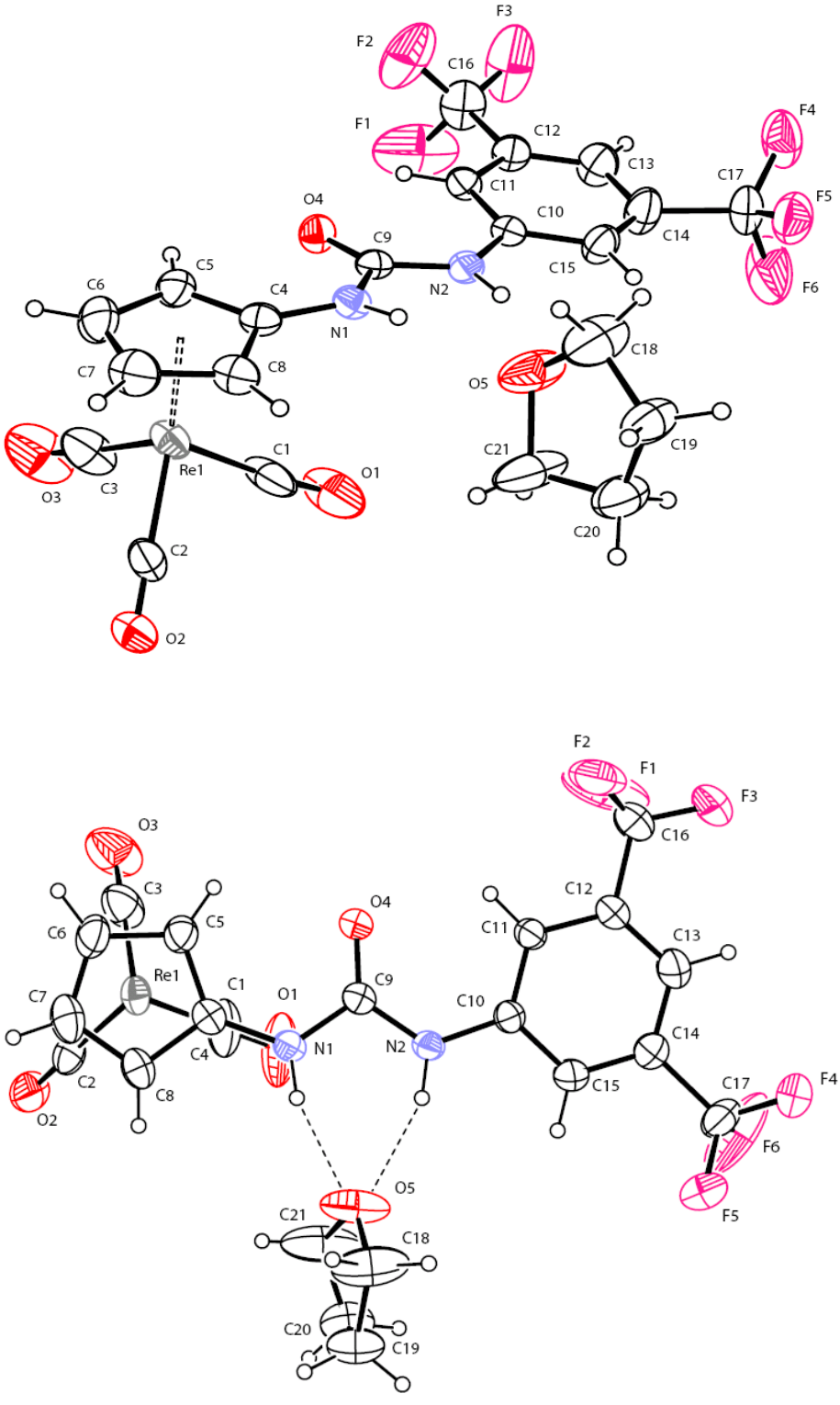


**Figure 4.22** Bis-hydrogen-bonding interaction between **21**.THF and a molecule of THF (ORTEP representation with selected atomic labels). Thermal ellipsoids are shown with a 30% probability level.

## 4.9 ($\eta^5$-$C_5H_4NHCONHC_6F_5$)$Re(CO)_3$ (22)

### 4.9.1 Preparation of 22

($\eta^5$-{[(pentafluorophenyl)carbamoyl]amino}cyclopentadienyl)(tricarbonyl)rhenium (**22**) was prepared according to the procedure described for the synthesis of 1-(3,5-bistrifluoromethyl-phenyl)-3-(cyclopentadienyltricarbonylrhenium)urea (**21**). $(C_5H_4NH_2)Re(CO)_3$ **15** was dissolved in a solution of chloroform and triethylamine (Scheme 4.15). 1.5 equivalents of triphosgene were added to the mixture and after 10 minutes, the reaction was treated with 1.5 equivalents of pentafluoroaniline. After workup and purification the yield of **22** was 30 %.

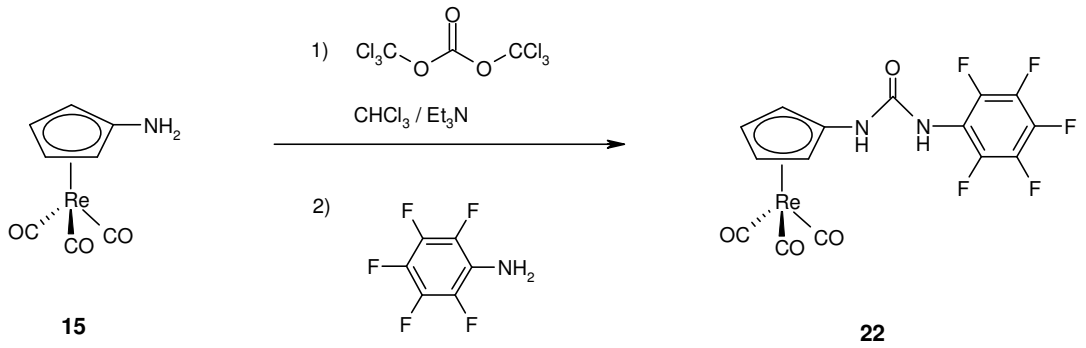


**Scheme 4.15**

### 4.9.2 Characterization of 22

An analytically pure sample of **22** was fully characterized by $^1H$, $^{13}C$, $^{19}F$ NMR, IR spectroscopy and mass spectroscopy. The $^1H$ NMR of **22** in $CD_3CN$ showed two triplets at 5.68 and 5.30 ppm assigned to the 4 protons of the $C_5H_4$ ring (Figure 4.22). The NH protons were found at chemical shifts of 7.10 and 7.67 ppm. The resonances of these NH protons are located at lower field than those of compound **21**, which might indicate that these protons are more acidic than the NH protons of **21**. The $^{13}C$ NMR spectrum of **22** showed a resonance at 196.1 ppm that was assigned to the C nuclei of the $Re(CO)_3$ unit. The resonance at 152.3 ppm was attributed to the carbonyl group of the urea function. The two resonances at 82.4 and 73.0 ppm were attributed to the C atoms of the ring in 2 and 3 positions. Then the other 5 resonances at 145.6, 143.7, 139.8, 137.9 and 120.5 ppm could not be definitively assigned.

They belong to aromatic carbon atoms and confirmed thus the presence of a phenyl group. According to our previous assignments with and the $C_{ipso}$ bound to the nitrogen of the urea function appears at either 137.9 or 139.8 ppm and could be one of the five signals not definitely assigned. The $^{19}F$ NMR spectrum of **22** in $CD_3CN$ displayed a doublet at -148.5, a triplet at -160.7 and another triplet at -166.0 ppm. For comparison pentafluoroaniline shows in $CD_3CN$ a doublet at -164.5 ppm, a triplet at -168.4 ppm and a multiplet at -178.4 ppm. The IR spectrum of **22** displayed two ν(CO) bands at 2007 (s) and 1895 (s) $cm^{-1}$ in accord with the local $C_{3v}$ symmetry of the $Re(CO)_3$ group. The mass spectrum of **22** showed the molecular-ion peak at m/z 583, which corresponds to the cation $[(\eta^5\text{-}C_5H_4NHCONHC_6F_5)Re(CO)_3 + Na]^+$.

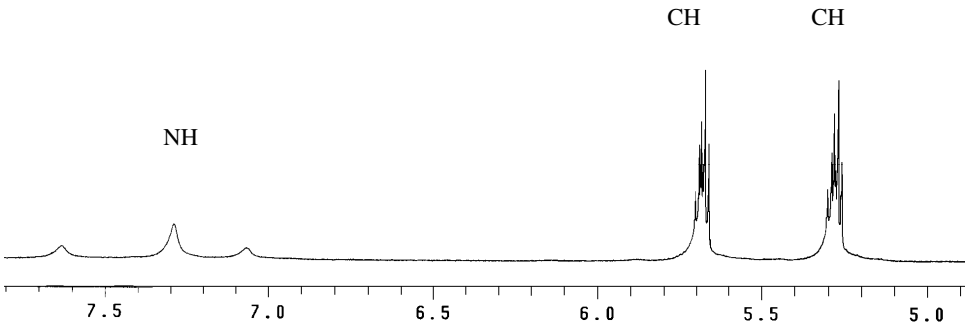


**Figure 4.23** $^1H$ NMR spectrum of **22** in acetonitrile-$d_3$ at 20 °C

## 4.10 Overview over the NMR and IR spectroscopic data of 14-22

**Table 4.8** Spectroscopic data of **14**-**22**

| Entry | Product | $^1$H (δ ppm, 200 MHz, [a]: $CD_3CN$, [b]: acetone-$d_6$, [c] :benzene-$d_6$, [d]: $CDCl_3$) | $^{13}$C (δ ppm, 200 MHz, [a]: $CD_3CN$, [b]: acetone-$d_6$, [c] :benzene-$d_6$, [d]: $CDCl_3$) | IR (KBr, $cm^{-1}$) |
|---|---|---|---|---|
| 1 | **14** | 5.53 (*pseudo* t, 2H), 5.36 (*pseudo* t, 2H)[a] | | |
| 2 | **15** | 5.11 (*pseudo* t, 2H), 4.94 (*pseudo* t, 2H), 4.05 (bs, 2H) [a] | 197.3, 135.7, 80.3, 66.4 [a] | 2012 (vs), 1917 (vs) |
| 3 | **16** | 8.41 (s, 1H), 7.82 (dd, 2H), 7.48 (m, 3H), 5.50 (*pseudo* t, 2H), 5.30 (*pseudo* t, 2H) [a] | 194.1, 164.9, 134.9, 132.2, 129.1, 128.9, 127.8, 84.5, 81.6 [a] | 2021 (vs), 1928 (vs) |
| 4 | **17** | 7.37-7.34 (m, 5H), 5.08 (*pseudo* t, 2H), 4.81 (*pseudo* t, 2H), 4.00 (s, 2H), 3.30 (bt, 1H) [d] | 195.4, 137.3, 134.4, 128.8, 127.9, 79.2, 64.4, 51.6 [d] | 3400, 2800 , 1910 |
| 5 | **18** | 7.81 (bs, 1H), 7.36-7.34 (m, 5H), 5.66 (*pseudo* t, 2H), 5.29 (*pseudo* t, 2H), 5.12 (s, 2H) [a] | 193.9, 152.5, 135.3, 128.7, 128.6, 128.2, 117.6, 80.4, 71.6, 67.8 [a] | 2020 (vs), 1907 (vs) |
| 6 | **19** | 5.20 (s,1H), 5.08 (*pseudo* t, 2H), 4.24 (*pseudo* t, 2H), 1.24 (s, 1H) [c] | 194.7, 80.1, 72.3, 23.0 [c] | 2020 (vs), 1908 (vs) |
| 7 | **20** | 5.23 (*pseudo* t, 2H), 4.71 (*pseudo* t, 2H), 2.87 (t, 2H), 1.91 (t, 2H) [a] | 196.9, 137.8, 80.6, 65.0, 51.2, 25.6 [a] | 3425 (bs), 2102 (vs), 2042 (vs), 1809 (vs), 1520 (s) |
| 8 | **21** | 8.00 (m, 3H), 7.62, 5.74 (*pseudo* t, 2H), 5.32 (*pseudo* t,2H) [a] | 196.2, 119.6, 81.9, 73.3 [a] | 2020 (vs), 1917 (vs) |
| 9 | **22** | 5.69 (*pseudo* t, 2H), 5.29 (*pseudo* t, 2H) [a] | 196.1, 152.3, 145.6-143.7, 141.9-139.8, 137.9-136.4, 114.1-113.9, 82.4, 73.0 [a] | 2020 (vs), 1908 (vs) |

## 4.11 Summary

Scheme 4.16 summarized the chemistry of NHR derivatives with $(\eta^5\text{-}C_5H_4)Re(CO)_3$ fragments. Besides the parent complex **15** other derivatives could be prepared varying in first place the NH acidity of the complexes. Amine, amide and urea functions wre chosen for the stake of potential hydrogen bonding to organic carbonyl compounds to enventually appear in nitrosyl substituted complexes.

## 4.12 Conclusion

We described the preparation of the complex $(\eta^5\text{-}C_5H_4NH_2)Re(CO)_3$ **15**, which was obtained by reduction of the azido complex $(\eta^5\text{-}C_5H_4N_3)Re(CO)_3$ **14** with $NaBH_4$. From **15**, a novel series of substituted cyclopentadienyl rhenium complexes $(\eta^5\text{-}C_5H_4R)Re(CO)_3$ (R = NCHPh **16**, R = $NHCH_2Ph$ **17**, R = NHCbz **18** R = NHCOMe **19**, R = $NHC_4H_8$ **20**, R = $NHCONHC_8H_3F_6$ **21**, R = $NHCONHC_6F_5$ **22)** was obtained.

This series includes various functions: imine, amide, carbamate, pyrrolidine, urea. The complex **18** is the protected form of **15**. It could be a good precursor for the preparation of the target molecule since the utilization of nitrosonium for the step of nitrosylation requires a protective group given that nitrosonium reacts with amine to give nitrosamine. The ureas **21** and **22** are very interesting. As postulated in this chapter, the preparation of a urea rhenium hydride could show very interesting features in terms of hydricity.

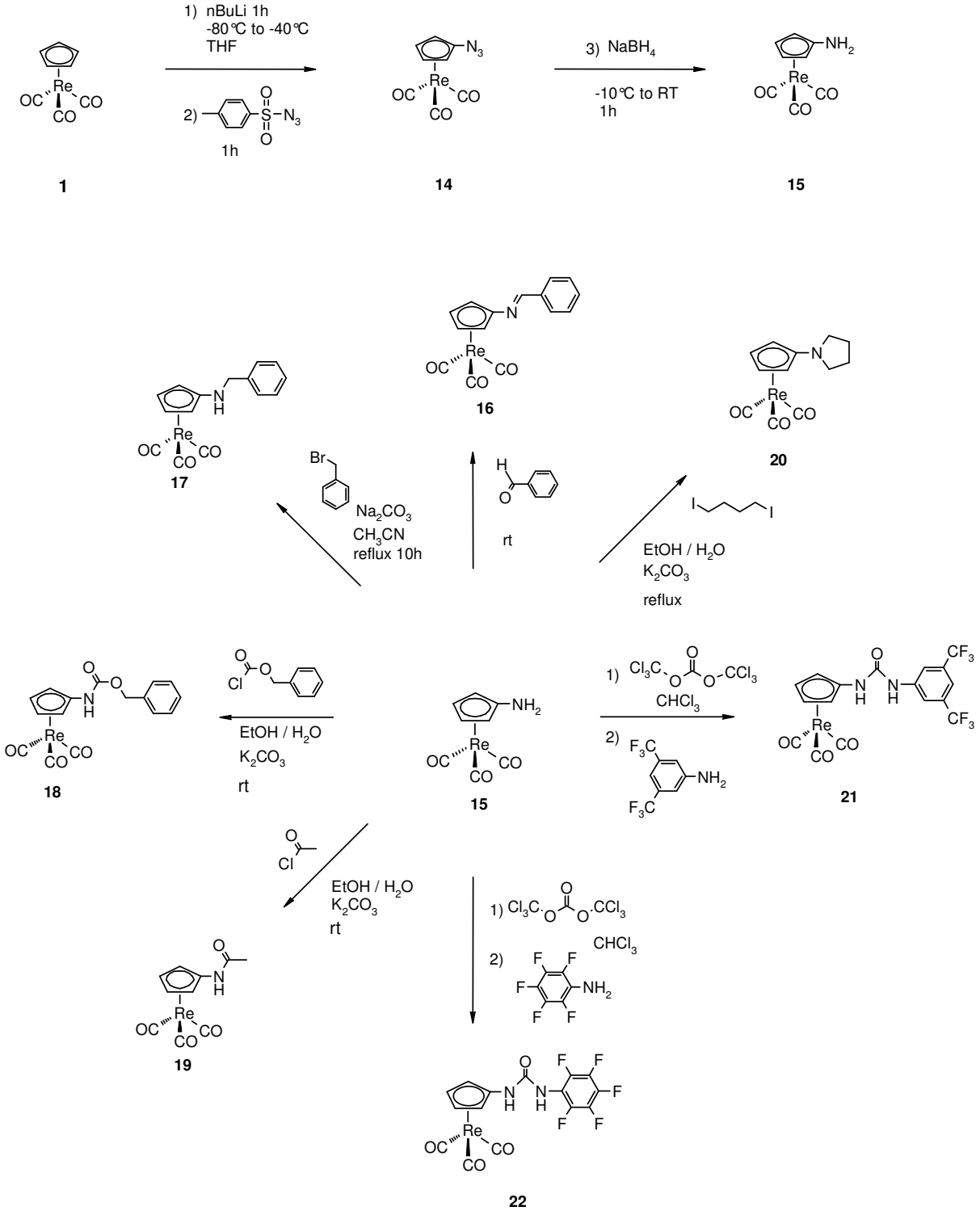
1) nBuLi 1h
-80°C to -40°C
THF
2)
1h
3) NaBH4
-10°C to RT
1h
1
14
15
16
17
18
19
20
21
22
Na2CO3
CH3CN
reflux 10h
rt
EtOH / H2O
K2CO3
reflux
EtOH / H2O
K2CO3
rt
CHCl3

**Scheme 4.16**

## 4.13 References


[1] T. C. Holovics, S. F. Deplazes, M. T. Toriyama, D. R. Powell, G. H. Lushington, M. V. Barybin, *Organometallics* **2004**, *23*, 2927.

[2] H. H. Strain, *J. Am. Chem. Soc.* **1928**, *50*, 2218. (b) L. A. Bigelow, H. Eatough, *Org. Synth.* 1941*, Collective Vol. 1,* 80.

[3] M. N. Ibrahim, H. K. Al-Deeb, *E-Journal of Chemistry* **2006**, *3*, 257.

[4] J. S. M. Samec, J. E. Bäckvall, *Chemistry-A European Journal* **2002**, *8*, 2955.

[5] E. Hadjoudis, *Mol. Eng.* **1995**, *5*, 301. M. Ilias, D. C. Barman, D. Prajapati, J. S. Sandhu, *Tetrahedron lett.* **2002**, *43*, 1877.

[6] P. Vachal, E. Jacobsen, *J. Am. Chem. Soc.* **2002**, *124*, 10012.

[7] R. S. Varma, R. Dahiya, *Synlett* **1997**, *11*, 1245.

[8] Z. Meić, G. Baranović, *Pure Appl. Chem.* **1989**, *61*, 2129

[9] V. M. S. Gil, M. E. L. Saraiva, *Tetrahedron* **1971**, *27*, 3007.

[10] B. T. Cho, S. K. Kang, *Tetrahedron* **2005**, *61*, 5725.

[11] A. K. Chakraborti, S. Bhagat, S. Rudrawar, *Tetrahedron lett.* **2004**, *45*, 7641.

[12] M. Hirano, S. Yakabe, H. Chikamori, J. H. Clark, T. Morimoto, *J. Chem. Res. Synop.,* **1998***, 12*, 770.

[13] R. Dalpozzo, A. De Nino, M. Nardi, B. Russo, A. Procopio, *Synthesis* **2006**, *7*, 1127.

[14] C. K. Z. Andrade, S. C. S. Takada, L. M. Alves, J. P. Rodrigues, P. A. Z. Suarez, R. F. Brandão, V. C. D. Soares, *Synlett* **2004**, *12*, 2135.

[15] S. Kumar, A. Saini, J. S. Sandhu, *Tetrahedron lett.* **2005**, *46*, 8737.

[16] M. Ilias, D. C. Barman, D. Prajapati, J. S. Sandhu, *Tetrahedron lett.* **2002**, *43*, 1877.

[17] B. J. E. Reich, E. E. Greenwald, A. K. Justice, B. T. Beckstead, J. H. Reibenspies, S. W. North, S. A. Miller, *J. Org. Chem.* **2005**, *70*, 8409.

[18] *Spectral Database for Organic Compounds* SDBS, SDBS No: 2145.

[19] M. C. Law, T. W. Cheung, K. Y. Wong, T. H. Chan, *J. Org. Chem.* **2007**, *72*, 923.

[20] T. N. Tuyen, T. S. Sin, H. P. Kim, H. Park, *Arch. Pharmacal Res.* **2005**, *28*(9), 1013.

[21] G. J. T. Kuster, L. W. A. van Berkom, M. Kalmoua, A. van Loevezijn, L. A. J. M Sliedregt, B. J. van Steen, C. G. Kruse, F. P. J. T. Rutjes, H. W. Scheeren, *J. Comb. Chem.* **2006**, *8*, 85.

[22] E. Pohl, R. Herbst-Irmer, K. Köhler, H. W. Roesky, G. M. Sheldrick, *Acta Crystallogr.* **1993**, *C49*, 2141.

[23] A. M. Herrera, S. Bernès, D. López, *Acta Crystallogr.* **2005**, *E61*, 2141.

[24] J. Harada, M. Harakawa, K. Ogawa, *Acta Crystallogr.* **2004**, *860*, 589.

[25] U. Braun, A. T. Shulgin, G. Braun, *J. Pharm. Sci.* **1980**, *69*, 192.

[26] L. Blackburn, R. J. K. Taylor, *Org. Lett.* **2001**, *3*, 1637.

[27] A. F. Abdel-Magid, K. G. Carson, B. D. Harris, C. A. Haryanoff, R. D. Shah, *J. Org. Chem.* **1996**, *61*, 3849.

[28] B. T. Cho, S. K. Kang, *Tetrahedron*, **2005**, *61*, 5725.

[29] D. B Repke, *J. Pharm. Sci.* **1979**, *67*, 1167.

[30] H. Kohmo, T. Iwakuma, K. Yamada, *Synth. Commun.* **1998**, *28*, 1935.

[31] Spectral Database for Organic Compounds SDBS, SDBS No: 18457.

[32] Spectral Database for Organic Compounds SDBS, SDBS No: 6170.

[33] Spectral Database for Organic Compounds SDBS, SDBS No: 17104.

[34] Spectral Database for Organic Compounds SDBS, SDBS No: 16370.

[35] Spectral Database for Organic Compounds SDBS, SDBS No: 16371.

[36] Spectral Database for Organic Compounds SDBS, SDBS No: 16372.

[37] Y. Ju, R. S Varma, *J. Org. Chem.* **2006**, *71*, 135.

[38] J. L Romera, J. M Cid, A. A. Trabanco, *Tetrahedron lett.* **2004**, *45*, 8797.

[39] Y. Ju, R. S Varma, *Green Chem.* **2004**, *6*, 119.

[40] F. Effenberger, F. Reisinger, K. H. Schoenwaelder, P. Baeuerle, J. J. Stezowski, K. H. Jogun, K.Schoellkopf, W. D. Stohrer, *J. Am. Chem. Soc.* **1987**, *109*, 882.

[41] Spectral Database for Organic Compounds SDBS, SDBS No: 18045.

[42] Spectral Database for Organic Compounds SDBS, SDBS No: 10636.

[43]

[44] M. C. Etter, Z. Urbanczyk-Lipkowska, M Zia-Ebrahimi, T. W. Panunto, *J. Am. Chem. Soc.* **1990**, *112*, 8415.

[45] Y. Takemoto, *Org. Biomol. Chem* **2005**, *3*, 4299.

[46] P. R. Schreiner, A. Wittkopp*, Org. Lett.* **2002**, *4*, 217.

[47] B. List, J. Woon Jang, *Science* **2006**, *313*, 1584.

[48] A. Zhang, Y. Han, K. Yamato, X. Cheng Zeng, B. Gong, *Org. Lett.* **2006**, *8*, 803.

[49] T. Okino, Y. Hoashi, Y. Takemoto, *J. Am. Chem. Soc.* **2003**, *125*, 12672.

[50] Y. Sohtome, A. Tanatani, Y. Hashimoto, K. Nagasawa, *Chem. Pharm. Bull.* **2004**, *52*, 477.

[51] G. Dessole, R. P. Herrera, A. Ricci, *Synlett* **2004**, *13*, 2374.

[52] F. Wang, J. Chien, X. Liu, X. Shen, X. He, H. Jiang, D. Bai*, Chem. Pharm. Bull.* **2006**, *54*, 372.

[53] P. Hantson, F. J. Baud, R. Garnier, *Hum. Tox.* **1996**, 661.

[54] W. F. Diller, R. Zante, *Zentralblatt für Arbeitsmedizin, Arbeitsschutz, Prophylaxe und Ergonomie* **1982**, *32*, 360, 366.

[55] M. A. Mehlman, *Defence Science Journal* **1987**, *37*, 269.

[56] S. A. Cucinell, *Arch. Environ. Health* **1974**, *28*, 272.

[57] D. Evison, D. Hinsley, P. Rice, *Br. Med. J.* **2002**, *324*, 332.

[58] A. M. Sciuto, *Inhalation Toxicology* (2nd Edition) **2006**, 457.

[59] J. Borak, W. F. Diller, *J. Occ. Env. Med.* **2001**, *43*, 110.

[60] J. Pauluhn, A. Carson, D. L. Costa, T. Gordon, U. Kodavanti, J. A. Last, M. A. Matthay, K. E. Pinkerton, A. M. Sciuto, *Inhalation Toxicology* **2007**, *19*, 789.

[61] W. F. Diller, *Pneumonologie* **1974**, *150*, 139.

[62] W. F. Diller, *Arch. Toxicol.***1980**, *46*, 199.

[63] W. F. Diller, *Tox. Ind. Health* **1985**, *1*, 7.

# 5 Preparation of Substituted Cyclopentadienyl Nitrosyl Rhenium Complexes

## 5.1 Introduction

This chapter concerns the preparation of nitrosyl rhenium complexes from selected substituted cyclopentadienyl tricarbonyl rhenium complexes and their conversion into hydride.

Nitrosylation of dicarbonyl(cyclopentadienyl)(nitrosyl)rhenium(1+)tetrafluoroborate was described by W. A. G. Graham[1-5]. The stirring of cyclopentadienyl tricarbonyl rhenium ($\eta^5$-$C_5H_5$)$Re(CO)_3$ with $NOBF_4$ in dichloromethane afforded the corresponding nitrosyl complex [($\eta^5$-$C_5H_5$)$Re(CO)_2(NO)]^+BF_4^-$. In 1972 W. A. G. Graham reported a method to produce the corresponding nitrosyl hydride ($\eta^5$-$C_5H_5$)Re(NO)(CO)H[6]. This hydride was obtained by reaction of the carbonyl cation [($\eta^5$-$C_5H_5$)$Re(NO)(CO)_2]^+BF_4^-$ with triethylamine in wet acetone. In 1982, William A. G and coworkers proposed a mechanism which involves a carboxylate anion as intermediacy[7]. They showed that the carboxylic acid, the product of the hydroxide attack on [($\eta^5$-$C_5H_5$)$Re(CO)_2(NO)]^+$, gave the hydride ($\eta^5$-$C_5H_5$)Re(NO)(CO)H under the conditions of the hydride preparation ($Et_3N$-$H_2O$, acetone, 50°, 1 hour). However, under anhydrous acetone and without triethylamine, the compound [($\eta^5$-$C_5H_5$)$Re(CO)_2(NO)]^+$ did not give the hydride ($\eta^5$-$C_5H_5$)Re(NO)(CO)H. The loss of $CO_2$ occurred only in the presence of triethylamine and water, which means that an intermediacy formed by reaction of the carboxylic acid with hydroxide anion. This anion was not isolated and is supposed no to exist since it would be strongly basic and would rapidly release $CO_2$.

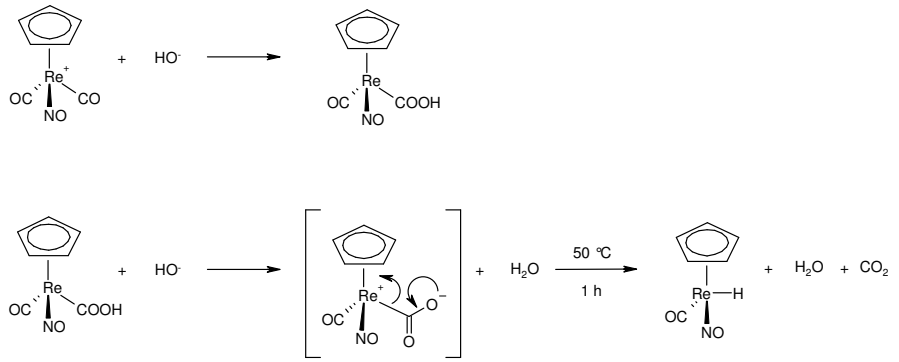


**Scheme 5.1**

## 5.2 $[(\eta^5\text{-}C_5H_4OCH_3)Re(CO)_2(NO)]^+BF_4^-$ (23)

$(\eta^5\text{-}C_5H_4OMeRe(CO)_3$ **7** was dissolved in dichloromethane and stirred with 2 equivalents of $NOBF_4$. Addition of $NOBF_4$ into the reaction mixture was followed by gas evolvement. After 24 hours the solvent was removed. The resulting yellow powder was washed with THF and dried *in vacuo* to afford **23** as a yellow solid in 70 % yield.

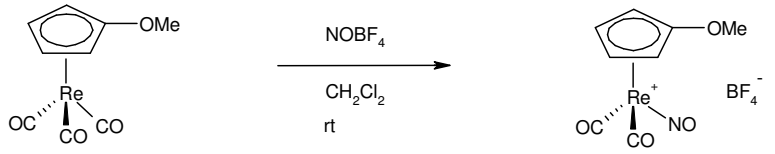


**7** **23**

**Scheme 5.2**

The structure of **23** was confirmed by $^1H$, $^{13}C$ NMR, IR and mas spectroscopy. Unfortunately, we failed to isolate an anatilically pure sample of **23** for elemental analysis. The $^1H$ NMR spectrum of **23** in acetone-$d_6$ displayed two triplets at 6.46 and 6.33 ppm attributed to the protons of the $C_5H_4$ group. The singlet at 5.32 ppm confirmed the existence of the methyl group (Figure 5.1). The $^{13}C$ NMR showed a resonance at 183.7 ppm which confirmed the existence of metal bound carbonyl groups. The resonance at 155.3 ppm was assigned to the $C_{ispso}$ of the $C_5H_4$ group and the resonances at 89.6 and 74.9 pm to the $C_5H_4$ ring carbon atoms. The $C_{Me}$ resonated at 60.9 ppm (Figure 5.2). The IR spectrum of **23** displayed two ν(CO) bands at 2100 and 2046 $cm^{-1}$ and a ν(NO) band at 1803 $cm^{-1}$ in accord with the the $Re(CO)_2(NO)$ pattern. The mass spectrum showed the correct molecular-ion peak for $[(\eta^5\text{-}C_5H_4OCH_3)Re(CO)_2(NO)]^+$ (Figure 5.3).

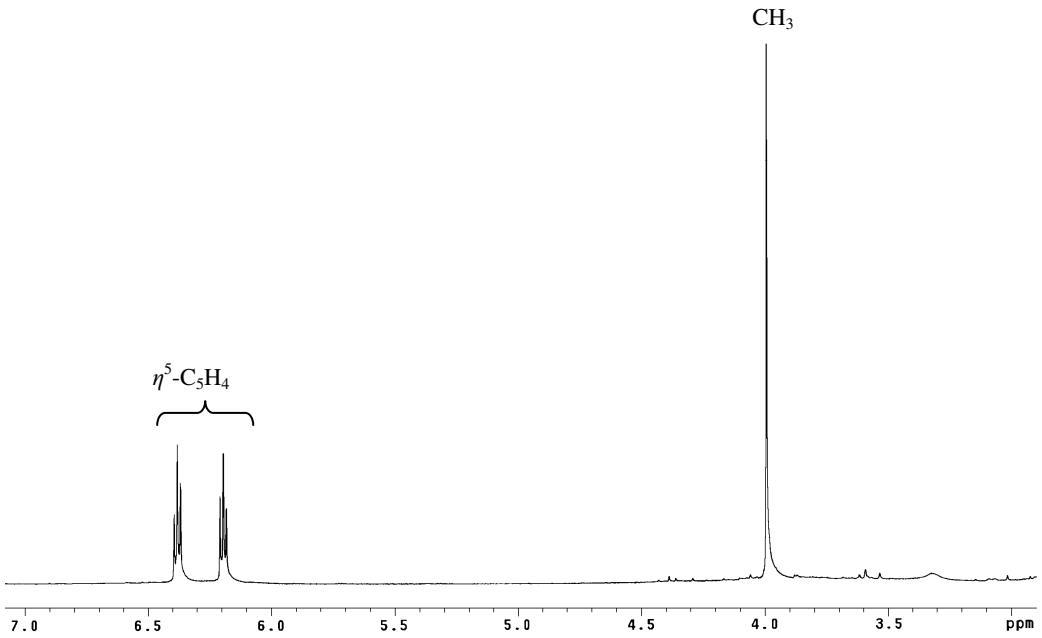


**Figure 5.1** $^{1}$H NMR of **23** in acetone-$d_6$.

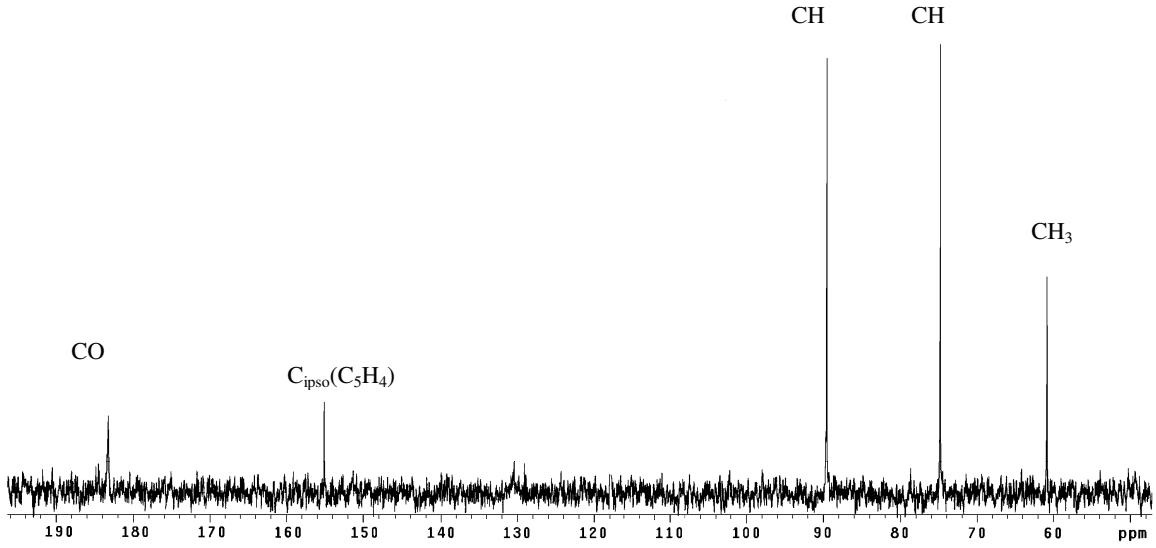


**Figure 5.2** $^{13}$C NMR of **23** in acetone-$d_6$.

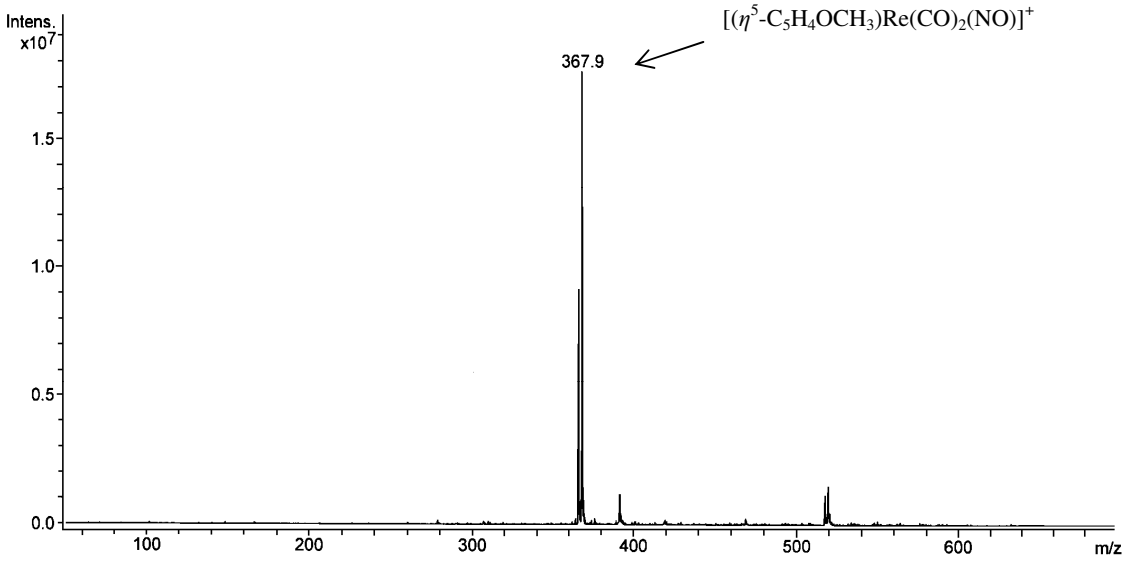


**Figure 5.3** Mas spectrum (ESI) of **23**.

## 5.3 $[(\eta^5\text{-}C_5H_4NHCOOCH_2Ph)Re(CO)_2(NO)]^+BF_4^-$ (24)

Reaction of ($\eta^5$-{[(benzyloxy)carbonyl]amino}cyclopentadienyl)(tricarbonyl)rhenium (**18**) with 2 equivalents of $NOBF_4$ in dichloromethane provided the corresponding nitrosyl complex **24**. The complex **24** was isolated as an orange-brown powder in a yield of 70 % (Scheme 5.3).

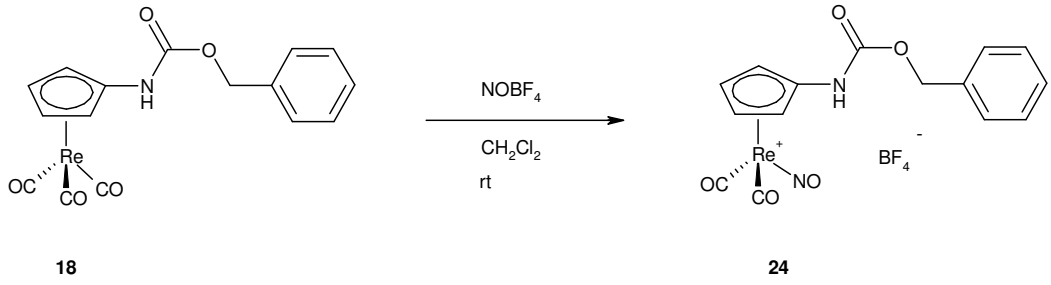


**Scheme 5.3**

The structure of **24** was confirmed by $^1H$, $^{13}C$ NMR, IR mass spectroscopy but unfortunately the sample was not analytically pure. Efforts to obtain analytically pure **24** by recrystallization in acetone / ether were ineffective.

The $^{1}H$ NMR of **24** in acetone-$d_6$ displayed a multiplet in the range 7.37-7.40 attributed to the protons of the phenyl group. The two triplets at 6.56 and 6.43 ppm were assigned to the $C_5H_4$ ring protons. The $^{13}C$ NMR spectrum showed a resonance at 183.9 ppm assigned to the carbonyl of the $Re(CO)_3$ unit. The carbonyl group of the carbamate gave rise to a signal at 153.6 ppm. The $^{13}C$, $^{1}H$ NMR correlation spectrum showed that the $^{13}C$ atoms resonating at 136.5 ppm 129.4, 129.3 and 128.9 ppm correspond to the carbon atoms of the phenyl group (Figure 5.4). The two $^{13}C$ resonances at 90.8 and 79.2 ppm correlated with the $^{1}H$ NMR signals assigned to the $C_5H_4$ ring protons. These two resonances were therefore attributed to the carbon atoms in proximal and distal position of OMe of the $C_5H_4$ group. By deduction, the resonance at 131.8 ppm was assigned to the $C_{ipso}$ of the $C_5H_4$ moiety and the signal at 79.2 ppm to the benzylic carbon. The IR spectrum of **24** in KBr displayed two ν(CO) bands at 2130 and 2076 $cm^{-1}$ and a ν(NO) band at 1823 $cm^{-1}$. The mass spectrum of **24** showed the correct molecular-ion peak for $[(\eta^5\text{-}C_5H_4ONHCbz)Re(CO)_2(NO)]^+$ (Figure 5.5).

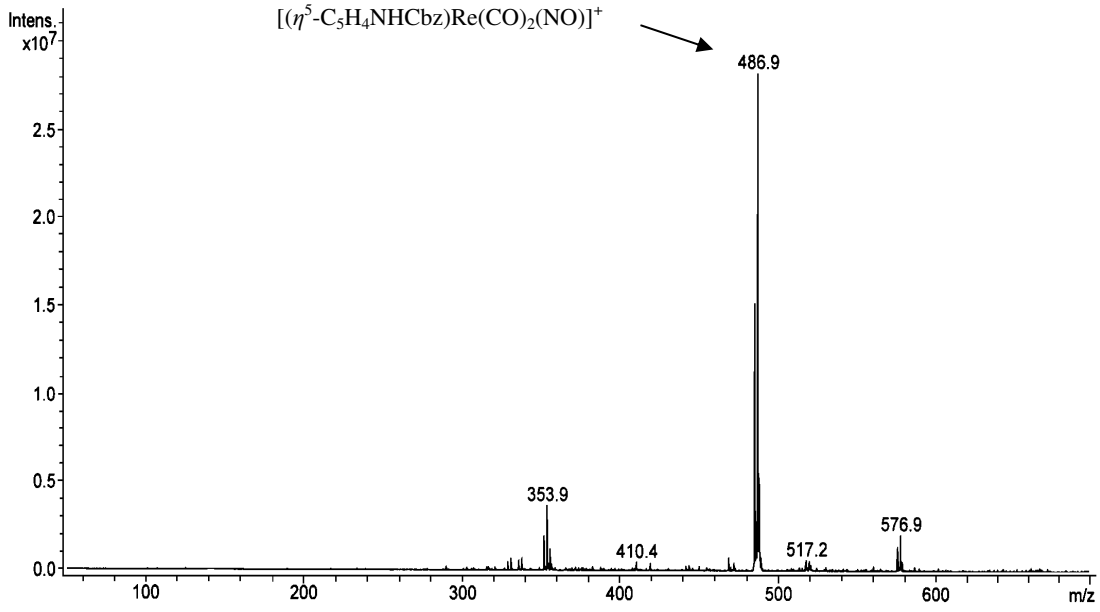


**Figure 5.5** Mass spectrum of **24**.

$C_5H_4$

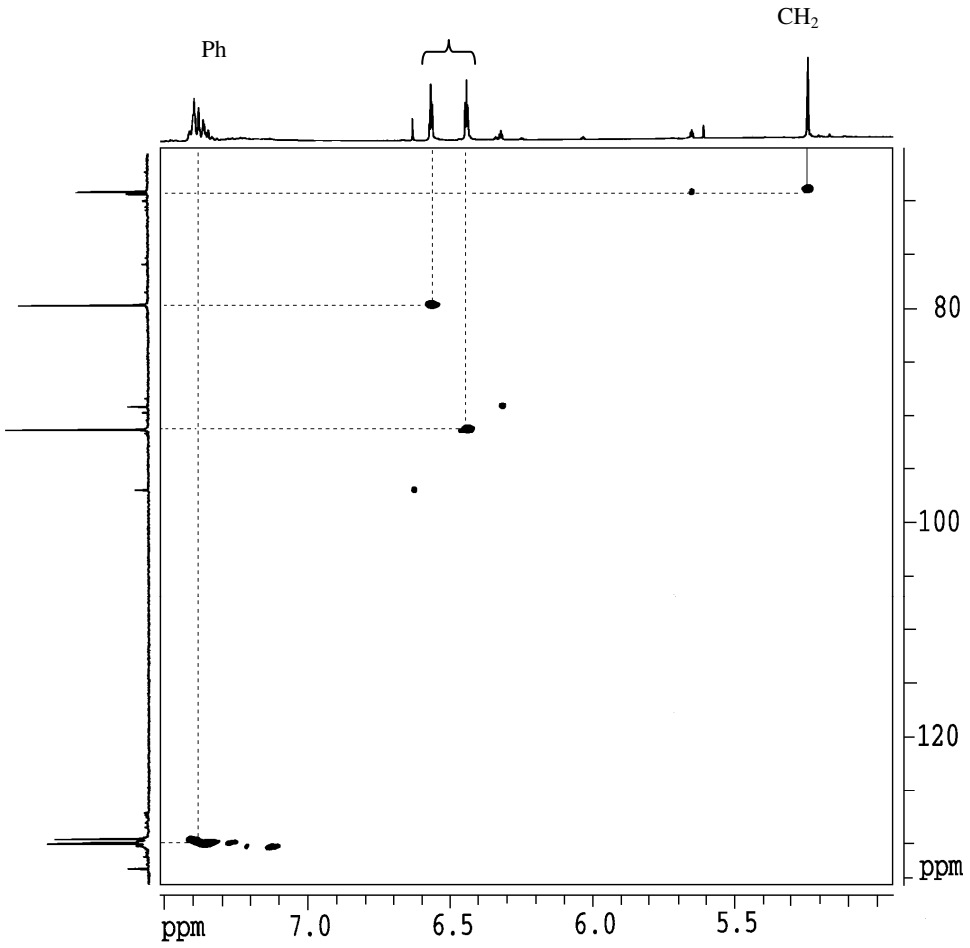


**Fifure 5.4** Long range $^{13}C$, $^{1}H$ correlation of **24** in acetone-$d_6$ at 20 °C.

### 5.3.1 [($\eta^5$-$C_5H_4OCH_2Ph$)$Re(CO)_2(NO)]^+BF_4^-$ (25)

### 5.3.2 Preparation of 25

$NOBF_4$ was added in four portions to a solution of **11** in dichloromethane. Addition of nitrosonium tetrafluoroborate into the reaction mixture was followed by gas evolvement. After 24 hours the solvent was removed *in vacuo*. The resulting yellow powder was washed with THF and dried *in vacuo* to afford **25** as a yellow powder in 70 % yield (Scheme 5.4).

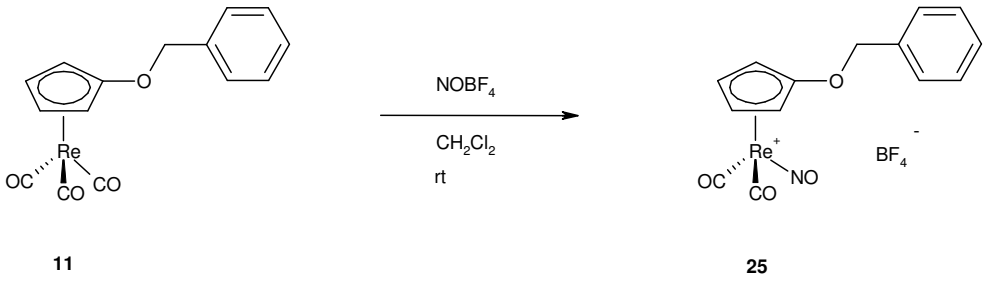


**11** **25**

**Scheme 5.4** Preparation of **25**

### 5.3.3 Characterization of 25

The structure of **25** was confirmed by $^{1}H$, $^{13}C$ NMR, IR and mass spectroscopy. Despite our efforts to purify and crystallize this complex, the sample was not analytically pure. As showed in Scheme 5.6, the $^{1}H$ NMR spectrum of **25** in acetone-$d_6$ displayed a multiplet in the range 7.45-7.35 ppm, assigned to the aromatics protons and two triplets at 6.46 and 6.33 ppm attributed to the $C_5H_4$ ring protons. The two benzylic protons appeared at 5.32 ppm. The $^{1}H$ NMR signals of **25** are situated in lower field than those of **11**. For comparison, the $^{1}H$ NMR spectrum of **11** displayed in acetone two triplets at 5.47 and 5.36 ppm and a singlet at 4.84 ppm in acetone. In the $^{13}C$ NMR spectrum of **25** in acetone-$d_6$ the $C_{CO}$ atoms gave rise to a signal at 179.7 ppm. The carbons of the $C_5H_4$ moiety resonated at 134.8, 89.6 and 75.8 ppm. The resonance at 75.6 ppm was assigned to the benzylic carbon and the resonances at 130.4, 130.0 129.7 and 129.2 ppm were attributed the phenyl group. The IR spectrum of **25** in KBr displayed two ν(CO) bands at 2100 and 2046 $cm^{-1}$ and a ν(NO) band at 1803 $cm^{-1}$ (Figure 5.7). The mass spectrum of **25** showed the correct molecular-ion peak for $[(\eta^5\text{-}C_5H_4OCH_2Ph)Re(CO)_2(NO)]^+$ (Figure 5.8)

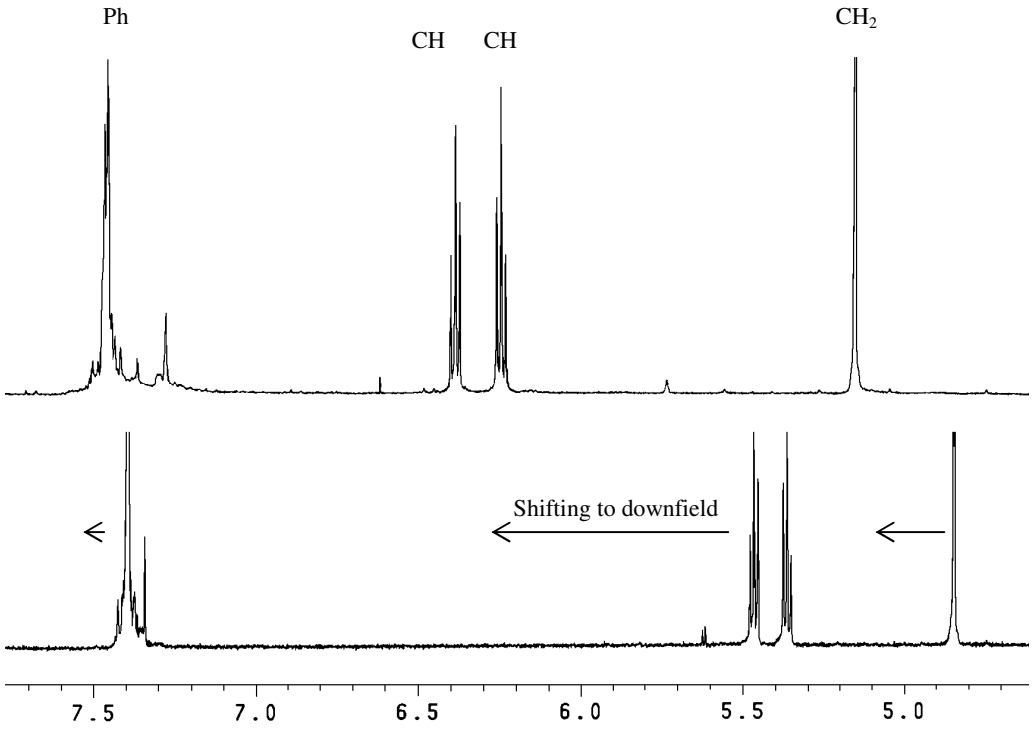


**Figure 5.6**. $^{1}$H NMR spectrum of **25** (top) and **11** (below) in acetone-$d_6$ at 20 °C

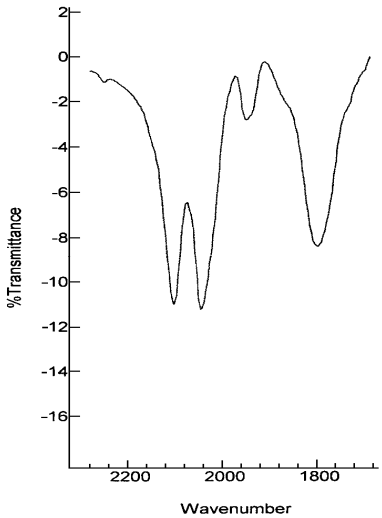


**Figure 5.7** IR spectrum of **25** in dichloromethane

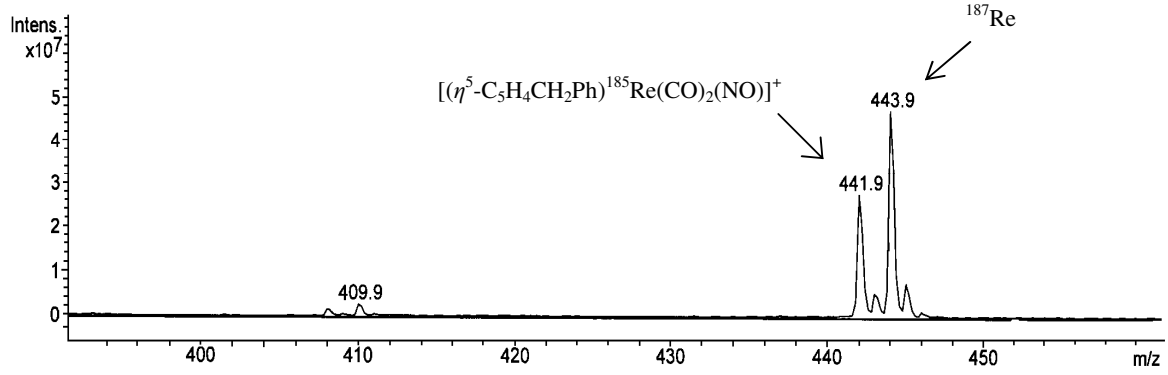


**Figure 5.8** Mass spectrum (ESI) of **25**.

## 5.4 ($\eta^5$-$C_5H_4OCH_2Ph$)Re(CO)(NO)H (26)

### 5.4.1 Preparation of 26

The compound **26** was dissolved in acetone and treated with 3 equivalents of trietylamine and 28 equivalents of $H_2O$. The mixture was heated to 50°C for one hour (Scheme 5.5). The product was extracted from the acetone solution with pentane. The solvent was removed from the pentane extract to afford **26** as a orange solid in the yield of 32%.

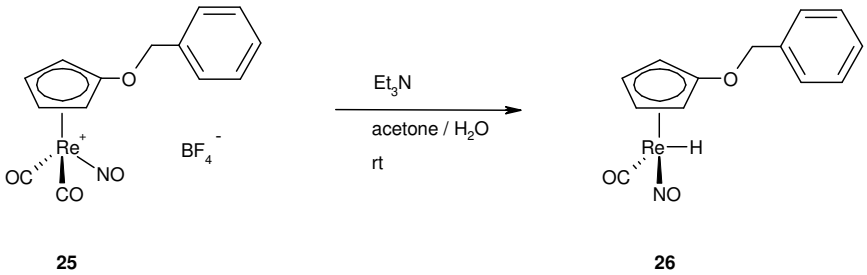


**25** **26**

**Scheme 5.5**

### 5.4.2 Characterization of 26

The new compound **26** was characterized by $^1H$, $^{13}C$ NMR , IR spectroscopy. The composition of **26** was confirmed by elemental analysis. Crystals suitable for X-ray

diffraction were obtained from dichloromethane/pentane. The X-ray diffraction study confirmed the structure of **26**.

The $^{1}H$ NMR spectrum of **26** in $CD_2Cl_2$ displayed a multiplet in the range 7.40 and 7.37 ppm, attributed to the phenyl group. Four quadruplets at 5.53, 5.42, 5,32 and 5.00 ppm were assigned to the protons of the $C_5H_4$ ring. The singlet at 4.79 ppm was assigned to the proton at the benzylic position and the singlet at -7.88 ppm was assigned to the hydridic proton. These assignations were confirmed by the integration ratio (Figure 5.9). The $^{1}H$ NMR signal at -7.88 ppm is a characteristic value of cyclopentadienyl hydrido rhenium complexes. For comparison, in the $^{1}H$ NMR spectrum of ($\eta^5$-$C_5H_5$)Re(NO)(CO)H in $CD_2Cl_2$ the hydridic proton appears at -8.50 ppm. In the $^{1}H$ NMR spectrum of [$\eta^5$-$C_5H_4CH_2CH_2N(CH_3)_2$]Re(NO)(CO)H in $CDCl_3$ the hydridic proton appears at -8.33 ppm. The $^{13}C$ NMR spectrum of **26** in $CD_2Cl_2$ displayed a resonance at 208.5 ppm which confirmed the existence of the $C_{CO}$ atom. Analysis of the long range $^{13}C$, $^{1}H$ correlation showed that the $^{13}C$ NMR resonances at 135.4, 129.0 and 128.3 ppm correlate with the $^{1}H$ NMR signal assigned to the phenyl group. It showed also that the $^{13}C$ NMR signal at 74.9 ppm correlates with the $^{1}H$ NMR signal at 4.79 ppm assigned to the benzylic position. The signals at 80.9, 79.4, 71.3 and 70.5 ppm were then assigned to the carbons of the $C_5H_4$ group. The signal of the carbon in the cyclopentadienyl ring bound to the oxygen is usually not much intense, situated in the range 120-130 ppm and therefore it was not observed. The IR spectrum of **26** in hexane showed a ν(CO) band at 1976 $cm^{-1}$ and a ν(NO) band at 1718 $cm^{-1}$ (Figure 5.10) X-ray diffraction studies showed that the compound **26** crystallized in the triclinic system P-1 (Figure 5.11). Selected bond distances and bond angles are listed in Table 5.1. The X-ray data collection and processing parameters are listed in Table 7.3.10.

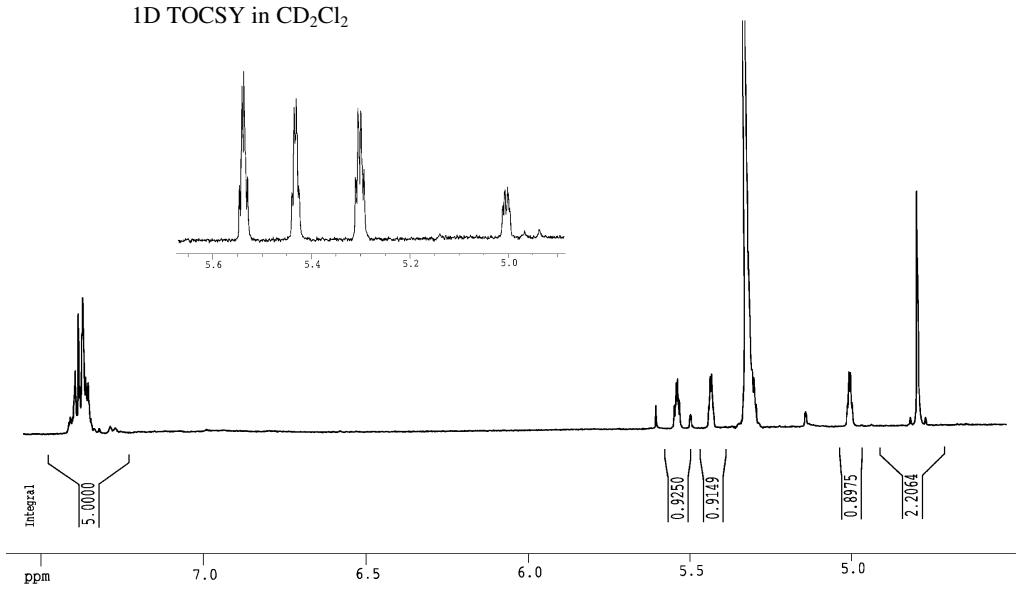


**Figure 5.9** $^1$H NMR spectra of **26** in $CD_2Cl_2$ at 20 °C (down) and 1D TOCSY (up)

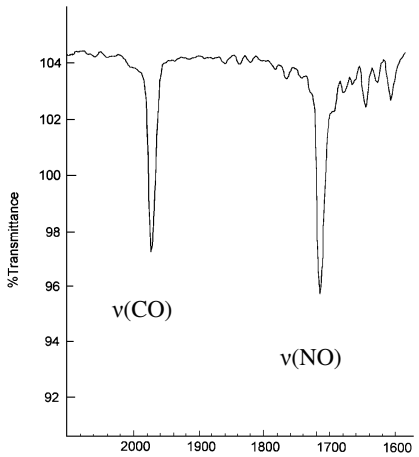


**Figure 5.10** IR spectrum of **26** in hexane.

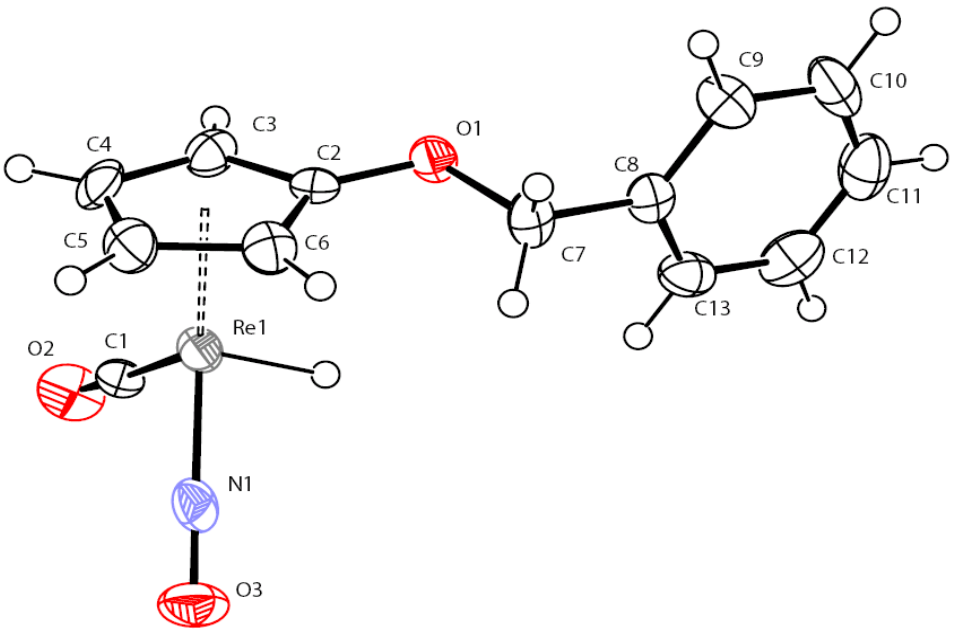


**Figure 5.11** X-ray structure of **26** (ORTEP representation with selected atomic labels). Thermal ellipsoids are shown with a 30% probability level.

**Table 5.1** Selected bond distances (Å) and bond angles (°) of **26**.

| Selected bond distances (Å) | | Selected angles (°) | |
|---|---|---|---|
| Re1-C1 | 1.856(6) | N1-Re1-H | 86.2(2) |
| Re1-N1 | 1.853(5) | C1-Re1-H | 97(3) |
| Re1-H | 1.500(6) | C3-C2-C6 | 108.0(5) |
| N1-O3 | 1.158(6) | C2-C3-C4 | 107.7(5) |
| C1-O2 | 1.155(7) | C3-C4-C5 | 108.7(5) |
| C2-O1 | 1.356(6) | C4-C5-C6 | 107.8(6) |
| C2-C3 | 1.425(7) | C5-C6-C2 | 107.6(5) |
| C4-C5 | 1.394(10) | | |
| C5-C6 | 1.437(8) | | |
| C6-C2 | 1.400(8) | | |

## 5.5 [$\eta^5$-$C_5H_4OH$)$Re(CO)_2(NO)]^+BF_4^-$ (27)

A solution of **6** with 2 equivalents of nitrosonium tetrafluoroborate was stirred 12 hours at room temperature (Scheme 5.6). The product **27** was isolated in 80 % yield as a yellow solid after washing with THF. Recrystallization from a mixture of acetone and ether afforded the analytically pure product **27**.

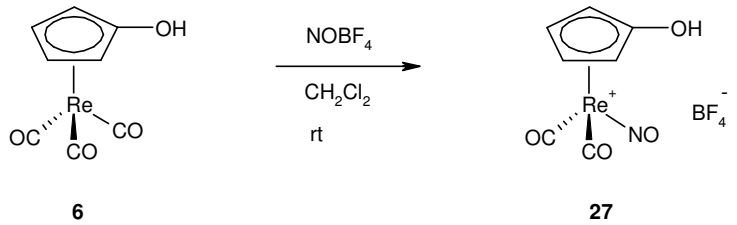


**6** **27**

**Scheme 5.6**

### 5.5.1 Characterization of 27

The composition of **27** was confirmed by elemental analysis. The IR spectrum of **27** displayed two ν(CO) bands at 2102 and 2042 $cm^{-1}$ and a ν(NO) band at 1809 $cm^{-1}$, which is in accord with the $Re(CO)_2NO$ pattern of **27**. Additionally the mass spectrum of **27** showed the expected molecular-ion peak at m/z 376, which corresponds to the nitrosyl cation [($\eta^5$-$C_5H_4OH$)$Re(CO)_2NO]^+$ (Figure 5.12).

Suitable crystals for X-ray diffraction were obtained by slow diffusion of ether into a solution of acetone at -30 °C. The X-ray studies confirmed the structure of **27** (Figure 5.13). Selected bond distances and bond angles are listed in Table 5.2. The X-ray data collection and processing parameters are listed in Table 3.11.

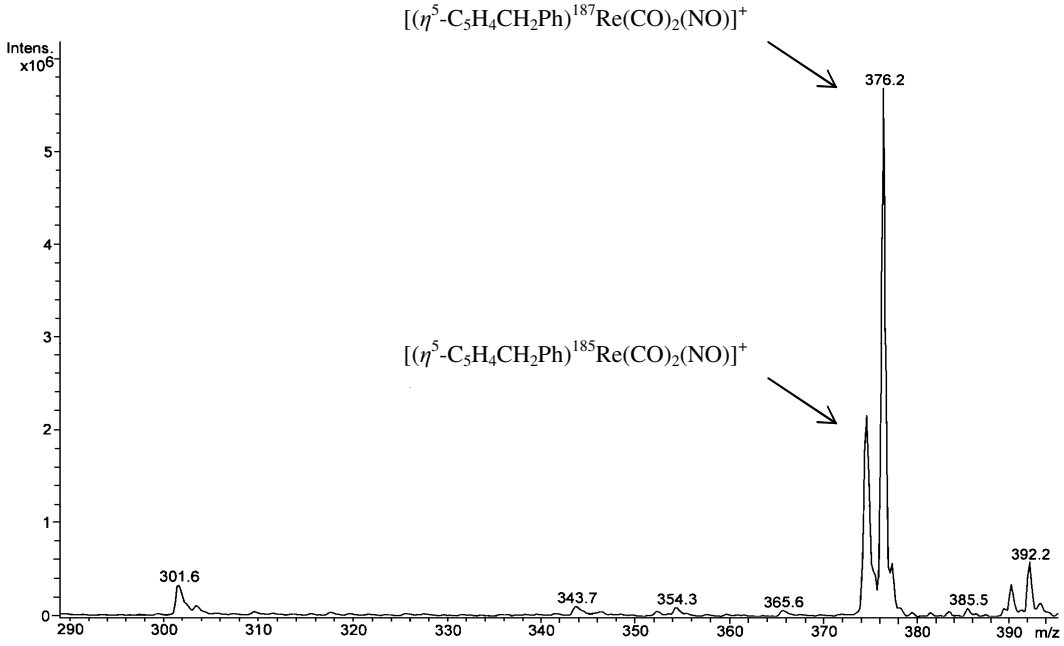


**Figure 5.12** Mass spectrum (EI) of **27**

**Table 5.2** Selected bond distances (Å) and bond angles (°) of **27**

| Selected bond distances (Å) | | Selected angles (°) | |
|---|---|---|---|
| Re1-N1 | 1.895(9) | C7-C3-O4 | 122.9(8) |
| N1-O3 | 1.152(10) | Re1-N1-O3 | 178.8(8) |
| C3-O4 | 1.337(11) | Re1-C1-O1 | 177.3(9) |
| C7-C3 | 1.403(12) | Re1-C2-O2 | 175.7(8) |
| C3-C4 | 1.437(13) | C3-C7-C6 | 107.1(8) |
| C5-C4 | 1.424(12) | C7-C6-C5 | 108.7(8) |
| C6-C5 | 1.409(14) | C6-C5-C4 | 107.9(9) |
| C6-C7 | 1.441(14) | C5-C4-C3 | 107.3(8) |

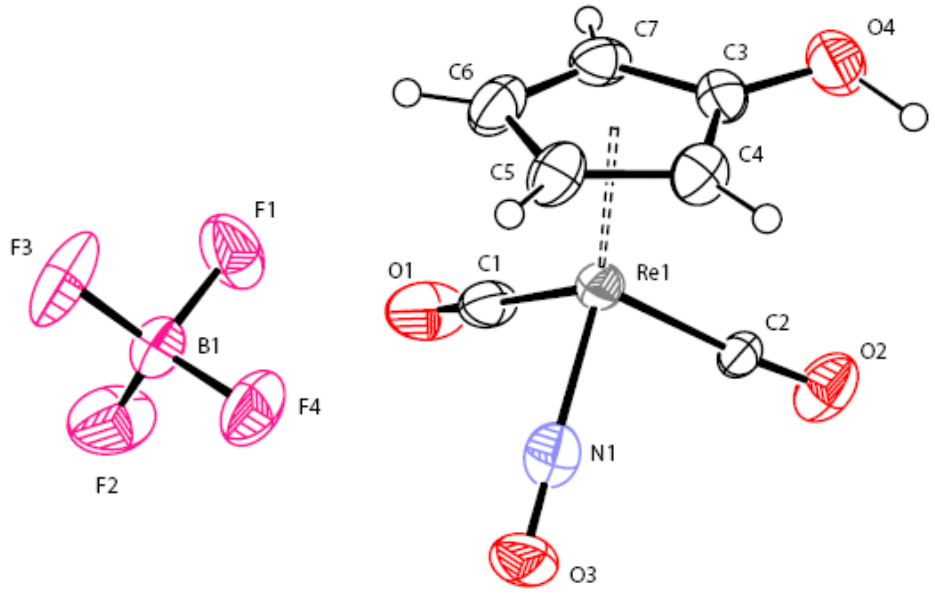


**Figure 5.13**. X-ray structure of **27** (ORTEP representation with selected atomic labels). Thermal ellipsoids are shown with a 30% probability level.

Unexpectedly the $^{1}$H NMR spectrum of **27** in acetone-$d_6$ revealed four triplets at 6.39, 6.27, 6.08 and 5.66 ppm. The $^{1}$H COSY NMR showed that the $^{1}$H NMR signal at 6.39 ppm (Ha) correlates with the $^{1}$H NMR signal at 6.08 ppm (Hc) and the $^{1}$H NMR signal at 6.27 ppm (Hb) correlates with the $^{1}$H NMR signal at 5.66 ppm (Hd) (Figure 5.14). This observation tends to show that **27** is in equilibrium with another species in acetone. The 1D NOESY spectra of **27** confirmed this hypothesis. The table 5.3 summarizes the NOESY experiments.

**Table 5.3** Summary of the 1D NOESY experiments

| Selective excitation | NOEs effects | |
|---|---|---|
| {Ha} | Ha-Hb | Ha-Hc |
| {Hb} | Hb-Ha | Hb-Hd |
| {Hc} | Hc-Ha | Hc-Hd |
| {Hd} | Hd-Hb | Hd-Hc |

When the signal of Ha was selectively excited, we observed NOEs effects between Ha and Hb and between Ha and Hc. Selective excitation of Hb gave NOEs effects between Hb and Ha and between Hb and Hd. After selective excitation of Hc, we observed NOEs effects between Hc and Ha and between Hc and Hd. When the signal of Hd was selectively excited, we observed NOEs effects between Hd and Hb and between Hd and Hc. The NOEs effects Ha-Hc and Hb-Hd are consistent with the 1D COSY NMR. The NOEs effects Ha-Hb and Hb-Hc indicates a proton exchange Ha-Hb and a proton exchange Hc-Hd, which proves that the compound **27** gives another species in acetone. The protons Ha and Hc were attributed to **27** by comparison with the $^{1}$H NMR spectra of compounds **23**, **24** and **2**5. The $^{1}$H NMR signals of the new species **28** are therefore Hb and Hd.

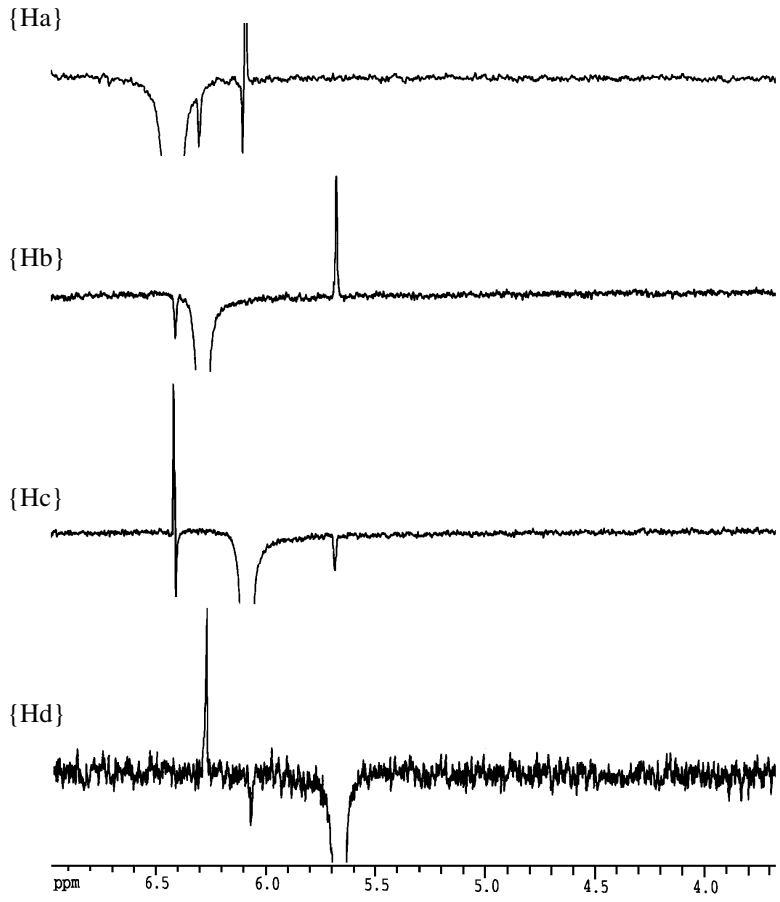


**Figure 5.15** 1D NOE experiments of **27** with selective excitation of Ha, Hb, Hc and Hd in acetone-$d_6$ at 20 °C.

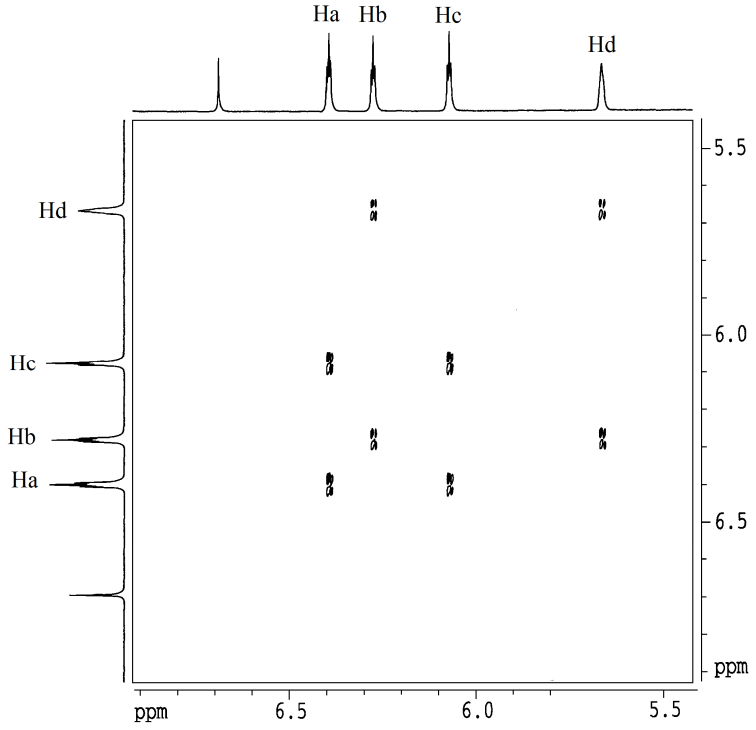


**Figure 5.14** 1D COSY spectrum of **27** in acetone-$d_6$ at 20 °C.

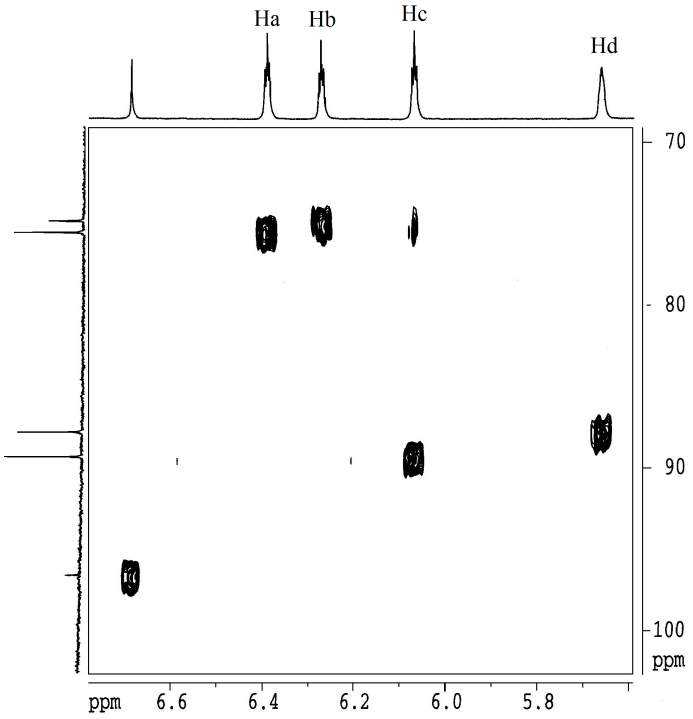


**Figure 5.16** Long range $^{13}C$, $^{1}H$ correlation of **27** in acetone-$d_6$ at 20 °C.

The $^{13}C$, $^{1}H$ correlation of **27** in acetone showed that the $^{1}H$ NMR signal of Ha correlates with the $^{13}C$ NMR signal at 75.6 ppm (Figure 5.16). The $^{1}H$ NMR signal of Hc correlates with the $^{13}C$ signal at 89.3 ppm. The $^{1}H$ NMR signal of Hb correlates with the $^{13}C$ NMR signal at 74.9 ppm and Hd with $^{13}C$ NMR signal at 87.8 ppm. The $^{13}C$ NMR spectrum displayed two resonances at 185.4 and 182.3 ppm attributed the $C_{CO}$ of the $Re(CO)_3$ unit of **27** and the unknown complex. For more clarity the $^{1}H$ and $^{13}C$ NMR signals of the two species **27** and the unknown complex are reported in Table 5.4.

**Table 5.4** $^{1}H$ NMR and $^{13}C$ NMR data for the two species **27** and the unknown complex

| | $^{1}H$ NMR δ (ppm) | $^{13}C$ NMR δ (ppm) |
|---|---|---|
| **27** | 6.39, 6.08 | 185.4, 158.6, 89.3, 75.6, |
| **Unknown complex** | 6.27, 5.66 | 184.5, 157.9, 87.8, 74.9 |

The $^{1}H$ NMR spectrum of **27** in acetonitrile-$d_3$ showed two triplets at 5.54 and 5.67 ppm and a broad signal at 9.25 ppm, which indicates the existence of an acidic proton. The chemical shift shows that the pKa of the OH group would be similar to a phenolic OH group. This acidic proton was assigned to the OH group of **27** since the proton of the OH group was expected to be acidic due to the presence of the rhenium(+1) unit. Thus the observed equilibrium could correspond to an acido-basic equilibrium between the acidic species **27** and its conjugate base **28** as showed below (Scheme 5.7).

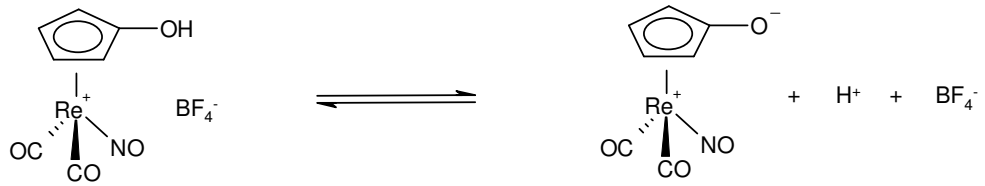


**27** **28**

**Scheme 5.7** Acido-basic equilibrium between **27** and **28**

The release of a proton could also lead to a neutral species such as **29** after formation of a cyclopentdienone moiety (Scheme 5.8). The hypothetic species **29** is a 18 electron rhenium complex with a $\eta^4$ rhenium-coordinated cycloptendienone.

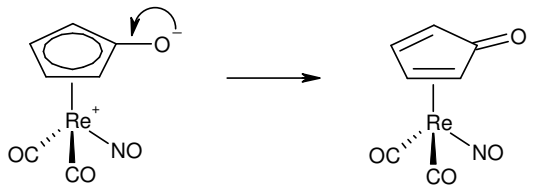


**29**

**Scheme 5.8** Hypothetic species **29**

### 5.5.2 Attempt to prepare the target molecule

The compound **26** was considered as a good precursor for the preparation of the target molecule ($\eta^5$-$C_5H_4OH$)Re(CO)(NO)H. We tried to deprotect **26** under pressure of dihydrogen in methanol in the presence of palladium but unfortunetly the deproctection failed (Scheme 5.10). The $^1$H NMR signals of **26** in the mixture were not anymore observable after a few hours.

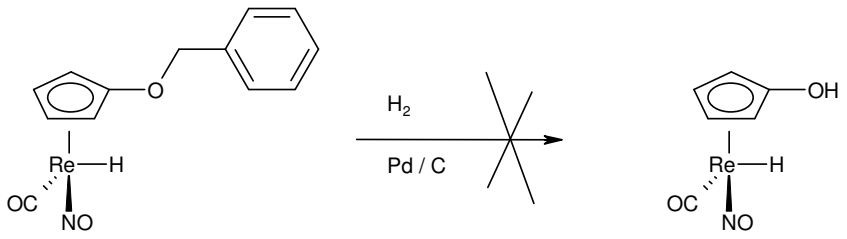


**26** target molecule

**Scheme 5.9**

The complex **27** was also a potential precursor for the preparation of the hydride ($\eta^5$-$C_5H_4OH$)Re(CO)(NO)H. **27** was treated with $Et_3N$ and $H_2O$, the conditions used for the prepration of the rhenium hydride **26**. The rhenium hydride $\eta^5$-$C_5H_4OH$)Re(CO)(NO)H was not observed and the complex **27** decomposed. No signal of substituted cyclopentadienyl group was observed in $^1$H NMR spectroscopy.

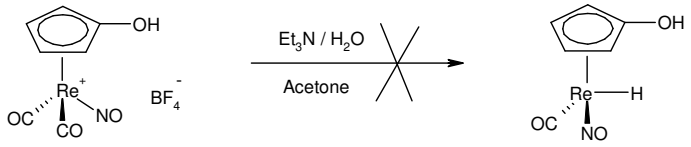


27 Target Molecule

**Scheme 5.10**

## 5.6 Summary

We prepared successfully the four novel nitrosyl complexes [($\eta^5$-$C_5H_4OMe$)$Re(CO)_2(NO)]^+BF_4^-$ (**23**), [($\eta^5$-$C_5H_4OCH_2Ph$)$Re(CO)_2(NO)]^+BF_4^-$ (**25**), [($\eta^5$-$C_5H_4OH$)$Re(CO)_2(NO)]^+BF_4^-$ (**27**), [($\eta^5$-$C_5H_4NHCbz$)$Re(CO)_2(NO)]^+BF_4^-$ (**24**) and the novel hydride ($\eta^5$-$C_5H_4OCH_2Ph$)Re(CO)(NO)H (**26**). But we failed to obtain the target molecule via the deprotection of **25** and from **27** under the triethylamine water conditions. It was demonstrated by NMR spectroscopy that compound **27** is in equilibrium in acetone with another species, which was suggested to be the conjugate base of **28** [($\eta^5$-$C_5H_4O^-$)$Re(CO)_2(NO)]^+BF_4^-$. However we did not exclude that **28** could rearrange to give the corresponding 18 electron and neutral $\eta^4$-cyclopentadienone nitrosyl rhenium complex ($\eta^4$-$C_4H_4CO$)$Re(CO)_2(NO)$ **29**. Further work would consist in the determination and the isolation of the structure of the unknown compound and in the determination of the right conditions permitting deprotection of **26.**

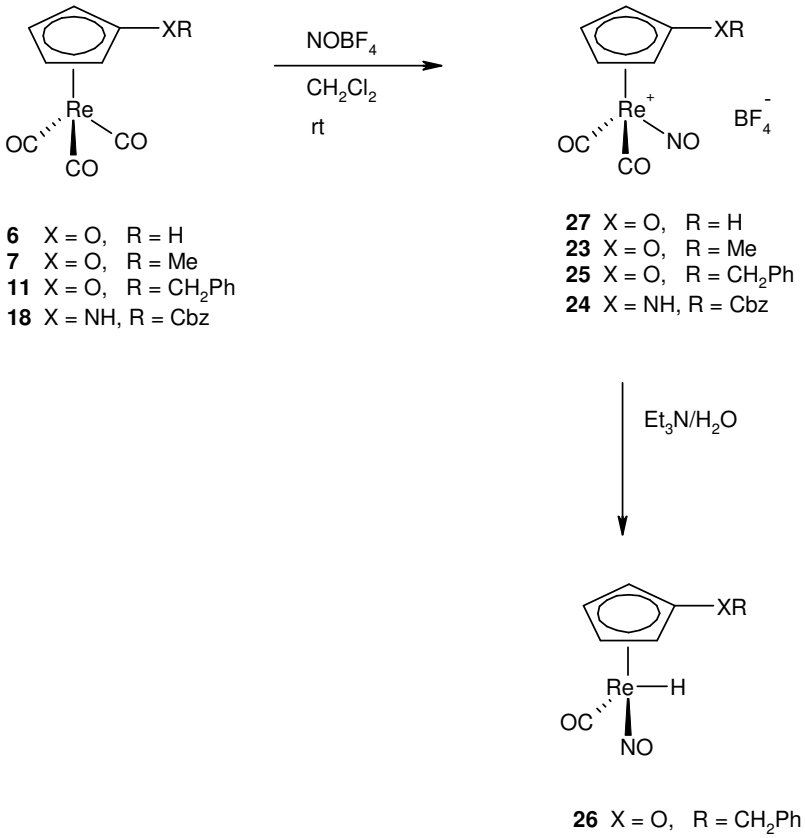


**6** X = O, R = H
**7** X = O, R = Me
**11** X = O, R = $CH_2Ph$
**18** X = NH, R = Cbz

**27** X = O, R = H
**23** X = O, R = Me
**25** X = O, R = $CH_2Ph$
**24** X = NH, R = Cbz

**26** X = O, R = $CH_2Ph$

**Scheme 5.11** Summary

## 5.7 References

[1] R. P. Stewart, N. K. Okamota, W. A. G. Graham, *J. Organomet. Chem.* **1972**, *42*, C32.

[2] A. N. Nesmeyanov, K. N Anisimov, N. E. Kolobova, L. L Krasnoslobodskaya, *Bull. Acad. Sci. USSR,* **1970**, 807 (*Izv. Aka. Nauk. SSSR*, Ser. Khim. **1970**, 860).

[3] C. P. Casey, M. A. Andrews, D. R. McAlister, J. E. Rinz, *J. Am. Chem. Soc.* **1980**, *102*, 1927.

[4] E. O. Fischer, H. Strametz, *Z. Naturforsch. B*, **1968**, *23*, 278.

[5] J. R. Sweet, W. A. G. Graham, *Organomet.* **1982**, *104*, 2811.

[6] C. P. Casey, M. A. Andrews, J. E. Rinz, *J. Am. Chem. Soc.* **1979**, *101*, 741.

[7] J. R. Sweet, W. A. G. Graham, *Organomet.* **1982**, *1*, 982.

# 6 Conclusion

We designed a new polar rhenium hydride with potential catalytic activity for ionic hydrogenation. Based on the Shvo's catalytic system, the isoelectronic 18 e complexes ($\eta^5$-$C_5H_4XH$)Re(CO)(NO)H (X = NR, X = O) bear acidic functions and a hydride. The transfer of $H^-$ and $H^+$ to an unsaturated substrate would give the 16 e $\eta^4$-cyclopentadienone coordinated rhenium complex [$\eta^4$-$C_5H_4(CO)$]Re(CO)(NO). The 18 e complex would be regenerated by heterolytic uptake of $H_2$.

We developed a new method to produce the complex ($\eta^5$-$C_5H_4OH$)$Re(CO)_3$ (**6**), which was obtained by reaction of the lithium complex ($\eta^5$-$C_5H_4Li$)$Re(CO)_3$ (**2**) with dioxybis(trimethylsilane) $(Me_3SiO)_2$. **6** was isolated in a moderate yield but the second product of the reaction ($\eta^5$-$C_5H_4SiMe_3$)$Re(CO)_3$ (**3**) could be recycled and thus the reaction yield could be considerably increased. This procedure implies only starting materials easy to prepare and to handle and it is therefore an excellent method to produce **6** in a large scale.

A series of various alkoxy and acyloxy cyclopentadienyl tricarbonyl rhenium complexes $\eta^5$-$C_5H_4R$)$Re(CO)_3$ ( R = OMe **7**, R = OEt **8**, R = O$^i$Pr **9**, R = OCHCH=$CH_2$ **10**, R = $OCH_2Ph$ **11**, R = OCOMe **12**, R = OCOPh **13**) has been prepared from **6**.

The new amino complex ($\eta^5$-$C_5H_4NH_2$)$Re(CO)_3$ **15** was obtained by reduction of the azido complex ($\eta^5$-$C_5H_4N_3$)$Re(CO)_3$ **14** with $NaBH_4$. A great variety of amino cyclopentadienyl rhenium complexes were synthesized ($\eta^5$-$C_5H_4R$)$Re(CO)_3$ (R = NCHPh **16**, R = $NHCH_2Ph$ **17**, R = NHCbz **18** R = NHCOMe **19**, R = $NHC_4H_8$ **20**, R = $NHCONHC_8H_3F_6$ **21**, R = $NHCONHC_6F_5$ **22**). The urea complexes **21**, **22** are of great interest since they could play a key role in the catalytic system. The acidic urea function could stabilize the substrate in the close vinicity to the hydride and the strong double hydrogen bonding between the substrate and the urea cyclopentadienyl rhenium complex could initiate the transfer of the hydride. Benzyl functions can be removed by hydrogenolysis. A benzyloxycarbonylamino, a benzylamino or a benzyloxy nitrosyl hydride could lead directly to the target molecule under pressure of $H_2$.

We prepared the new nitrosyl complexes $[(\eta^5\text{-}C_5H_4R)Re(CO)_2(NO)]^+BF_4^-$ (R = OH **27**, R = $OCH_3$ **23**, R = $OCH_2Ph$ **25**, R = NHCbz **24**). **27** exhibited an interesting behavior in solution. When **27** was dissolved in acetone, an equilibrium occurred. The species **28** in equilibrium with **27** was not identified but spectroscopic data suggests that **28** is the conjugate base $[(\eta^5\text{-}C_5H_4O^-)Re(CO)_2(NO)]^+BF_4^-$ of **27** or the $\eta^4$ cyclopentadienone rhenium coordinated complex $[(\eta^4\text{-}C_5H_4(C{=}O)]Re(CO)_2(NO)$.

# 7 Experimental Section

## 7.1 General Considerations

All manipulations of air sensitive compounds were carried out either in a glove box under recirculating dry nitrogen or under dry nitrogen by conventional Schlenk techniques. Solvents were distilled from appropriate drying agents and freshly distilled under nitrogen prior to use (e.g. diethylether, hexane, pentane, benzene, toluene, xylene and THF were purified by refluxing over sodium/benzophenone; dichloromethane was refluxed either over calcium hydride or $P_2O_5$).
The deuterated solvents ($C_6D_6$, $CDCl_3$, $CD_3CN$, $CD_2Cl_2$, toluene-$d_8$ and THF-$d_8$) were also obtained from commercial suppliers and distilled from appropriate drying agents and vacuum transferred for storage in Schlenk flasks fitted with Teflon stopcocks.

Elemental analyses were measured with a *Leco CHN(S)-932* analyzator.

IR spectra were recorded on the spectrometer *Digilab FTS-40 Pro* using solid samples on a ATR device, in compressed KBr-pellets or $CaF_2$ liquid cells.

NMR spectra were recorded on the following spectrometers:

| | |
|---|---|
| $^{1}$H NMR | *Brucker Avance DRX-500, 500.2 MHz* |
| | *Varian-Gemini-300, 300.1 MHz* |
| | *Varian-Gemini-200, 200.0 MHz* |
| $^{31}$C{$^{1}$H} NMR | *Brucker Avance DRX-500, 125.8 MHz* |
| | *Varian-Gemini-300, 75.4 MHz* |
| | *Varian-Gemini-200, 50.3 MHz* |
| $^{19}$F NMR | *Varian-Gemini-200, 200.0 MHz* |
| $^{29}$Si{$^{1}$H} NMR | *Brucker Avance DRX-500, 99.30 MHz* |

Chemical shifts are reported relative to residual solvent protons as reference.

Electrospray ionization mass spectra (ESI-MS) were recorded on a spectrometer, a Finnigan MAT8400 instrument was used for fast atom bombardment mass spectroscopy with an EI source (70 ev) (EI-MS); values are reported for the $^{187}$Re isotope.

## 7.2 Syntheses

### 7.2.1 Preparation of dioxybis(trimethylsilane), $(Me_3SiO)_2$

Method 1[1]:

1,4-diazabicyclo[2.2.2]octane (DABCO) (10 g, 89 mmol) was dissolved in THF (150 mL) in a 500 mL round bottom flask equipped with a dropping funnel. The flask was placed in an ice bath and a solution of hydrogen peroxide (20 mL, 30 %) was added to the mixture drop wise with magnetic stirring. A white precipitate formed. After 6 hours of stirring, the solvent was removed with a canular equipped with a filter. The complex DABCO.$2H_2O_2$ was dried under vacuum for 5 hours at 30 °C. DABCO.$2H_2O_2$ (10 g, 55.5 mmol) and DABCO (10 g, 89 mmol) were added in a 500 mL round bottom flask placed in an ice bath. Dichloromethane (300 mL) was cooled to 0 °C and added to the mixture with a canular. Then chlorotrimethylsilane (27.6 mL, 220 mmol) was added dropwise with a dropping funnel and the slurry mixture was stirred during 3 hours at 0 °C. The whole volatiles were distilled with a short Vigreux column. The distillate was redistilled carefully in order to remove dichloromethane with a 30 cm Vigreux column. The temperature was controlled with a thermometer on the top of the distillation column (40 °C). The residue was redistilled with a smaller Vigreux. The receiver was cooled to -200 °C with liquid nitrogen and the pressure was reduced. Pure dioxybis(trimethylsilane) was collected as a colorless oil. Yield: 3.5 g (19.6 mmol, 40 %).

Method 2[2]:

In a round bottom flask of 1 L equipped with a stirring bar and a Friedrich condenser of 10 cm, were introduced urea (26.9 g, 0.45 mol), hexamethyldisilazane (104 mL, 0.50 mol) and freshly distilled acetonitrile (250 mL). The mixture was heated under reflux for 6 hours (81-82°C). Then the mixture was cooled to room temperature and the white precipitate was filtered and washed with acetonitrile on a Buchner filter funnel. Finally the white solid was dried *in vacuo* for 5 hours at 30°C to give 84.5 g of 1,3-bis(trimethylsilyl)urea (0.41 mol, 91%). Tablets of 1 g of urea hydrogen peroxide (37 g, 0.39 mol) were finely ground with a mortar pestle under nitrogen in a glove-box and introduced into a 250 mL round bottom flask. 1,3-bis(trimethylsilyl)urea (84.5 g, 0.41 mol) was suspended in dichloromethane (250 mL) in

a round bottom flask of 1 L equipped with a Friedrich condenser and the fine powder of urea hydrogen peroxide was added through a 105° bend adapter. The mixture was heated at reflux for 12 hours with magnetic stirring. The resulting thick slurry mixture was allowed to cool to room temperature and the volatiles were distilled under nitrogen using a distilling head with a short Vigreux of 10 cm. The distillate was redistilled with a 30 cm Vigreux in order to remove dichloromethane. The top of the Vigreux column was equipped with a thermometer to control the temperature (40°). The residue was transferred to a flask of 50 mL and redistilled with a short Vigreux column to give pure dioxybis(trimethylsilane). Yield: 42 g (0.24 mol, 60 %). $^1$H NMR (200 MHz, $CDCl_3$, 20 °C): δ = 0.20 (s) ppm. EI-MS: *m/z* 178 $[M]^+$, 163 $[M - CH_3]^+$, 148 $[M - 2CH_3]^+$, 133 $[M - 3CH_3]^+$, 117 $[M - 4CH_3]^+$, 105 $[M - (CH_3)_3Si]^+$, 89 $[M - (CH_3)_3SiO]^+$, 75 $[M - 2CH_3 - (CH_3)_3Si]^+$.

### 7.2.2 Preparation of dirhenium heptoxide, $Re_2O_7$ [3]

A ceramic boat containing rhenium metal (28 g, 150 mmol) was introduced in a quartz tube. Rhenium metal was heated to 1000°C with a benzene burner under a steady stream of dry oxygen gas. Rhenium heptoxide was collected as a green crystalline powder in a flask filled with nitrogen gas. Yield: 32 g (66 mmol, 88 %).

### 7.2.3 Preparation of sodium perrhenate, $NaReO_4$[4]

Rhenium heptoxide $Re_2O_7$ (32 g, 66 mmol) was dissolved in water to give perrhenic acid $HReO_4$. The corresponding anion perrehnate was obtained by addition of a sodium hydroxide into the aqueous solution of perrhenic acid. The dry perrehnate is a white powder stable under ambient atmosphere. Yield: 34 g ( 124 mmol, 94 %).

### 7.2.4 Preparation of decacarbonyl dirhenium, $Re_2(CO)_{10}$[5]

Rhenium decacarbonyl was prepared from sodium perrhenate (30 g, 110 mmol) under high pressure of CO in dry methanol with a catalytic amount of copper chips in autoclave. Yield: 32.8 g (50.3 mmol, 91 %) . IR ($cm^{-1}$, $CH_2Cl_2$, 20 °C) $\nu_{CO}$ 2070 s, 2014 s, 1968 s.

### 7.2.5 Preparation of (bromo)(pentacarbonyl)rhenium, $ReBr(CO)_5$[6]

$Re_2(CO)_{10}$ (8.7 g, 13.33 mmol, 1 equiv.) was dissolved in $CH_2Cl_2$ in a round bottom flask equipped with a magnetic bar. $Br_2$ ( 0.82 mL, 16.00 mmol, 1.2 equiv.) was added dropwise with a syringe to the mixture cooled to 0 °C with an ice bath. The solution turned orange due to excess of $Br_2$ and $BrRe(CO)_5$ precipitated as a white solid. The solvent was removed and the product was filtered on a Buchner funnel, washed with dichloromethane and dried *in vacuo* to give a white solid. Yield: 9.7 g (23.89 mmol, 90 %). IR ($cm^{-1}$, $CH_2Cl_2$, 20 °C) $\nu_{CO}$ 2046 vs, 1988 s.

### 7.2.6 Preparation of ($\eta^5$-cyclopentadienyl)thallium(1+), ($\eta^5$-$C_5H_5$)Tl[7]

Thallium sulphate (15 g, 29.7 mmol) was added into a 250 mL round bottom flask to a solution of KOH (6.67 g, 11.9 mmol) in water (100 mL) at room temperature with magnetic stirring. The mixture was warmed to 40°C for complete dissolution. A precipitate formed. The mixture was filtered on a Buchner filter funnel and the filtrate was transferred to a round bottom flask equipped with a dropping funnel. Freshly distilled cyclopentadiene (17 mL, mmol) was added to the filtrate dropwise and after complete addition the mixture was stirred for 30 min. The precipitate was filtered on a Buchner funnel and washed successively with water (35 mL), methanol (35 mL) and ether (35 mL). The brown residue was dried *in vacuo* for several hours to give a brown powder. Yield: 15 g (55.7 mmol, 94 %).

### 7.2.7 Preparation of ($\eta^5$-cyclopentadienyl)(tricarbonyl)rhenium, ($\eta^5$-$C_5H_5$)$Re(CO)_3$, (1)

Method 1[8]:

$Re_2(CO)_{10}$ (5 g, 7.7 mmol) and dicyclopentadiene (8.6 mL, 6.4 mmol) were heated under reflux for 12 hours in a round bottom flask equipped with magnetic stirring and a condenser. Then the mixture was allowed to cool to room temperature and it was extracted with acetone. After removal of the solvent, **1** was purified by chromatography. Rf = 0.40 (silica gel, Hexane/ACOEt, 9:1). Yield: 2.5 g (7.5 mmol, 49 %).

Method 2[9]:

In a round bottom flask equipped with a condenser, were added ($\eta^5$-cyclopentadienyl)thallium(1+) (7.1 g, 26 mmol, 1.1 equiv.), THF and $ReBr(CO)_5$ (9.7 g, 24 mmol, 1 equiv.). The mixture was heated to reflux for 16 hours. The mixture was filtered on a Buchner funnel and the solvent was removed to give the product as a white brown powder. 1 was purified by sublimation to give a white solid. Yield: 7.8 g (23 mmol, 96 %). $^1$H NMR (200 MHz, $CDCl_3$, 20 °C): δ = 5.38 (s, 5H, $C_5H_5$) ppm. $^{13}C\{^1H\}$ NMR (200 MHz, $CDCl_3$, 20 °C): δ = 193.8 (s, CO), 84.5 (s, $C_5H_4$) ppm. IR ($cm^{-1}$, $CH_2Cl_2$, 20 °C): $\nu_{CO}$ 2024 s, 1926 vs. Anal. Calcd. for $C_8H_5O_3Re$ (351.33): C 28.65, H 1.50. Found: C 28.30, H 1.56. EI-MS: m/z 336 $[M]^+$, 308 $[M - CO]^+$, 280 $[M - 2CO]^+$, 252 $[M - 3CO]^+$.

### 7.2.8 Preparation of ($\eta^5$-hydroxycyclopentadienyl)(tricarbonyl)rhenium, ($\eta^5$-$C_5H_4OH$)$Re(CO)_3$, (6)

**1** (4 g, 12 mmol, 1 equiv.) was added into a round bottom flask and dissolved in THF (40 mL). The mixture was cooled to -78 °C and nBuLi (14mL, 1.6 M, 14 mmol, 1.2 equiv.) was added dropwise to the mixture. After 30 min, the mixture was allowed to warm to room temperature and bis(trimethylsilyl)peroxide $(Me_3SiO)_2$ (2.7 mL, 12 mmol, 1 equiv.) was added in one portion with a syringe. The mixture was stirred for 2 hours and the solvent was removed *in vacuo*. The residue, a brown solid, was transferred to a sublimation apparatus. At 130°C *in vacuo* **3** sublimed and crystallized on the cooling finger. **5** remains at the bottom of

the flask . **5** can be used for the preparation of **6** without further purification. Additional purification could be effected by recrystallization from THF/pentane at -30 °C.
**5** was dissolved in a solution of dichloromethane (40 mL) and $HCl_{aq}$ (2 mL, 32%). The mixture was stirred for 20 min and filtered on celite. Then the filtrate was dried over $MgSO_4$. and dichloromethane was removed *in vacuo*. **6** and **3** were separated by chromatography on silica gel (ether). Compounds **6** and **3** were isolated as white solids. Additional purification of **3** can be effected by recrystallisation from hexane/$CH_2Cl_2$.

**3**: Yield: 2.15 g (5.28 mmol, 44 %). $^1$H NMR (500.2 MHz, $CDCl_3$, 20 °C): δ = 5.42 (*pseudo* t, 2H, *J* = 1.8 Hz, $C_5H_4$), 5.40 (pseudo t, 2H, *J* = 1.8 Hz, $C_5H_4$), 0.25 (s, 9H, $Si(CH_3)_3$) ppm. $^{13}C\{^1H\}$ NMR (125.8 MHz, $CDCl_3$, 20 °C): δ = 194.2 (s, CO), 91.8 (s, 2C, $C_5H_4$), 86.3 (s, 2C, $C_5H_4$), 0.0 (s, $Si(CH_3)_3$) ppm. $^{29}Si\{^1H\}$NMR (99.4 MHz, $CDCl_3$, 20 °C): δ = -3.12 (s, $Si(CH_3)_3$) ppm. IR ($cm^{-1}$, $CH_2Cl_2$, 20 °C) $\nu_{CO}$ 2021 s, 1922 s. Anal. Calcd. for $C_{11}H_{13}O_3ReSi$ (407.51): C 32.42, H 3.22 Found C 32.43, H 3.19. EI-MS: *m/z* 408 $[M]^+$, 393 $[M - CH_3]^+$, 365 $[M - CH_3 - CO]^+$, 350 $[M - 2CH_3 - CO]^+$, 335 $[M- 3CH_3 - CO]^+$, 322 $[M - 2CH_3 - 2CO]^+$, 307 $[M- 3CH_3 - 2CO]^+$, 279 $[M - 3CH_3 - 3CO]^+$.

**6**: Yield: 1.39 g (4 mmol, 33 %). $^1$H NMR (200 MHz, $CDCl_3$, 20 °C): δ = 5.10 (*pseudo* t, 2H, *J* = 2.2 Hz, $C_5H_4$), 5.03 (pseudo t, 2H, *J* = 2.2 Hz, $C_5H_4$) ppm. $^{13}C\{^1H\}$ NMR (50.3 MHz, $CDCl_3$, 20 °C): δ = 194.4 (s, CO), 140.1 (s, $C_{ipso}(C_5H_4)$), 78.4 (2C, $C_5H_4$), 67.8 (2C, $C_5H_4$) ppm. IR ($cm^{-1}$, $CH_2Cl_2$, 20 °C) $\nu_{OH}$ 3100 (w), $\nu_{CO}$ 2021 s, 1923 vs. Anal. Calcd. for $C_8H_5O_4Re$ (351.33): C 27.35, H 1.43. Found C 27.30, H 1.60. EI-MS: *m/z* 352 $[M]^+$, 324 $[M - CO]^+$, 296 $[M - 2CO]^+$, 268 $[M - 3CO]^+$, 242 $[M - 3CO - C_2H_2]^+$.

### 7.2.9 Deprotection of 3 to yield 1

**3** (346 mg, 0.85 mmol) was dissolved in THF and tetrabutyl ammonium fluorate ($nBu_4N^+F^-$) (190 g, 1.27 mmol) were added to the mixture in several portions. The colorless solution became brown after a few minutes. After 2 hours of stirring at room temperature, the solvent was removed *in vacuo* and **1** purified by flash chromatography. Additional purification of **1** can be effected by recrystallization in ether or sublimation. Yield: 273 mg (0.81 mmol, 96 %).

$^1$H NMR (200 MHz, $CDCl_3$, 20 °C): δ = 5.38 (s, 5H, $C_5H_5$) ppm. IR ($cm^{-1}$, $CH_2Cl_2$, 20 °C) $\nu_{CO}$ 2021 s, 1922 s.

### 7.2.10 Preparation of ($\eta^5$-methoxycyclopentadienyl)(tricarbonyl)rhenium, ($\eta^5$-$C_5H_4OCH_3$)$Re(CO)_3$, (7)

**6** (100 mg, 0.29 mmol, 1 equiv.) was dissolved in acetonitrile (20 mL). $Na_2CO_3$ (61 mg, 0.58 mmol, 2 equiv.) and iodomethane (54 µL, 0.87 mmol, 3 equiv.) were added to the solution of **6**. The mixture was stirred and heated to reflux. After 10 h the reaction mixture was allowed to cool to room temperature and the solvent was removed *in vacuo*. The brown residue was redissolved in benzene and filtered through a short plug of celite. Solvent removal *in vacuo* gave the product **7** as a white powder. The product is air stable and thermally stable under ambient conditions. Recrystallisation may be effected from hexane/dichloromethane. Yield: 64 mg (0.17 mmol, 60 %). $^1$H NMR (200 MHz, $CDCl_3$, 20 °C): δ = 5.08 (m, 4H, $C_5H_4$), 3.59 (s, 3H, $CH_3$) ppm. $^{13}C\{^1H\}$ NMR (50.3 MHz, $CDCl_3$, 20 °C): δ = 194.1 (s, CO), 145.1 (s, $C_{ipso}(C_5H_4)$), 78.3 (s, 2C, $C_5H_4$), 66.1 (s, 2C, $C_5H_4$), 58.3 (s, $CH_3$) ppm. IR ($cm^{-1}$, $CH_2Cl_2$, 20 °C) $\nu_{CO}$ 2021 s, 1924 s. Anal. Calcd. for $C_9H_7O_4Re$ (365.36): C 29.59, H 1.93. Found C 29.42, H 1.99. EI-MS: *m/z* 366 $[M]^+$, 338 $[M - CO]^+$, 310 $[M - 2CO]^+$, 282 $[M - 3CO]^+$.

### 7.2.11 Preparation of ($\eta^5$-ethoxycyclopentadienyl)(tricarbonyl)rhenium, ($\eta^5$-$C_5H_4OCH_2CH_3$)$Re(CO)_3$, (8)

**6** (50 mg, 0.14 mmol, 1 equiv.) was dissolved in acetonitrile (10 mL). $Na_2CO_3$ (0 mg, 0.28 mmol, 2 equiv.) and ethylbromide (32 µL, 0.42 mmol, 3 equiv.) were added to the solution of **6**. The mixture was stirred and heated to reflux. After 10 h reaction mixture was allowed to cool to room temperature and the solvent was removed *in vacuo*. The brown residue was redissolved in benzene and filtered through a short plug of celite. Solvent removal *in vacuo* gave the product **8** as a white powder. The product is air stable and thermally stable under ambient conditions. Recrystallization may be effected from hexane/dichloromethane. Solvent removal *in vacuo* afforded **8** as a white solid. Recrystallisation may be effected from

hexane/dichloromethane. Yield: 35 mg (0.09 mmol, 65 %). $^{1}$H NMR (200 MHz, $CDCl_3$, 20 °C): δ = 5.06 (m, 4H, $C_5H_4$), 3.77 (quart, 2H, *J* = 7.0 Hz, $CH_2$), 1.33 (t, 3H, *J* = 7.0 Hz, $CH_3$) ppm. $^{13}C\{^{1}H\}$ NMR (50.3 MHz, $CDCl_3$, 20 °C): δ = 194.3 (s, CO), 144.4 (s, $C_{ipso}(C_5H_4)$), 78.4 (s, 2C, $C_5H_4$), 67.4 (s, 2C, $C_5H_4$), 66.2 (s, $CH_2$), 14.4 (s, $CH_3$) ppm. IR ($cm^{-1}$, $CH_2Cl_2$, 20 °C) $\nu_{CO}$ 2021 s, 1922 s. Anal. Calcd. for $C_{10}H_9O_4Re$ (379.38): C 31.66, H 2.39. Found C 31.54, H 2.37. EI-MS: *m/z* 380 $[M]^+$, 352 $[M - CO]^+$, 324 $[M - 2CO]^+$, 296 $[M - 3CO]^+$, 266 $[M - 3CO - C_2H_5 - H]^+$.

### 7.2.12 Preparation of ($\eta^5$-isopropoxycyclopentadienyl)(tricarbonyl)rhenium, [$\eta^5$-$C_5H_4OCH(CH_3)_2$]$Re(CO)_3$, (9)

**6** (31 mg, 0.09 mmol, 1 equiv.) was dissolved in acetonitrile (10 mL). $Na_2CO_3$ (19 mg, 0.18 mmol, 2 equiv.) and isopropylbromide (25 µL, 0.27 mmol, 3 equiv.) were added to the solution of **6**. The mixture was stirred and heated to reflux. After 10 h the reaction mixture was allowed to cool to room temperature and the solvent was removed *in vacuo*. The brown residue was redissolved in benzene and filtered through a short plug of celite. Solvent removal *in vacuo* gave the product **9** as a white powder. The product is air stable and thermally stable under ambient conditions. Recrystallization may be effected from hexane/dichloromethane. Yield: 24 mg (0.06 mmol, 68 %). $^{1}$H NMR (200 MHz, $CDCl_3$, 20 °C): δ = 5.06 (*pseudo* t, 2H, *J* = 2.2 Hz, $C_5H_4$), 5.02 (*pseudo* t, 2H, *J* = 2.2 Hz $C_5H_4$), 4.03 (quart, 1H, *J* = 6.0 Hz, CH), 1.30 (d, 6H, *J* = 6.0 Hz, $CH(CH_3)_2$) ppm. $^{13}C\{^{1}H\}$ NMR (50.3 MHz, $CDCl_3$, 20 °C): δ = 194.5 (s, CO), 144.22 (s, $C_{ipso}(C_5H_4)$), 78.4 (s, 2C, $C_5H_4$), 67.8 (s, 2C, $C_5H_4$), 66.3 (s, $CH(CH_3)_2$), 21.9 (s, 2C, $CH(CH_3)_2$) ppm. IR ($cm^{-1}$, $CH_2Cl_2$, 20 °C) $\nu_{CO}$ 2020 s, 1921 s. Anal. Calcd. for $C_{11}H_{11}O_4Re$ (393.41): C 33.58, H 2.82. Found C 32.41, 2.59 H. EI-MS: *m/z* 394 $[M]^+$.

### 7.2.13 Preparation of [$\eta^5$-(allyloxy)cyclopentadienyl](tricarbonyl)rhenium, ($\eta^5$-$C_5H_4OCH_2CH=CH_2$)$Re(CO)_3$, (10)

**6** (60 mg, 0.17 mmol, 1 equiv.) was dissolved in acetonitrile (10 mL). $Na_2CO_3$ (40 mg, 0.38 mmol, 2 equiv.), allylchloride (14 µL, 0.17 mmol, 1 equiv.) and a crystal of KI were added to the solution of **6**. The mixture was stirred and heated to reflux. After 10 h the reaction mixture was allowed to cool to room temperature and the solvent was removed *in vacuo*. The brown residue was redissolved in benzene and filtered through a short plug of celite. Solvent removal *in vacuo* afforded **10** as a colorless oil. The product is air stable and thermally stable under ambient conditions. Yield: 46 mg (0.06 mmol, 70 %). $^1$H NMR (200 MHz, $CDCl_3$, 20 °C): δ = 6.04-5,84 (m, 1H), 5.36 (dquart, 1H), 5.34 (t, 1H), 5.29 (quart, 1H), 5.09 (m, 4H, $C_5H_4$), 4.23 (dt, 2H) ppm. $^{13}C\{^1H\}$ NMR (50.3 MHz, $CDCl_3$, 20 °C): δ = 194.1 (s, CO), 143.8 (s, $C_{ipso}(C_5H_4)$), 131.4 (s, *C*H=$CH_2$), 119.2 (s, CH=*C*$H_2$), 78.4 (s, 2C, $C_5H_4$), 72.4 (s, 2C, $C_5H_4$), 66.7 (s, $OCH_2$) ppm. IR ($cm^{-1}$, KBr, 20 °C) $\nu_{CO}$ 2020 s, 1914 s. Anal. Calcd. for $C_{11}H_9O_4Re$ (391.39): C 33.76, H 2.32. Found C 33.81, 2.36 H. EI-MS: *m/z* 392 $[M]^+$, 364 [M - CO]$^+$, 336 [M - 2CO]$^+$, 308 [M - 3CO]$^+$, 278 [M - 3CO - $C_2H_5$ - H]$^+$.

### 7.2.14 Preparation of [$\eta^5$-(benzyloxy)cyclopentadienyl](tricarbonyl)rhenium, ($\eta^5$-$C_5H_4OCH_2C_6H_5$)$Re(CO)_3$, (11)

**6** (500 mg, 1.43 mmol, 1 equiv.) was dissolved in acetonitrile (10 mL). $Na_2CO_3$ (303 mg, 2.86 mmol, 2 equiv.) and benzyl bromide (187 µL, 1.57 mmol, 1.1 equiv.) were added to the solution of **6**. The mixture was stirred and heated to reflux. After 10 h the reaction mixture was allowed to cool to room temperature and the solvent was removed *in vacuo*. The brown residue was redissolved in benzene and filtered through a short plug of celite. Solvent removal *in vacuo* afforded **11** as a white powder. The product is air stable and thermally stable under ambient conditions. Recrystallization may be effected from hexane/dichloromethane.Yield: 540 mg (1.2 mmol, 85 %). $^1$H NMR (200 MHz, $CDCl_3$, 20 °C): δ = 7.38 (m, 5H, $C_6H_5$), 5.13 (*pseudo* t, 2H, *J* = 2.5 Hz, $C_5H_4$), 5.11 (pseudo t, 2H, *J* = 2.5 Hz, $C_5H_4$), 4.73 (s, 2H, $CH_2$) ppm. $^{13}C\{^1H\}$ NMR (50.3 MHz, $CDCl_3$, 20 °C): δ = 194.19 s, (s, CO), 143.81 (s, $C_{ipso}(C_5H_4)$), 134.72 (s, 1C, $C_6H_5$), 128.78 (s, 2C, $C_6H_5$), 128.21 (s, 2C,

$C_6H_5$), 78.53 (s, 2C, $C_5H_4$), 73.71 (s, 2C, $C_5H_4$), 66.78 (s, $CH_2$) ppm. IR ($cm^{-1}$, $CH_2Cl_2$, 20 °C) $\nu_{CO}$ 2020 s, 1930 s. Anal. Calcd. for $C_{15}H_{11}O_4Re$ (441.45): calcd. C 40.81, H 2.51. Found C 40.99, H 2.37. EI-MS: *m/z* 442 $[M]^+$, 386 $[M - 2CO]^+$, 358 $[M - 3CO]^+$, 351 $[M - C_6H_5CH_2]^+$, 267 $[M - 3CO - C_6H_5CH_2]^+$, 91 $[C_6H_5CH_2]^+$.

### 7.2.15 Deprotection of 11 to yield 6

Under nitrogen, in a NMR tube (Schlenk-type), were added 2 mL deuterated methanol, **11** and palladium on activated carbon. Slightly the tube was frozen with liquid nitrogen and the pressure in the tube was gradually reduced. Then the tube was refilled with dihydrogen. This operation was repeated four times. Finally the pressure of dihydrogen was raised to 1.5 bar abs. The tube was heated to ~70°C in an oil bath. The reaction was followed by $^1$H NMR.

### 7.2.16 Preparation of ($\eta^5$-acetoxycyclopentadienyl)(tricarbonyl)rhenium, ($\eta^5$-$C_5H_4OCOCH_3$)$Re(CO)_3$, (12)

Method 1:

**1** (580 mg, 1.74 mmol, 1 equiv.) was dissolved in THF into a flask under nitrogen equipped with a stirring bar. The mixture was cooled to -78° C and nBuLi (1.20 mL, 1.6 M, 1.92 mmol, 1.1 equiv.) was added dropwise with a syringe to the mixture. After 30 min, $(Me_3SiO)_2$ (0.39 mL, 1.74 mmol, 1 equiv.) was added in one portion at room temperature. After 20 min, acetyl chloride (410 mg, 5.22 mmol, 3 equiv.) was added with a syringe and the reaction mixture was stirred for 4 hours. The solvent was removed *in vacuo*. The products of the reaction were separated by column chromatography. Rerystallisation of **12** was effected from ether at -20 °C.

**12** : Yield: 150 mg (0.38 mmol, 22 %). Rf = 0.2 (UV: λ = 254 nm, silica gel, Hexane / Ether, 9:1). $^1$H NMR (200 MHz, $CDCl_3$, 20 °C): δ = 5.56 (*pseudo* t, 2H, *J* = 2.5 Hz, $C_5H_4$), 5.16 (*pseudo* t, 2H, *J* = 2.5 Hz, $C_5H_4$), 2.19 (s, 3H, $CH_3$) ppm. $^{13}C\{^1H\}$ NMR (50.3 MHz, $CDCl_3$, 20 °C): δ = 193.4 (s, $Re(CO)_3$), 167.4 (s, $COCH_3$), 128.8 (s, $C_{ipso}(C_5H_4)$), 79.4 (s, 2C, $C_5H_4$), 74.5 (s, 2C, $C_5H_4$), 20.8 (s, $COCH_3$) ppm. IR ($cm^{-1}$, $CH_2Cl_2$, 20 °C) $\nu_{CO}$ 2026 s, 1929 s. Anal.

Calcd. for $C_{10}H_7O_5Re$ (393.37): C 30.53, H 1.79. Found C 30.01, H 1.83. EI-MS: *m/z* 394 $[M]^+$, 366 $[M - CO]^+$, 352 $[M - CH_2CO]^+$, 338 $[M - 2CO]^+$, 324 $[M - CH_2CO - CO]^+$, 310 $[M - 3CO]^+$, 296 $[M - CH_2CO - 2CO]^+$, 268 $[M - CH_2CO - 3CO]^+$.

**3** : Yield: 390 mg (0.96 mmol, 55 %). Rf = 0.6 (UV: λ = 254 nm, silica gel, Hexane/Ether, 9:1). $^1$H NMR (500.2 MHz, $CDCl_3$, 20 °C): δ = 5.42 (*pseudo* t, 2H, *J* = 1.8 Hz, $C_5H_4$), 5.40 (*pseudo* t, 2H, *J* = 1.8 Hz, $C_5H_4$), 0.25 (s, 9H, $Si(CH_3)_3$) ppm.

Method 2:

**6** (100 mg, 0.286 mmol, 1 equiv.) was dissolved in acetonitrile (10 mL). $Na_2CO_3$ (61 mg, 0.572 mmol, 2 equiv.) and acetylchloride (122 µL, 1.716 mmol, 6 equiv.) were added to the acetonitrile solution of **6**. The flask was placed in an oil bath and heated to reflux. After 10 h, the reaction mixture was allowed to cool to room temperature and then the solvent was removed *in vacuo*. The white residue was redissolved in benzene and filtered through a short plug of celite and silica gel. Solvent removal *in vacuo* gave **12** as a white powder. The product is air stable and thermally stable under ambient conditions. Yield: 75 mg (0.191 mmol, 67 %). $^1$H NMR (200 MHz, $CDCl_3$, 20 °C): δ = 5.56 (*pseudo* t, 2H, *J* = 2.5 Hz, $C_5H_4$), 5.16 (*pseudo* t, 2H, *J* = 2.5 Hz, $C_5H_4$), 2.19 (s, 3H, $CH_3$) ppm.

### 7.2.17 Preparation of [$\eta^5$-(benzoyloxy)cyclopentadienyl](tricarbonyl)rhenium, ($\eta^5$-$C_5H_4OCOPh)Re(CO)_3$, (13)

Method 1:

($\eta^5$-$C_5H_5$)$Re(CO)_3$ (300 mg, 0.90 mmol, 1 equiv.) was dissolved in THF into a flask under nitrogen equipped with a stirring bar. The mixture was cooled to -78 °C and nBuLi (0.62 mL, 1.6 M, 0.99 mmol, 1.1 equiv.) was added drop wise with a syringe. After 30 min, $(Me_3SiO)_2$ (0.39 mL, 1.74 mmol, 1 equiv.) was added in one portion at room temperature. After 20 min, benzoyl chloride (151.7 mg, 1.08 mmol, 1.2 equiv.) was added with a syringe and the reaction mixture was stirred for 4 hours. The solvent was removed *in vacuo* and the products of the reaction **13** and **3** were separated by chromatography on silica gel. Recrystallisation of **13** may be effected from ether.

**13**: Yield: 102 mg (0.22 mmol, 25 %). Rf = 0.2 (UV: λ = 254 nm, silica gel, Hexane/Ether, 9:1). $^{1}$H NMR (200 MHz, $CDCl_3$, 20 °C): δ = 8.07-8.05 (m, 2H, $C_6H_5$), 7.64 (t, 1H, *J* = 7.8 Hz, $C_6H_5$), 7.49 (t, 2H, *J* = 7.8 Hz, $C_6H_5$), 5.69 (*pseudo* t, 2H, *J* = 2.4 Hz, $C_5H_4$), 5.24 (*pseudo* t, 2H, *J* = 2.4 Hz, $C_5H_4$) ppm. $^{13}$C{$^{1}$H} NMR (50.3 MHz, $CDCl_3$, 20 °C): δ = 193.4 (s, $Re(CO)_3$), 163.4 (s, COPh), (s, $C_{ipso}(C_5H_4)$), 130.2 (s, 2C, $C_{ipso}(C_6H_5)$), 129.3 (s, $C_6H_5$), 128.8 (s, $C_6H_5$), 127.9 (s, $C_6H_5$), 79.9 (s, 2C, $C_5H_4$), 74.8 (s, 2C, $C_6H_4$) ppm. IR ($cm^{-1}$, $CH_2Cl_2$, 20 °C) $\nu_{CO}$ 2026 s, 1929 s. Anal. Calcd. for $C_{15}H_9O_5Re.½Et_2O$ (492.49): C 41.46, H 2.87. Found C 41.36, H 2.53. (The presence of ether in the crystals was confirmed by $^{1}$H NMR spetroscopy.) EI-MS: *m/z* 456 $[M]^+$, 428 $[M - CO]^+$, 400 $[M - 2CO]^+$, 372 $[M - 3CO]^+$, 323 $[M – CO - C_6H_5CO]^+$, 267 $[M - 3CO - C_6H_5CO]^+$, 121 $[C_6H_5COO]^+$, 105 $[C_6H_5CO]^+$, 77 $[C_6H_5]^+$. **3**: Yield: 209 mg (0.51 mmol, 57 %). $^{1}$H NMR (500.2 MHz, $CDCl_3$, 20 °C): δ = 5.42 (*pseudo* t, 2H, *J* = 1.8 Hz, $C_5H_4$), 5.40 (*pseudo* t, 2H, *J* = 1.8 Hz, $C_5H_4$), 0.25 (s, 9H, $Si(CH_3)_3$) ppm.

Method 2:

A flask equipped with a stirring bar and a condenser was charged with ($\eta^5$-$C_5H_4OH$)$Re(CO)_3$ (100 mg, 0.286 mmol, 1 equiv.), acetonitrile (10 mL), $Na_2CO_3$ (61 mg, 0.572 mmol, 2 equiv.) and benzoylchloride (40 µL, 0.343 mmol, 1.2 equiv.). The flask was placed in an oil bath and heated to reflux. After 10 hours, the reaction mixture was allowed to cool to room temperature and then the solvent was removed *in vacuo*. The white residue was redissolved in ether and filtered on a funnel with a filter paper. Solvent removal *in vacuo* gave the product **13** as a white powder. The product is air stable and thermally stable under ambient conditions. Yield: 89 mg (0.194 mmol, 68 %). $^{1}$H NMR (200 MHz, $CDCl_3$, 20 °C): δ = 8.07-8.05 (m, 2H, $C_6H_5$), 7.64 (t, 1H, *J* = 7.8 Hz, $C_6H_5$), 7.49 (t, 2H, *J* = 7.8 Hz, $C_6H_5$), 5.69 (*pseudo* t, 2H, *J* = 2.4 Hz, $C_5H_4$), 5.24 (pseudo t, 2H, *J* = 2.4 Hz, $C_5H_4$) ppm.

### 7.2.18 Preparation of ($\eta^5$-aminocyclopentadienyl)(tricarbonyl)rhenium, ($\eta^5$-$C_5H_4NH_2$)$Re(CO)_3$, (15)

A solution of BuLi in hexanes (2.3 mL, 1.6 M, 3.6 mmol, 1.2 equiv. ) was added dropwise to a cold solution (-78 °C) of **1** (1000 mg, 3.00 mmol, 1.0 equiv.) in THF. After 1 hour of

stirring, *p*-toluenesulfonylazide was added to the mixture and the resulting orange solution was allowed to cool to room temperature. Conversion of **1** into **14** was controlled by $^{1}$H NMR spectroscopy. Then a solution of $NaBH_4$ (113 mg, 3.00 mmol, 1.0 equiv.) in ethanol was added dropwise to the mixture at –10 °C and then warmed to room temperature. The reaction evolves $N_2$ and gas evolution was observed. After 6 h of stirring, the solvents were removed *in vacuo*. The resulting brown solid was transferred to a sublimation apparatus. The product **15** crystallized on the cold finger. **15** is white solid air stable and thermally stable under ambient conditions. **14**: $^{1}$H NMR (200 MHz, $CD_3CN$, 20 °C): δ = 5.53 (*pseudo* t, 2H, *J* = 2.2 Hz, $C_5H_4$), 5.36 (*pseudo* t, 2H, *J* = 2.2 Hz, $C_5H_4$) ppm. **15**: Yield: 420 mg (1.20 mmol, 40 %). $^{1}$H NMR (200 MHz, $CD_3CN$, 20 °C): δ = 5.11 (*pseudo* t, 2H, *J* = 2.2 Hz, $C_5H_4$), 4.94 (*pseudo* t, 2H, *J* = 2.2 Hz, $C_5H_4$), 4.02 (broad s, 2H, $NH_2$) ppm. $^{13}$C{$^{1}$H} NMR (50.3 MHz, $CD_3CN$, 20 °C): δ = 197.3 (s, CO), 135.7 (s, $C_{ipso}(C_5H_4)$), 80.3 (s, 2C, $C_5H_4$), 66.4 (s, 2C, $C_5H_4$) ppm. IR ($cm^{-1}$, KBr, 20 °C) $\nu_{CO}$ 2012 s, 1917 s. Anal. Calcd. for $C_8H_6NO_3Re$ (350.35): C 27.43, H 1.73, N 4.00. Found C 27.51, H 1.70 N 3.94. ESI-MS: *m/z* 353 $[M + 2H]^+$.

### 7.2.19 Preparation of [$\eta^5$-(phenylmethyleneamino)cyclopentadienyl](tricarbonyl)-rhenium, ($\eta^5$-$C_5H_4N{=}CHC_6H_5$)$Re(CO)_3$, (16)

**15** (50 mg, 0.14 mmol, 1.0 equiv.) was dissolved in ethanol (5 mL) with benzaldehyde (15 mg, 0.14 mmol, 1.0 equiv.). The mixture was stirred overnight at room temperature. After evaporation of the solvent *in vacuo*, **16** was isolated by crystallization from a solution dichloromethane/hexane to give colorless crystals. Yield: 40 mg (0.09 mmol, 65 %). $^{1}$H NMR (200 MHz, $CD_3CN$, 20 °C): δ = 8.41 (s, 1H, CH), 7.82 (m, 2H, $C_6H_5$), 7.48 (m, 3H, $C_6H_5$), 5.50 (*pseudo* t, 2H, *J* = 2.2 Hz, $C_5H_4$), 5.30 (*pseudo* t, 2H, *J* = 2.2 Hz, $C_5H_4$) ppm. $^{13}$C{$^{1}$H} NMR (50.3 MHz, $CD_3CN$, 20 °C): δ = 194.1 (s, CO), 164.9 (s, N=CH), 134.9 (s, $C_6H_5$), 132.2 (s, $C_5H_4$), 129.1 (s, $C_6H_5$), 128.8 (s, $C_6H_5$), 127.8 (s, $C_6H_5$), 84.5 (s, 2C, $C_5H_4$), 81.6 (s, 2C, $C_5H_4$) ppm. IR ($cm^{-1}$, KBr, 20 °C) $\nu_{CO}$ 2021 s, 1928 s. Anal. Calcd. for $C_{15}H_{10}NO_3Re$ (438.45): C 41.09, H 2.30, N 3.19. Found C 41.28, H 2.35, N 3.11. ESI-MS: *m/z* 441 $[M + 2H]^+$.

### 7.2.20 Preparation of [$\eta^5$-(benzylamino)cyclopentadienyl](tricarbonyl)rhenium, ($\eta^5$-$C_5H_4NHCH_2C_6H_5$)$Re(CO)_3$, (17)

The imine **16** (40 mg, 0.091 mmol, 1.0 equiv.) was dissolved in ethanol and stirred at room temperature. A solution of $NaBH_4$ in ethanol was added dropwise to the ethanol solution of **16** and the mixture was stirred overnight. After removal of the solvent, **17** was isolated by chromatography on silica gel. **17** is was isolated as a white powder and crystallized in ether. Yield: 25 mg (0.057 mmol, 63 %). $^1$H NMR (200 MHz, $CDCl_3$, 20 °C): δ = 7.37-7.34 (m, 5H, $C_6H_5$), 5.08 (*pseudo* t, 2H, *J* = 2.4 Hz, $C_5H_4$), 4.81 (*pseudo* t, 2H, *J* = 2.4 Hz, $C_5H_4$), 4.00 (d, 2H, *J* = 5.2 Hz, $CH_2$), 3.30 (bt, 1H, NH) ppm. $^{13}$C{$^1$H} NMR (50.3 MHz, $CDCl_3$, 20 °C): δ = 195.2 (s, CO), 137.3 (s, $C_{ipso}(C_6H_5)$), 134.4 (s, $C_{ipso}(C_5H_4)$), 128.8 (s, $C_6H_5$), 127.9 (s, $C_6H_5$), 79.2 (s, $C_5H_4$), 64.4 (s, $C_5H_4$), 51.6 (s, $CH_2$) ppm. IR (cm$^{-1}$, KBr, 20 °C) $\nu_{NH}$ 3400 s, $\nu_{CO}$ 2008 s, 1910 s. Anal. Calcd. for $C_{15}H_{12}NO_3Re.½Et_2O$ (585.62): C 34.87, H 4.99, N 2.39. Found C 35.08, H 4.95, N 2.13. (The presence of ether was confirmed by $^1$H NMR spetroscopy.) ESI-MS: *m/z* 442 $[M + H]^+$.

### 7.2.21 Preparation of ($\eta^5$-{[(benzyloxy)carbonyl]amino}cyclopentadienyl)(tricarbonyl)-rhenium, ($\eta^5$-$C_5H_4NHCOOCH_2C_6H_5$)$Re(CO)_3$, (18)

**15** (200 mg, 0.57 mmol, 1.0 equiv.) was dissolved in 4 mL of ether with Benzyl chlroformate (CbzCl) (81 µL, 0.57 mmol, 1.0 equiv.). A solution of $K_2CO_3$ (240 mg, 1.71 mmol, 3.0 equiv.) in 4 mL of water was added to the mixture, which was heated to reflux. After 12 h the mixture was allowed to cool to room temperature and the organic layer was extracted with ether and washed with a saturated solution of NaCl. The ether phase was dried over $MgSO_4$ and the solvent was removed *in vacuo*. The product **18** was isolated as a white powder. Additional purification by recrystallization of **18** from dichloromethane/hexane afforded colorless crystals. Yield: 96 mg (0.19 mmol, 70 %). $^1$H NMR (200 MHz, $CD_3CN$, 20 °C): δ = 7.81 (bs, 1H, NH), 7.36-7.34 (m, 5H, $C_6H_5$), 5.66 (*pseudo* t, 2H, *J* = 2.4 Hz, $C_5H_4$), 5.29 (*pseudo* t, 2H, *J* = 2.4 Hz, $C_5H_4$), 5.12 (s, 2H, $CH_2$) ppm. $^{13}$C{$^1$H} NMR (50.3 MHz, $CD_3CN$, 20 °C): δ = 193.9 (s, $Re(CO)_3$), 152.5 (s, NHCO), 135.3 (s, $C_6H_5$), 128.7 (s, $C_6H_5$), 128.6 (s, $C_6H_5$), 128.2 (s, $C_6H_5$), 117.6 (s, $C_6H_5$), 80.4 (s, $C_5H_4$), 71.6 (s, $C_5H_4$), 67.8 (s, $CH_2$) ppm. IR

($cm^{-1}$, KBr, 20 °C) $\nu_{CO}$ 2020 s, 1907 s. Anal. Calcd. for $C_{16}H_{12}NO_5Re$ (484.48): C 39.67, H 2.50, N 2.89. Found C 40.01, H 2.67, N 2.87. ESI-MS: *m/z* 508 $[M + Na]^+$.

### 7.2.22 Preparation of ($\eta^5$-acetamidocyclopentadienyl)(tricarbonyl)rhenium, ($\eta^5$-$C_5H_4NHCOCH_3$)$Re(CO)_3$, (19)

**15** (20 mg, 0.057 mmol, 1.0 equiv.) was dissolved in ether 5 mL with acetylchloride (23 mg, 0.285 mmol, 5 equiv.). An aqueous solution of $K_2CO_3$ (16 mg, 0.114 mmol, 2.0 equiv.).was added to the mixture, which was stirred overnight under reflux. After removal of the solvent *in vacuo*, the organic phase was extracted with ether and washed with a saturated solution of NaCl. The ether phase was dried over $MgSO_4$ and the solvent was removed *in vacuo*. Then **19** was isolated by chromatography on silica gel. **19** is a white solid. Yield: 15 mg (0.038 mmol, 67 %). $^1H$ NMR (200 MHz, $C_6D_6$, 20 °C): δ = 5.20 (bs, 1H, NH), 5.08 (*pseudo* t, 2H, *J* = 2.4 Hz, $C_5H_4$), 4.24 (*pseudo* t, 2H, *J* = 2.4 Hz, $C_5H_4$), 1.24 (s, 3H, $CH_3$) ppm. $^{13}C$ NMR (50.3 MHz, $C_6D_6$, 20 °C): δ = 194.7 (s, CO), 80.1 (s, 2C, $C_5H_4$), 72.3 (s, 2C, $C_5H_4$), 23.0 (s, $CH_3$) ppm. IR ($cm^{-1}$, KBr, 20 °C) $\nu_{CO}$ 2020 s, 1908 s. Anal. Calcd. for $C_{10}H_8NO_4Re$ (392.38): C 30.61, H 2.06, N 3.57. Found C 30.71, H 2.23, N 3.39. ESI-MS: *m/z* 416 $[M + Na]^+$.

### 7.2.23 Preparation of ($\eta^5$-pyrrolidinylcyclopentadienyl)(tricarbonyl)rhenium, ($\eta^5$-$C_5H_4NHC_4H_8$)$Re(CO)_3$, (20)

**15** (150 mg, 0.42 mmol, 1.0 equiv.) and butyldiodide (60 µL, 0.46 mmol, 1.1 equiv.) were dissolved in acetontrile in a young schlenk. $Na_2CO_3$ was added to the mixture and the mixture was heated under reflux overnight. The mixture was allowed to cool to room temperature and the organic layer was extracted with ether. The ether phase was washed with a saturated solution of NaCl and dried over $MgSO_4$. The product was finally purified by chromatography on silica gel. **20** is a white powder wich cristallized in dichloromethane/hexane. Yield: 102 mg (0.252 mmol, 60 %). $^1H$ NMR (200 MHz, $CD_3CN$, 20 °C): δ = 5.23 (*pseudo* t, 2H, *J* = 2.4 Hz, $C_5H_4$), 4.71 (*pseudo* t, 2H, *J* = 2.4 Hz, $C_5H_4$), 2.87 (t, 2H, *J* = 5.3 Hz, $OCH_2$), 1.91 (t, 2H, *J* = 5.3 Hz, $CH_2$) ppm. $^{13}C\{^1H\}$ NMR (50.3 MHz, $CD_3CN$, 20 °C): δ = 196.9 (s, CO), 137.8

(s, $C_{ipso}(C_5H_4)$), 80.6 (s, $C_5H_4$), 65.0 (s, $C_5H_4$), 51.2 (s, 2C, $OCH_2$), 25.6 (s, 2C, $CH_2$) ppm. IR ($cm^{-1}$, KBr, 20 °C) $\nu_{CO}$ 2007, 1895 s. Anal. Calcd. for $C_{12}H_{12}NO_3Re$ (404.44): C 35.64, H 2.99, N 3.46. Found C 35.76, H 2.94, N 3.43. ESI-MS: *m/z* 406 $[M + H]^+$.

### 7.2.24 Preparation of [$\eta^5$-({[3,5-bis(trifluoromethyl)phenyl]carbamoyl}amino)-cyclopentadienyl](tricarbonyl)rhenium, [$\eta^5$-$C_5H_4NHCONH(C_8H_3F_6)$]$Re(CO)_3$, (21)

**15** (100 mg, 0.286 mmol, 1.0 equiv.) was dissolved in 10 mL of chloroform and 1 mL of triethylamine. A solution of triphosgene (115 mg, 0.429 mmol, 1.5 equiv.) in 2 mL of chloroform was added to the mixture at room temperature. After 10 minutes of stirring, bis(trifluoromethyl)aniline (66 µL, 0.429 mmol, 1.5 equiv.) was added to the mixture. After 1 hour, the solvent was removed *in vacuo* and the product was purified by chromatography. **21** is a white powder which crystallizes in dichloromethane/hexane. Yield: 120 mg (0.200 mmol, 70 %). $^1$H NMR (500.2 MHz, $CD_3CN$, 20 °C): δ = 8.00 (m, 3H, NH + Ar), 7.62 (m, 2H, NH + Ar), 5.74 (*pseudo* t, 2H, *J* = 2.0 Hz, $C_5H_4$), 5.32 (*pseudo* t, 2H, *J* = 2.0 Hz, $C_5H_4$) ppm. $^{13}C\{^1H\}$ NMR (125.8 MHz, $CD_3CN$, 20 °C): δ = 196.2 (s, $Re(CO)_3$), 119.6 (s, Ar), 81.9 (s, 2C, $C_5H_4$), 73.3 (s, 2C, $C_5H_4$) ppm. $^{19}F\{^1H\}$ NMR (282.2 MHz, $CD_3CN$, 20 °C): δ = -65.2 (s, $CF_3$) ppm. IR ($cm^{-1}$, KBr, 20 °C) $\nu_{CO}$ 2020 s, 1917 s. Anal. Calcd. for $C_{17}H_9F_6N_2O_4Re$.½THF (641.51): C 35.57, H 2.04, N 4.37. Found C 35.42, H 2.31, N 4.44. (**21** cocrystallized with THF as shown in the X-ray study). ESI-MS: *m/z* 629 $[M + Na]^+$.

### 7.2.25 Preparation of ($\eta^5$-{[(pentafluorophenyl)carbamoyl]amino}-cyclopentadienyl)(tricarbonyl)rhenium, ($\eta^5$-$C_5H_4NHCONHC_6F_5$)$Re(CO)_3$, (22)

**15** (100 mg, 0.286 mmol, 1.0 equiv.) was dissolved in 10 mL of chloroform and 1 mL of triethylamine. A solution of triphosgene (115 mg, 0.429 mmol, 1.5 equiv.) in 2 mL of choloroform was added to the mixture at room temperature. After 10 minutes of stirring, pentafluoroaniline (78 mg, 0.429 mmol, 1.5 equiv.) was added to the mixture. After 1 hour, the solvent was removed *in vacuo* and the product was purified by flash chromatography. **22** is a white solid. Yield: 48 mg (0.086 mmol, 30 %). $^1$H NMR (200 MHz, $CD_3CN$, 293 K): δ =

5.69 (*pseudo* t, 2H, *J* = 2.5 Hz, $C_5H_4$), 5.29 (*pseudo* t, 2H, *J* = 2.5 Hz, $C_5H_4$) ppm. $^{19}F\{^1H\}$ NMR (188.1 MHz, $CD_3CN$, 20 °C): δ = -148.5 (d, *J* = 14.7 Hz), -160.7 (t, *J* = 20.9 Hz), -166.0 (t, *J* = 20.9 Hz) ppm. $^{13}C\{^1H\}$ NMR (50.3 MHz, $CD_3CN$, 20 °C): δ = 196.1 (s, $Re(CO)_3$), 152.3 (s, NHCO), 145.6- 143.7 (m, o-$C_6F_5$), 141.9-139.8 (m, p-$C_6F_5$), 137.9-136.4 (m, m-$C_6F_5$), 114.1-113.9 (m, $C_{ipso}(C_6F_5)$), 82.4 (s, 2C, $C_5H_4$), 73.0 (s, 2C, $C_5H_4$) ppm. IR ($cm^{-1}$, KBr, 20 °C) $\nu_{CO}$ 2016 s, 1910 s. Anal. Calcd. for $C_{15}H_6F_5N_2O_4Re$ (559.42): C 32.20, H 1.08, N 5.01. Found C 31.95, H 1.14, N 4.95. ESI-MS: *m/z* 583 $[M + Na]^+$.

### 7.2.26 Preparation of dicarbonyl($\eta^5$-methoxycyclopentadienyl)(nitrosyl)-rhenium(1+)tetrafluoroborate(1-), [($\eta^5$-$C_5H_4OCH_3$)$Re(CO)_2(NO)]^+BF_4^-$, (23)

**7** (55 mg, 0.15 mmol, 1 equiv.) was dissolved in acetonitrile (10 mL) in a 20 mL vial and $NOBF_4$ (35 mg, 0.30 mmol, 2 equiv.) was added in 4 portions with stirring. After addition of $NOBF_4$, the mixture turned deep yellow and orange and finally darkened to give a deep brown slurry mixture. The solution was stirred overnight and then the solvent was removed *in vacuo*. Unfortunately, we failed to isolate an anatilically pure sample of **23** for elemental analysis.Yield: 50 mg (0.11 mmol, 73 %). $^1H$ NMR (200 MHz, Acetone-$d_6$, 20 °C): δ = 6.46 (*pseudo* t, 2H, *J* = 2.4 Hz, $C_5H_4$), 6.33 (*pseudo* t, 2H, *J* = 2.4 Hz, $C_5H_4$), 5.32 (s, 3H, $CH_3$) ppm. $^{13}C\{^1H\}$ NMR (50.3 MHz, Acetone-$d_6$, 293 K): δ = 183.7 (s, CO), 155.3 (s, $C_{ipso}(C_5H_4)$), 89.6 (s, 2C, $C_5H_4$), 74.9 (s, 2C, $C_5H_4$), 60.9 (s, $CH_3$) ppm. IR ($cm^{-1}$, KBr, 20 °C) $\nu_{CO}$ 2100 s, 2046 s, $\nu_{NO}$ 1803 s. ESI-MS: *m/z* 368 $[M - BF_4]^+$.

### 7.2.27 Preparation of ($\eta^5$-{[(benzyloxy)carbonyl]amino}cyclopentadienyl)(dicarbonyl)-(nitrosyl)rhenium(1+) tetrafluoroborate(1-), [($\eta^5$-$C_5H_4NHCOOCH_2C_6H_5$)$Re(CO)_2(NO)]^+BF_4^-$, (24)

**18** (100 mg, 0.20 mmol, 1 equiv.) was dissolved in dichloromethane, then $NOBF_4$ (48 mg, 0.40 mmol, 2 equiv.) was added to the solution and the mixture was stirred overnight. When $NOBF_4$ was added, the colorless solution turned to orange and gas release was observed. The solvent was evaporated and the resulting brown orange powder was washed with THF to

afford **24** as an orange powder. Efforts to obtain analytically pure **24** by recrystallization in acetone/ether were ineffective. Yield: 109 mg (0.19 mmol, 95 %). $^{1}$H NMR (500.2 MHz, Acetone-$d_6$, 20 °C): δ = 7.39-7.37 (m, 5H, $C_6H_5$), 6.56 (*pseudo* t, 2H, *J* = 2.4 Hz, $C_5H_4$), 6.43 (*pseudo* t, 2H, *J* = 2.4 Hz, $C_5H_4$), 5.25 (s, 2H, $CH_2$) ppm. $^{13}$C{$^{1}$H} NMR (125.8 MHz, Acetone-$d_6$, 20 °C): δ = 183.9 (s, $Re(CO)_3$), 153.6 (s, NHCO), 136.5 s, (s, $C_{ipso}(C_6H_5)$), 131.8 (s, $C_{ipso}(C_5H_4)$), 129.4 (s, $C_6H_5$), 129.3 (s, $C_6H_5$), 128.9 (s, $C_6H_5$), 90.8 (s, 2C, $C_5H_4$), 79.2 (s, 2C, $C_5H_4$), 68.7 (s, $CH_2$) ppm. IR (cm$^{-1}$, KBr, 20 °C) $\nu_{CO}$ 2130, 2076 s, $\nu_{NO}$ 1823 s. ESI-MS: *m/z* 487 $[M - BF_4]^+$.

### 7.2.28 Preparation of [$\eta^5$-(benzyloxy)cyclopentadienyl](dicarbonyl)(nitrosyl)-rhenium(1+) tetrafluoroborate(1-), [($\eta^5$-$C_5H_4OCH_2C_6H_5$)$Re(CO)_2(NO)]^+BF_4^-$, (25)

($\eta^5$-$C_5H_4OCH_2Ph$)$Re(CO)_3$ (540 mg, 1.22 mmol, 1 equiv.) was dissolved in acetonitrile (10 mL) in a 20 mL vial and $NOBF_4$ (171 mg, 1.46 mmol, 1.2 equiv.) was added in 4 portions with stirring. After addition of $NOBF_4$, the mixture turned deep yellow and orange and finally darkened to give a brown mixture. The solution was stirred overnight and then the solvent was removed *in vacuo*. The residue can be used without further purification for the preparation of the corresponding hydride **26**. Additional purification can be effected by precipitation and washing of the residue in THF. Elemental Analysis: Despite the efforts to purify and crystallize this complex, the sample could not be obtained in analytically pure form. Yield: 496 mg (0.936 mmol, 77 %). $^{1}$H NMR (200 MHz, Acetone-$d_6$, 20 °C): δ = 7.46-7.44 (m, 5H, $C_6H_5$), 6.46 (*pseudo* t, 2H, *J* = 2.4 Hz, $C_5H_4$), 6.33 (*pseudo* t, 2H, *J* = 2.4 Hz, $C_5H_4$), 5.32 (s, 2H, $CH_2$) ppm. $^{13}$C{$^{1}$H} NMR (50.3 MHz, Acetone-$d_6$, 20 °C): δ = 179.7 (s, CO), 134.8 (s, $C_{ipso}(C_5H_4)$), 130.4 (s, $C_{ipso}(C_6H_5)$), 130.0 (s, $C_6H_5$), 129.7 (s, $C_6H_5$), 129.2 (s, $C_6H_5$), 89.6 (s, 2C, $C_5H_4$), 75.8 (s, 2C, $C_5H_4$), 75.6 (s, $CH_2$) ppm. IR (cm$^{-1}$, KBr, 20 °C) $\nu_{CO}$ 2046 s, $\nu_{NO}$ 1803 s. ESI-MS: *m/z* 444 $[M - BF_4]^+$.

### 7.2.29 Preparation of [$\eta^5$-(benzyloxy)cyclopentadienyl](carbonyl)hydrido(nitrosyl)-rhenium, ($\eta^5$-$C_5H_4OCH_2C_6H_5$)Re(CO)(NO)H, (26)

**25** (500 mg, 1.12 mmol, 1 equiv.), $H_2O$ (0.5 mL, 27.8 mmol, 28 equiv.) and triethylamine (0.5 mL, 3.59 mmol, 3.2 equiv.) were heated in a round bottom flask equipped with a condenser in acetone at 50°C. After one hour the mixture was allowed to cool to room temperature and the solvent was removed *in vacuo*. The brown residue was triturated with pentane to extract the product. The pentane turned orange. After several extractions the pentane was evaporated *in vacuo* to give an orange-brown powder. Crystallization of the powder from $CH_2Cl_2$/pentane afforded orange crystals. Yield: 150 mg (0.36 mmol, 32 %). $^1$H NMR (500.2 MHz, $CD_2Cl_2$, 20 °C): δ = 7.39-7.35 (m, 5H, $C_6H_5$), 5.53 (quart, 1H, *J* = 2.1 Hz), 5.42 (quart, 1H, *J* = 2.1 Hz), 5.32 (quart, 1H, *J* = 2.1 Hz), 5.00 (quart, 1H, *J* = 2.1 Hz), 4.79 (s, 2H, $CH_2$), -7.88 (s, 1H, ReH) ppm. $^{13}$C{$^1$H} NMR (125.8 MHz, $CD_2Cl_2$, 20 °C): δ = 208.6 (s, CO), 135 (s, $C_6H_5$), 129.0 (s, $C_6H_5$), 128.3 (s, $C_6H_5$), 80.9 (s, $C_5H_4$), 79.4 (s, $C_5H_4$), 74.9 (s, $CH_2$), 71.3 (s, $C_5H_4$), 70.5 (s, $C_5H_4$) ppm. IR (cm$^{-1}$, Hexane, 20 °C) $\nu_{CO}$ 1976 s, $\nu_{NO}$ 1718 s. Anal. Calcd. for $C_{13}H_{12}NO_3Re$ (416.45): C 37.49, H 2.90; N 3.36. Found C 37.96, H 2.60, N 3.49.

### 7.2.30 Preparation of dicarbonyl($\eta^5$-hydroxycyclopentadienyl)(nitrosyl)-rhenium(1+)tetrafluoroborate(1-), [$\eta^5$-$C_5H_4OH$)$Re(CO)_2(NO)]^+BF_4^-$, (27)

**6** (200 mg, 0.57 mmol, 1 equiv.) was dissolved in $CH_2Cl_2$ (10 mL) in a 20 mL vial under nitrogen with a stirring bar. $NOBF_4$ (133 mg, 1.14 mmol, 2 equiv.) was added in 2 portions. The reaction evolved CO gas. The mixture was stirred 12 hours and the solvent was removed *in vacuo*. The residue, a yellow-brown powder, was extracted with acetone. The acetone solution was filtered on celite and ether was added to get a yellow precipitate. Crystallization from acetone/ether gave yellow crystals. The product is air stable and thermally under ambient conditions. Yield: 202 mg (0.46 mmol, 80 %). $^1$H NMR (500.2 MHz, Acetone-$d_6$, 20 °C): δ = 6.39 (*pseudo* t, 2H, *J* = 2.4 Hz, $C_5H_4$), 6.08 (*pseudo* t, 2H, *J* = 2.4 Hz, $C_5H_4$) ppm. $^{13}$C{$^1$H} NMR (125.8 MHz, Acetone-$d_6$, 20 °C): δ = 185.4 (s, CO), 154.0 (s, $C_{ipso}(C_5H_4)$), 89.3 (s, $C_5H_4$), 75.6 (s, $C_5H_4$) ppm. IR (cm$^{-1}$, KBr, 20 °C) $\nu_{OH}$ 3425 w, $\nu_{CO}$ 2102 s, 2042 s,

$\nu_{NO}$ 1809 s. Anal. Calcd. for $C_7H_6NO_4Re.BF_4$ (440.13): C 19.10, H 1.15, N 3.18. Found C 19.34, H 1.34, N 3.26. ESI-MS: *m/z* 376 $[M - BF_4 + Na]^+$.

## 7.3 X-ray Structure Analysis

Most of the compounds were not sensitive to moisture and air. Thus most of the crystals were grown and prepared under ambient atmosphere. Crystals sensitive to moisture (water) and air (oxygen) were grown and prepared under nitrogen atmosphere in a glove box. Thus these crystals are embedded in polybutene oil within the glove box before the crystal quality can be examined under polarized light. The polarizing microscope is the most important tool in the choice of good quality single crystal for the X-ray diffraction studies. Twinning and intergrown crystals or crystals with too large intrusions can easily be neglected.

The selected single crystal is mounted using polybutene oil on the top of a glass fiber fixed on a goniometer head and transferred to the Stoe IPDS diffractometer (Imaging Plate Detector System with graphite-monochromated MoKα radiation, λ = 0.71073 Å) [10] and cooled to 183(2) K using a cold $N_2$-gas stream from an Oxford Cryogenic System. Data collection was performed with the program EXPOSE[10]. The crystal system and the unit cell parameters were determined with the programs DISPLAY, INDEX and CELL[10]. The intensities were integrated (INTEGRATE[10]) after using a dynamic peak profile analysis (PROFILE[10]) and an estimated mosaic spread check (EMS[10]) to prevent overlapping intensities. The data were finally corrected for Lorentz and polarization effects and a numerical absorption correction[11] based on measured and indexed crystal faces was applied with the programs FACEitVIDEO and XRED.[10] The Patterson method was used to solve the crystal structure by applying the software options of the program SHELXS-97. [12] The structure refinement was performed with the program SHELXL-97. [12] The program PLATON[13] was used to check the result of the X-ray analysis and the program ORTEP[14] used to give a representation of the structure. All softwares used to prepare material for publication are included in the WINGX software.

**Lithium ($\eta^5$-oxidocyclopentadienyl)(tricarbonyl)rhenium tetrahydrofuran (1:2), (5)**

A colorless plate (0.41 x 0.30 x 0.14 $mm^3$) was chosen for the X-ray diffraction study. A number of 200 images were exposed at a constant times of 3.0 min per image. The crystal-to-image distance was set to 50 mm and the ϕ-oscillation scan mode was selected with the ϕ increment of 1.1°. For the cell parameter refinement, 8000 reflections were selected out of the whole limiting sphere with intensities $I > 6\sigma$ (I). A total of 22911 reflections were collected of

which 5374 were unique after performing data reduction and absorption correction ($R_{int}$ = 0.0686). A total of 11 indexed crystal faces were used for the numerical absorption correction ($T_{min}$ = 0.111, $T_{max}$ = 0.414).[11]

Compound **5** crystallizes in the centrosymmetric space group $P2_1/n$. The asymmetric unit consists of one neutral rhenium $Re(CO)_3(\eta^5\text{-}C_5H_4OLi(OC_4H_8)_2)$ complex. The positions of all hydrogen atoms were calculated after each refinement cycle (riding model) and all non-hydrogen atoms were anisotropically refined.

**($\eta^5$-Hydroxycyclopentadienyl)(tricarbonyl)rhenium, (6)**

A colorless plate (0.45 x 0.45 x 0.14 $mm^3$) was chosen for the X-ray diffraction study. A number of 175 images were exposed at a constant times of 3.0 min per image. The crystal-to-image distance was set to 50 mm and the ϕ-rotation scan mode was selected with the ϕ increment of 1.6°. For the cell parameter refinement, 8000 reflections were selected out of the whole limiting sphere with intensities $I > 6\sigma$ (I). A total of 14120 reflections were collected of which 2411 were unique after performing data reduction and absorption correction ($R_{int}$ = 0.0843). A total of 6 indexed crystal faces were used for the numerical absorption correction ($T_{min}$ = 0.029, $T_{max}$ = 0.162). [11]

Compound **6** crystallizes in the centrosymmetric space group $P2_1/c$. The asymmetric unit consists of one neutral rhenium $(C_5H_4OH)Re(CO)_3$ complex. The hydrogen atom of the hydroxy group was located by difference electron density calculations and its coordinates and isotropic thermal parameter were freely refined. The positions of all other hydrogen atoms were calculated after each refinement cycle (riding model) and the other non-hydrogen atoms were anisotropically refined.

**($\eta^5$-Methoxycyclopentadienyl)(tricarbonyl)rhenium, (7)**

A colorless tablet (0.34 x 0.27 x 0.19 $mm^3$) was chosen for the X-ray diffraction study. A number of 220 images were exposed at a constant times of 2.0 min per image. The crystal-to-image distance was set to 50 mm and the ϕ-rotation scan mode was selected with the ϕ increment of 1.5°. For the cell parameter refinement, 8000 reflections were selected out of the whole limiting sphere with intensities $I > 6\sigma$ (I). A total of 9238 reflections were collected of

which 2571 were unique after performing data reduction and absorption correction ($R_{int}$ = 0.1123). A total of 12 indexed crystal faces were used for the numerical absorption correction ($T_{min}$ = 0.045, $T_{max}$ = 0.161).[11]

Compound **7** crystallizes in the centrosymmetric space group P-1. The positions of all hydrogen atoms were calculated after each refinement cycle (riding model) and the other non-hydrogen atoms were anisotropically refined. The OMIT –2 50 was used in the SHELXL refinement to truncate the data set to a lower angle ($\theta_{max}$ = 25°) in order to get rid of the level A alert of the check CIF/PLATON validation routine (completeness = 90.9 < 95%). The new value of 94.0% for the data completeness still remains a low value probably due to a "misorientation" of the crystal (crystal parallel to glas fibre) which then often results in a completeness of about 90% for our type of IPDS diffractometer.

**[$\eta^5$-(Benzyloxy)cyclopentadienyl](tricarbonyl)rhenium, (11)**

A colorless plate (0.24 x 0.19 x 0.08 $mm^3$) was chosen for the X-ray diffraction study. A number of 280 images were exposed at a constant times of 5.0 min per image. The crystal-to-image distance was set to 50 mm and the ϕ-oscillation scan mode was selected with the ϕ increment of 0.8°. For the cell parameter refinement, 8000 reflections were selected out of the whole limiting sphere with intensities $I > 6\sigma$ (I). A total of 18465 reflections were collected of which 4092 were unique after performing data reduction ($R_{int}$ = 0.0383). A total of 10 indexed crystal faces were used for the numerical absorption correction ($T_{min}$ = 0.211, $T_{max}$ = 0.541).[11]

Compound **11** crystallizes in the centrosymmetric space group $P2_1/c$. The positions of all hydrogen atoms were calculated after each refinement cycle (riding model) and all non-hydrogen atoms were anisotropically refined.

**[$\eta^5$-(Benzoyloxy)cyclopentadienyl](tricarbonyl)rhenium, (13)**

A colorless plate (0.20 x 0.20 x 0.08 $mm^3$) was chosen for the X-ray diffraction study. A number of 273 images were exposed at a constant times of 2.0 min per image. The crystal-to-image distance was set to 50 mm and the ϕ-rotation scan mode was selected with the ϕ increment of 1.2°. For the cell parameter refinement, 8000 reflections were selected out of the

whole limiting sphere with intensities $I > 6\sigma$ (I). A total of 14483 reflections were collected of which 3753 were unique after performing data reduction and absorption correction ($R_{int}$ = 0.0549). A total of 6 indexed crystal faces were used for the numerical absorption correction ($T_{min}$ = 0.222, $T_{max}$ = 0.486).[11]

Compound **13** crystallizes in the centrosymmetric space group P-1. The asymmetric unit consists of one neutral rhenium $(C_5H_4OCOPh)Re(CO)_3$ complex. The positions of all hydrogen atoms were calculated after each refinement cycle (riding model) and all non-hydrogen atoms were anisotropically refined.

**[$\eta^5$-(phenylmethyleneamino)cyclopentadienyl](tricarbonyl)rhenium, (16)**

A flat colorless needle (0.50 x 0.17 x 0.03 $mm^3$) was chosen for the X-ray diffraction study. A number of 226 images were exposed at a constant times of 3.0 min per image. The crystal-to-image distance was set to 50 mm and the $\phi$-oscillation scan mode was selected with the $\phi$ increment of 0.8°. For the cell parameter refinement, 8000 reflections were selected out of the whole limiting sphere with intensities $I > 6\sigma$ (I). A total of 14214 reflections were collected of which 3654 were unique after performing data reduction and absorption correction ($R_{int}$ = 0.0942). A total of 6 indexed crystal faces were used for the numerical absorption correction ($T_{min}$ = 0.111, $T_{max}$ = 0.753).[11]

Compound **16** crystallizes in the centrosymmetric space group $P2_1/c$. The asymmetric unit consists of one neutral rhenium $Re(CO)_3(\eta^5\text{-}C_5H_4NCHPh)$ complex. No classical intermolecular hydrogen bonds have been found in the structure. The positions of all hydrogen atoms were calculated after each refinement cycle (riding model) and all non-hydrogen atoms were anisotropically refined. The OMIT –2 50 was used in the final SHELXL refinement to truncate the data set to a lower angle $\theta_{max}$ = 25° (3654 → 2197 unique reflections) in order to get rid of the level A alert of the checkCIF/PLATON validation routine (completeness = 91.5 < 95%). The new value of 93.7 % for the data completeness still remains a low value probably due to a “misorientation” of the crystal (crystal parallel to glas fibre) which then often results in a completeness of about 90% for our type of IPDS diffractometer.

**($\eta^5$-{[(Benzyloxy)carbonyl]amino}cyclopentadienyl)(tricarbonyl)rhenium, (18)**

A colorless prism (0.24 x 0.12 x 0.10 $mm^3$) was chosen for the X-ray diffraction study. A number of 142 images were exposed at a constant times of 2.5 min per image. The crystal-to-image distance was set to 50 mm and the ϕ-rotation scan mode was selected with the ϕ increment of 1.3° ($\theta_{max}$ = 30.36°). For the cell parameter refinement, 7998 reflections were selected out of the whole limiting sphere with intensities I > 6σ (I). A total of 13 indexed crystal faces were used for the numerical absorption correction ($T_{min}$ = 0.307, $T_{max}$ = 0.494).[11] A total of 16799 reflections were collected of which 4459 were unique after performing data reduction ($R_{int}$ = 0.0473).

Compound **18** crystallizes in the centrosymmetric space group $P2_1/c$. The asymmetric unit is composed of one neutral $Re(CO)_3(\eta^5\text{-}C_5H_4N(H)CO_2CH_2Ph)$ species. The positions of all hydrogen atoms were calculated after each refinement cycle (riding model) and all non-hydrogen atoms were anisotropically refined. A short intermolecular distance of 2.01 Å is observed between $H(1)_N$ and the carbonyl oxygen O(4).

**($\eta^5$-Pyrrolidinylcyclopentadienyl)(tricarbonyl)rhenium, (20)**

A colorless prism (0.45 x 0.25 x 0.23 $mm^3$) was chosen for the X-ray diffraction study. A number of 195 images were exposed at a constant times of 2.0 min per image. The crystal-to-image distance was set to 50 mm and the ϕ-rotation scan mode was selected with the ϕ increment of 1.2°. For the cell parameter refinement, 7998 reflections were selected out of the whole limiting sphere with intensities I > 6σ (I). A total of 15063 reflections were collected ($\theta_{max}$ = 28°) of which 3187 were unique after performing data reduction ($R_{int}$ = 0.0998) and 3119 were observed with I > 2σ (I). A total of 6 indexed crystal faces were used for the numerical absorption correction.[11]

Compound **20** crystallizes in the non centrosymmetric space group $P2_12_12_1$. All non-hydrogen atoms were refined with anisotropic thermal parameters and the hydrogen atoms were included in idealized positions, their $U_{iso}$ values were set to ride on the $U_{eq}$ values of the parent carbon atoms.

**[$\eta^5$-({[3,5-Bis(trifluoromethyl)phenyl]carbamoyl}amino)cyclopentadienyl](tricarbonyl) rhenium, (21)**

A colorless block (0.42 x 0.40 x 0.21 $mm^3$) was chosen for the X-ray diffraction study. A number of 400 images were exposed at a constant times of 3.0 min per image. The crystal-to-image distance was set to 56 mm and the ϕ-oscillation scan mode was selected with the ϕ increment of 0.6°. For the cell parameter refinement, 8000 reflections were selected out of the whole limiting sphere with intensities $I > 6\sigma$ (I). A total of 27459 reflections were collected of which 5718 were unique after performing data reduction and absorption correction ($R_{int}$ = 0.0736, $\phi_{max}$ = 28°). A total of 13 indexed crystal faces were used for the numerical absorption correction.[11]

Compound **21** crystallizes in the centrosymmetric space group C2/c. The asymmetric unit is composed of one rhenium molecule and one solvent molecule of tetrahydrofurane. The disorder observed for one $CF_3$ group was treated with the PART instruction of SHELXL-97 and anisotropically refined. The positions of all hydrogen atoms were calculated after each refinement cycle (riding model). All non-hydrogen atoms were anisotropically refined.

**[$\eta^5$-(Benzyloxy)cyclopentadienyl](carbonyl)hydrido(nitrosyl)rhenium, (26)**

A pale orange plate (0.37 x 0.13 x 0.05 $mm^3$) was chosen for the X-ray diffraction study. A number of 314 images were exposed at a constant times of 5.0 min per image. The crystal-to-image distance was set to 50 mm and the ϕ-oscillation scan mode was selected with the ϕ increment of 0.7°. For the cell parameter refinement, 8000 reflections were selected out of the whole limiting sphere with intensities $I > 6\sigma$ (I). A total of 16932 reflections were collected of which 3536 were unique after performing data reduction and absorption correction ($R_{int}$ = 0.0611). A total of 6 indexed crystal faces were used for the numerical absorption correction ($T_{min}$ = 0.169, $T_{max}$ = 0.633).[11]

Compound **26** crystallizes in the centrosymmetric space group $P2_1/c$. The hydride atom was located by difference electron density calculations and its coordinates and isotropic thermal parameter were freely refined. Nevertheless, the Re1-H bond distance of 1.50(6) Å is clearly too short and should not be used for comparisons. The positions of all other hydrogen atoms were calculated after each refinement cycle (riding model) and the other non-hydrogen atoms were anisotropically refined. The OMIT –2 50 was used in the SHELXL refinement to

truncate the data set to a lower angle ($\theta_{max}$ = 25°) in order to get rid of the level A alert of the checkCIF/PLATON validation routine (completeness = 91.8 < 95%). The new value of 94.5% for the data completeness still remains a low value probably due to a "misorientation" of the crystal (crystal parallel to glas fibre) which then often results in a completeness of about 90% for our type of IPDS diffractometer.

**Dicarbonyl($\eta^5$-hydroxycyclopentadienyl)(nitrosyl)rhenium(1+) tetrafluoroborate(1-), (27)**

An irregular yellow crystal (0.23 x 0.22 x 0.21 $mm^3$) was chosen for the X-ray diffraction study. A number of 162 images were exposed at a constant times of 3.5 min per image. The crystal-to-image distance was set to 50 mm and the ϕ-oscillation scan mode was selected with the ϕ increment of 1.2°. For the cell parameter refinement, 8000 reflections were selected out of the whole limiting sphere with intensities I > 6σ( (I). A total of 12675 reflections were collected of which 3281 were unique after performing data reduction and absorption correction ($R_{int}$ = 0.1276). A total of 10 indexed crystal faces were used for the numerical absorption correction ($T_{min}$ = 0.107, $T_{max}$ = 0.198).[11]

Compound **27** crystallizes in the centrosymmetric space group $P2_1/c$. The asymmetric unit is composed of one cationic $Re(C_5H_4OH)(NO)(CO)_2^+$ species and its corresponding $BF_4^-$ counter-ion. The NO ligand was not distinguished from the CO ligands with bond distances but testing the different possibilties and the behavior of the $R_1$ and $wR_2$ values (0.0375/0.0886 ; 0.0371/0.0886 ; 0.0366/0.0866). The OH hydrogen atom was located by difference electron density calculations and the coordinates and isotropic thermal parameters were freely refined. The positions of all other hydrogen atoms were calculated after each refinement cycle (riding model) and the non-hydrogen atoms were anisotropically refined. The OMIT –2 52 command was used in the SHELXL refinement to truncate the data set to a lower angle ($\theta_{max}$ = 26°: 3281 → 2165 unique reflections) in order to get rid of the high residual peaks close to the metal center.

**Table 7.3.1** Crystallographic data and structure refinements for **5**

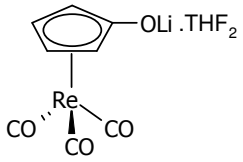


**5**

| | |
|---|---|
| Empirical formula | $C_{16}H_{20}LiO_6Re$ |
| Colour | colorless |
| Formula weight [g/mol$^{-1}$] | 501.46 |
| Crystal system | Monoclinic |
| Crystal size (mm) | 0.41 x 0.30 x 0.14 |
| Space group | P $2_1$/n |
| a(Å) | 9.9410(13) |
| b(Å) | 10.3114(9) |
| c(Å) | 17.700(2) |
| α (deg) | 90(2) |
| β(deg) | 90.135(15) |
| γ (deg) | 90 |
| V(Å$^3$) | 1814.3(4) |
| Z | 4 |
| Calculated density (g/cm$^{-3}$) | 1.836 |
| Absorption coefficient μ (mm$^{-1}$) | 6.723 |
| Temperature (K) | 183(2) |
| Wavelength (Å) | 0.71073 |
| Theta range for data collection (deg) | 2.85-30.25 |
| Reflections collected | 22911 |
| Independent reflections | 5374 |
| Data/restraints/parameters | 5374 / 0 / 218 |
| Goodness-of-fit on $F^2$ | 0.952 |
| Final R indices [I> 2σ(I)] | R1 = 0.0273, wR2 = 0.0655 |
| R indices (all data) | R1 = 0.0433, wR2 = 0.0743 |
| Largest diff. Peak and hole (e Å$^{-3}$) | 1.398 and –1.685 |

**Table 7.3.2** Crystallographic data and structure refinements for **6**

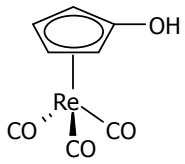


**6**

| | |
|---|---|
| Empirical formula | $C_8H_5O_4Re$ |
| Colour | colorless |
| Formula weight [g/mol$^{-1}$] | 351.32 |
| Crystal system | Monoclinic |
| Crystal size (mm) | 0.45 x 0.45 x 0.14 |
| Space group | $P2_1/c$ (n° 14) |
| a(Å) | 5.8799(9) |
| b(Å) | 12.4403(14) |
| c(Å) | 11.6443(19) |
| α (deg) | 90.0 |
| β(deg) | 91.788(19) |
| γ (deg) | 90.0 |
| V(Å$^3$) | 851.3(2) |
| Z | 4 |
| Calculate density (g/cm$^{-3}$) | 2.741 |
| Absorption coefficient μ (mm$^{-1}$) | 14.248 |
| Temperature (K) | 183(2) |
| Wavelenght (Å) | 0.71073 |
| Theta range for data collection (deg) | 3.28-30.32 |
| Reflections collected | 14120 |
| Independent reflections | 2411 |
| Data/restraints/parameters | 2411 / 0 / 122 |
| Goodness-of-fit on $F^2$ | 1.129 |
| Final R indices [I> 2σ(I)] | R1 = 0.0285, wR2 = 0.0760 |
| R indices (all data) | R1 = 0.0339, wR2 = 0.0897 |
| Largest diff. Peak and hole (e Å$^{-3}$) | 1.139 and –3.589 |

**Table 7.3.3** Crystallographic data and structure refinements for **7**

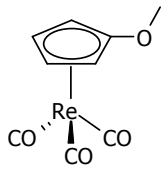


**7**

| | |
|---|---|
| Empirical formula | $C_9H_7O_4Re$ |
| Colour | colorless |
| Formula weight [g/mol$^{-1}$] | 365.36 |
| Crystal system | Triclinic |
| Crystal size (mm) | 0.34 x 0.27 x 0.19 |
| Space group | P -1 |
| a(Å) | 5.7724(10 |
| b(Å) | 8.8059(15) |
| c(Å) | 9.4765(16) |
| α (deg) | 83.16(2) |
| β(deg) | 81.92(2) |
| γ (deg) | 88.25(2) |
| V(Å$^3$) | 473.48(14) |
| Z | 2 |
| Calculate density (g/cm$^{-3}$) | 2.563 |
| Absorption coefficient μ (mm$^{-1}$) | 12.815 |
| Temperature (K) | 183(2) |
| Wavelenght (Å) | 0.71073 |
| Theta range for data collection (deg) | 3.38-24.99 |
| Reflections collected | 9238 |
| Independent reflections | 1564 |
| Data/restraints/parameters | 1564 / 0 / 128 |
| Goodness-of-fit on $F^2$ | 1.146 |
| Final R indices [I> 2σ(I)] | R1 = 0.0539, wR2 = 0.1324 |
| R indices (all data) | R1 = 0.0556, wR2 = 0.1337 |
| Largest diff. Peak and hole (e Å$^{-3}$) | 5.389 and –5.992 |

**Table 7.3.4** Crystallographic data and structure refinements for **11**

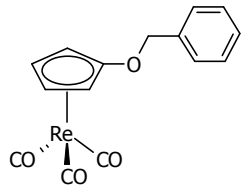


**11**

| | |
|---|---|
| Empirical formula | $C_{15}H_{11}O_4Re$ |
| Colour | colorless |
| Formula weight [g/mol$^{-1}$] | 441.45 |
| Crystal system | Monoclinic |
| Crystal size (mm) | 0.24 x 0.19 x 0.08 |
| Space group | P $2_1$/c (n°14) |
| a(Å) | 10.7532(6) |
| b(Å) | 6.3032(3) |
| c(Å) | 22.2064(14) |
| α (deg) | 90 |
| β(deg) | 113.092(7) |
| γ (deg) | 90 |
| V(Å$^3$) | 1384.54(15) |
| Z | 4 |
| Calculate density (g/cm$^{-3}$) | 2.118 |
| Absorption coefficient μ (mm$^{-1}$) | 8.785 |
| Temperature (K) | 183(2) |
| Wavelenght (Å) | 0.71073 |
| Theta range for data collection (deg) | 3.38-30.29 |
| Reflections collected | 18465 |
| Independent reflections | 4092 |
| Data/restraints/parameters | 4092 / 0 /181 |
| Goodness-of-fit on $F^2$ | 1.050 |
| Final R indices [I> 2σ(I)] | R1 = 0.0213, wR2 = 0.0619 |
| R indices (all data) | R1 = 0.0275, wR2 = 0.0628 |
| Largest diff. Peak and hole (e Å$^{-3}$) | 2.001 and –.0830 |

**Table 7.3.5** Crystallographic data and structure refinements for **13**

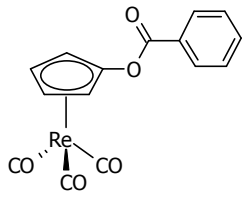


**13**

| | |
|---|---|
| Empirical formula | $C_{15}H_9O_5Re$ |
| Colour | colorless |
| Formula weight [g/mol$^{-1}$] | 455.42 |
| Crystal system | Triclinic |
| Crystal size (mm) | 0.20 x 0.20 x 0.08 |
| Space group | P-1 |
| a(Å) | 6.7284(5) |
| b(Å) | 7.1091(6) |
| c(Å) | 15.3920(12) |
| α (deg) | 91.911(10) |
| β(deg) | 99.044(10) |
| γ (deg) | 107.285(9) |
| V(Å$^3$) | 691.75(9) |
| Z | 2 |
| Calculate density (g/cm$^{-3}$) | 2.186 |
| Absorption coefficient μ (mm$^{-1}$) | 8.801 |
| Temperature (K) | 183(2) |
| Wavelenght (Å) | 0.71073 |
| Theta range for data collection (deg) | 3.01-30.33 |
| Reflections collected | 14483 |
| Independent reflections | 3753 |
| Data/restraints/parameters | 3753 / 0 / 190 |
| Goodness-of-fit on $F^2$ | 1.044 |
| Final R indices [I> 2σ(I)] | R1 = 0.0272, wR2 = 0.0677 |
| R indices (all data) | R1 = 0.0323, wR2 = 0.0684 |
| Largest diff. Peak and hole (e Å$^{-3}$) | 1.866 and –0.831 |

**Table 7.3.6** Crystallographic data and structure refinements for **16**

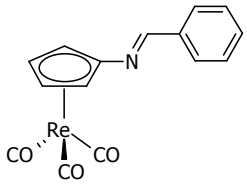


**16**

| | |
|---|---|
| Empirical formula | $C_{15}H_{10}NO_3Re$ |
| Colour | colorless |
| Formula weight [g/mol$^{-1}$] | 438.45 |
| Crystal system | Monoclinic |
| Crystal size (mm) | 0.50 x 0.17 x 0.03 |
| Space group | P $2_1$/c |
| a(Å) | 6.0691(4) |
| b(Å) | 21.3738(13) |
| c(Å) | 10.5171(7) |
| α (deg) | 90 |
| β(deg) | 103.116(8) |
| γ (deg) | 90 |
| V(Å$^3$) | 1328.69(15) |
| Z | 4 |
| Calculate density (g/cm$^{-3}$) | 2.192 |
| Absorption coefficient μ (mm$^{-1}$) | 9.151 |
| Temperature (K) | 183(2) |
| Wavelenght (Å) | 0.71073 |
| Theta range for data collection (deg) | 3.58-25.00 |
| Reflections collected | 14214 |
| Independent reflections | 2197 |
| Data/restraints/parameters | 2197 / 0 / 181 |
| Goodness-of-fit on $F^2$ | 1.114 |
| Final R indices [I> 2σ(I)] | R1 = 0.0269, wR2 = 0.0807 |
| R indices (all data) | R1 = 0.0298, wR2 = 0.0821 |
| Largest diff. Peak and hole (e Å$^{-3}$) | 2.526 and –0.831 |

**Table 7.3.7** Crystallographic data and structure refinements for **18**

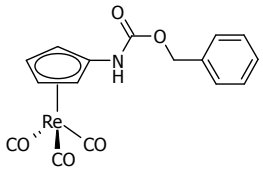


**18**

| | |
|---|---|
| Empirical formula | $C_{16}H_{12}NO_5Re$ |
| Colour | red |
| Formula weight [g/mol$^{-1}$] | 484.48 |
| Crystal system | Monoclinic |
| Crystal size (mm) | 0.24 x 0.12 x 0.10 |
| Space group | P $2_1$/c |
| a(Å) | 13.227(8) |
| b(Å) | 12.3692(9) |
| c(Å) | 9.4038(6)) |
| α (deg) | 90 |
| β(deg) | 96.789(7) |
| γ (deg) | 90 |
| V(Å$^3$) | 1527.25(18) |
| Z | 4 |
| Calculate density (g/cm$^{-3}$) | 2.107 |
| Absorption coefficient μ (mm$^{-1}$) | 7.981 |
| Temperature (K) | 183(2) |
| Wavelenght (Å) | 0.71073 |
| Theta range for data collection (deg) | 2.73-30.36 |
| Reflections collected | 16799 |
| Independent reflections | 4459 |
| Data/restraints/parameters | 4459 / 0 / 208 |
| Goodness-of-fit on $F^2$ | 1.079 |
| Final R indices [I> 2σ(I)] | R1 = 0.0233, wR2 = 0.0767 |
| R indices (all data) | R1 = 0.0355, wR2 = 0.0774 |
| Largest diff. Peak and hole (e Å$^{-3}$) | 1.133 and –574 |

**Table 7.3.8** Crystallographic data and structure refinements for **20**

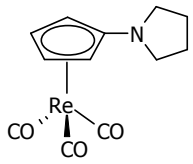


**20**

| | |
|---|---|
| Empirical formula | $C_{12}H_{12}NO_3Re$ |
| Colour | colorless |
| Formula weight [g/mol$^{-1}$] | 404.44 |
| Crystal system | Orthorhombic |
| Crystal size (mm) | 0.32 x 0.28 x 0.10 |
| Space group | P $2_1$ $2_1$ $2_1$ |
| a(Å) | 9.0755(9) |
| b(Å) | 10.9084(11) |
| c(Å) | 12.1523(16) |
| α (deg) | 90 |
| β(deg) | 90 |
| γ (deg) | 90 |
| V(Å$^3$) | 1203.1(2) |
| Z | 4 |
| Calculate density (g/cm$^{-3}$) | 2.233 |
| Absorption coefficient μ (mm$^{-1}$) | 10.095 |
| Temperature (K) | 183(2) |
| Wavelenght (Å) | 0.71073 |
| Theta range for data collection (deg) | 2.80-29.00 |
| Reflections collected | 15063 |
| Independent reflections | 3187 |
| Data/restraints/parameters | 3187 / 0 / 154 |
| Goodness-of-fit on $F^2$ | 1.044 |
| Final R indices [I> 2σ(I)] | R1 = 0.0209, wR2 = 0.0496 |
| R indices (all data) | R1 = 0.0216 wR2 = 0.0498 |
| Largest diff. Peak and hole (e Å$^{-3}$) | 1.313 and –1.659 |

**Table 7.3.9** Crystallographic data and structure refinements for **21**

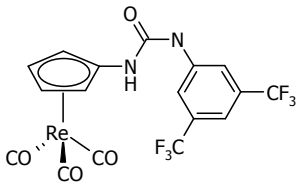


**21**

| | |
|---|---|
| Empirical formula | $C_{17}H_9F_6N_2O_4Re$, $C_4H_8O$ |
| Colour | colorless |
| Formula weight [g/mol$^{-1}$] | 677.57 |
| Crystal system | Monoclinic |
| Crystal size (mm) | 0.42 x 0.40 x 0.21 |
| Space group | C 2/c |
| a(Å) | 24.628(3) |
| b(Å) | 15.1292(13) |
| c(Å) | 12.9687(19) |
| α (deg) | 90 |
| β(deg) | 100.973(16) |
| γ (deg) | 90 |
| V(Å$^3$) | 4743.8(10) |
| Z | 8 |
| Calculate density (g/cm$^{-3}$) | 1.897 |
| Absorption coefficient μ (mm$^{-1}$) | 5.205 |
| Temperature (K) | 183(2) |
| Wavelenght (Å) | 0.71073 |
| Theta range for data collection (deg) | 2.86-28.00 |
| Reflections collected | 27459 |
| Independent reflections | 5718 |
| Data/restraints/parameters | 5718 / 0 / 352 |
| Goodness-of-fit on $F^2$ | 1.033 |
| Final R indices [I> 2σ(I)] | R1 = 0.0395, wR2 = 0.1032 |
| R indices (all data) | R1 = 0.0599, wR2 = 0.1135 |
| Largest diff. Peak and hole (e Å$^{-3}$) | 1.220 and –1.067 |

**Table 7.3.10** Crystallographic data and structure refinements for **26**

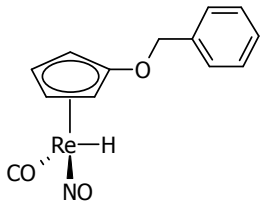


**26**

| | |
|---|---|
| Empirical formula | $C_{13}H_{12}NO_3Re$ |
| Colour | orange |
| Formula weight [g/mol$^{-1}$] | 416.45 |
| Crystal system | Monoclinic |
| Crystal size (mm) | 0.37 x 0.13 x 0.05 |
| Space group | P $2_1$/c |
| a(Å) | 6.4533(8) |
| b(Å) | 22.927(2) |
| c(Å) | 9.0410(11) |
| α (deg) | 90 |
| β(deg) | 106.289(14) |
| γ (deg) | 90 |
| V(Å$^3$) | 1284.0(3) |
| Z | 4 |
| Calculate density (g/cm$^{-3}$) | 2.154 |
| Absorption coefficient μ (mm$^{-1}$) | 9.463 |
| Temperature (K) | 183(2) |
| Wavelenght (Å) | 0.71073 |
| Theta range for data collection (deg) | 2.94-25.00 |
| Reflections collected | 16932 |
| Independent reflections | 2144 |
| Data/restraints/parameters | 2144 / 0 / 167 |
| Goodness-of-fit on $F^2$ | 0.931 |
| Final R indices [I> 2σ(I)] | R1 = 0.0244, wR2 = 0.0601 |
| R indices (all data) | R1 = 0.0308, wR2 = 0.0612 |
| Largest diff. Peak and hole (e Å$^{-3}$) | 0.613 and –1.658 |

**Table 7.3.11** Crystallographic data and structure refinements for **27**

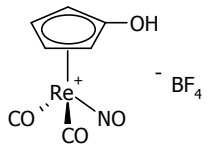


**27**

| | |
|---|---|
| Empirical formula | $C_7H_5BF_4NO_4Re$ |
| Colour | yellow |
| Formula weight [g/mol$^{-1}$] | 440.13 |
| Crystal system | Monoclinic |
| Crystal size (mm) | 0.23 x 0.22 x 0.21 |
| Space group | P $2_1$/c |
| a(Å) | 11.8112(17) |
| b(Å) | 7.4219(6) |
| c(Å) | 15.906(2) |
| α (deg) | 90 |
| β(deg) | 127.707(13) |
| γ (deg) | 90 |
| V(Å$^3$) | 1103.8(2) |
| Z | 4 |
| Calculate density (g/cm$^{-3}$) | 2.648 |
| Absorption coefficient μ (mm$^{-1}$) | 11.069 |
| Temperature (K) | 183(2) |
| Wavelenght (Å) | 0.71073 |
| Theta range for data collection (deg) | 3.19-25.99 |
| Reflections collected | 12675 |
| Independent reflections | 2165 |
| Data/restraints/parameters | 2165 / 0 / 185 |
| Goodness-of-fit on $F^2$ | 0.941 |
| Final R indices [I> 2σ(I)] | R1 = 0.0366, wR2 = 0.0844 |
| R indices (all data) | R1 = 0.0464, wR2 = 0.0866 |
| Largest diff. Peak and hole (e Å$^{-3}$) | 1.365 and –2.241 |

## 7.4 References


[1] P. Dembech, A. Ricci, G. Seconi, M. Taddei, *Organic Syntheses*, Coll. Vol. 9, p.91 (1998); Vol. 74, p.84 (1997).

[2] D. Reeves, C. Ruppin, G. Drivon, *European Patent*, Publication number: EP1059297, Application number: 20000401547 20000531, Priority number: FR 9907206 19990608.

[3] H. V. A. Briscoe, P. L. Robinson, A. J. Rudge, *Nature* **1932**, *129*, 618.

[4] I. Noddak, W. Noddak, *Z. Anorg. Allg. Chem.* **1933**, *215*, 129.

[5] W. Hieber, H. Fuchs, *Z. Anorg. Allg. Chem.* **1941**, *248*, 256.

[6] S. P. Schmidt, W.C. Trogler, F. Basolo, *Inorg. Syn.* **1990**, *2*, 154.

[7] G. V. Bindu Madhavan, J. C. Martin , *J. Org. Chem.* **1986,** *51*, 1287.

[8] K. H. Franzreb, C. G. Kreiter, *J. Organomet. Chem.* **1983**, *246*, 189.

[9] P. C. Heah, A. Patton, T. Alan, T. A. Gladysz *J. Am.. Chem. Soc.* **1986***, 108,* 1185.

[10] STOE-IPDS Software package, Version 2.87 5/1998; STOE & Cie, Darmstadt, Germany 1998.

[11] Coppens, P., Leiserowitz, L.; Rabinovich, D. *Acta Crystallogr.* **1965**, *18*, 1035.

[12] SHELX97 n(including *SHELXS97* and *SHELXL97*) – *Programs for Crystal Structure Analysis* (Release 97-2). Sheldrick, G. M., Institüt für Anorganische Chemie der Universität, Göttingen, Germany, 1998.

[13] (a) Spek, A. L. Acta Crystallogr., Sect A 1990, 46, C34. (b) PLATON, *A Multipurpose Crystallographic Tool*, Utrecht University, Utrecht, The Netherlands, Spek, A. L. 1998.

[14] ORTEP-3 for Windows. Farrugia, L. A. *J. Appl. Cryst.* **1997**, *30*, 565.

# 8 Summary

Organometallic chemistry with its important branch of homogeneous catalysis really arose in the fifties and has literally exploded during the last twenty years. Homogeneous catalysts have become an irreplaceable tool in many industrial processes (pharma, petrochemistry), naturally also in laboratory syntheses and it even plays a major role in biological catalysis. Nowadays, several millions tonnes of organic compounds are produced worldwide via organometallic processes. Homogeneous catalysis represents the royal way to develop processes permitting a perfect chemo, regio and stereo selectivity control.

Transition metal mediated hydrogen transfer reactions are the basis of catalytic hydrogenation. They have attracted considerable attention. Many noble metal complexes of ruthenium, iridium and rhodium have been found to be active catalysts. Homogeneous catalytic reduction of polar functional groups mediated by transition metal complexes has emerged as an alternative to stoichiometric reduction by main group metal hydrides such as $LiAlH_4$ and $NaBH_4$.

The main purpose of this project was the development of a new polar rhenium hydride with potential catalytic activity for hydrogenation. The design of this complex was based on the Shvo catalytic system, which involves a diruthenium complex ($\eta^5$-$C_4Ph_4CO$-H-$OCC_4Ph_4$-$\eta^5$)(μ-H)$(CO)_4Ru_2$ capable of hydrogenating unsaturated substrates. The potential catalyst is a cyclopentadienyl nitrosyl rhenium hydride ($\eta^5$-$C_5H_4XH$)Re(NO)(CO)(H) (X = O, NH), isoelectronic to the Shvo catalyst, bearing an acidic function and a hydride.

We developed simple synthetic routes to obtain oxy and amino cyclopentadienyl tricarbonyl rhenium complexes. We synthesized the following comlexes ($\eta^5$-$C_5H_4R$)$Re(CO)_3$ (R = OH **6**, R = OMe **7**, R = OEt **8**, R = O$^i$Pr **9**, R = OCHCH=$CH_2$ **10**, R = $OCH_2Ph$ **11**, R = OCOMe **12**, R = OCOPh **13**, R = $N_3$ **14**, R = $NH_2$ **15**, R = N=CHPh **16**, R = $NHCH_2Ph$ **17**, R = NHCOMe **19**, R = NHCbz **18**, R = $NHC_4H_8$ **20**, R = $NHCONHC_8H_3F_6$ **21**, R = $NHCONHC_6F_5$ **22**). Subsequently the compounds **6**, **7**, **11** and **18** were reacted with nitrosonium tetrafluoroborate $NOBF_4$ to give the corresponding nitrosyl cationic complexes [($\eta^5$-$C_5H_4OR$)$Re(CO)_2(NO)]^+BF_4^-$ (R = OH **27**, R = $OCH_3$ **23**, R = $OCH_2Ph$ **25**, R = NHCbz **24**).

We were very interested in the cationic complex $[(\eta^5\text{-}C_5H_4OH)Re(CO)_2(NO)]^+BF_4^-$ (**27**). As expected the proton of the hydroxyl group was found to be acidic. Moreover it was demonstrated that an equilibrium occurs when this complex is dissolved in acetone. This new species could not be isolated and determined, but the spectroscopic data indicated that the unknown complex could correspond to the conjugate base $[(\eta^5\text{-}C_5H_4O^-)Re(CO)_2(NO)]^+BF_4^-$ **28** or to a $\eta^4$-cyclopentadienone nitrosyl rhenium complex $(\eta^5\text{-}C_5H_4CO)Re(CO)_2(NO)$ **29**, which would be the first example of a $\eta^4$ rhenium-coordinated cyclopentadienone.

Cyclopentadienyl dicarbonyl nitrosyl rhenium complexes are of great interest since they can generate hydride in one step. In an appropriate basic medium, one carbonyl group of the nitrosyl dicarbonyl rhenium unit undergoes oxidation to COOH. At 50 °C the release of $CO_2$ results in the formation of hydride. We used this method to generate the novel hydride $(\eta^5\text{-}C_5H_4OCH_2Ph)Re(NO)(CO)(H)$ (**26**) which is the protected form of the target molecule $(\eta^5\text{-}C_5H_4OH)Re(NO)(CO)H$.

Further work should focus on the deprotection of an appropriate protected hydride complex of the type $(\eta^5\text{-}C_5H_4OR)Re(NO)(CO)H$ (R = protective group) and on the study of the features of the complex **27**.

# 9 Zusammenfassung

Organometallische Chemie und mit ihr auch eines ihrer wichtigen Teilgebiete über homogene Katalysen kam in den 50er-Jahren auf und entwickelte sich in den letzten zwanzig Jahren explosionsartig. Homogene Katalysatoren sind heute ein unersetzliches Instrument in vielen industriellen Prozessen (Pharmaindustrie, Petrochemie), in der Laborsynthese und sie spielen sogar in vielen biologischen Katalysatoren eine grosse Rolle. Heutzutage werden weltweit mehrere Millionen Tonnen organischer Verbindungen über organometallische Katalyse hergestellt. Homogene Katalysatoren bieten den strategisch besten Weg, um Prozesse zu entwickeln, welche eine perfekte Kontrolle über die Chemo-, Regio- und Stereoselektivität erlauben.

Wasserstoff-Transfer-Reaktionen katalysiert durch Uebergangsmetalle bilden die Basis für katalytische Hydrogenation. Sie haben bemerkenswerte Beachtung gefunden. Viele hochwertige Metalverbindungen von Ruthenium, Iridium und Rhodium wurden als aktive Katalysatoren erkannt. Die homogene katalytische Reduktion von polaren fuktionellen Gruppen katalysiert durch Uebergangsmetalle hat sich als eine Alternative zur stöchiometrischen Reduktion durch Hauptgruppen Metallhydride wie zum Beispiel $LiAlH_4$ und $NaBH_4$ herausgestellt.

Der Grundgedanke in diesem Projekt war die Entwicklung von neuen polaren Rheniumhydriden, welche sich durch eine potentielle katalytische Aktivität für Hydrierung auszeichnen. Ein Design solche Verbindung geht auf den Shvo-Katalysator zurück, welcher als Diruthenium-Komplex ($\eta^5$-$C_4Ph_4CO$-H-$OCC_4Ph_4$-$\eta^5$)(μ-H)$(CO)_4Ru_2$ Basis für die Hydrierung ungesättigter Substrate ist. Die potenziellen Katalysatoren sind Cyclopentadienylhydridonitrosylrhenium ($\eta^5$-$C_5H_4XH$)Re(NO)(CO)(H)-Systeme (X = O, NH), isoelektrisch zu Shvo-Katalysatoren, mit einer saueren Funktion $H^+$ und einem Hydrid $H^-$ als $H_2$ Equivalent.

Wir fanden einen einfachen Weg, um Oxy- und Amino Cyclopentadienyltricarbonylrhenium-Verbindungen ($\eta^5$-$C_5H_4R$)$Re(CO)_3$ (R = OH **6**, R = OMe **7**, R = OEt **8**, R = $O^iPr$ **9**, R = $OCHCH{=}CH_2$ **10**, R = $OCH_2Ph$ **11**, R = OCOMe **12**, R = OCOPh **13**, R = $N_3$ **14**, R = $NH_2$ **15**,

R = N=CHPh **16**, R = $NHCH_2Ph$ **17**, R = NHCOMe **19**, R = NHCbz **18**, R = $NHC_4H_8$ **20**, R = $NHCONHC_8H_3F_6$ **21**, R = $NHCONHC_6F_5$ **22)**. Anschliessend liessen wir die Verbindungen **6**, **7**, **11** und **18** mit Nitrosonium-Salz reagieren, um die korrespondierenden Nytrosyl-kationischen Verbindungen $[(\eta^5\text{-}C_5H_4R)Re(CO)_2(NO)]^+BF_4^-$ (R = OH **27**, R = $OCH_3$ **23**, R = $OCH_2Ph$ **25**, R = NHCbz **24**) zu synthetisieren.

Die kationische Verbindung $[(\eta^5\text{-}C_5H_4OH)Re(CO)_2(NO)]^+BF_4^-$ (**27**) weckte unser Interesse sehr. Wie erwartet stellte sich das Proton der Hydroxyl-Gruppe als sehr sauer heraus. Weiter noch konnte aufgezeigt werden, dass ein Gleichgewicht entsteht, wenn diese Verbindung in Aceton aufgelöst wird. Diese neuen Speziens, welche aus **27** hervorgingen, konnten nicht isoliert und voll charakterisert werden. Aber in Anbetracht der NMR-Spektrometrie stellten wir fest, dass die unbekannte Verbindung zur konjugierten Base $[(\eta^5\text{-}C_5H_4O^-)Re(CO)_2(NO)]^+BF_4^-$ **28** oder eine $\eta^4$-Cyclopentadienone nitrosyl rhenium-Verbindung $(\eta^5\text{-}C_5H_4CO)Re(CO)_2(NO)$ **29** sein könnte, was ein erstes Beispiel eines Rhemium-koordinierten Cyclopentadienon-Liganden darstellt.

Cyclopentadienyl Diacarbonyl Nitrosyl Rhenium-Verbindungen sind von grossem Interesse, da sie Hydride in einem Schritt generieren können. In einem passendem basischen Medium kann eine Carbonyl-Gruppe der Nitrosyldicarbonylrhenium-Einheit zu einem COOH-Rest oxidieren. Bei 50°C geschieht die Abgabe von $CO_2$ und Bildung von Hydriden. Wir brauchten diese Methode um das neue Hydrid $(\eta^5\text{-}C_5H_4OCH_2Ph)Re(NO)(CO)(H)$ (**26**) zu generieren, welches die geschützte Form von $(\eta^5\text{-}C_5H_4OH)Re(NO)(CO)H$ ist.

Weitere Forschung sollte den Fokus auf die Entfernung der Schutzgruppe eines geeigneten geschützten Hydrido-Komplex $(\eta^5\text{-}C_5H_4OR)Re(NO)(CO)H$ (R = Schutzgruppe) und auf die Erforschung der Eigenschaften von Komplex **27** richten.

# Acknowledgements

I wish to express my thankfulness to Prof. Dr. Heinz Berke, for giving me the opportunity to work in his group and for having introduced me to an interesting research field.

I would also like to thank,
Prof. Dr. Roger Alberto
Dr. Thomas Fox for performing NMR measurements
Dr. Helmut W. Schmalle for crystallographic studies
Dr. Olivier Blacque for crystallopgraphic studies
Beatrice Spichtig for MS measurements and administrative help
Ferdinand Wild and Felix Zelder for MS measurements
Heinz Spring for the elemental analyses
Hanspeter Stalder for providing always excellent solutions to our technical problems

I would like to thank particularly Tristan Corbière, Ivan Timokhin, Nikolay Vostrikov, Sergey Semenov, Dr. Marcello Bertoli, Dr. Marta Tymcio, Dr. Elisabetta Macaroni, Shiva Taghipourian, Praveen Sreedevi, Yanfeng Jiang, Balz Dudle, Alexander Dybov, Dr. Venkatesan Koushik, Stéphane Masi, Javier Fraga Hernandez, and Alberto Lopez for their help, cooperation, suggestions and encouragement.

I would also like to thank all the members of the ACI who have always been helpful and welcoming in all the little day-to-day details which add up to the whole experience.

I express my sincere thanks to all those who have extended their help directly or indirectly to make the study a success.

I am very thankful to the University of Zürich and the Swiss National Science Foundation for financial support.

I would also like express my Scincere Thanks to My Friends.

Finally I would Like to Express My Sincere and Heartfelt Gratitude to

My sweet Stephanie
Heidi and Christian Maeder for their kindness

All My Family
My dearest Mother
My beloved sister and brothers, Johanne, Frédéric and Jean-Raymond
I embrace my cute and playful nephews and nieces:
Lise, Flavie, Mirtille, Leon, Yvon, Edmon and Konstantin
My Father
My Grand-Mother Mério

# Curriculum Vitae

**Gabriel LASTENNET**

Magdalenenstrasse 48 · 8050 Zürich · Switzerland

Email: gabriel_lastennet@yahoo.fr

Home Phone: +41 43 536 56 08

Mobile: +41 78 712 78 24

Date of Birth: 01.01.1979

## Education

2003 - Present

- **PhD - Organometallic Chemistry**

  **Thesis:** "Synthesis of Oxy and Amino Cyclopentadienyl Rhenium Complexes"

  Institute of Inorganic Chemistry, University of Zürich, Switzerland

2002 - 2003

- ***Diplôme d'Etudes Approfondies (DEA) de Chimie Organique***

  **Master of Science - Organic Chemistry**

  **Thesis:** "Interaction of Nucleophiles with Carbene Complexes of Chromium: Diastereo and Enantioselective Synthesis of Polycyclic Butenolides"

  University Paris VI, France

1999 - 2002

- ***Ingénieur-Maître en Chimie Fine***

  **Bachelor of Science - Fine Chemistry**

  **Thesis:** "Parallel Synthesis of Amidocarbamates"

  University-Based Professional Institute (IUP) of Chemistry, Nantes, France

**Relevant Experience**

10.2003 - 11.2007

**Institute of Inorganic Chemistry**

University of Zürich,

Zürich, Switzerland

**Postgraduate Assistant**

01.2003 - 07.2003

**Laboratoire de Chimie Organique (CNRS)**

**Equipe de Synthèse Organique et Organométallique**

Université Pierre et Marie Curie Paris VI,

Paris, France

**Graduate Assistant**

03.2002 - 09.2002

**Sanofi-Synthélabo**

CNS (Central Nervous System) Research Department

Bagneux, France

Pharmaceutical company

**Intern in the Department of Parallel Synthesis**

06.2001 - 09.2001

**Armor Proteines**

Loudéac, France

Specialist in Milk Fractionation

**Intern in the Quality Control Department**

**Publication**

Henri Rudler, André Parlier, Victor Certal, Gabriel Lastennet, Max Audouin and Jacqueline Vaisserman, *"Interaction of Dihydropyridines and nucleophiles with Carbene Complexes of Chromium: Diastereo and Enantioselective Synthesis of Polycyclic Butenolides."* **European Journal of Organic Chemistry**, **2004**, 2471-2502.

**Conference Contributions**

Gabriel Lastennet, H.W. Schmalle, O. Blacque and Heinz Berke: *"Synthesis of Substituted Cyclopentadienyl Tricarbonyl Rhenium Complexes. Ester and Ether Derivatives of Hydroxycyclopentadienyltricarbonylrhenium."* Oral Presentation. X$^{th}$ International Seminar of Ph.D. Students on Organometallic and Coordination Chemistry (**X$^{th}$ ISPSOC 2006**), Pardubice, Czech Republic, 17-21 September 2006.

Gabriel Lastennet, H.W.Schmalle, O. Blacque and Heinz Berke: *"Synthesis of Substituted Cyclopentadienyl Tricarbonyl Rhenium Complexes"*, Fall Meeting of the Swiss Chemical Society, Zürich, Switzerland, 13.10.2006. Abstract: **Chimia 2006**, 60, 423.

Gabriel Lastennet, H.W. Schmalle, O. Blacque and Heinz Berke: *"Design of a new Rhenium Catalyst"*, Fall Meeting of the Swiss Chemical Society, Lausanne, Switzerland, 13.10.2005. Abstract: **Chimia 2005**, 59, 629.